

COMMUNICATIONS QUARTERLY

THE JOURNAL OF
COMMUNICATIONS
TECHNOLOGY

Spring 1991

\$9.95



■ The Quad Antenna:
Rectangular and
Square Loops

■ Digital Signal
Processing:
Image Processing

■ A 4800 Baud
Modem Daughter
Board for Packet

■ A High-Performance
1296 MHz Converter

■ The Traveling-Wave
Amplifier

■ Solid-State
75S-3 Receiver

■ VLF-LF and the
Loop Aerial

■ HF Modems for
Data Transmission

INTRODUCING

I C - 2 2 9



HM-56 DTMF
Autodialer
Microphone



ACTUAL
SIZE

STATE OF THE ART IN SMALL MOBILES

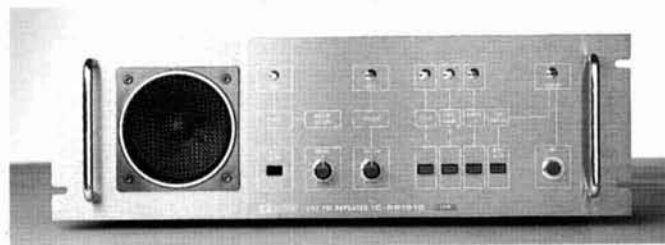
ICOM enhances your mobiling experience with a sleek design perfect for today's automobiles. Big rig performance and maximum frequency coverage are yours with the ultra-compact IC-229A/H 2-Meter and IC-449 440MHz mobile transceivers.

Incomparable ICOM quality and an array of alluring features ensure endless hours of operating enjoyment: 20 memory channels store operating offset and subaudible tone frequencies; up to 50 watts power output; call channel; and unique auto dialing function for excellent autopatching and repeater control.

The IC-229/H and IC-449 will exceed your mobiling expectations.

Test tune one today

at your quality ICOM amateur dealer and see what mobiling can be. For full details call the ICOM Brochure Hotline at 1-800-999-9877.



IC-RP1510
2-Meter
Repeater

ICOM

CORPORATE HEADQUARTERS: ICOM America, Inc., 2380-116th Ave., N.E., Bellevue, WA 98004
CUSTOMER SERVICE HOTLINE (206) 454-7619
CUSTOMER SERVICE CENTERS: 3150 Premier Drive, Suite 126, Irving, TX 75063
1777 Phoenix Parkway, Suite 201, Atlanta, GA 30349
3071 - #5 Road, Unit B, Richmond, B.C. V6X 2T4 Canada
2380-116th Ave., N.E., Bellevue, WA 98004
All stated specifications are subject to change without notice or obligation. All ICOM radios significantly exceed FCC regulations limiting spurious emissions. 2291090

BREAKING THE BARRIER OF DUAL BAND COMMUNICATION



The dual banders of the future are here! ICOM's IC-24AT dual band handheld and IC-3220 dual band mobile provide you all the advantages with the most feature packed, power packed dual banders available.

Whether your needs require the mobility of the IC-3220 or the convenience of the IC-24AT mini-handheld, ICOM has the dual bander fit for you.

The IC-24AT mini-handheld and the IC-3220 mobile give you full operation on the 2-meter and 440MHz

amateur bands with outstanding flexibility and performance!

The IC-24AT offers 40 memories, 5 watts, programmable scanning, priority watch, a battery saver, plus a DTMF pad for autopatching...the list is endless. Among the many features

of the compact IC-3220 are a built-in duplexer, simultaneous dual band receive, auto dialing and a memory transfer function. For full details and specs on the IC-24AT and IC-3220, call the ICOM Brochure hotline at 1-800-999-9877. See them today at your quality ICOM amateur dealer.

ICOM
First in Communications

CORPORATE HEADQUARTERS: ICOM America, Inc.
2380-116th Ave. N.E., Bellevue, WA 98004
CUSTOMER SERVICE HOTLINE (206) 454-7619
CUSTOMER SERVICE CENTERS:
3150 Premier Drive, Suite 126, Irving, TX 75063
1777 Phoenix Parkway, Suite 201, Atlanta, GA 30349
3071 - #5 Road, Unit 9, Richmond, B.C. V6X 2T4 Canada
2380-116th Ave. N.E., Bellevue, WA 98004

All stated specifications are subject to change without notice or obligation. All ICOM radios significantly exceed FCC regulations limiting spurious emissions: 3220990.

KENWOOD

Compact Champion!

TH-27A/47A

2 m and 70 cm Super Compact HTs

Here is a great new addition to Kenwood's HT family — the all new TH-27A for 2 meters and TH-47A for 70 cm! Super compact and beautifully designed, these pocket-sized twins give you full-size performance.

- **Large capacity NiCd battery pack supplied.** The standard battery pack is 7.2 volts, 700 mAh, providing extended transmit time with 2.5 watts. (TH-47A: 1.5 W.)
- **Extended receive coverage.** TH-27A: 118–165 MHz; TH-47A: 438–449,995 MHz. TX on Amateur bands only, (TH-27A modifiable for MARS/CAP, Permits required. Specifications guaranteed for Amateur bands only.)
- **Multi-function scanning.** Band and memory channels can be scanned, with time operated or carrier operated scan stop.
- **Frequency step selectable for quick QSX.** Choose from 5, 10, 12.5, 15, 20, or 25 kHz steps.
- **Built-in digital clock with programmable timer.**
- **Dual Tone Squelch System (DTSS).** Compatible with the TH-26AT Series and the TM-941A Triple bander, as well as other Kenwood series transceivers, this selective calling system uses standard DTMF to open squelch.
- **Five watts output** when operated with PB-14 battery pack or 13.8 volts.
- **T-Alert for quiet monitoring.** Tone Alert beeps when squelch is opened.
- **Auto battery saver, auto power off function, and economy power mode extends battery life.**
- **DTMF memory.** The DTMF memory function can be used as an auto-dialer. All characters from the 16-key pad can be stored, allowing repeater control codes to be stored!

- **41 memories.** All channels store receive and transmit separately for "odd split"
- **DC direct in operation.** Allows external DC to be used (7.2 – 16 volts). When external power is used, the batteries are being charged. (PB-13 only.)

Optional accessories:

- BC-14: Wall charger for PB-13, 14
- BC-15: Rapid charger for PB-13, 14
- BH-6: Swivel mount
- BT-8: Six cell AA Alkaline battery case
- HMC-2: Headset with VOX and PTT
- PB-13: 7.2 V, 700 mAh NiCd pack
- PB-14: 12 V, 300 mAh NiCd pack
- PG-3F: DC cable with filter and cigarette lighter plug
- PG-2W: DC cable
- SC-30: Soft case
- SMC-31: Standard speaker mic
- SMC-32: Compact speaker mic
- SMC-33: Compact speaker mic with controls
- WR-2: Water resistant bag.



- **Automatic offset selection (TH-27A).**
- **Direct keyboard frequency entry.** The rotary dial can also be used to select memory, frequency, frequency step, CTCSS, and scan direction.
- **CTCSS encode/decode built-in.**
- **Supplied accessories:** Rubber flex antenna, battery pack, wall charger, belt hook, wrist strap, dust caps.

KENWOOD U.S.A. CORPORATION
COMMUNICATIONS & TEST EQUIPMENT GROUP
P.O. BOX 22745, 2201 E. Dominguez Street
Long Beach, CA 90801-5745
KENWOOD ELECTRONICS CANADA INC.
P.O. BOX 1075, 959 Gana Court
Mississauga, Ontario, Canada L4T 4C2

KENWOOD

...pacesetter in Amateur Radio

Specifications and features are subject to change without notice or obligation.
Complete service manuals are available for all Kenwood transceivers and most accessories.

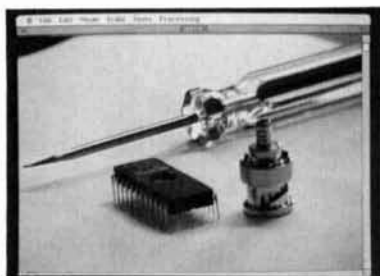
COMMUNICATIONS QUARTERLY

THE JOURNAL OF
COMMUNICATIONS
TECHNOLOGY

CONTENTS

Volume 1, Number 2

Spring 1991



NUIN, page 23

11 The Quad Antenna: Rectangular and Square Loops

R.P. Haviland, W4MB

23 Digital Signal Processing: Image Processing

Bryan Bergeron, NUIN

37 Solid-State 75S-3 Receiver

Jim Larson, KF7M

54 VLF-LF and the Loop Aerial

Lloyd Butler, VK5BR

62 A 4800-Baud Modem Daughter Board for Packet TNC

Glenn Leinweber, VE3DNL, Max Pizzolato, VE3DNM, John Vanden Berg, VE3DVV, Jack Botner, VE3LNY

74 HF Modems for Data Transmission

Dr. Alan Chandler, PHd EE, K6RFK

79 Yagi Optimization and Observations on Frequency Off-set and Element Taper Problems

William Orr, W6SAI

86 What's the Electromagnetic Capability of Your Antenna?

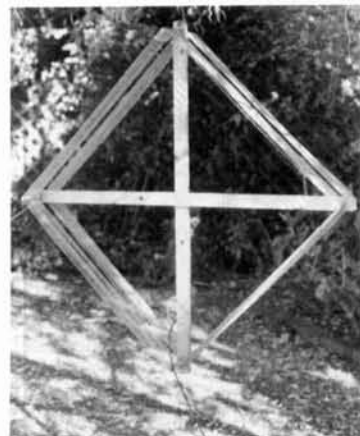
John A. Wick, W1HIR

95 The Traveling-Wave Amplifier

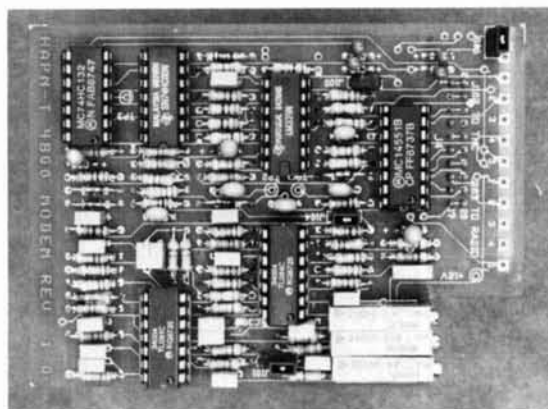
Michael Gruchalla, P.E.

101 A High-Performance 1296-MHz Converter

Norman J. Foot, WA9HUV



VK5BR, page 54



VE3DNL, VE3DNM, VE3DVV, VE3LNY, page 62

Who's Responsible? Automatically controlled packet radio suffers a setback.

Recent regulatory and enforcement actions taken by the FCC against eleven east coast Amateur packet radio BBS operators have left many hams concerned about the future of automatically controlled packet radio.

On January 5, 1991, a message giving information about a (900) telephone number which could be called to support efforts to keep the United States out of a war in the Middle East was initiated by one station and automatically retransmitted over the eastern-central portion of the U.S. The message passed through a number of packet stations before it was questioned by a ham in the Norfolk, Virginia area, who brought it to the attention of his local FCC office.

Shortly thereafter, the FCC Engineer-in-Charge of the Norfolk FCC field office issued citations to a number of packet stations for their role in transmitting this message. In essence, the letter said that these hams were in violation of Part 97.113(a) and had used Amateur Radio to facilitate the business activities of the *Coalition to Stop U.S. Intervention in the Middle East*.

Make no mistake about it, this message was in violation of the FCC rules and should have never been posted into the Amateur Radio packet system. The question which arises concerns the liability of packet BBS operators for messages transmitted automatically through their stations.

Many operators of automatic packet systems have assumed that they cannot be held responsible for messages passing through their system. This is a logical assumption when you look at the volume of mail going through some of the more active packet nodes. It quickly becomes apparent that a sysop's ability to censor messages is limited. At W3IWI, one of the named "offenders" in this morass, a minimum of 10,000 messages per month were being handled prior to the FCC action. There is no way W3IWI, or any other sysop, can screen all messages passing through the packet system. Jobs, family, and other obligations also require attention. The technology which has led to automatic control of packet switches has been a boon to traffic handlers. Messages can now zip across the country in a matter of hours via high-speed packet radio.

As an assistant sysop of a local DX packet cluster, I am quite concerned over our liability should someone post an "illegal" message on our

system. The operative question is: who is really responsible for the content of a message—the originator, or a BBS where the message resides.

In grade school, teachers often punish the whole class for the indiscretion of one student. The FCC's action in this case smacks of similar treatment. While the originator of the (900) message should be punished, I see no need to do the same to every other station that unknowingly passed the message on before it was stopped. While punishing the group for the sins of a few is a very simple solution, it rarely gets to the root of the problem.

But the fact remains that Amateur radio rule Part 97.113(a) provides that the licensee of an Amateur station is responsible for its proper operation. Part of that responsibility involves not passing business communications over the Amateur frequencies.

Finding a solution isn't easy. Messages involving business communications are in clear violation of the FCC rules. However, the FCC's response to the problem is unpalatable and harkens back to the early days of repeaters. You'll remember that initial regulations regarding repeaters were quite restrictive. Many of us wondered if they were designed to limit repeaters because of actual abuses, or were handed down by an FCC that didn't like repeaters and was bound and determined to slow, if not stop, their growth.

Is the FCC against technological advances in Amateur Radio? Was it when repeaters made their appearance? How will the FCC's recent findings impact on the implementation of state-of-the-art technology by Amateur Radio operators?

I'm afraid I don't know the answer to these questions. We need to have the support of the FCC if Amateur Radio is to grow and prosper. We do not need to have the commission throw roadblocks in the path of technological developments which make the service more efficient. Hopefully, there will be a resolution to this question before the FCC stymies further developments in packet technology or frightens computer-oriented Amateurs away.

We'll know soon enough.

J. Craig Clark, NX1G
Associate Publisher

EDITORIAL STAFF

Editor

Terry Northup, KA1STC

Consulting Technical Editor

Robert Wilson, WA1TKH

Senior Technical Editor

Alfred Wilson, W6NIF

Technical Editor

Peter Bertini, K1ZJH

Editorial Assistant

Elizabeth McCormack

EDITORIAL REVIEW BOARD

Forrest Gehrke, K2BT

Michael Gruchalla, P.E.

Hunter Harris, W1SI

Bob Lewis, W2EBS

Walter Maxwell, W2DU

William Orr, W6SAI

Joseph J. Schroeder, W9JUV

BUSINESS STAFF

Publisher

Richard Ross, K2MGA

Associate Publisher

J. Craig Clark, Jr., NX1G

Advertising Manager

Arnie Sposato, N2IQO

Sales Assistant

Tracy Parbst

Production Manager

Dorothy Kehrwieler

Controller

Frank Fuzia

Circulation Manager

Catherine Ross

Data Processing

Melissa Kehrwieler

Customer Service

Carol Minervini

A publication of

CQ Communications, Inc.

76 North Broadway

Hicksville, NY 11801-USA

Editorial Offices: Main Street, Greenville, NH 03048. Telephone: (603) 878-1441. FAX: (603) 878-1951.

Business Offices: 76 North Broadway, Hicksville, NY 11801. Telephone: (516) 681-2922. FAX: (516) 681-2926.

Communications Quarterly is published four times a year by CQ Communications, Inc. Subscription prices: Domestic—one year \$29.95; Foreign—\$39.95; Foreign Air Mail—\$60.95. Contents copyrighted CQ Communications, Inc. 1991. Communications Quarterly does not assume responsibility for unsolicited manuscripts. Allow six weeks for change of address.

Second-class postage paid pending at Hicksville, NY and additional mailing offices.

Postmaster: Please send change of address to Communications Quarterly, CQ Communications, Inc., 76 North Broadway, Hicksville, NY 11801.

ISSN 1053-9433



Kantronics D4-10

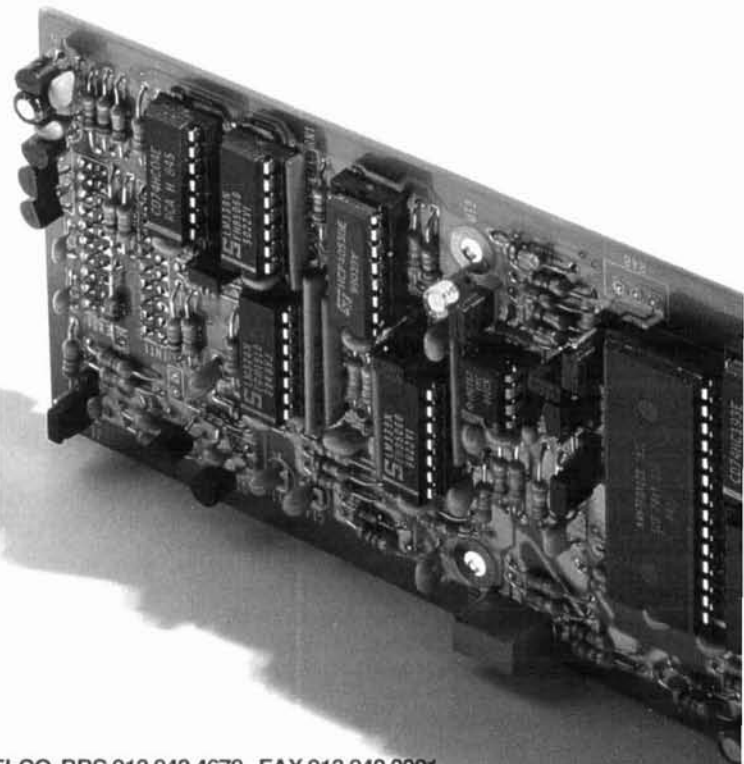
19,200 off the shelf

No tweaking, no kludges, no kidding . . . The new Kantronics D4-10 transceiver provides robust 19,200 baud operation off the shelf, today. Manufactured to respond to your requests for a faster more powerful transceiver, the D4-10 represents state of the art design equalling that found in our DataEngine and beyond that found anywhere else in the industry.

The Kantronics D4-10 features user selectable narrow and wide bandwidth operation (60 KHZ). This provides conventional and high speed data modes at 1200, 9600, and up to 19,200 baud and beyond with our DataEngine and DE19200 plug-in module.

Add features like a DVR2-2 plug compatible analog port for experimentation, TTL port which supports internal DFSK modulation and threshold demodulation, fast TR switching and you have a 70 cm transceiver that is as fun to use as it is technologically advanced.

The Kantronics D4-10 transceiver, the state of the art available off the shelf from Kantronics.



LETTERS

Pleasant surprise

I waited with curiosity for the first issue of *Communications Quarterly*. I am pleased and surprised at what you accomplished.

Large schematics (you could reduce them to 1/2 and still be clear to my bifocals). Excellent narration.

Most articles were perused with interest.

Even though I'll never build it, N6NWP's article, "High Range Dynamic Range Receiver," was fascinating reading because of the excellent narration which included references to the NEARBY schematics. A few more photos of the development breadboards would add interest.

I am probably in the minority but I suggest some of the heavier data found in this issue should be relegated to "Proceedings of the IEEE," etc.

Congratulations for a great technical issue.

**Allen Bell, W4IKV,
Cape Canaveral, Florida**

There's a typo in my article

Congratulations on the Premier Issue of *Communications Quarterly*! Job well done!

Hope we can do something else together in the future.

I have noticed a typo on page 84 in the beginning of the Appendix section:

| | |
|------------------------|------------|
| Noise | Noise |
| Figure 7.1 should read | Factor 7.1 |
| (NFt) | (NFt) |

**Jacob Makhinson, N6NWP,
Burbank, California**

The right blend

I received the premier issue of *Communications Quarterly* during the first week in January.

You have created a pleasant blend of subjects of interest to all in the communications field. I enjoyed all the articles.

The initial article in the 432-MHz EME series is very interesting; I'm looking forward to reading more of

Steve Powlishen's writing in later issues.

Well done.

**Robert W. Jones, KH6O,
Kaneohe, Hawaii**

Please add these corrections

Regrettably, an error crept into my article "Radio Propagation by Tropospheric Scattering," page 119, Winter 1991. On page 122, the variation in path loss as a function of radio index refraction is correctly given as:

$$L_n = 0.2(N_s - 310)(dB)$$

However, this factor should be subtracted from the total path loss, *not added*, as shown in the equation at the foot of page 122, the top of page 123, and in the listing on page 124. Thus, the equation at the top of page 124 should read:

$$L = 56 + 20\log_{10}(d) + 30\log_{10}(f) - 0.2(N_s - 310) + 10(\theta) + 1.8(\theta/\alpha) - 0.063(\theta/\alpha)^2$$

and line 39 of listing 1 should read:

$$tpl = 56 + 20 * \log(d3)/2.303 + 30 * \log(f)/2.303 + 10 * tsa - ln + lamc$$

I apologize for any inconvenience these errors may have caused.

**Bob Atkins,
KA1GT, Millington, New Jersey**

Balance and variety

I'm glad I followed my instinct and subscribed to *Communications Quarterly*. I enjoyed reading all of the articles and think you and your staff did a great job at selecting a balanced variety.

I wouldn't mind the articles being a bit more technical, but I'm a microwave engineer (BSEE '68) and enjoy theory as much as practical information. Personally, I enjoy antenna articles the most, followed by wide dynamic range receiver related topics. I'd be particularly interested in articles on better noise blankers, especially for the new United States-based woodpecker radars.

Keep up the quality work.

**Bill Shanney, KJ6GR,
Torrance, California**

Many subjects to cover

I just received the premier issue of *Communications Quarterly*. I am very impressed with the quality of the articles and the format. I was disappointed when *Ham Radio* magazine was cancelled. I believe your magazine will fill that void very nicely. I would like to see more DSP articles in future issues. Last year at Dayton there was a new DSP newsletter out called *Ham Pute*. It didn't materialize beyond the first issue. The editor of *Ham Pute* was Richard Blasco, NX6R, MSEE, with 20 years DSP experience. Maybe he could contribute to your magazine in this area.

Another area that really hasn't been addressed in Amateur Radio is frequency synthesizers (direct synthesis). Fred Williams of TRW has written articles for *QST* (1984-1985), and A & A Engineering produces a unit that he designed, but that is all I have seen. Could we see articles in this area?

When is the last time anyone has designed a modern solid-state multi-band HF rig? This may sound crazy with the fine equipment that is available today but, with computers to control and modular construction, maybe a spread-spectrum rig with DSP could be a great stride in advancing Amateur Radio. Military contractors have already done this.

I think the article "Interface Your Computer to the Poor Man's Spectrum Analyzer" shows that, with today's modular technology, this once expensive gear can be built at reasonable cost. I have a poor man's spectrum analyzer in the works, so I will make good use of the article.

In closing, I think that your magazine is off to a good start. Keep the format as is. It's worth waiting a quarter for a high-quality publication that we all can be proud of. Good job.

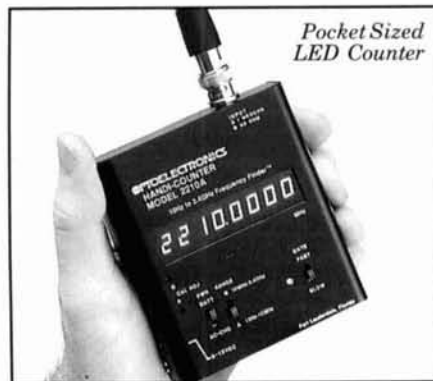
**Jim Brude, WB0SCD,
Amelia, Ohio**

OPTOELECTRONICS

"the State of the Art"

The new 10 digit LCD Handi-Counters™ from Optoelectronics redefine the state of the art. Our new HIGH SPEED ASIC (230MHz) makes the difference.

Select from our family of LCD, LED as well as computer based counters.



Pocket Sized
LED Counter

| Model | 8030 | 3000 | 2600H | 2600HA | 2210A | 1300H/A | PC10 |
|------------------------------|--|--|--------------------------------|--------------|-------------|-------------|------------------|
| Function | Freq, Period Ratio, Interval Avg, Prescale | Freq, Period Ratio, Interval Avg, Prescale | Frequency | Frequency | Frequency | Frequency | * |
| Range | 10Hz-2.6GHz | 10Hz-2.6GHz | 1MHz-2.6GHz | 1MHz-2.6GHz | 10Hz-2.4GHz | 1MHz-1.3GHz | 1Hz-2.4GHz |
| Display | 10 Digit LCD w/Function Annunciators | 10 Digit LCD w/Function Annunciators | 10 Digit LCD | 10 Digit LCD | 8 Digit LED | 8Digit LED | 14 Digit Monitor |
| RF Signal Strength Indicator | 16 Segment Adjustable Bargraph | 16 Segment Adjustable Bargraph | 16 Segment Adjustable Bargraph | . | . | . | . |
| Price | \$579. | \$375. | \$325. | \$225. | \$239. | \$179. | **\$339. |

Sensitivity: <1 to <10mV typical. Time Base: ± 1 ppm.; ± 5 ppm. add \$75 - LED Models; ± 2 ppm add \$80. - LCD Models. Nicads & AC charger/adaptor included. Carry case and a full line of probes and antennas are available. One year parts & labor warranty on all products.

* PC10: Universal Counter Timer Board for the PC. Windows 3.0 based software. Frequency, Period, Ratio, Time Interval, Pulse Width, Reciprocal Count, Data Logging, Direct Tune a Radio Receiver, Auto Calibrate, Configure Units of Time & Frequency.

* Price includes on board 50ohm, 2.5MHz to 2.4GHz input. Companion model AP10H, Dual High Impedance Amplifier is an additional \$299.

**FACTORY DIRECT
ORDER LINE
1-800-327-5912**

FL(305)771-2050 • FAX(305)771-2052

5821 NE 14th Avenue • Fort. Lauderdale, FL 33334
Visa, MC, COD, Cash, M.O. accepted. Personal Check allow
3 weeks. 5% Shipping, Handling. (Maximum \$10) U.S. &
Canada. 15% outside continental U.S.A.



ASTRON POWER SUPPLIES

• HEAVY DUTY • HIGH QUALITY • RUGGED • RELIABLE •



MODEL VS-50M

SPECIAL FEATURES

- SOLID STATE ELECTRONICALLY REGULATED
- FOLD-BACK CURRENT LIMITING Protects Power Supply from excessive current & continuous shorted output
- CROWBAR OVER VOLTAGE PROTECTION on all Models except RS-3A, RS-4A, RS-5A, RS-4L, RS-5L
- MAINTAIN REGULATION & LOW RIPPLE at low line input Voltage
- HEAVY DUTY HEAT SINK • CHASSIS MOUNT FUSE
- THREE CONDUCTOR POWER CORD except for RS-3A
- ONE YEAR WARRANTY • MADE IN U.S.A.

PERFORMANCE SPECIFICATIONS

- INPUT VOLTAGE: 105-125 VAC
- OUTPUT VOLTAGE: 13.8 VDC \pm 0.05 volts (Internally Adjustable: 11-15 VDC)
- RIPPLE Less than 5mv peak to peak (full load & low line)
- All units available in 220 VAC input voltage (except for SL-11A)

SL SERIES



| MODEL | Colors Gray Black | Continuous Duty (Amps) | ICS* (Amps) | Size (IN) H x W x D | Shipping Wt. (lbs.) |
|--------|----------------------|---------------------------|----------------|------------------------|------------------------|
| SL-11A | • • | 7 | 11 | 2 1/4 x 7 1/2 x 9 3/4 | 11 |

- LOW PROFILE POWER SUPPLY

RS-L SERIES



| MODEL | Continuous Duty (Amps) | ICS* (Amps) | Size (IN) H x W x D | Shipping Wt. (lbs.) |
|-------|---------------------------|----------------|------------------------|------------------------|
| RS-4L | 3 | 4 | 3 1/2 x 6 1/2 x 7 1/4 | 6 |
| RS-5L | 4 | 5 | 3 1/2 x 6 1/2 x 7 1/4 | 7 |

- POWER SUPPLIES WITH BUILT IN CIGARETTE LIGHTER RECEPTACLE



RM SERIES

MODEL RM-35M

| MODEL | Continuous Duty (Amps) | ICS* (Amps) | Size (IN) H x W x D | Shipping Wt. (lbs.) |
|--------|---------------------------|----------------|------------------------|------------------------|
| RM-12A | 9 | 12 | 5 1/4 x 19 x 8 1/4 | 16 |
| RM-35A | 25 | 35 | 5 1/4 x 19 x 12 1/2 | 38 |
| RM-50A | 37 | 50 | 5 1/4 x 19 x 12 1/2 | 50 |
| RM-60A | 50 | 55 | 7 x 19 x 12 1/2 | 60 |

- 19" RACK MOUNT POWER SUPPLIES

- Separate Volt and Amp Meters

RS-A SERIES



MODEL RS-7A

| MODEL | Colors Gray Black | Continuous Duty (Amps) | ICS* (Amps) | Size (IN) H x W x D | Shipping Wt. (lbs.) |
|--------|----------------------|---------------------------|----------------|------------------------|------------------------|
| RS-3A | • • | 2.5 | 3 | 3 x 4 1/4 x 5 3/4 | 4 |
| RS-4A | • • | 3 | 4 | 3 3/4 x 6 1/2 x 9 | 5 |
| RS-5A | • • | 4 | 5 | 3 1/2 x 6 1/2 x 7 1/4 | 7 |
| RS-7A | • • | 5 | 7 | 3 3/4 x 6 1/2 x 9 | 9 |
| RS-7B | • • | 5 | 7 | 4 x 7 1/2 x 10 3/4 | 10 |
| RS-10A | • • | 7.5 | 10 | 4 x 7 1/2 x 10 3/4 | 11 |
| RS-12A | • • | 9 | 12 | 4 1/2 x 8 x 9 | 13 |
| RS-12B | • • | 9 | 12 | 4 x 7 1/2 x 10 3/4 | 13 |
| RS-20A | • • | 16 | 20 | 5 x 9 x 10 1/2 | 18 |
| RS-35A | • • | 25 | 35 | 5 x 11 x 11 | 27 |
| RS-50A | • • | 37 | 50 | 6 x 13 3/4 x 11 | 46 |

RS-M SERIES



MODEL RS-35M

| MODEL | Continuous Duty (Amps) | ICS* (Amps) | Size (IN) H x W x D | Shipping Wt. (lbs.) |
|--------|---------------------------|----------------|------------------------|------------------------|
| RS-12M | 9 | 12 | 4 1/2 x 8 x 9 | 13 |
| RS-20M | 16 | 20 | 5 x 9 x 10 1/2 | 18 |
| RS-35M | 25 | 35 | 5 x 11 x 11 | 27 |
| RS-50M | 37 | 50 | 6 x 13 3/4 x 11 | 46 |

- Switchable volt and Amp meter

- Separate volt and Amp meters

VS-M AND VRM-M SERIES



MODEL VS-35M

- Separate Volt and Amp Meters • Output Voltage adjustable from 2-15 volts • Current limit adjustable from 1.5 amps to Full Load

| MODEL | Continuous Duty (Amps) | ICS* (Amps) | Size (IN) H x W x D | Shipping Wt. (lbs.) |
|--------|--------------------------------|----------------|------------------------|------------------------|
| VS-12M | 9 @ 13.8VDC 5 @ 10VDC 2 @ 5VDC | 12 @ 13.8V | 4 1/2 x 8 x 9 | 13 |
| VS-20M | 16 9 4 | 20 | 5 x 9 x 10 1/2 | 20 |
| VS-35M | 25 15 7 | 35 | 5 x 11 x 11 | 29 |
| VS-50M | 37 22 10 | 50 | 6 x 13 3/4 x 11 | 46 |

- Variable rack mount power supplies

| | | | | | | |
|---------|----|----|----|----|---------------------|----|
| VRM-35M | 25 | 15 | 7 | 35 | 5 1/4 x 19 x 12 1/2 | 38 |
| VRM-50M | 37 | 22 | 10 | 50 | 5 1/4 x 19 x 12 1/2 | 50 |

RS-S SERIES



MODEL RS-12S

| MODEL | Colors Gray Black | Continuous Duty (Amps) | ICS* Amps | Size (IN) H x W x D | Shipping Wt. (lbs.) |
|--------|----------------------|---------------------------|--------------|------------------------|------------------------|
| RS-7S | • • | 5 | 7 | 4 x 7 1/2 x 10 3/4 | 10 |
| RS-10S | • • | 7.5 | 10 | 4 x 7 1/2 x 10 3/4 | 12 |
| RS-12S | • • | 9 | 12 | 4 1/2 x 8 x 9 | 13 |
| RS-20S | • • | 16 | 20 | 5 x 9 x 10 1/2 | 18 |

- Built in speaker

Wide Dynamic Range and Low Distortion – The Key to Superior HF Data Communications

- Dynamic Range > 75 dB
- 400 to 4000 Hz
- BW Matched to Baud Rate
- BER < 1×10^{-5} for S/N = 0 dB
- 10 to 1200 Baud
- Linear Phase Filters



ST-8000 HF Modem

Real HF radio teleprinter signals exhibit heavy fading and distortion, requirements that cannot be measured by standard constant amplitude BER and distortion test procedures. In designing the ST-8000, HAL has gone the extra step beyond traditional test and design. Our noise floor is at -65 dBm, not at -30 dBm as on other units, an extra 35 dB gain margin to handle fading. Filters in the ST-8000 are all of linear-phase design to give minimum pulse

distortion, not sharp-skirted filters with high phase distortion. All signal processing is done at the input tone frequency; heterodyning is NOT used. This avoids distortion due to frequency conversion or introduced by abnormally high or low filter Q's. Bandwidths of the input, Mark/Space channels, and post-detection filters are all computed and set for the baud rate you select, from 10 to 1200 baud. Other standard features of the ST-8000 include:

- 8 Programmable Memories
- Set frequencies in 1 Hz steps
- Adjustable Print Squelch
- Phase-continuous TX Tones
- Split or Transceive TX/RX
- CRT Tuning Indicator
- RS-232C, MIL-188C, or TTL Data
- 8, 600, or 10K Audio Input
- Signal Regeneration
- Variable Threshold Diversity
- RS-232 Remote Control I/O
- 100-130/200-250 VAC, 44-440 Hz
- AM or FM Signal Processing
- 32 steps of M/S filter BW
- Mark or Space-Only Detection
- Digital Multipath Correction
- FDX or HDX with Echo
- Spectra-Tune and X-Y Display
- Transmitter PTT Relay
- 8 or 600 Ohm Audio Output
- Code and Speed Conversion
- Signal Amplitude Squelch
- Receive Clock Recovery
- 3.5" High Rack Mounting

Write or call for complete ST-8000 specifications.



HAL Communications Corp.

Government Products Division
Post Office Box 365
Urbana, Illinois 61801
(217) 367-7373

VERSATILITY PLUS +



L.L. Grace introduces our latest product, the **DSP-12 Multi-Mode Communications Controller**. The **DSP-12** is a user programmable, digital signal processing (DSP) based communications controller.

FEATURES

- Multi-tasking operating system built in
- PC-compatible (V40) architecture allows development of custom applications using normal PC development tools and languages
- Motorola DSP56001 DSP processor
- Serial interface speeds from 110 to 19200 bps
- Optional 8-channel A-to-D & DAC for voice and telemetry applications
- 12-bit conversion architecture
- V40 source code and schematics available
- RAM expandable to one megabyte. Useable for mailbox feature, voice mail and development
- EPROM expandable to 384k bytes
- Low power requirements: 10-15vdc, 750ma
- 3 analog radio connectors. RX & TX can be split in any combination. Programmable tuning outputs are available on each connector
- Many modems available in the basic unit, including Packet, RTTY, ASCII, and PSK modems for high speed packet and satellite work
- Both V40 and DSP programs can be down-line-loaded from your PC or a bulletin board. You can participate in new development!
- Built in packet mailbox
- V40 and DSP debuggers built in
- Open programming architecture
- Free software upgrades
- Low cost unit
- Room for future growth

APPLICATIONS

- HF Packet
- HF RTTY & ASCII, including inverted mark/space and custom-split applications
- VHF Packet
- 400bps PSK (satellite telemetry)
- 1200bps PSK (satellite & terrestrial packet)
- V26.B 2400bps packet
- 9600bps direct FSK (UO-14)
- Morse Code

CUSTOM APPLICATIONS

- Voice compression
- Telemetry acquisition
- Message Store-and-Forward
- Voice Mail

COMING ATTRACTIONS

(Remember, software upgrades are free!)

- WEFAX and SSTV demodulators
- NAVTEX
- AMTOR and SITOR
- Multi-tone Modems
- ARINC ACARS

Commercial inquiries are welcomed. We offer rapid prototyping of custom commercial, civil, and government applications including intelligent radio, wireline, and telephone modems.

| | |
|---|-----------|
| DSP-12 Multi-mode Communications Controller | \$ 595.00 |
| One Megabyte RAM Expansion Option | 149.00 |
| Date/Time Clock Backup Option | 29.00 |
| 8-Channel A-To-D Telemetry/Experimentation Option | 49.00 |
| Wall-Mount Power Supply for DSP-12 (110 vac) | 19.00 |

We accept MasterCard & VISA and can ship C.O.D. within the USA. All orders must be paid in US Dollars. Shipping & Handling: \$5 (\$20 International).

L. L. Grace Communications Products, Inc.

41 Acadia Drive, Voorhees, NJ 08043, USA

Telephone: (609) 751-1018

FAX: (609) 751-9705

Compuserve: 72677,1107

1/91

L. L. Grace also manufactures the Kansas City Tracker family of satellite antenna aiming systems. Call or write for more information.

THE QUAD ANTENNA: RECTANGULAR AND SQUARE LOOPS

Design and performance data for any square, rectangular, or diamond loop

The classic quad is made from a pair of square loops. The usual feedpoint for these is at the bottom center, and occasionally the side center. Some variations change from a square to a rectangular shape. A more common variation rotates the square by 45 degrees, making a diamond. Again, the feed is usually at the bottom point of the diamond, less commonly at the side. "Squashed" diamonds are often advertised, but most are really fat dipoles rather than quad loops.

Notes on the quad literature

There's a lot of Amateur literature on quad loops used both alone and in arrays. In contrast, scientific and engineering material is sparse. The only theoretical studies I've found are King¹ and Prasad². King's study places a generator at each corner of the loop, allowing a set of four independent currents using symmetrical components. The theory is complex; the only practical usable result is that a first approximation of the current distribution is given by its distribution on a transmission line, as for the circular loop. As a consequence, the tables of circular loop admittance, or Storer's curves³, can be used as approxima-

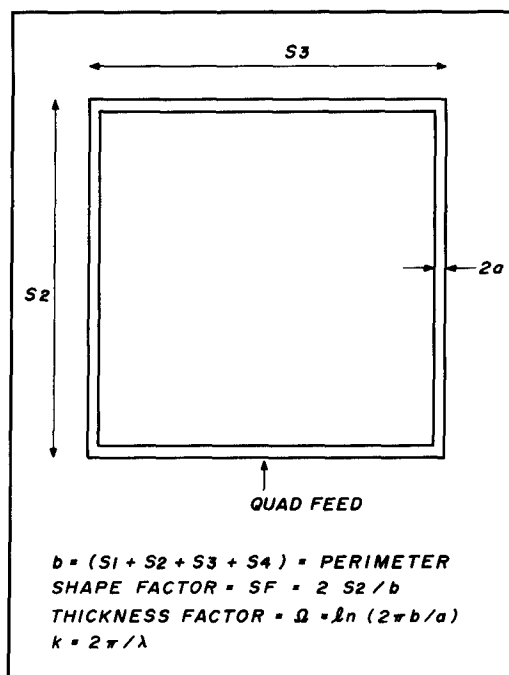


Figure 1. Geometry and nomenclature of a quad loop. The circular loop circumference is redefined to be the perimeter of the loop. The quantity kb is the perimeter in wavelengths, and is also, more generally, the conductor length. Shape factor is defined in terms of a rectangle, but can be used for any regular figure.

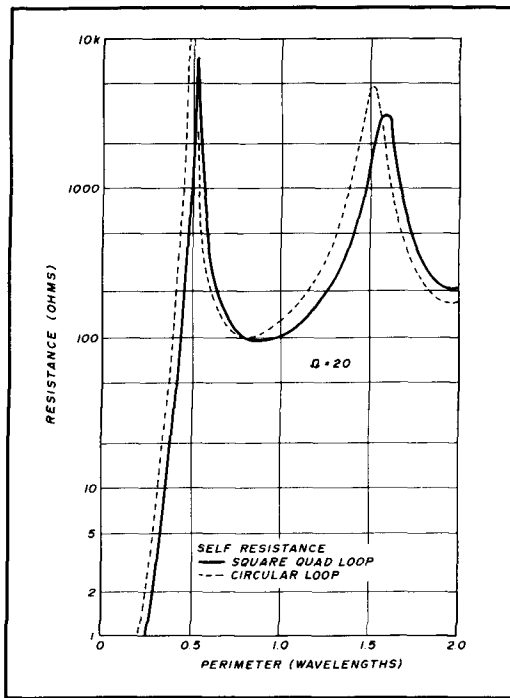


Figure 2. Self-resistance of a square quad loop. The self or driving-point resistance is shown as a function of perimeter for a thickness factor of 20. The circular loop curve is for comparison. See also Figures 4A and 9A of Reference 6.

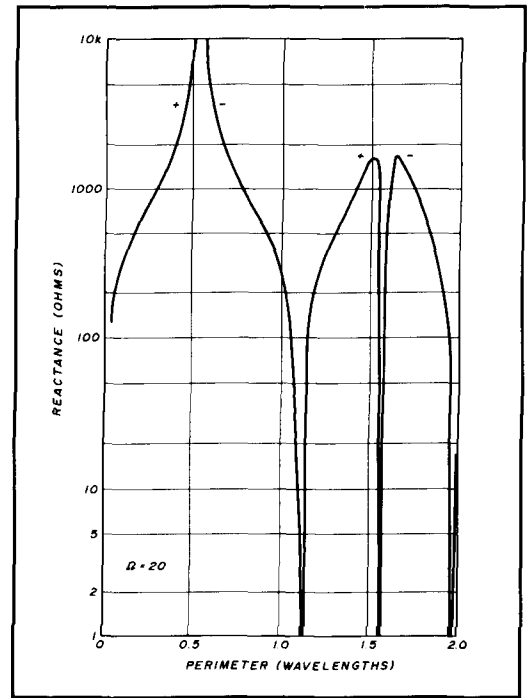


Figure 3. Self-reactance of a square quad loop. Shown is the self or driving-point reactance of a quad loop as a function of perimeter for a thickness factor of 20. Compare this with Figures 4B and 9B of Reference 6.

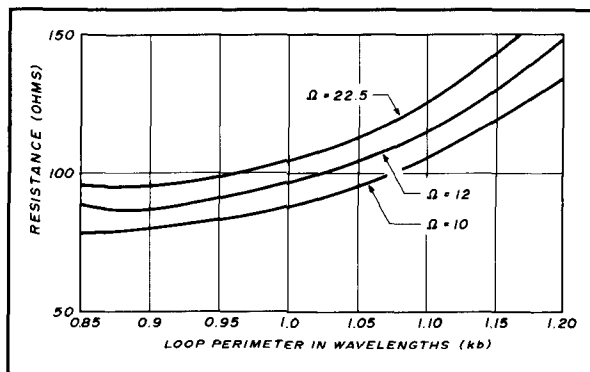


Figure 4. Self-resistance of a square quad loop near resonance. Self-resistance is plotted against perimeter for three values of thickness factor. See also Figure 5.

tions for all quad loops. The approximation will be better for square loops than for markedly rectangular ones. Diamond and square loops are identical to this degree of approximation.

Kennedy⁴ has reported measurements for thick conductors, typically $\omega = 11$. Feed impedances and current distributions are given for a limited number of conditions. The measurements confirm the close relationship between circular and square loops.

Orr⁵ gives the best summary of Amateur findings. His work mainly concerns the quad array of loops and gives estimates of size, performance, feed impedance, and con-

struction details. Almost all other Amateur material relates to construction, with occasional reports of measurements of drive impedances and performance.

Quad loop literature reflects a lack of useful theoretical analysis. The material which follows is intended to correct this, at least to the extent that full design data is available for all common quad types and for a number of the less popular ones.

I used the MININEC analysis program* to obtain data for a selected family of loops. The resulting material was organized into a format I believe to be both useful and explanatory.

MININEC gives approximate answers. The accuracy of the data in this section should be sufficient for any practical purpose. Analyses have been made with a total of 16 segment divisions of the loop perimeter. For the most important data, this is also 16 segments per wavelength. The smallest segmentation is 8 per wavelength, usually sufficient to give 10 percent accuracy.

Quad loop geometry

The general geometry and nomenclature for this loop family is shown in Figure 1.

*Copies of MININEC are available from CQ's Ham Radio Bookstore for \$39.95. Ask for "Practical Antenna Design and Analysis," by W4MB.

The previous nomenclature of a = conductor radius is retained. The perimeter (analogous to circumference and denoted by b) is used to define the conductor thickness factor, ω . New quantities introduced are: s = side length and sf = shape factor (defined as twice the length of a vertical side divided by the perimeter). This factor is 0.5 for a square loop, zero for a horizontal folded dipole, and 1.0 for a vertical transmission line, all fed at the bottom center.

Square loop drive impedance

The self- or drive resistance of a typical square loop is shown in **Figure 2** for wavelengths from 0.05 to 2.0. The theoretical curve for a circular loop is shown for comparison.

The general pattern of these two types is the same, with parallel resonance points at 0.5 and 1.5 wavelengths, and series resonant minima at 1.0 and 2.0 wavelengths. There's appreciable difference in the resonant frequencies and some difference in the magnitudes.

Figure 3 shows the corresponding reactance curve; the comparison curve has been omitted for clarity. Circular data was given in a previous article⁶ Comparison shows nearly identical curve shape and close correspondence in magnitude, but appreciable shift in resonant frequency with the square

loop resonance occurring at a larger loop size.

Remember that this pair of calculated values results from two different theories, so some of the difference may be due to approximation errors. This factor appears to be negligible for practical purposes. The shift in resonant frequency is close to that measured by Kennedy⁴ and in the same direction but greater than that implied by Orr⁵ However, Orr's values are to secure zero reactance in the quad, rather than in an isolated loop. This shift will be discussed later.

Table 1 summarizes the source data for the entire family of square and quad loops for the size range from $kb = 0.05$ to $kb = 2.0$, and for selected thickness factors of $\omega = 10$ to $\omega = 22.5$. (Similar data for rectangular and diamond loops are discussed later and given in **Table 2**.) Use the nearest table value for estimations. Interpolate for exact perimeter and thickness for accuracy within a few percent. You'll need the values of this table for calculation of array performance.

I've mentioned using Storer's curves³ as approximations for any loop. You can also use **Table 1** of this article. If you need better accuracy, I suggest you do the following: measure the resonant frequency of the design loop, or a scale model. Use the percentage offset of the desired frequency to

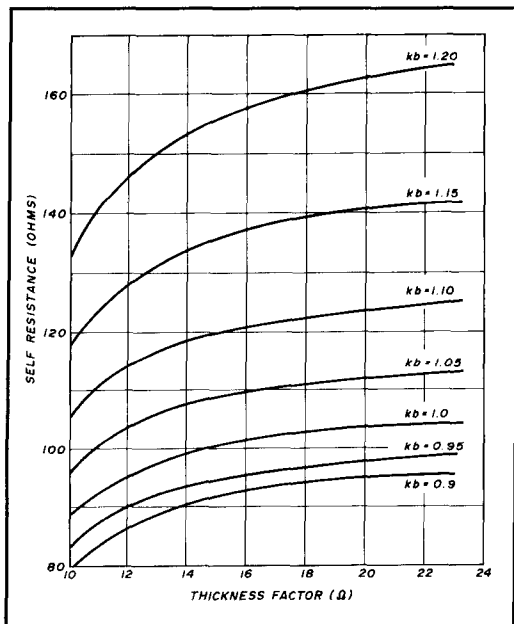


Figure 5. Self-resistance of a square quad loop near resonance. Here self-resistance is plotted against the thickness factor, with selected values of perimeter as the curve parameter. For a typical one-wavelength HF loop, the self-resistance is about 105 ohms.

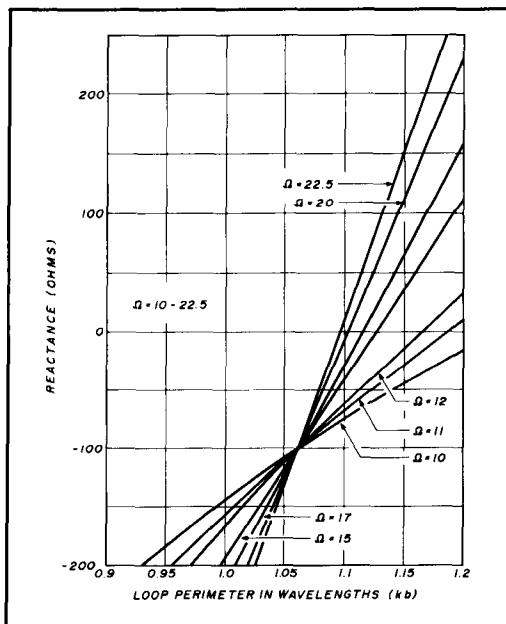


Figure 6. Self-reactance of a square quad loop near resonance. Self-reactance is plotted against perimeter, with selected values of thickness factor as a parameter. Resonance is indicated by the zero reactance intercept. Compare with *Figures 5B and 10 of Reference 6*.

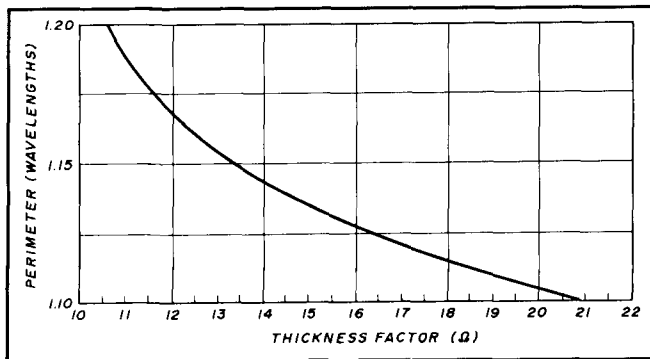


Figure 7. Resonant frequency of a square quad loop. Resonant point data from Figure 6 is plotted against thickness factor. Compare with Figures 6 and 11 of Reference 6.

enter the table as a percent change from its corresponding resonance. If you use a scale model, don't forget to correct the resonant frequency for the change in wire thickness factor.

Drive impedance near resonance

The normal use of loops is at or close to

the first series-resonance point, with the circumference close to 1 wavelength. Figure 4 shows the self-resistance for kb between 0.85 and 1.2, with the thickness factor as the parameter. In Figure 5 the data is plotted against thickness factor, with perimeter as the parameter.

Typical self-supporting VHF/UHF loops have thickness factors in the range of 10 to 12. For these, the drive resistance can be taken as 100 ohms. HF loops with wire conductors have a drive resistance close to 110 ohms.

Figure 6 shows the drive reactance versus perimeter, with thickness factor (ω) as the parameter. As with the other loops and with dipoles, there's a point where reactance is independent of thickness factor (in this case a value of -100 ohms at a perimeter of 1.063). The reactance at this point of crossover is essentially the same as for the circular and octagonal loops, but the common point occurs at a perimeter which is about 5 and 3 percent larger, respectively.

The zero-reactance point on these curves

| kb | ADMITTANCE OF SQUARE QUAD LOOPS | | | | | | | |
|------|---------------------------------|-----------------|-----------------|-----------------|-----------------|-----------------|-----------------|--|
| | Omega=10 | Omega=11 | Omega=12 | Omega=15 | Omega=17 | Omega=20 | Omega=22.5 | |
| .05 | .0003-j19.3072 | .0002-j16.6672 | .0002-j14.6462 | .0001-j10.7208 | .0001-j 9.1118 | .0001-j 7.4230 | .0001-j 6.4038 | |
| .10 | .0012-j 9.4046 | .0009-j 8.1273 | .0007-j 7.1448 | .0004-j 5.2355 | .0003-j 4.4492 | .0002-j 3.6260 | .0001-j 3.1286 | |
| .15 | .0028-j 5.9916 | .0021-j 5.1859 | .0016-j 4.5637 | .0008-j 3.3496 | .0006-j 2.8481 | .0004-j 2.2222 | .0003-j 2.0044 | |
| .20 | .0053-j 4.1984 | .0039-j 3.6421 | .0031-j 3.2100 | .0016-j 2.3586 | .0012-j 2.0101 | .0008-j 1.6403 | .0006-j 1.4164 | |
| .25 | .0089-j 3.0489 | .0066-j 2.6542 | .0052-j 2.3446 | .0028-j 1.7290 | .0020-j 1.4754 | .0013-j 1.2053 | .0010-j 1.0416 | |
| .30 | .0139-j 2.2174 | .0105-j 1.9405 | .0081-j 1.7200 | .0044-j 1.2753 | .0032-j 1.0902 | .0021-j .8922 | .0016-j .7718 | |
| .35 | .0211-j 1.5629 | .0159-j 1.3794 | .0123-j 1.2294 | .0067-j .9194 | .0049-j .7880 | .0033-j .6467 | .0024-j .5602 | |
| .40 | .0310-j 1.0138 | .0234-j .9090 | .0182-j .8182 | .0010-j .6210 | .0073-j .5349 | .0049-j .4410 | .0037-j .3830 | |
| .45 | .0450-j .5289 | .0341-j .4936 | .0267-j .4550 | .0146-j .3574 | .0107-j .3111 | .0072-j .2590 | .0054-j .2261 | |
| .50 | .0648-j .0819 | .0492-j .1103 | .0386-j .1195 | .0212-j .1134 | .0159-j .1046 | .0104-j .0902 | .0078-j .0805 | |
| .55 | .0929+j .3458 | .0708+j .2574 | .0556+j .2029 | .0308+j .1222 | .0232+j .0986 | .0152+j .0733 | .0114+j .0606 | |
| .60 | .1330+j .7689 | .1018+j .6225 | .0802+j .5241 | .0447+j .3584 | .0338+j .3030 | .0222+j .2381 | .0167+j .2032 | |
| .65 | .1910+j 1.1999 | .1469+j .9969 | .1162+j .8552 | .0653+j .6043 | .0495+j .5167 | .0326+j .4112 | .0246+j .3534 | |
| .70 | .2758+j 1.6509 | .2136+j 1.3925 | .1699+j 1.2077 | .0965+j .7011 | .0734+j .7488 | .0487+j .6005 | .0368+j .5182 | |
| .75 | .4013+j 2.1338 | .3138+j 1.8221 | .2516+j 1.5947 | .1450+j 1.1683 | .1111+j 1.0114 | .0742+j .8168 | .0563+j .7075 | |
| .80 | .5901+j 2.6601 | .4678+j 2.3001 | .3791+j 2.0323 | .2234+j 1.5163 | .1725+j 1.3215 | .1164+j 1.0758 | .0890+j .9361 | |
| .85 | .8785+j 3.2381 | .7100+j 2.8410 | .5846+j 2.5395 | .3559+j 1.9394 | .2784+j 1.7053 | .1910+j 1.4036 | .1473+j 1.2288 | |
| .90 | 1.3249+j 3.8645 | 1.1014+j 3.4539 | .9284+j 3.1355 | .5943+j 2.4746 | .4745+j 2.2045 | .3341+j 1.8451 | .2616+j 1.6308 | |
| .95 | 2.0181+j 4.5023 | 1.7474+j 4.1211 | 1.5258+j 3.8212 | 1.0584+j 3.1683 | .8743+j 2.8833 | .6444+j 2.4832 | .5184+j 2.3224 | |
| 1.00 | 3.0704+j 5.0313 | 2.8132+j 4.7336 | 2.5874+j 4.5091 | 2.0445+j 4.0206 | 1.7962+j 3.7937 | 1.4464+j 3.4464 | 1.2312+j 3.2071 | |
| 1.05 | 4.5374+j 5.1725 | 4.4529+j 4.9448 | 4.3822+j 4.8006 | 4.2016+j 4.5795 | 4.1049+j 4.5118 | 3.9412+j 4.4329 | 3.8166+j 4.3878 | |
| 1.10 | 6.1843+j 4.5134 | 6.4142+j 4.0894 | 6.6583+j 3.7226 | 7.3606+j 2.6607 | 7.6932+j 1.9784 | 8.0230+j .6364 | 7.9836-j .4714 | |
| 1.15 | 7.3145+j 2.9334 | 7.5535+j 1.9410 | 7.6588+j .9708 | 7.0230-j 1.5839 | 6.1725-j 2.5952 | 4.5238-j 3.4388 | 3.4412-j 3.5373 | |
| 1.20 | 7.3452+j 1.0751 | 7.0571-j .2716 | 6.5152-j 1.3599 | 4.3811-j 2.9724 | 3.3298-j 3.1343 | 2.0751-j 2.9086 | 1.4795-j 2.6118 | |
| 1.25 | 6.5262-j .2650 | 5.7191-j 1.4586 | 4.8229-j 2.1875 | 2.6905-j 2.6998 | 1.9396-j 2.5441 | 1.1612-j 2.1500 | .8204-j 1.8685 | |
| 1.30 | 5.4653-j .9012 | 4.4419-j 1.7651 | 3.5288-j 2.1600 | 1.7991-j 2.1665 | 1.2745-j 1.9559 | .7563-j 1.5976 | .5348-j 1.3732 | |
| 1.35 | 4.5151-j 1.0379 | 3.4819-j 1.6303 | 2.6700-j 1.8329 | 1.3048-j 1.6718 | .9194-j 1.4804 | .5456-j 1.1911 | .3871-j 1.0189 | |
| 1.40 | 3.7679-j .8948 | 2.8066-j 1.3150 | 2.1086-j 1.4271 | 1.0107-j 1.2456 | .7119-j 1.0927 | .4239-j .8723 | .3019-j .7442 | |
| 1.45 | 3.2117-j .6066 | 2.3396-j .9320 | 1.7378-j 1.0115 | .8274-j .8726 | .5840-j .7622 | .3496-j .6053 | .2500-j .5151 | |
| 1.50 | 2.8138-j .2421 | 2.0226-j .5234 | 1.4945-j .6021 | .7128-j .5331 | .5052-j .4651 | .3044-j .3670 | .2187-j .3107 | |
| 1.55 | 2.5479+j .1664 | 1.8206-j .1019 | 1.3449-j .1967 | .6473-j .2100 | .4615-j .1835 | .2804-j .1413 | .2026-j .1168 | |
| 1.60 | 2.4007+j .6033 | 1.7174+j .3313 | 1.2748+j .2122 | .6242+j .1123 | .4488+j .0978 | .2757+j .0855 | .2006+j .0789 | |
| 1.65 | 2.3726+j 1.0583 | 1.7132+j .7775 | 1.2853+j .6330 | .6468+j .4483 | .4706+j .3937 | .2934+j .3270 | .2153+j .2889 | |
| 1.70 | 2.4766+j 1.5156 | 1.8235+j 1.2334 | 1.3932+j 1.0704 | .7306+j .8129 | .5404+j .7207 | .3439+j .5998 | .2553+j .5292 | |
| 1.75 | 2.7346+j 1.9425 | 2.0791+j 1.6804 | 1.6340+j 1.5170 | .9109+j 1.2186 | .6900+j 1.0965 | .4522+j .9262 | .3412+j .8226 | |
| 1.80 | 3.1633+j 2.2748 | 2.5200+j 2.0651 | 2.0633+j 1.9333 | 1.2586+j 1.6630 | .9883+j 1.5336 | .6779+j 1.3345 | .5245+j 1.2040 | |
| 1.85 | 3.7399+j 2.4113 | 3.1634+j 2.2750 | 2.7357+j 2.2081 | 1.9013+j 2.0776 | 1.5810+j 1.9955 | 1.1719+j 1.8360 | .9485+j 1.7109 | |
| 1.90 | 4.3543+j 2.2502 | 3.9263+j 2.1469 | 3.6126+j 2.1275 | 2.9731+j 2.1845 | 2.6958+j 2.2163 | 2.2861+j 2.2362 | 2.0213+j 2.2206 | |
| 1.95 | 4.8107+j 1.7858 | 4.5569+j 1.5931 | 4.4037+j 1.4994 | 4.1962+j 1.4126 | 4.1467+j 1.4018 | 4.1058+j 1.3963 | 4.0945+j 1.3938 | |
| 2.00 | 4.9481+j 1.1725 | 4.7710+j .7859 | 4.6703+j .4989 | 4.5064-j .1617 | 4.4116-j .4981 | 4.1701-j 1.0440 | 3.9178-j 1.4038 | |

Table 1. Source Data for the entire family of square quad loops for the size range from $kb = 0.05$ to $kb = 2.0$.

gives the resonant frequency of an isolated loop. This is plotted against the thickness factor in **Figure 7**. Note that the resonant perimeter approaches 1 wavelength as the conductor becomes smaller, as with a dipole. However, the direction of change is just opposite the direction of change with dipoles.

When dealing with arrays of antennas, it's often convenient to use numerical values from equations rather than from graphs. The data in **Figures 5** through **7** can be approximated by the following relationships:

resistance

$$\text{thick loop} = 100 \text{ ohms}$$

$$\text{thin loop} = 110 \text{ ohms}$$

perimeter for resonance, RP

$$RP = 1.057 + 0.24/OM + 13.57/OM$$

reactance

$$X = 100 \left(\frac{kb - RP}{RP - 1.063} \right)$$

where OM is the thickness factor, ω , RP is the perimeter at resonance, and the loop perimeter, kb, is within 20 percent of unity.

Gain of the square loop

The MININEC-calculated gain of the square loop is shown in **Figure 8**. This is the magnitude of the lobe at 90 degrees to the plane of the loop, on the axis of symmetry. The comparison curve shows the gain below that of a circular loop, as expected from area considerations. The gain increases with size, up to about 1.4 wavelength circumference. The gain is greater than for the corresponding dipole, by about 1.0 dB at kb = 1 and about 1.5 dB at kb = 1.4. Conductor size has a small effect on gain, as shown in **Figure 9**. This is not of practical significance.

From the viewpoint of gain, better performance is obtained by operating with kb above unity — that is, above resonance. As for the circular loop, kb = 1.2 appears to be a good compromise value. As for the circular loop, wideband operation is feasible for at least the range from one-half to twice the nominal design frequency. You'll need transmission line that will withstand high VSWR without puncture or excessive loss. Open wire, ladder twin lead, or Teflon™-insulated coax will work. Solid-state transmitters, in particular, will need a matchbox.

Current distribution on a square loop

Figure 10 shows a typical current distribution for kb = 1.0 and a thickness factor of 17.8. The maximum current is larger for

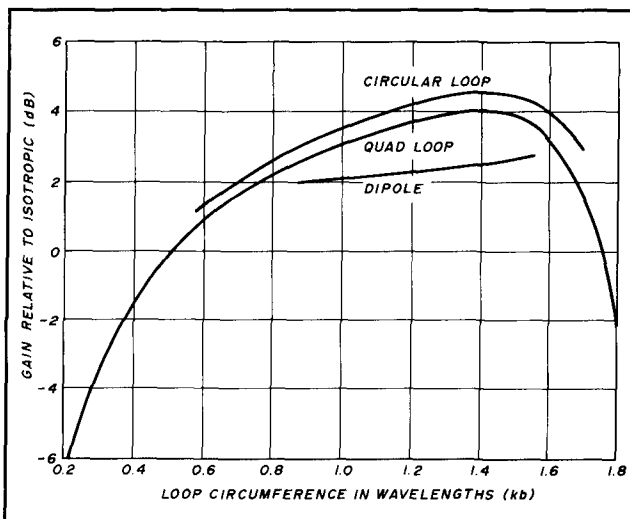


Figure 8. The gain of a square quad loop as a function of circumference. The gain of a circular loop and a folded dipole are shown for comparison. The gain is for the lobe at right angles to the plane of the loop, along the line of symmetry. The differences are partly due to area change and partly to differences in separation of the high-current points.

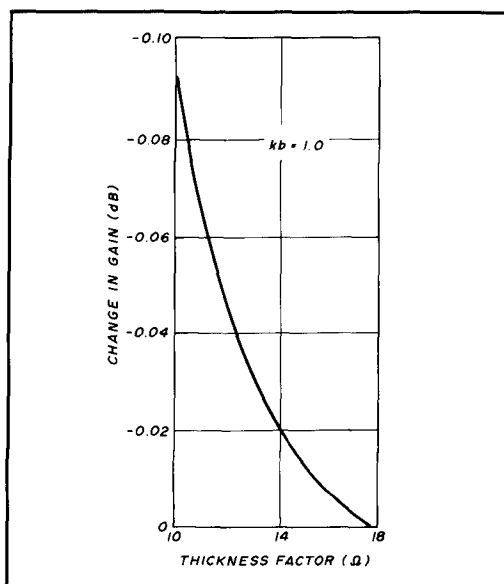


Figure 9. Effect of thickness on loop gain. The small effect appears to be due to the effective reduction in area by conductor blockage. The change is negligible in a practical sense.

the square loop, reflecting its lower impedance, compared with the distribution for an octagon⁶. The general shape of the magnitude and angle curves is the same. See **Reference 4** or **7** for the overall agreement with circular loops.

Radiation patterns of square loops

Figure 11 shows the horizontally polarized radiation pattern of a square loop at kb

| kb | Admittances of Rectangular and Diamond Loops | | | | | | | | | | | |
|------|--|---------|-----------|---------|-----------|--------|----------|--------|----------|--------|----------|--------|
| | SF=.875 | | SF=.75 | | SF=.625 | | SF=.25 | | DIAMOND | | | |
| .50 | .0019-j | .1672 | .0057-j | .0911 | .0099-j | .0910 | .0162-j | .1176 | .0174-j | .1563 | .0125-j | .0690 |
| .55 | .0025+j | .0343 | .0078+j | .1021 | .0138+j | .0963 | .0244+j | .0720 | .0276+j | .0399 | .0181+j | .1170 |
| .60 | .0032+j | .2340 | .0106+j | .2950 | .0194+j | .2839 | .0371+j | .2646 | .0438+j | .2414 | .0261+j | .3028 |
| .65 | .0042+j | .4398 | .0145+j | .4948 | .0275+j | .4790 | .0568+j | .4685 | .0705+j | .4581 | .0381+j | .4954 |
| .70 | .0056+j | .6602 | .0200+j | .7101 | .0394+j | .6898 | .0882+j | .6937 | .1155+j | .7023 | .0563+j | .7029 |
| .75 | .0075+j | .9063 | .0283+j | .9517 | .0575+j | .9270 | .1403+j | .9536 | .1948+j | .9911 | .0851+j | .9358 |
| .80 | .1167+j | .9418 | .0402+j | 1.2768 | .0917+j | 1.2432 | .2373+j | 1.2897 | .3467+j | 1.3619 | .1388+j | 1.2413 |
| .85 | .1433+j | 1.3919 | .0668+j | 1.6466 | .1431+j | 1.6029 | .4055+j | 1.6855 | .6385+j | 1.8071 | .2246+j | 1.5856 |
| .90 | .1860+j | .9827 | .1079+j | 2.1433 | .2367+j | 2.0810 | .7357+j | 2.1917 | 1.2495+j | 2.3195 | .3854+j | 2.0338 |
| .95 | .2645+j | 2.8217 | .1918+j | 2.8785 | .4281+j | 2.2772 | 1.4343+j | 2.7996 | 2.4942+j | 2.5910 | .7198+j | 2.6491 |
| 1.00 | .4381+j | 4.1590 | .4040+j | 4.1423 | .8976+j | 3.8906 | 2.9217+j | 3.1807 | 4.1113+j | 1.5678 | 1.5173+j | 3.4988 |
| 1.05 | .9504+j | 6.7131 | 1.2119+j | 6.9670 | 2.4643+j | 5.9364 | 5.0234+j | 1.9466 | 4.1101-j | .5127 | 3.6399+j | 4.2287 |
| 1.10 | 3.6996+j | 13.5819 | 10.7764+j | 17.3337 | 10.1740+j | 7.3369 | 4.9892-j | .8090 | 2.9074-j | 1.4354 | 7.0262+j | 1.7086 |
| 1.15 | 63.7356+j | 13.8577 | 6.6962-j | 13.8007 | 9.2204-j | 6.5827 | 3.3438-j | 1.9172 | 1.9756-j | 1.4644 | 5.1970-j | 2.4017 |
| 1.20 | 3.8913-j | 14.7580 | 1.1239-j | 5.7745 | 2.6748-j | 5.0409 | 2.1680-j | 1.8629 | 1.4227-j | 1.2545 | 2.6759-j | 2.5939 |
| 1.25 | 1.2454-j | 8.0592 | .4519-j | 3.3796 | 1.1838-j | 3.2802 | 1.5090-j | 1.5570 | 1.0922-j | 1.0140 | 1.5434-j | 1.9966 |
| 1.30 | .6766-j | 5.5879 | .2506-j | 2.2318 | .6769-j | 2.2656 | 1.1296-j | 1.2434 | .8842-j | .7887 | 1.0138-j | 1.4692 |
| 1.35 | .4644-j | 4.2971 | .1658-j | 1.5307 | .4499-j | 1.6085 | .8988-j | .9631 | .7466-j | .5834 | .7320-j | 1.0599 |
| 1.40 | .3621-j | 3.4947 | .1241-j | 1.0342 | .3314-j | 1.1318 | .7465-j | .7142 | .6520-j | .3936 | .5652-j | .7353 |
| 1.45 | .3051-j | 2.9405 | .1030-j | .6444 | .2653-j | .7527 | .6462-j | .4871 | .5857-j | .2132 | .4588-j | .6668 |
| 1.50 | .2702-j | 2.5298 | .0942-j | .3117 | .2296-j | .4272 | .5797-j | .2723 | .5394-j | .0361 | .3871-j | .2352 |

Table 2. Source data for rectangular and diamond loops.

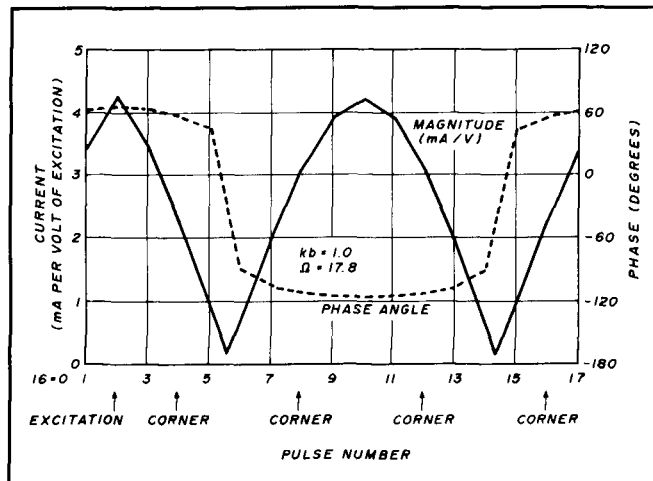


Figure 10. Current distribution on a square quad loop. Comparison with Figure 15 and published data on circular loops shows near identity in distribution, with some change in magnitude, reflecting the difference in drive impedance.

= 1.0 in the horizontal plane. The beam width is just less than 90 degrees. The pattern is identical in shape to that of the corresponding octagon, but the gain is slightly less — 3.076 dB compared with 3.397 dB.

Figure 12 shows the vertically polarized component in the horizontal plane. The lobes are about 18 dB smaller than those in the H-lobe, and somewhat larger than for the octagon because of the relatively longer wire component in the vertical direction. This component is essentially ignored in the literature; its importance is yet to be determined.

Figure 13 shows the total radiation in the H-plane. Because of the vertically polarized

component, the front-to-side ratio is only 18 dB, compared with the theoretical infinite value for a dipole⁸

Figure 14 shows the total radiation in the plane of the loop, with zenith at the right. Note that the reference is the maximum lobe size in this plane, in the direction of the feedpoint. The zenith lobe is a bit smaller, reflecting the slightly smaller current in the upper part of the loop.

Figure 15 shows the pattern at right angles to the loop, in the vertical plane. Front-to-top ratio is very small, about 3 dB. The V-plane beam width is essentially 180 degrees.

There are both similarities and differences in the pattern at other frequencies. Figure 16 shows the H-component, H-plane pattern for kb = 0.5. The direction of maximum gain is not at right angles to the loop; the gain in this direction is down about 2.5 dB. The beam width is slightly less than 90 degrees.

The vertical component pattern for this plane is shown in Figure 17. The intensity of the vertically polarized component is markedly increased — only 4.3 dB below maximum gain. This is the lobe used in the usual, but smaller, direction-finding loop.

The total component pattern in the plane of the loop for kb = 0.5 is shown in Figure 18. Compared with Figure 14, the side-directed radiation has increased and the pronounced dip has disappeared. The up-and-down components are nearly the same. The differences are a consequence of the more uniform current distribution around the loop.

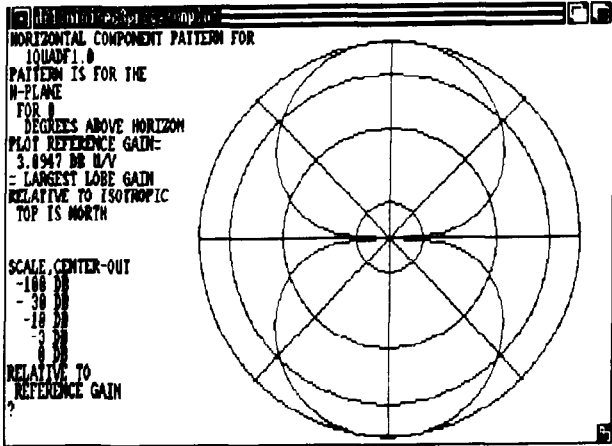


Figure 11. H-H radiation pattern for a quad loop near resonance. Showing the horizontally polarized radiation component in the horizontal plane. In this and all following patterns, the loop is vertical, fed at the bottom, and lies in the X-Z plane (from right to left in this figure). The pattern is essentially that of a magnetic dipole. See Figure 12.

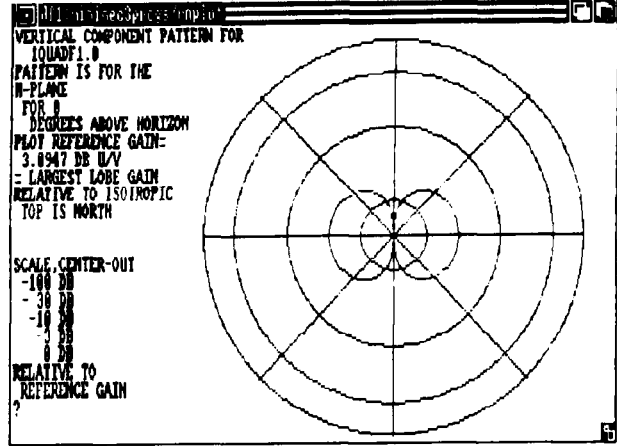


Figure 12. V-H pattern for a quad loop near resonance. Similar to Figure 11, but for the vertically polarized component. The presence of this component is a major difference from a resonant dipole. (See Figure 13).

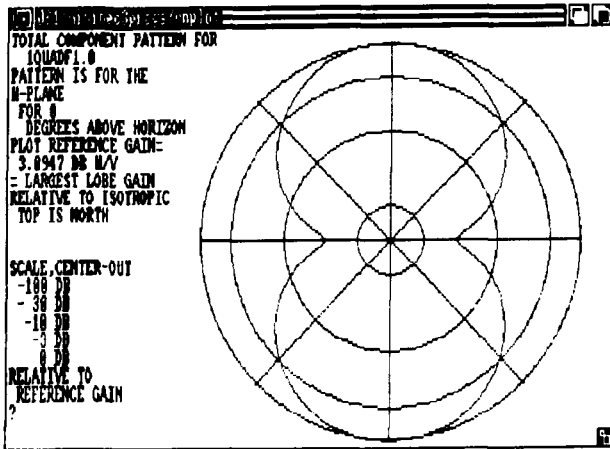


Figure 13. T-H pattern for a quad loop near resonance. Similar to Figure 11, but for the total radiation component. The effect of the vertical component shows in the radiation along the line of the loop, from right to left in the figure.

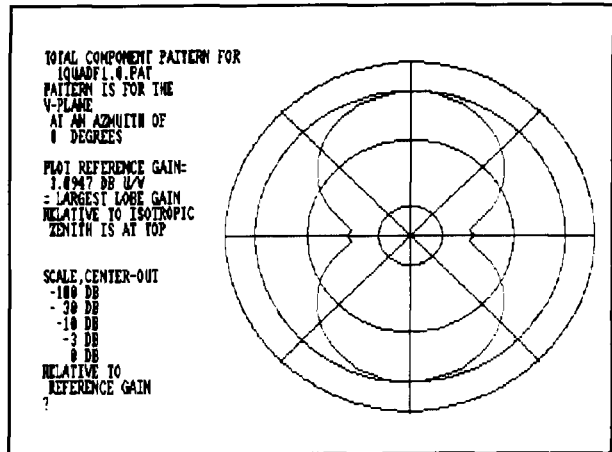


Figure 14. T-V pattern of a quad loop near resonance. The total component is shown for the vertical plane, which contains the loop. Zenith is at the right of the figure.

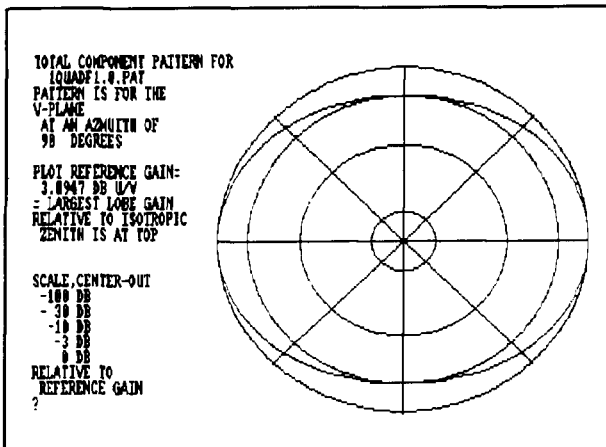


Figure 15. Orthogonal T-V pattern of a quad loop near resonance. The total component is shown for the plane at right angles to the loop. Zenith is at the right of the figure.

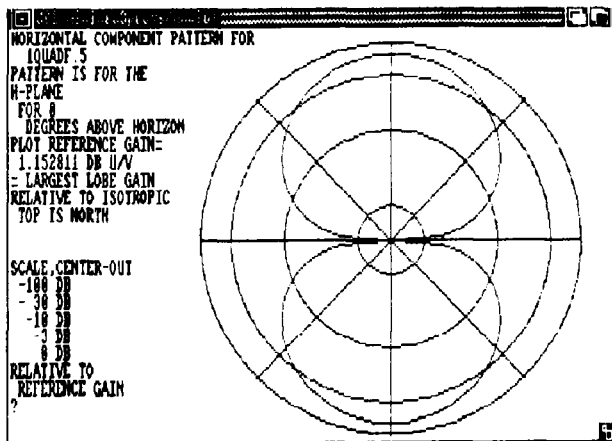


Figure 16. H-H pattern for a 0.5-wavelength quad loop. The horizontally-polarized component is shown for the horizontal plane. Compare to Figure 11.

At $kb = 1.5$, the H-component, H-plane pattern of **Figure 19** is nearly the same. The major difference is an increase in gain. The V-component pattern (**Figure 20**) has increased to about 6 dB below the main lobe. The major difference is in the plane of the loop (**Figure 21**). Because there are three points of maximum current around the loop, the pattern shows three lobes — one toward the zenith, the others at an angle of about 120 degrees. At a still higher frequency, $kb = 2.0$, the H-component in the H-plane has become small (**Figure 22**). It's about 12 dB below the main lobe. In contrast, the V-component lobe in this plane (**Figure 23**) has increased, and is only 1 dB below the maximum radiation. Note that the maximum radiation at right angles to the loop has decreased with respect to that for $kb = 1.5$.

Again, the major difference is in the plane of the loop (**Figure 24**). There are now four lobes reflecting the four current max-

ima around the loop. This multi-lobe pattern persists for all larger values of kb^9

At right angles to the loop plane the component toward the horizon becomes small, as seen in **Figure 25**. At exact resonance, the minimum would occur at the horizon, rather than below it.

Rectangular loops

Several changes occur as the shape of a square loop becomes rectangular. One is a shift of driving resistance from the 300-ohm value of a folded dipole to the zero resistance of a shorted ideal line. The MININEC-calculated pattern of change is shown in **Figure 26**. The change is not linear with shape factor, but nearly square law. The associated reactance change is also shown. At the folded dipole end (shape factor less than 0.15 for this conductor size) the

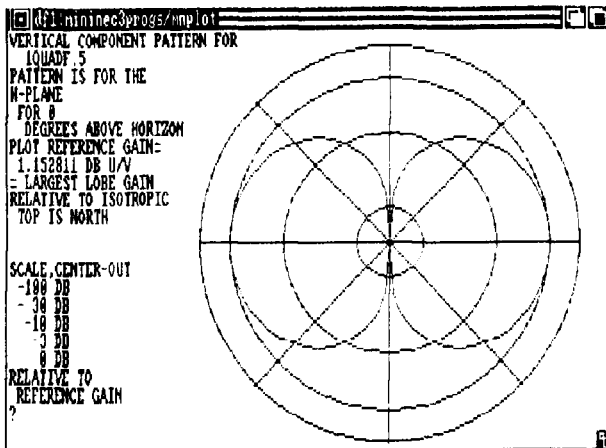


Figure 17. V-H pattern for a 0.5-wavelength quad loop. Note the growth of this component as compared to *Figure 12*.

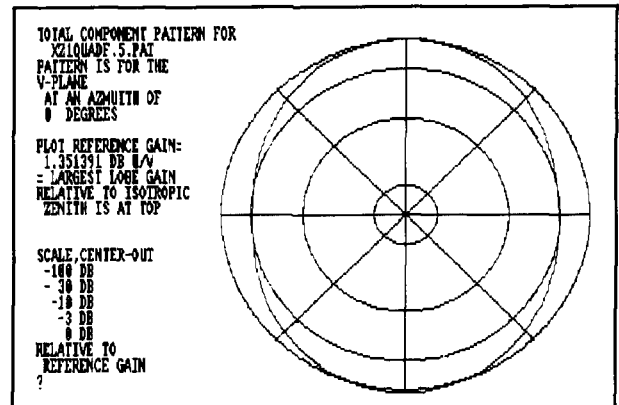


Figure 18. T-V pattern for a 0.5-wavelength quad loop. Total component pattern is in the plane of the loop. Zenith is at the right. Note the growth of the component toward the horizontal as compared to *Figure 14*.

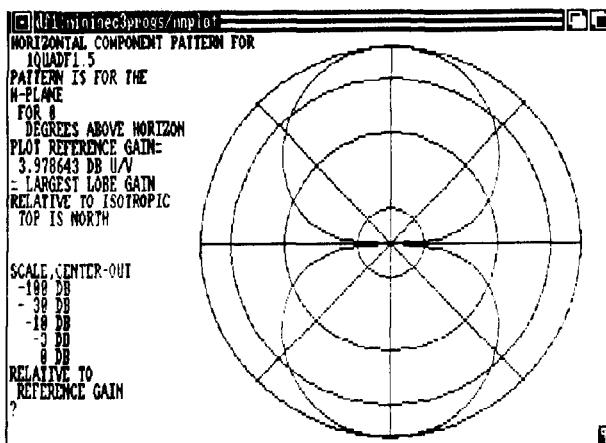


Figure 19. H-H pattern for a quad loop of 1.5-wavelength perimeter. Despite the dimension change, the pattern is essentially that of a magnetic dipole.

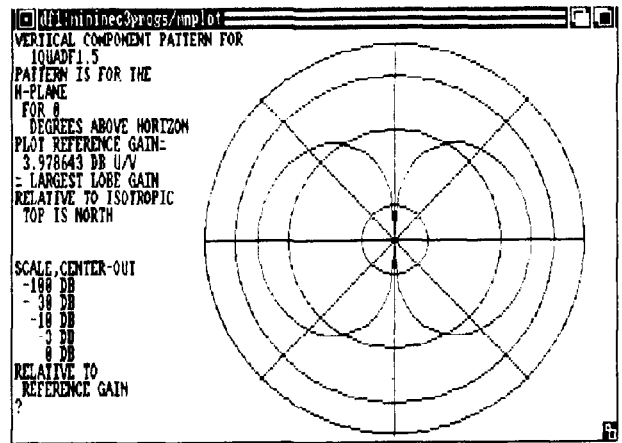


Figure 20. V-H pattern for a 1.5-wavelength loop. Compare to *Figures 12 and 17*.

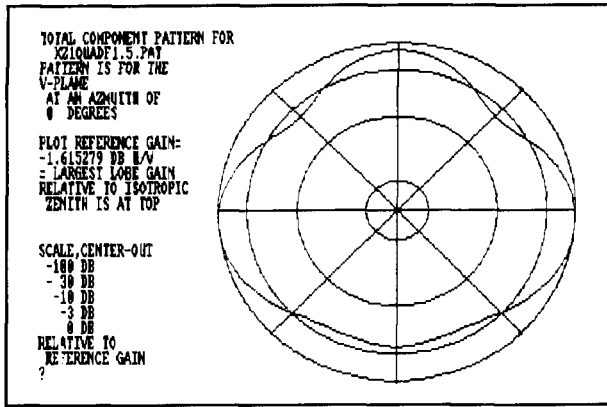


Figure 21. T-V pattern for a 1.5-wavelength loop in the plane of the loop. Zenith is at the right. The three lobes reflect the three high-current points around the loop, one being opposite the feedpoint, the other approximately 120 degrees away.

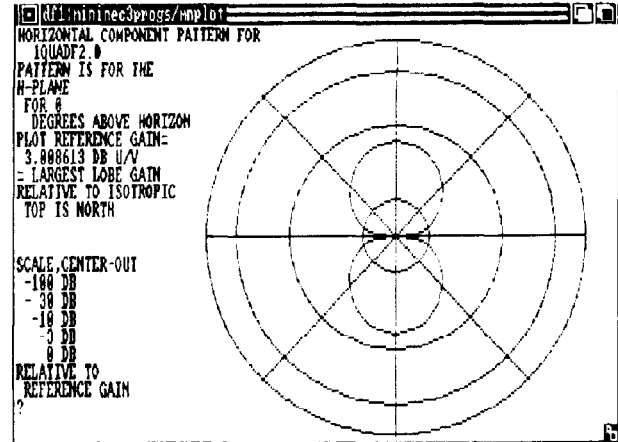


Figure 22. H-H pattern for a 2.0-wavelength loop. Note the marked decrease as compared to Figure 11.

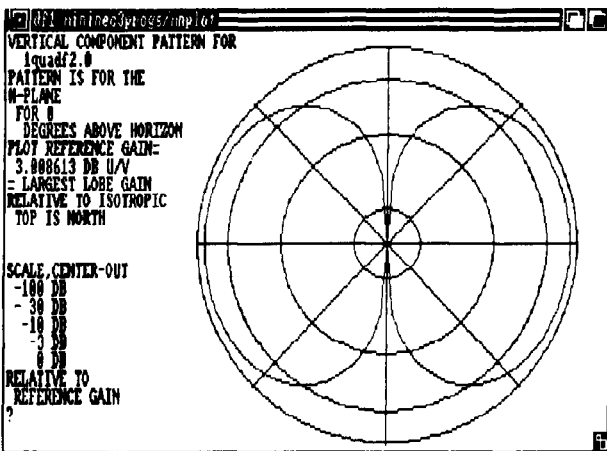


Figure 23. V-H pattern for the 2.0-wavelength loop. Note the marked increase as compared to Figure 12.

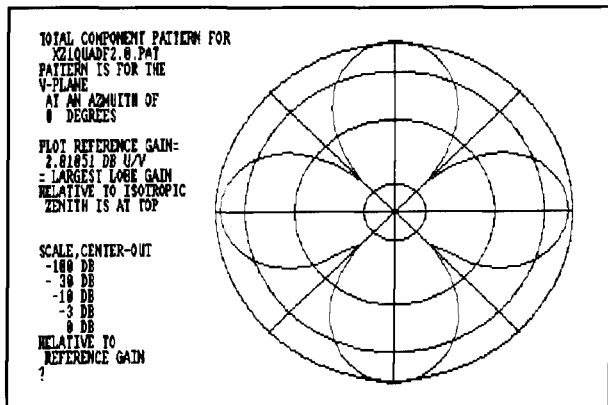


Figure 24. T-V pattern for the 2.0-wavelength loop in the plane of the loop. There are now four high-current points and four lobes. A multi-leaved pattern occurs for all higher integral values of kb .

reactance is positive, so the loop/dipole is above resonance. Dipoles and loops with small shape factors must be shortened for resonance. For shape factors greater than 0.15, a loop with perimeter $kb = 1.0$ will be below resonance. The curves are dotted for shape factors greater than 0.75 because MININEC calculation errors become large if segment lengths are too small. In the extreme, calculated values of radiation resistance may even become negative — a physical impossibility. No attempt has been made to find calculation conditions that give good results because it seems unlikely that very large shape factors will find practical use.

Gain is affected by two factors in these rectangular loops. The lower area implies lower gain, but the increased separation of the high current points implies increased gain. Figure 27 indicates that the area loss is the least important, because the gain increases to at least $sf = 0.75$.

Lawson¹⁰ estimated the gain of square

loops, considering both the separation of current points and the length of the high-current part of the loop. His calculated values are also shown in Figure 27. Agreement is reasonably good, but he ignored the

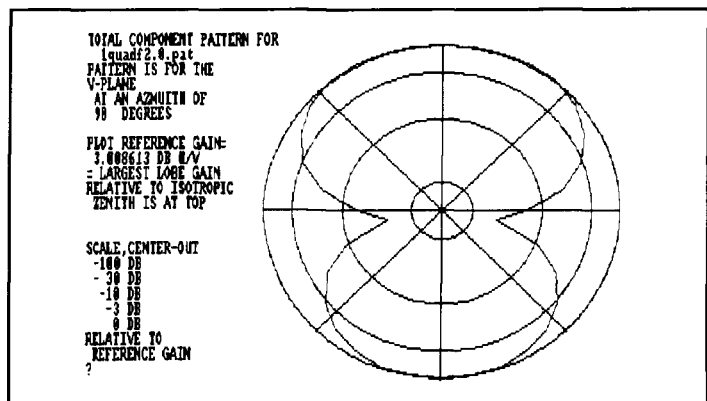


Figure 25. T-V pattern for the 2.0-wavelength loop at right angles to the loop plane. Zenith is at the right. At resonance, the minimum would be at the horizon.

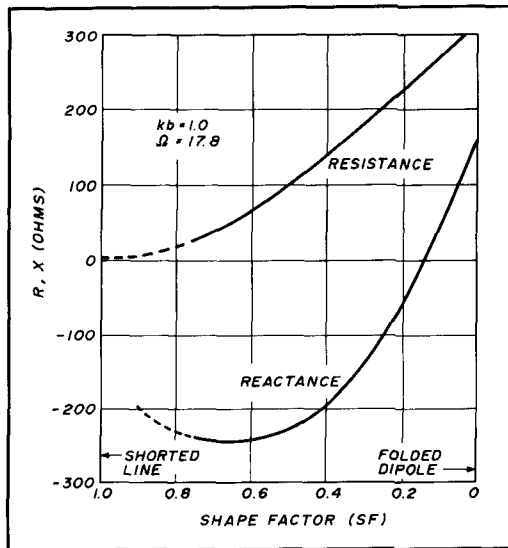


Figure 26. Self-impedance of a typical rectangular quad loop as a function of shape factor. At $sf = 1.0$, both resistance and reactance must be zero, the values for a perfect shorted transmission line. Change in resistance with conductor size would be relatively small, but reactance change would be sizable. The pattern is related to those of Figures 5 and 6.

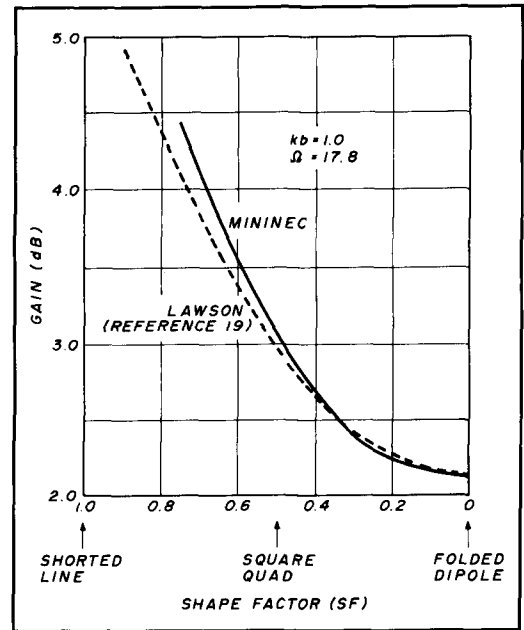


Figure 27. Gain of rectangular loops around 1.0-wavelength perimeter. The loops with high shape factor are related to the skeleton slot loop used in VHF/UHF stacked beams.

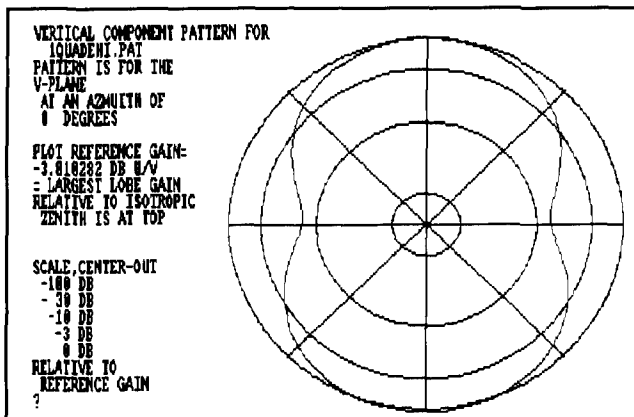


Figure 28. V-V pattern for a rectangular loop at right angles to the loop plane. With $sf = 0.75$, this is one of the skeleton-slot family. Maximum gain is toward the horizon.

vertically polarized component, so his values are smaller than the MININEC results where this component is large.

Lawson¹⁰ shows the gain increasing to at least $sf = 0.9$. However, MININEC results at $sf = 0.875$ imply a marked reduction in gain. As discussed above, the value cannot be considered trustworthy, so it isn't shown on the curve. Practically, the gain must reach a maximum somewhere around $sf = 0.9$ and fall to zero for a shorted line.

The added gain must have some effect on the radiation pattern. The only plane where this is found to be important is shown in Figure 28. Comparison of this with Figure 15 shows that the up-down directed compo-

nents have decreased by about 5 dB — not an important change.

The overall conclusion is that rectangular loops are just as useful as square ones. The high and narrow loops will have slightly higher gain, but lower drive resistance. The flattened ones will show reduced gain and higher drive resistance. If maximum gain is needed, the narrow loops operated at kb greater than unity offer interesting possibilities.

The diamond loop

The quad literature indicates that the square and diamond loops have identical performance. This is found to be nearly the case, but there are some differences.

Figure 29 shows the major difference — the variation of self- or drive resistance with loop size. At $kb = 1.0$ the values are identical, but there is some difference at all other values of kb . The difference reaches some 55 percent for $kb = 1.15$. In contrast, there's only a small difference in self-reactance, as shown in Figure 30. Over the range from $kb = 0.9$ to 1.02, the difference is about 7 percent.

The current distribution on the diamond is shown in Figure 31. The maximum current is slightly lower than in the square loop (Figure 10); this current difference does induce some small pattern changes. Comparison of Figures 31 and 11 shows a slight increase in gain for the diamond. Other pat-

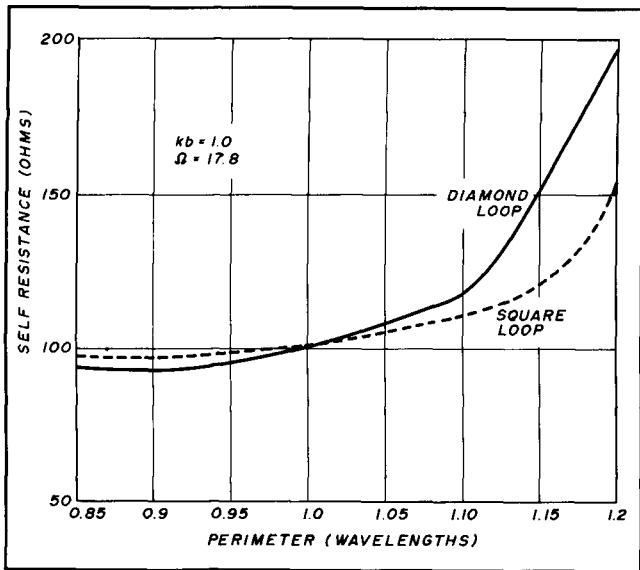


Figure 29. Self-resistance of a diamond loop close to resonance. The curve for a square loop is shown for comparison. While the resistance components are identical at perimeter = 1.0 wavelength, there is appreciable departure above perimeter = 1.1. This is related to the way current maxima change position.

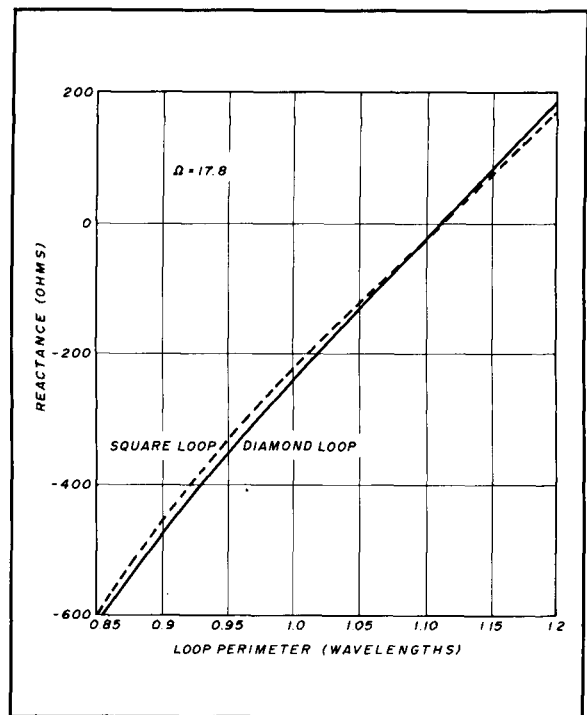


Figure 30. Self-reactance of diamond and square loops near resonance. Practically, the small difference is negligible.

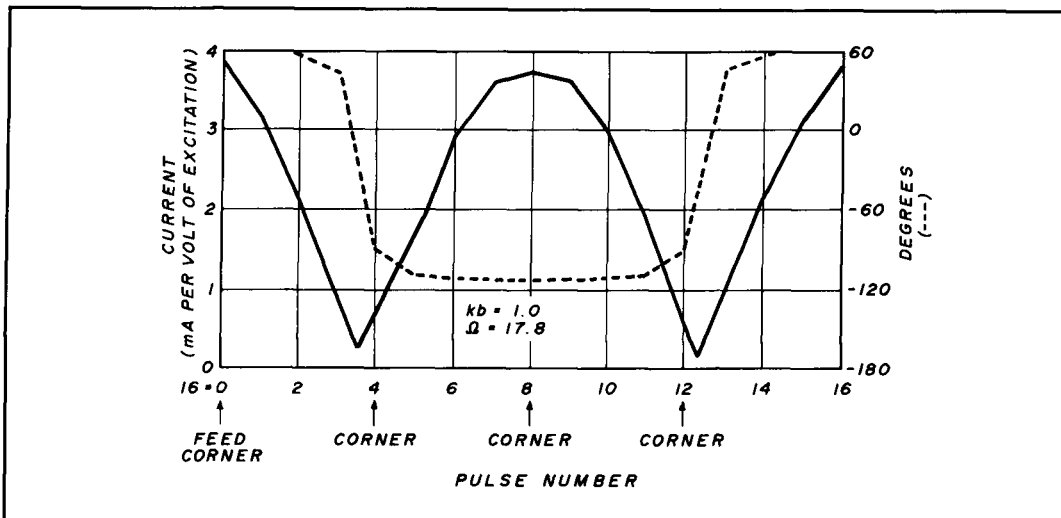


Figure 31. Current distribution on a diamond. Compare with Figure 10.

tern characteristics are essentially identical, as seen by comparing Figures 32, 33, and 34 with Figures 11, 12, and 14. These data indicate that the diamond and square loops are fully interchangeable in a practical sense. A small size adjustment is indicated if resonant operation is needed but other differences are negligible, especially if line matching is used. The size adjustment may be important in arrays. This is a factor to be studied. Basically, however, the choice between the diamond and quad loop (and even between these and rectangular ones) can be based on mechanical design and installation considerations.

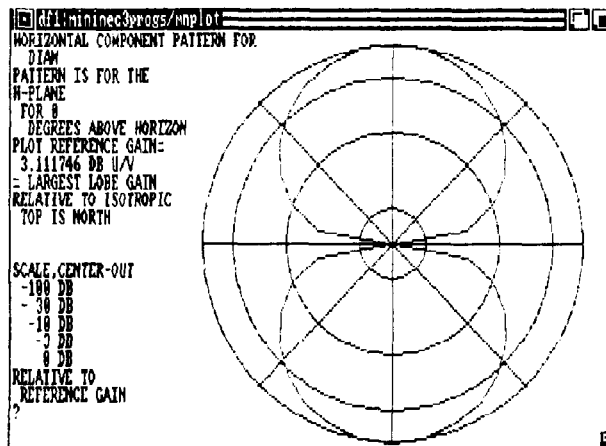


Figure 32. H-H pattern for a diamond. Compare with Figure 11.

ELNEC

Advanced Antenna Analysis Program

Fast to learn and easy to use, ELNEC lets you analyze nearly any type of antenna in its actual operating environment. Describe your antenna with ELNEC's unique menu structure and spreadsheet-like entry system and watch it generate azimuth and elevation plots, report beamwidth, front/back ratio, takeoff angle, gain, and more. Save and recall antenna files. Print plots on your dot-matrix or laser printer.

ELNEC uses the full power, versatility, and accuracy of MININEC computing code while making antenna description, analysis, and changes worlds easier. With ELNEC there's no messing with "pulses" - just tell it where on a wire you want a source or load to go, and ELNEC puts it there. And keeps it there, even if you change the antenna. Interested in phased arrays? ELNEC has true current sources for accurate analysis.

ELNEC runs on any PC-compatible computer with at least 360k RAM, CGA/EGA/VGA/Hercules, and 8/9 or 24 pin Epson-compatible or HP LaserJet/DeskJet printer. Two versions are available, optimized for use with and without a coprocessor.

There's no copy-protection hassle with ELNEC - it's not copy protected. And of course there's extensive documentation.

ELNEC is a terrific value for only \$49.00 postpaid. (Please add \$3.00 for airmail outside N. America.) VISA and MasterCard orders are accepted - please include card number and expiration date. Specify coprocessor or noncoprocessor version. Order or write for more information from:

Roy Lewallen, W7EL
P.O. Box 6658
Beaverton, OR 97007

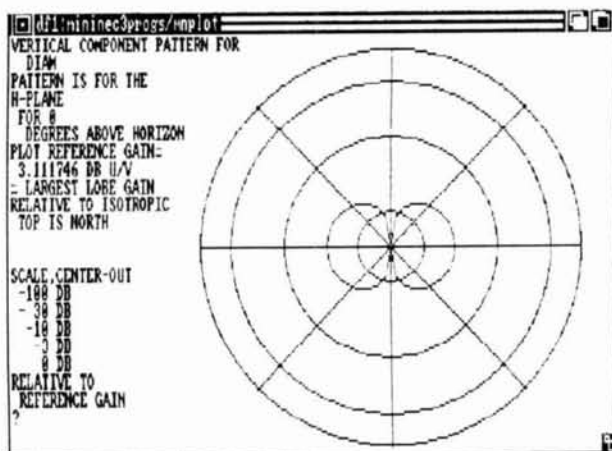


Figure 33. V-H pattern for a diamond. Compare with Figure 12.

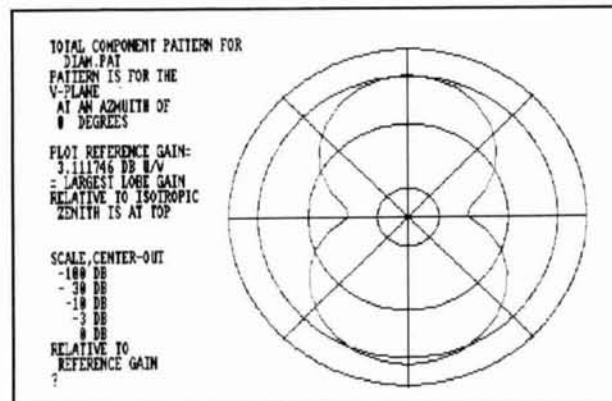


Figure 34. T-V pattern for a diamond in the plane of the loop. Compare to Figure 14 noting the difference in reference level. These patterns confirm the common view that a square and diamond loop have practically identical properties.

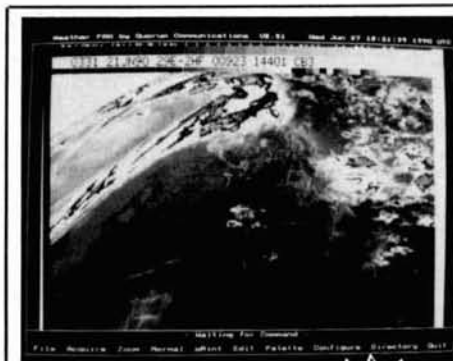
Summary

The curves and tables shown here are sufficient to design any practical square, rectangular, or diamond loop, and to estimate performance. The data also provides the basic building blocks for the development of arrays using these loops. ■

References

1. Ronald King, "Theory of the Corner-Driven Square Loop Antennas," *IEEE Antennas and Propagation AP-4*, July 1956.
2. Sheila Prasad, "Theory of Corner-Driven Coupled Square Loop Antennas," *ONR Report NR-371-016*, Harvard University, Cambridge, February 1959.
3. Storer, "Impedance of Thin-Wire Loop Antennas," *Cruft Laboratory Technical Report 212*, May 1955.
4. Phyllis A. Kennedy, "Loop Antenna Measurements," *IRE Transactions, Antenna Propagation*, October 1956.
5. William I. Orr, W6SAI, *All About Cubical Quad Antennas*, Radio Publications, Wilton, Connecticut, 1971.
6. R.P. Haviland, W4MB, "The Quad Antenna: Part 2, Circular and Octagonal Loops," *Ham Radio*, June 1988, pages 54-67.
7. Storer, "Impedance of Thin-Wire Loop Antennas," *Transactions of AIEE Communications*, November 1956.
8. R.P. Haviland, W4MB, "The Quad Antenna: Part 3, Circular Loop and Octagonal Arrays," *Ham Radio*, August 1988, pages 34-47.
9. R.P. Haviland, W4MB, "The Quad Antenna: Part 1, General Concepts," May 1988, pages 43-52.
10. James L. Lawson, *Yagi Antenna Design*, ARRL Newington, Connecticut, 1986.

Editor's Note: Haviland's work on the quad antenna will soon be available in book form from the CQ Bookstore.



Quorum introduces the first totally integrated system for the reception of weather satellite images directly on your personal computer. Selection of HF NAFAX, GOES WEFAX, GOESTAP, METEOSAT, NOAA and METEOR APT (including satellite downlink frequency selection) are made under complete program control from your PC keyboard.

The easy to learn and use Menu driven program allows you to capture, store, retrieve, view and print images with a few simple keystrokes. Images can be colorized from a palette of up to 262,000 colors when using a VGA display.

System configurations capable of NAFAX reception start at \$399.00 while fully capable systems can be configured for \$1500 to \$2000.00, providing professional quality at low prices.

For complete information and a Demo Disk, call or write:

Quorum Communications, Inc., 1020 S. Main St. Suite A, Grapevine, TX 76051 (817) 488-4861. Or, download a demo from our Bulletin Board by calling (817) 421-0228 using 2400 baud, 8 data bits and No parity.



Receive
Weather Satellite
Images and Charts
on your PC
with Quorum's
Totally Integrated
and Affordable
Weather Facsimile
System

QUORUM COMMUNICATIONS

DIGITAL SIGNAL PROCESSING

Image processing

Why are the major players in the electronic's industry scurrying to develop systems based on digital signal processing (DSP) technology? DSP research and development is at an all-time high, partly due to the emergence of powerful, affordable DSP ICs which can replace more expensive or less capable conventional circuitry! Plug-in cards containing these chips can transform a common desktop microcomputer into a high-speed, flexible, and affordable DSP research and development workstation. As discussed in previous articles in this series^{2,3,4}, a variety of computer algorithms and approaches have been developed over the years to facilitate the development of efficient DSP systems. These approaches, which include both time and frequency domain processing, as well as the application of artificial intelligence (AI) techniques, are commonly discussed in terms of one-dimensional data; for example, audio signals.

DSP techniques aren't limited to simple chronological data. However, all of the commonly used DSP techniques which have been applied to one-dimensional data, like the Fast Fourier Transform, have multi-dimensional equivalents. The field of digital image processing (DIP), a subset of DSP, is perhaps the most active arena of multi-dimensional DSP research and development. One reason for the resurgence of interest in DIP systems—which are concerned with enhancing, measuring, classifying, or matching images—is that DIP systems are being built around the new generation of powerful and inexpensive DSP chips. This article examines the field of digital image processing, and illustrates

how DIP techniques can be applied to amateur image communications systems.

Introduction

Practical DIP has the distinction of being a by-product of America's space program⁵. In the late 1960s, a small group of scientists in NASA's Jet Propulsion Laboratory (JPL) used DSP techniques to process analog pictures of the moon sent to earth from the Ranger 7 spacecraft. In this and other early applications of DIP, the analog signals were first digitized so the data could be manipulated by a digital computer (in this case an IBM 360/44). In the Image Processing Laboratory of the JPL, digital image enhancement techniques were developed to correct for defects in the onboard camera, interference from other satellite equipment, motion artifacts, and other sources of noise.

In later years, with the deployment of digital camera systems on board satellites, it became desirable to perform image processing before transmitting the image to earth; for example, performing data compression on the camera output to minimize transmission time. Realizing that the development of a practical space-based DIP system was constrained by hardware, and not the availability of computer algorithms, researchers at NASA set out to develop lightweight alternatives to massive mainframe systems. The result was a series of parallel (Harvard) architecture very large scale integration (VLSI) chips that outperform even the fastest mainframe-based DIP systems. These chips, which make it possible for a satellite system to process an image before it's

beamed to earth, are able to outperform conventional mainframe systems because each component in the chip works in parallel with others. That is, in normal operation, part of a DSP chip performs certain functions, passes its intermediate results to the next specialized component, and then operates on new data. In comparison to the highly parallel DSP systems in which components are rarely idle, the serial (von Neumann) architecture of conventional mainframe (and microcomputer) systems requires that each calculation be handled sequentially.

As was the case in the JPL, the main attraction of DIP to those involved in image communications is that it can be used to uncover information within an image. That is, DIP can be used to increase the image signal/noise ratio. Extensions of traditional DSP techniques (like the 2-D Fast Fourier Transform) can be used to isolate noise spikes, remove them, and then transform the data into a noise-free image. Similarly, images can be subtracted from each other to highlight changes, or averaged to remove noise. Regardless of how it's implemented, DIP can be classified into one of four categories: restoration, enhancement, coding, and understanding⁶

The objective of *image restoration* is to reduce or eliminate the effects of noise, image blurring, or geometric distortion in order to bring the image back to its original state. *Image enhancement* is intended to improve the appearance of an image; in other words, to improve image quality, intelligibility, or visual appearance. Unlike a restored image, an enhanced image may bear little resemblance to the original. The purpose of *image coding* is to represent an image in as compact a representation as possible; that is, image compression, for more economic archiving or use of a communications channel. *Image understanding* systems are designed to symbolically repre-

sent the contents of an image, for use in robotics, computer vision, and target identification. In this area of AI research, traditional DSP techniques—digital high-pass filtering, for example—are applied to an image before higher-level operations, like knowledge-based manipulations of objects detected in the image, are performed. Before the characteristics of the software and hardware required for these types of processing are discussed, a brief detour into the specifics of image communications systems is in order. A summary of the more pertinent characteristics of the image systems used by amateurs follows.

TV and video

The two basic types of television available to amateurs—conventional or Fast Scan TV (FSTV) and Slow Scan TV (SSTV)—differ in many respects. These differences include bandwidth requirements, communications range, likely sources of noise and distortion, and permissible operating bands. Because of the bandwidth requirements (approximately 6 MHz for FSTV and only a few kHz for SSTV), FSTV is limited to 420 MHz and above. Below 50 MHz, the bandwidth of FM and AM SSTV signals is limited to that of a standard SSB signal, or about 3 kHz (see Table 1). Between 50 and 225 MHz, SSTV SSB signals must be no wider than voice signals. An SSTV DSB signal should be wider than an AM voice signal—about 7 kHz. The FM signal limit in this frequency range is 20 kHz.

Fast scan television

FSTV, sometimes referred to as Amateur Television or ATV, is in many respects identical to standard National Television System Committee (NTSC) TV. As such, most ATV stations are constructed with unmodified commercial NTSC video equipment. NTSC standard TV signals are allotted 6 MHz for video, audio, and color (see Figure 1). The video signal, which decreases in amplitude with increasing light intensity, is amplitude modulated, with lower sideband partially suppressed (vestigial sideband). The audio signal is frequency modulated with pre-emphasis for an increased signal/noise ratio. The image carrier is 1.25 MHz above the lower limit of the channel, and the sound subcarrier is 4.5 MHz above the visual carrier. The color subcarrier is 3.579545 MHz above the visual carrier⁸

There are 525 horizontal scanning lines in an NTSC signal, interlaced at 262.5 per field, with a vertical scanning frequency of

| Frequency Range | Maximum Bandwidth Allowed |
|-----------------|--|
| < 50 MHz | 3 KHz (FM & AM) |
| 50 - 225 MHz | 3 KHz (SSB), 7 KHz (DSB), 20 KHz (FM) |
| > 420 MHz | ~6 MHz |

Table 1. Bandwidth limitations for video communications as a function of operating frequency.

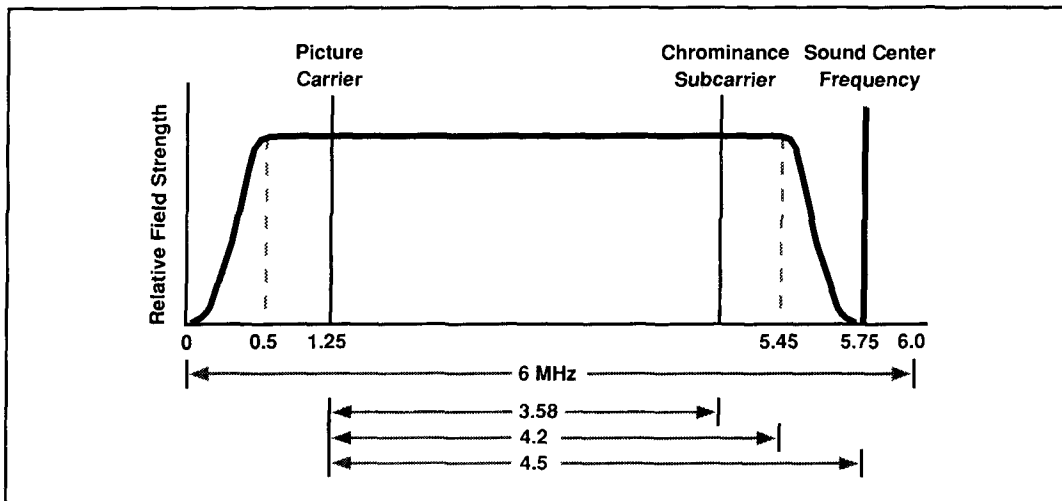


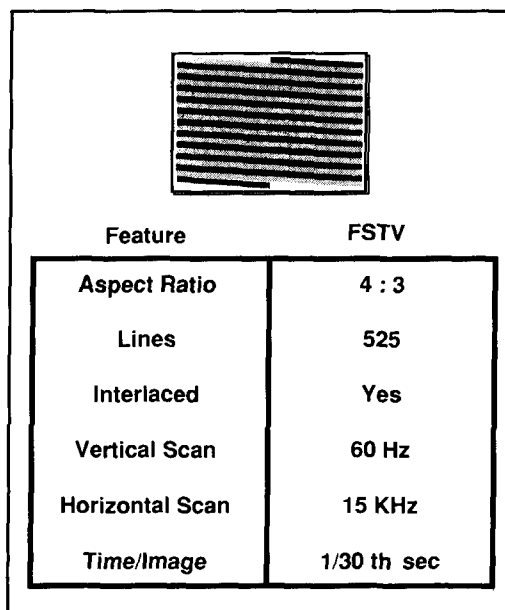
Figure 1. The spectrum allotment for standard NTSC color TV. Frequencies are all in MHz.

60 Hz for monochrome and 59.94 for color (see Figure 2). This means that each image is composed of two alternating fields repainted approximately 30 times/second; that is, a field of 162.5 lines is displayed every 1/60th of a second. The horizontal scanning frequency is 15,750 Hz for monochrome and 15,734.264 Hz for color, and the image horizontal-to-vertical or aspect ratio is 4:3.

A color NTSC TV camera produces three simultaneous signals — red, green, and blue (RGB)—which are combined to produce a luminance (brightness) signal and two chrominance (color) signals. The two chrominance signals modulate two components of a 3.58 MHz chrominance subcarrier that are in phase quadrature. Double sideband, suppressed carrier modulation is used, and the output of each of the two modulators is added to the luminance signal. In composite signals, the luminance information is applied directly to the modulator, making it compatible with monochrome receivers. Composite NTSC video is created by combining chrominance, luminance, and synchronization information.

Its commercial longevity in this country notwithstanding, the NTSC video standard of the 1950s is not without its shortcomings. *Flicker* is often present when there is even a slight variation in the composition of fine lines from one field to the next. And although the NTSC standard specifies 512 horizontal lines, up to 30 percent of the image display is typically lost due to over-scanning, blanking, and maladjustment. Furthermore, image sharpness and color definition are lost when color and brightness information are combined, as in NTSC composite video. Studios compensate for these and other NTSC video shortcomings by carefully composing scenes and choosing

particular colors, graphics, and type styles. Amateurs have responded by developing systems that depart from the NTSC standard. Some of these systems avoid the complex transmitter arrangement by frequency modulating the AM video carrier (at the expense of requiring modified receiving equipment), instead of modulating a separate subcarrier. Another approach is that of Fast Scan Frequency Modulated Television (FMTV), which is gaining popularity in the 24-cm band. FMTV provides a number of advantages over NTSC standard TV, including improved signal/noise ratio through use of transmitter pre-emphasis and receiver de-emphasis, as well as immunity from both co-channel interference and fading.⁹ Because



| Feature | FSTV |
|-----------------|-------------|
| Aspect Ratio | 4 : 3 |
| Lines | 525 |
| Interlaced | Yes |
| Vertical Scan | 60 Hz |
| Horizontal Scan | 15 KHz |
| Time/Image | 1/30 th sec |

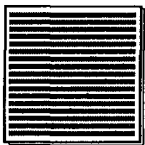
Figure 2. Characteristics of NTSC standard FSTV.

most ATV activity is in the 70 and 23-cm bands (requiring a Technician Class license or higher), amateur communications based on NTSC video are limited to line of sight.

Slow scan television

To a casual observer, the most obvious features of SSTV are the low resolution, still pictures, and lack of sound. Instead of 525 interlaced lines every 1/30th of a second, standard SSTV supports only one frame, composed of 120 noninterlaced lines, every 8 seconds (see **Figure 3**). Additional features include a horizontal sweep rate of only 15 Hz, and square images; that is, an aspect ratio of 1:1. Since SSTV signals lie within the audio range, conventional communications equipment can be used to receive and transmit the signals. Either SSB or FM may be used on the HF bands.

The key component in any modern SSTV system is a *digital scan converter*.¹⁰ This device allows unmodified fast scan equipment—a home video camera, for example—to be used for SSTV image input/display. In transmit mode, the scan converter translates the video image into an audio signal which can be fed into the audio input of an unmodified transceiver. The video-to-audio translation is accomplished through the use of a *frame grabber*, which includes a high-speed Analog-to-Digital converter and enough memory (about 64 K of RAM for a monochrome image) to store a single frame from a standard NTSC video camera. The digital data acquired by the frame grabber is used to control a tone



| Feature | SSTV |
|-----------------|----------|
| Aspect Ratio | 1 : 1 |
| Lines | 120 |
| Interlaced | No |
| Vertical Scan | 0.125 Hz |
| Horizontal Scan | 15 Hz |
| Time/Image | 8 sec |

Figure 3. Characteristics of SSTV. Note the contrast with the features of NTSC TV (*Figure 2*).

generator which supplies the transmit audio input. For color images, each of the three components of the original RGB signal are sent separately, requiring 8×3 or 24 seconds per color picture.

On receive, incoming signals are digitized and stored by the scan converter. When the image memory or buffer is full (after a frame of video has been processed), the data is sent line by line to a Digital-to-Analog converter, and video synchronization voltages are added. The resulting video signals can either be sent directly to a video monitor, or can be used to modulate a VHF oscillator attached to the front end of an NTSC TV receiver. Color scan converters store each of the three color signals in different memory locations, and then combine the three to form a composite color signal.

Because of its bandwidth limitations, SSTV can be used on any band (with a General or higher class license), including the HF bands, for worldwide communications. Multipath distortion and high atmospheric noise, uncommon in ATV, are therefore commonly observed with SSTV signals.⁹

Applicability of DIP to image communications systems

From the preceding discussion, it should be obvious that amateur communications systems based on both FSTV and SSTV can benefit from DIP technology. Both modes can use techniques that result in noise reduction and contrast enhancement. One source of distraction in FSTV systems, flicker, can be circumvented by using DIP to convert a conventional interlaced NTSC signal into a noninterlaced signal. The image which results is displayed on a special monitor, and can be redrawn in its entirety every 1/60th of a second—without flicker.

Because of the prominence of multipath distortion on HF SSTV signals, DIP techniques that filter the effects of this type of distortion can be applied. In addition, SSTV methods have need for real-time compression (on transmit) and expansion (on receive) to allow for faster image transfer rates. PC-based digital image compression systems with real-time expansion have already been developed for compact disk read only memory (CD ROM) applications. For example, a DIP system called Digital Video Interactive (DVI), developed by General Electric's Sarnoff Laboratory in New Jersey, can compress motion video by a factor of 100:1, and decompress the images

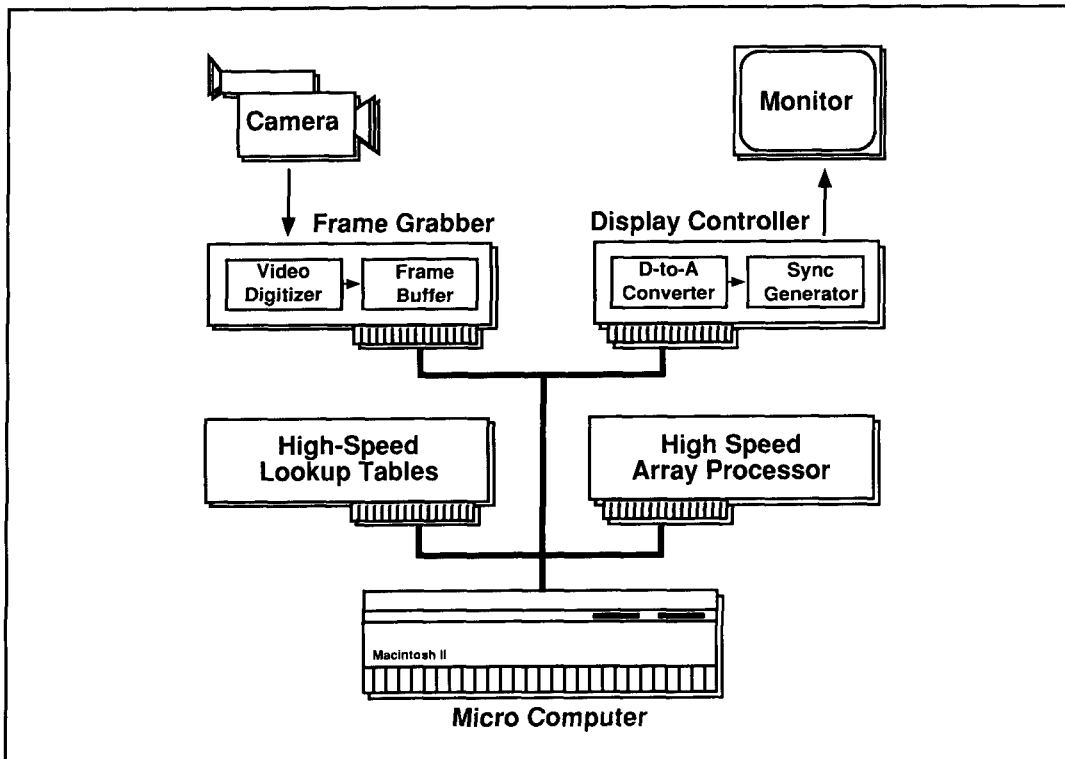


Figure 4. The hardware associated with a typical DIP system. Image acquisition hardware includes a video camera or other video source, a frame grabber, and a frame buffer. In some systems, the actual DIP is performed with generic computer hardware. In others, such as the system depicted above, video array processors and lookup tables implemented in hardware are used to increase computational throughput. The display controller, which may also consist of generic computer display hardware, converts the digital image data into a form suitable for display on a monitor.

in real time. The same techniques could potentially be applied to SSTV video, resulting in an image transfer rate of several frames/second, while adhering to current bandwidth limitations.

Given that DIP techniques are applicable to amateur image communications systems, the next step is to examine the software and hardware issues surrounding this technology. An especially attractive feature of SSTV is that the relatively slow data transfer rates make it possible to use inexpensive DSP hardware and simple software algorithms for image processing. In comparison, DIP of FSTV images requires fast, special-purpose hardware and low-level, efficiently written software. A more detailed discussion of the software and hardware issues surrounding DIP technology follows.

Digital image processing hardware

With the current practice of incorporating image processing functions in hardware applications, the distinction between DIP hardware and software is becoming blurred. However, most experts would agree that a minimal DIP system includes an image cap-

ture device, a computer, and a display device!¹ These three classes of DIP hardware are outlined next.

Image capture hardware

As illustrated in **Figure 4**, image acquisition hardware minimally includes a: (1) video source, (2) frame grabber, and (3) frame buffer!² The video source is commonly a video camera with an NTSC analog output. Other popular video sources include VCRs and video disk players.

Given a video source, the purpose of a *frame grabber* is to transform the analog video signal into a matrix of digital values in the frame buffer. In general, the speed and bit conversion capability of the Analog-to-Digital converter within the frame grabber defines the limits of any image acquisition system. That is, high sampling rates are required for fine details to be captured from the analog signal, and the shades of grey or colors available in a system are a function of the number of bits available to describe a given pixel (picture element). For example, with an n -bit Analog-to-Digital converter, a frame grabber will capture only 2^n levels of grey or intensity. To capture four levels of

grey, a 2-bit converter would be required. Since the human eye can distinguish up to 64 levels of grey or intensity,¹³ image acquisitions systems commonly use at least 6-bit converters.

The *frame buffer*, a memory matrix or array of high-speed RAM, is used to store the initial or pre-processed digital image. Each value in the matrix represents the pixel (picture element) image intensity at a point in the image. The rows of a frame buffer matrix correspond to the horizontal lines of the image; the columns represent samples along the x-axis of each line. Where a monochrome system might have only one frame buffer matrix, color systems typically have four—one each for the red, green, and blue images, and one that serves as a placeholder for intermediate calculations.

Computer hardware

Once an analog video image has been digitized and stored in computer-accessible form, virtually any computer system—from a Commodore-64 to a powerful CRAY supercomputer—can be used to execute the large assortment of available DIP algorithms. With the introduction of dedicated DSP chips, the most popular platform for DIP work has become the desktop microcomputer. In many respects, the new DSP chips are analogous to the common math co-processor chips available for microcomputers in that they offload intensive math calculations from the main CPU. Circuits containing these DSP chips, in the form of add-on cards (see **Figure 4**), offload the burden of image processing computations from the main CPU to an onboard processor. This special-purpose processor is usually equipped with its own high speed RAM and support software in ROM, and may be supported by its own co-processor chips.¹⁴

The result is typically a ten to twenty-fold increase in image processing performance over the unaided capabilities of the host microcomputer. The basis for this significant increase in computational throughput is the parallel hardware architectures of the new DSP chips that support more efficient data transfer between the image memory, image co-processor, and the display circuitry.¹⁵ The inclusion of fast *video array processors* and *lookup tables* implemented in hardware also contribute to the computational efficiency of image processors. Video array processors, which are specifically designed to work with frame buffers, allow image processing systems to work in real time on small computer systems. These

array processors are able to process an image in less than 1/30th of a second while the next frame is being loaded into the buffer.

Lookup tables (see **Figure 4**) implemented in hardware also decrease processing times by rapidly mapping function input values to predefined transformations.¹² Due to the large amount of overhead associated with repeatedly performing operations on each pixel value in an image, image processing transformations are rarely performed directly on the matrix of image intensity values. For example, in any practical DIP system, a lookup table similar to that shown in **Figure 5** would be used to determine the square root of a pixel value. Instead of using a dozen or more machine cycles to calculate the square root of a given number (26, for example), the lookup table can provide the answer quickly, often within two or three machine cycles.

Because of these and other special features of DIP hardware systems, image data transfer bandwidths of 80 Mbytes/second and more are attainable with image co-processor hardware. The improvements in throughput are so remarkable that the traditional tests and standards applied to von Neumann machines simply do not apply to DIP hardware. Specialized DIP benchmarks have been developed to intelligently compare DIP hardware systems.¹⁶

Image display device

The purpose of the image display device in a DIP system is to translate the digital data in the frame buffer into a viewable form. A central component in the display device is the *display controller*, which reads data from the frame buffer, provides Digital-to-Analog conversion, and passes the analog video signal to a CRT or other monitor, with the appropriate refresh rate. In most microcomputer-based systems, the output of the display controller is a standard RD-170 composite signal. In more capable systems, higher resolution RGB output is used. RGB video provides separate 1-volt peak-to-peak signals for each of the three color components. Synchronization may be provided by a separate signal, or superimposed on the green signal!¹⁴ The best systems bypass the standard composite and RGB formats entirely, in favor of specialized, noninterlaced displays. Several of the better DIP systems are add-on processing boards used to produce a flicker-free, noninterlaced signal. In addition to preventing flicker, the special video cards make it possible to use monitors which support more

| Input Value | Output Value |
|-------------|--------------|
| 20 | 4.4721 |
| 21 | 4.5826 |
| 22 | 4.6904 |
| 23 | 4.7958 |
| 24 | 4.8990 |
| 25 | 5.0000 |
| 26 | 5.0990 |

Figure 5. An example of a square root lookup table. In this partial table, input values on the lefthand side of the table are mapped directly to output values on the right. A simple lookup routine requires significantly less time than does calculating the square root of each value as it is needed. Other, more complex functions (exponentials and trigonometric expressions, for example) are also amenable to lookup-table processing.

than the standard 64 levels of grey, at an increased image density or pixels/inch. These added features increase the perceived quality of the image displayed.

Digital image processing algorithms

The basic data manipulations involved in image processing (simple addition, subtraction, multiplication, and division), are rela-

tively trivial. However the large number of data points that must enter into image processing calculations, demand the use of powerful and efficient algorithms. These algorithms can be implemented in hardware to minimize execution time, as in the lookup table described earlier, or as software designed to run on generic computer hardware.

Regardless of how they are implemented, the basic image processing manipulations can be categorized as either *radiometric*, *spatial*, *multiple-image*, or *data compression*!² Contrast stretching and density slicing are examples of radiometric operations. Both operations manipulate the intensity of individual pixels within an image. Contrast stretching forces the darkest values in an image to black and the lightest values to white, and varies all of the intermediate values linearly. Density slicing displays only those pixels within a certain intensity range, to highlight or remove objects that have a characteristic brightness or color. Spatial operations include registration procedures and filtering. Forcing an image to overlay another by projecting a curved image onto a flat surface, or using high-pass filtering to enhance an image, are examples of spatial operations. Multiple-image operations are concerned with image overlays and frame comparisons. The subtraction of one image from another to highlight frame-to-frame differences, is a common multiple-image operation. Data compression, as discussed earlier, is especially important in the efficient transmission of large images.

The computer algorithms developed to support these basic manipulations can be classified as either *point*, *area*, *geometric*, or

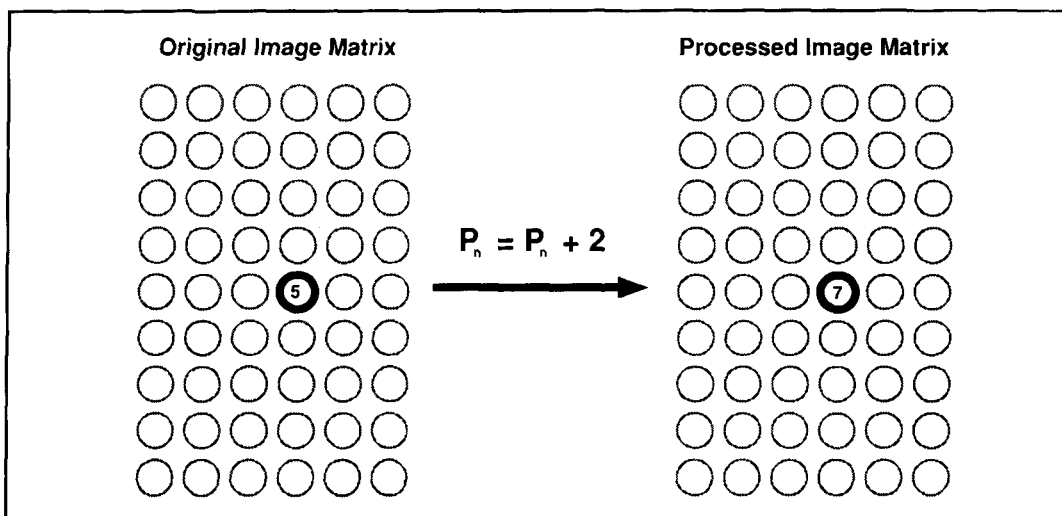


Figure 6. Point process algorithms compute a pixel's value as a function of its current value. In the example above, image brightness in the original image (left) is increased by adding 2 to the intensity value of every pixel in the image (0 = black; 255 = white). The final image matrix (right) holds the updated pixel values.

frame processes!¹¹ Point process algorithms compute a pixel's value as a function of its value only, without regard to the other pixel values in the image. Adding a constant to all pixels in an image to increase image brightness, or pseudocoloring a monochrome image (assigning arbitrary colors to specific grey levels) are two examples of point process algorithms (see **Figure 6**). In contrast to point process algorithms, area process algorithms depend on neighboring pixel values to compute a given pixel's value. For example, high and low-pass spatial filtering, used to sharpen or smooth an image, respectively, are area process operations.

Geometric process algorithms modify the position or arrangement of pixels in an image by rotating part or all of an image to correct for distortions caused by imperfect optics, or simply magnifying an area of interest. The first class of problems tackled by DSP was that of geometric distortion of images resulting from nonuniform rates of scanning in an image tube⁵. Frame process algorithms make use of two or more images in assigning individual pixel values; for example, as in image subtraction to detect image differences. Frame averaging, assigning the average value of a given pixel, across several images, to the final pixel value, can be used to increase the image signal/noise ratio.

Although each of the four classes of image processing algorithms have situations in which they are most useful, virtually all DIP applications employ some sort of area processing algorithms!¹¹ Area processing algorithms can be linear (based on simple mathematical operations like addition and multiplication) or nonlinear (based on trigonometric, exponential, and root functions). Although significantly more computationally demanding, nonlinear area process algorithms can provide a higher signal/noise ratio in the final image than can linear process algorithms. Despite the theoretical advantages of nonlinear algorithms, the simplicity and power of linear area algorithms has made them the practical standard for DIP applications. Of the linear area process algorithms, *convolution* is by far the most popular.

Convolution

In its most basic form, convolution is simply a filtering process that amplifies or attenuates particular pixels in an image, in order to identify features of interest. Convolution is a powerful algorithm. The same basic algorithm can be used to provide a

variety of image processing functions. These functions include: high and low-pass filtering, noise filtering, edge enhancement, image inversion, etc. While the generic convolution algorithm is relatively trivial, practical implementations are challenging because of the large number of repetitive calculations that must be performed on every pixel in an image.

Convolution replaces a pixel's value with the sum of the pixel's value and that of its neighbors—each weighed or multiplied by a factor (see **Figure 7**). The matrix of weighting factors, or *convolution kernel* may be of virtually any dimension; for example, 3×3 , 3×6 , 4×4 , 5×9 , and so on, with the larger kernels requiring significantly more computational resources. A 3×3 matrix is commonly used on microcomputer-based systems, although a larger matrix will allow you to identify edges more precisely—especially diagonals at other than 45 degrees!¹⁷

In the convolution example illustrated in **Figure 7**, a simple 3×3 smoothing kernel is used to minimize sudden changes in pixel intensities; that is, it provides low-pass spatial filtering. The intensity value of the highlighted pixel in the original image, 27, is obviously out of line with the intensity values of its neighboring pixels to the top, bottom, and either side. The smoothing kernel replaces the current pixel intensity value with the mean intensity value of the four neighboring pixels (see the equation in the lower middle of **Figure 7**). Note that the new pixel intensity value does not replace the original value in the original image matrix, but is placed in the same position within the processed image matrix. This avoids the possibility of using the convolution output values from previous calculations as the inputs to new convolution operations. After computing the new value of a particular pixel, the next step is to apply the same convolution kernel to subsequent pixels in the original image matrix, until all of the pixel intensity values have been processed. In this example, the pixel immediately to the right of the highlighted pixel (original value = 6) would be next in the queue for convolution processing.

Convolution is a time consuming operation, since the convolution function is repeated for every pixel in the image. Convoluting an image of size X by Y with a kernel of size n by m can require up to $X \times Y \times m \times n$ multiplications and additions or subtractions; that is, a 3×3 kernel can require almost 600,000 multiply/add operations for a 256×256 pixel image! The con-

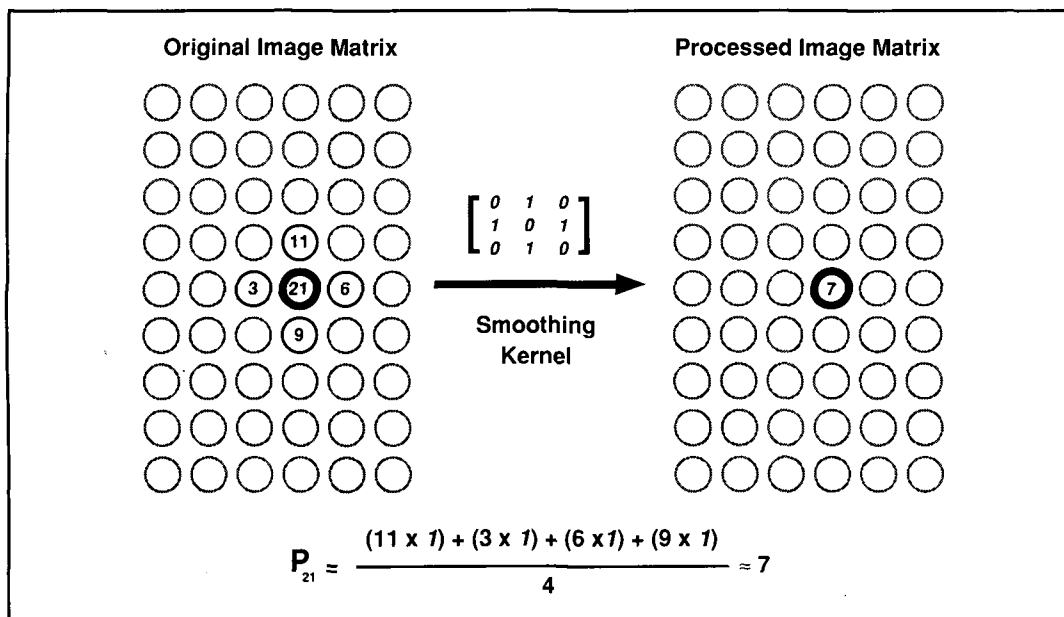


Figure 7. Convolution replaces the target pixel value with the sum of the current target pixel value and its neighbors, each multiplied by a factor defined in the convolution kernel. In the above example, a simple smoothing kernel is used to calculate the new value of the highlighted pixel (original value = 21; smoothed value = 7). For clarity, only the four nonzero values in the kernel are shown in the above calculation. In an actual calculation with a 3×3 kernel, nine kernel values and nine original image matrix values would enter into the calculations. Note the use of separate source and destination to avoid overlapping the convolution output values with the inputs to the convolution.

convolution process not only requires considerable computational resources, but also demands significant quantities of high-speed RAM. For example, during the convolution process, the results of each operation—the new pixel values—must be stored in a second frame buffer. Only original pixel values are used in the convolution computations.

Practical implementation issues associated with convolution algorithms include how to handle image edges, as well as positive and negative overflow conditions. A common method of handling the garbage produced at the image border (due to missing data values) is to assign either 0 (black) or a neighboring pixel's value to a border pixel's value. Overflow conditions, which occur when the value computed for a pixel exceeds the number of bits allotted to represent the value, are commonly handled by scaling. However, simply dividing each pixel value by a constant introduces internal rounding errors (noise). Another approach to handling overflow conditions—error checking—places additional computational demands on a system. It is also necessary to know how negative convolution output values will be handled. If you decide to store negative results, an additional bit will be required per pixel for the sign (\pm) value. The popular approach of storing all negatives as 0 has the benefit of minimizing storage requirements. But this is done at the

expense of internal inaccuracy. Performing the reverse convolution process will not recreate the original image, because some image data was lost when the negative values were truncated to 0.

Digital image processing examples

The best way to appreciate DIP techniques like convolution is to work with them firsthand. However, since few of you may have ready access to DIP workstations, I have included pictures of digitally processed images, along with descriptions of the processing method used. To produce these images, I used the NTSC composite output of a Panasonic Professional video camera. An eight-bit frame grabber, the Color Space II (Mass Micro System, Inc.), was installed on an Apple Macintosh II computer equipped with a standard Apple eight-bit video card and color monitor (used in monochrome mode). The image processing software used to manipulate the images was version 1.0 of ReView (Orange Micro, Inc.) and version 1.03 of Image (National Institutes of Health). To record the images from the computer monitor, I used a Nikon FE-2 camera with Nikkor 50mm 1:1.4 lens and a Kiron MC7 2X teleconverter. I used Kodak TMX-100 black & white print film.

Photo A shows the digitized image before

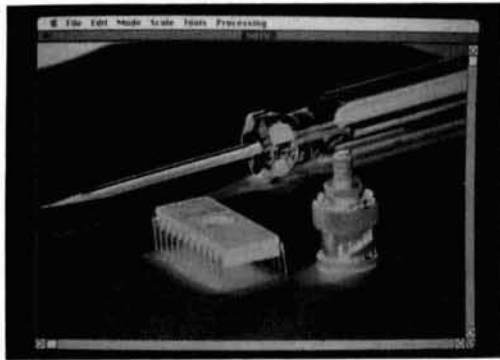


Photo A. The original, digitized image of a standard screwdriver with a colorless, transparent handle, a BNC connector, and a 24-pin EPROM, displayed on a standard eight-bit Apple Macintosh II color monitor in monochrome mode. Note the clarity of the EPROM markings, and the vertical herringbone pattern throughout the eight-bit image.

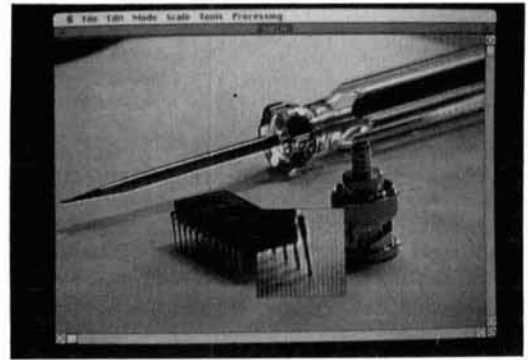


Photo B. The original image after convolution processing with a sharpening kernel. Note the increased clarity of the finer details in the photo, especially in the EPROM markings. Also note the increased prominence of the vertical herringbone pattern throughout the image. In the magnified panel (lower middle of the photo) you can see a close-up view of the EPROM leads.

any processing was performed. As you can see, the image consists of a 24-pin EPROM, a 3-inch screwdriver with a transparent handle, and a BNC connector. White paper was used as a backdrop. If you look closely at the extreme upper right-hand corner of the image, you can see a slight vertical herringbone pattern. This pattern, distributed uniformly throughout the image, is due to color information from the NTSC composite camera signal. The images were digitized in monochrome mode, even though a color camera was used, in order to make more publishable prints. Although a monochrome camera would have been a better choice for a video source in this situation, the noise introduced by the color signal is actually advantageous for the discussion on filtering techniques which follows.

Photo B shows the effects of convolution processing the image shown in **Photo A** (hereafter referred to as the original image) with the following 3×3 sharpening kernel:

$$\begin{array}{ccc} -1 & -1 & -1 \\ 1 & 9 & -1 \\ 1 & -1 & -1 \end{array}$$

This kernel adds the output of high-pass filtering to the original image. As you can see by looking at **Photo B**, the result is a sharper and somewhat noisier image. Certain features, like the EPROM leads, the markings on the EPROM, and the details on the BNC connector are crisper. The screwdriver handle, while somewhat blurred in the original image, also appears crisp and well delineated from the background. The price paid for this added definition is that the vertical herringbone pattern, only mar-

ginally obvious in the original image, is now markedly pronounced in all areas of the image. This noise is especially obvious in the X2 magnified view of some of the EPROM leads, shown in the lower middle of the photo.

Photo C shows the effects of convolution processing the original image with the following 3×3 median kernel:

$$\begin{array}{ccc} 1 & 1 & 1 \\ 1 & 1 & 1 \\ 1 & 1 & 1 \end{array}$$

This is called a median filter because it replaces the center pixel with the median value of that pixel and the neighboring pixel's values. After convolution, the algorithm first sorts the pixel values in ascending or descending order, and then

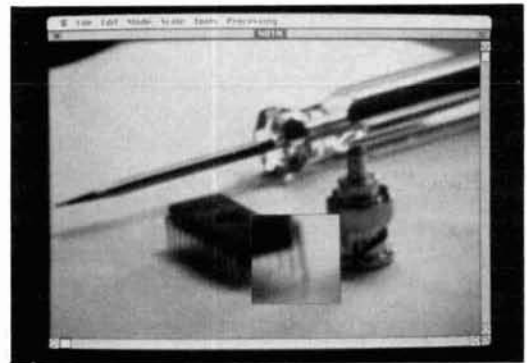


Photo C. After low-pass filtering with a median convolution kernel, most of the noise in the image has been removed—along with the smaller details in the image. Notice also the absence of noise or of the herringbone pattern present in *Photos A* and *B*.

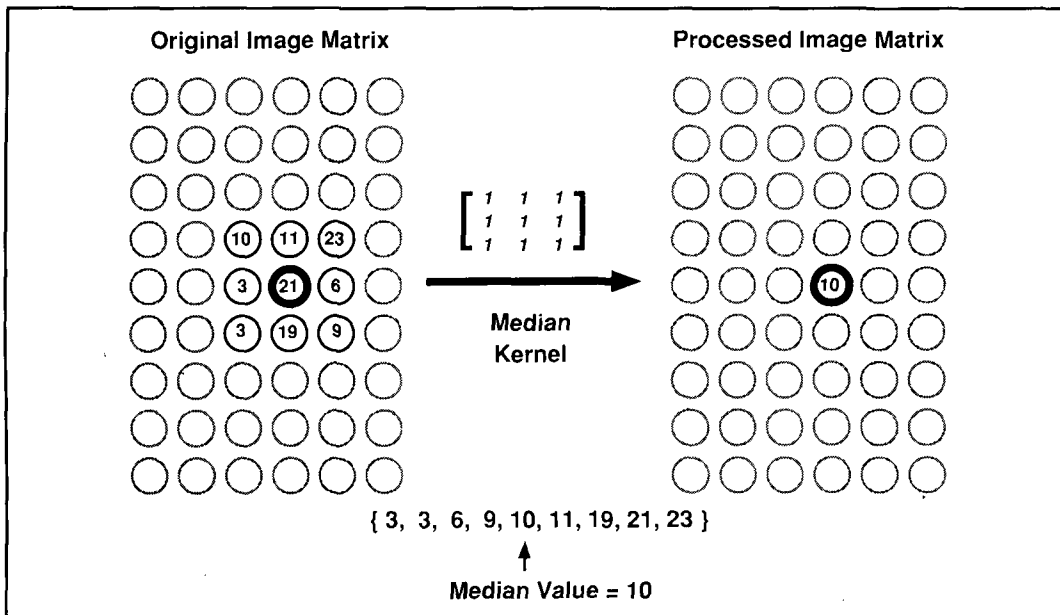


Figure 8. Convolution with a median kernel replaces the center pixel with the median or middle value of it and the neighboring pixel's values. In the original image matrix (left), the median value of the central pixel (value 21) and its eight neighbors is 10. This median value is used for the pixel's new value in the processed image matrix (right). Median filtering attenuates the higher spatial frequencies, and therefore tends to remove spot noise, as well as edges, textures, and other fine details from an image.

assigns the middle value to the pixel being processed.

Refer to **Figure 8**. Assume the nine original pixel intensity values are: {10, 11, 23, 3, 21, 6, 3, 19, 9}. Note that the central pixel (the pixel being processed) has an initial intensity value of 21. Since all values within the kernel are 1 or unity, the convolution process per se does not alter the actual pixel intensity value, but rather defines the scope of neighboring pixels which will have an effect on the processed pixel's value. A 3×3 median kernel will have markedly different effects on an image than will a 3×7 or 5×5 median kernel, because different numbers of neighboring pixel values will be involved in the calculations. Given the nine pixel intensity values above, an ordered list of intensity values appears as in **Figure 8**, with a median value of 10. This median value is now assigned to the central pixel; that is, the pixel with original intensity value of 21 now has a value of 10. Although this algorithm is more involved than that of the simple smoothing filter described in **Figure 7** (a type of *mean* filter, because it is based on the average pixel value), it also produces better results.

As is illustrated in **Photo C**, the median filter removes spot noise, as well as edges, textures, and other fine details from an image. This means it provides low-pass filtering. The vertical herringbone noise pattern is virtually absent in the image. How-

ever, if you look at the magnified area, you'll see that the individual EPROM leads are barely visible. When applying a median filter, you must be willing to sacrifice image details. You wouldn't use this type of filtering if the markings on the EPROM were of interest, but it would be applicable if you were mainly concerned with the relative positions of the three objects in the image.

Photo D illustrates image brightness enhancement—a common point process. The control panel in the upper left corner of the display has two slider controls that were used to control image brightness and contrast. The top slider has been adjusted to decrease the overall brightness of the image, making the details of the transparent screwdriver handle more apparent. In this instance, overall image brightness was reduced by subtracting a constant from all pixels in the image. As you might expect, the computation time required to process the image in this way is significantly less than that required for a convolution. On my system, in which all image manipulations are handled in generic hardware (the frame grabber does *not* function during image processing), altering the brightness of the image took less than one second. In comparison, the convolution operations used to create the two previous images each required approximately 10 seconds of computer time (the Macintosh II computer uses a 32-bit

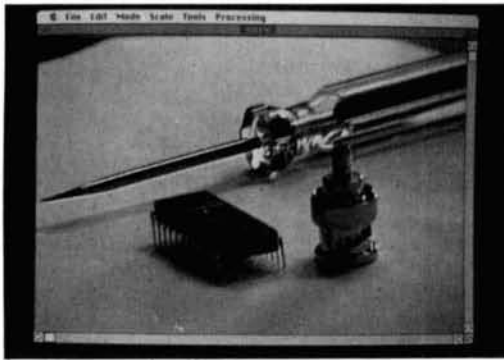


Photo D. Brightness enhancement of the original image. Notice the Brightness Histogram panel, in the upper lefthand corner of the display, which was used to vary the brightness and contrast of the image (or a selected region within the image). Normally, the controls are adjusted so that data points displayed are distributed evenly throughout the range of the histogram. In this photo, most of the data points are on the righthand side of the histogram, indicating below normal image brightness.

68020 CPU, in addition to a math co-processor, at a clock speed of approximately 16 MHz).

Photo E illustrates the effects of image inversion, another point process. In this example, the individual pixel values were simply inverted, without regard to the value of neighboring pixels. That is, in this case where pixels can be assigned values from 0 to 255, a pixel with an original value of 10 would be assigned a value of $255 - 10$, or 245. Similarly, a pixel with an original value of 245 would be assigned a value of $255 - 245$, or 10. Inversion can sometimes highlight details in an image that are not apparent in a noninverted original. Notice, for example, the increased clarity of the details in the BNC connector.

Photo F shows the effects of another con-

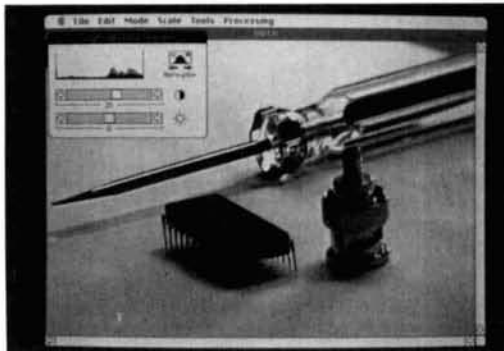


Photo E. Simple inversion of the original image. Notice that some details (for example, those of the BNC connector) are more evident in the inverted image than in the original image.

volution process with the following 3×3 horizontal edge enhancement kernel:

$$\begin{array}{ccc} -1 & -1 & -1 \\ 0 & 0 & 0 \\ 1 & 1 & 1 \end{array}$$

This convolution kernel illustrates how a kernel can be thought of as smaller image of what you want to detect or emphasize in the larger image. The kernel both resembles and enhances horizontal edges. Notice how this “horizontal-pass” filter de-emphasizes objects, patterns, and other details in the image that lack horizontal components. As you can see in the magnified area of the display, the horizontal edge of the EPROM is



Photo F. Horizontal-edge enhancement, through convolution with a horizontal-edge enhancement kernel, attenuates all lines and edges of the original image not in the horizontal plane. Note the prominence of the EPROM body, relative to the pins, in the magnified panel.

obvious, while the vertical EPROM leads are barely discernable. The shadows from the EPROM leads, which have a major horizontal component, are actually more prominent than the leads themselves. Notice, also, that the vertical herringbone noise pattern is completely absent from the image.

Photo G shows the effects of convoluting the original image with a 3×3 vertical edge enhancement kernel of the following form:

$$\begin{array}{ccc} -1 & 0 & 1 \\ -1 & 0 & 1 \\ -1 & 0 & 1 \end{array}$$

Note the similarity of this kernel to the previous one. This “vertical-pass” filter, which both resembles and enhances vertical edges, is essentially a horizontal-pass filter turned on its side. Only objects with a vertical component are visible in the image. In sharp contrast with the previous image, you

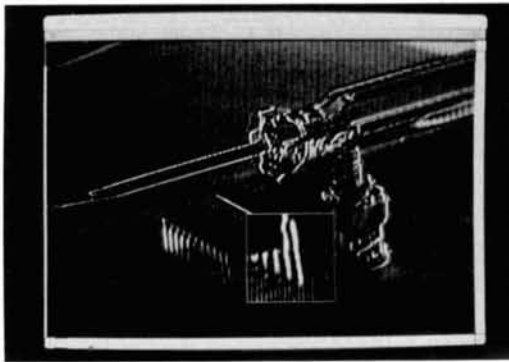


Photo G. Vertical-edge enhancement through convolution effectively attenuates all edges and lines not in the vertical plane of the image. Note the prominence of the vertical EPROM pins, relative to the horizontal EPROM body, in the magnified panel. Note also the emphasized vertical noise pattern.

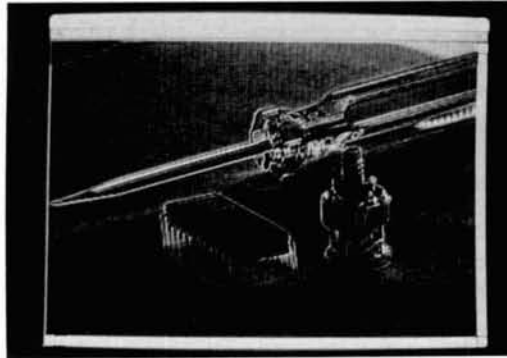


Photo H. Convolution with a Laplacian kernel emphasizes high spatial frequencies in all planes. The effect is similar to that observed with the sharpening kernel, in which higher spatial frequencies were added to the original image (see *Photo B*). In this case, however, *only* the higher frequencies in the original image appear in the final image.

can see in the magnified area of the display that the horizontal edge of the EPROM is now barely visible, while the vertical EPROM leads are now quite pronounced. Notice, too, that the vertical herringbone noise pattern is prominent throughout the image.

The last photo in the series, **Photo H**, illustrates the effects of convoluting the original image with the following 3×3 Laplacian kernel:

$$\begin{array}{ccc} -1 & -1 & -1 \\ -1 & 8 & -1 \\ -1 & -1 & -1 \end{array}$$

Note the similarity of this kernel to the sharpening kernel used to produce **Photo B**. Like the sharpening kernel, the Laplacian filter provides high-pass filtering, and therefore enhances abrupt intensity changes in any direction; that is, edges. Unlike the sharpening filter, which combines the higher spatial frequencies that pass through the filter with the original image, the Laplacian filtered image is composed of *only* the edges or higher spatial frequencies. The Laplacian image is therefore usually much darker than the original image, as you can see in the photo. Also evident is the prominence of the vertical herringbone noise pattern.

Summary

Photos A through **H** show why the type of image processing used on an image is quite case specific. The optimum filter (or series of filters) depends not only on the subject matter, type of noise present, and other external factors, but also on the object

of interest in the image. If, for example, you are concerned with minimizing all sources of noise in your image transmission system, you might want to examine your ATV or SSTV system video output after Laplacian convolution. Since any high frequency noise present in your system would be made obvious by the processing, you would be able to detect subtle changes in noise content as you adjust your video equipment. On receive, a sharpening filter would likely enhance the images from strong stations. On the other hand, noisy, weak signals would probably benefit most from some type of low-pass filtering. Spot noise or snow would be handled best by a median filter.

In addition to the potential benefits of image compression on transmit and expansion on receive noted earlier, other types of pre- and post-processing are applicable to video communications. Consider, for example, the effect of using the spatial equivalents of pre-emphasis (sharpening) on images to be transmitted, either in real time (for ATV) or offline (most applicable for SSTV), and de-emphasis (smoothing) on receive. On the receive end, filters that remove higher frequency components, such as a median convolution filter, could be used to remove high frequency noise with little degradation of the actual image. The overall effect would be to increase the effective range of an image communications system.

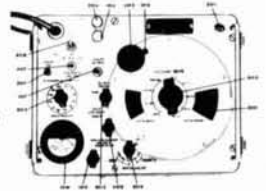
As software and hardware prices continue to drop, DIP will become more commonplace in the amateur's arsenal of communications equipment. Even as it stands today, it takes a relatively small investment to enter

N.E. Litsche Air Navigation Industries, Inc.

P.O. Box 191, Canandaigua, NY 14421-0191
716-394-9099 FAX 716-394-8329

All Prices FOB Canandaigua, NY

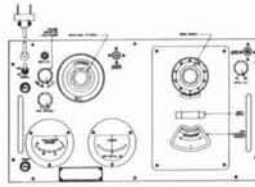
- 10 KHz-50 MHz in 8 Bands
- Sub-Microvolt to 2 Volt RF Output
- Resistive Attenuator
- Crystal Calibrator
- Checked out with schematic



\$125.00
Accessories Available
\$25.00 Additional

Signal Generators
SG-103/URM-25F

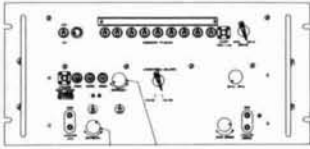
- 2-400 MHz in 6 Bands
- Sub-Microvolt to .1 Volt RF Output
- Piston Attenuator
- Checked out with schematic



\$100.00

TS-497 B/URR

- 30 or 60 MHz Center Frequency
- 3 or 20 MHz Sweep Width
- 9 Crystal Marker Capability (Five Equipped)
- Variable Marker with External Oscillator
- Operators Manual Reprint & Schematic Included

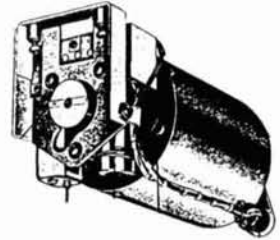


\$125.00

Sweep Generator
SG-336/U-KAY 380

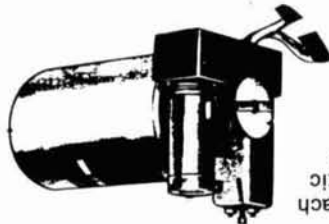
*** Pin Diodes, Set of 4...\$5.00 Call For Details***

Only \$65.00 Complete
Ready To Install In Your Radio



R-390A
VFO Subchassis
U.S. Government Depot Rebuild & Tested

\$12.50 Each
Schematic
Included



R-392
VFO Subchassis/Mixer
With 26D6 Tube Used Pulls

Easily Transistorized
Make Super Transmitter VFO!



CU-1280/RD-10
500 KHz-32 MHz Multi-Receiver
Solid State, Antenna Coupler

- Run 16 Receivers From One Antenna
- Great For Any HF Wideband Signal
- Built-in Supply And Transistor Condition
- Metering
- BNC Connectors On All Ports

Only \$125.

REFERENCES

1. D.A. Mindell, "Dealing with a Digital World," *Byte*, 14(8): 1989, page 246.

2. B.P. Bergeron, NUIJN, "Digital Signal Processing: The Fundamentals," *Ham Radio*, April 1990, page 24.

3. B.P. Bergeron, NUIJN, "Digital Signal Processing: Working in the Frequency Domain," *Communications Quarterly*, November 1990, page 45.

4. B.P. Bergeron, NUIJN, "Digital Signal Processing: Artificial Intelligence Techniques," *Communications Quarterly*, February 1990, page 77.

5. K. Sheldon, "Probing Space by Camera: The Development of Image Processing at NASA's Jet Propulsion Laboratory," *Byte*, March 1987, page 143.

6. J.S. Lim, "Two-Dimensional Signal Processing," *Advanced Topics in*

the world of digital image communications. Inexpensive data controllers, such as the MFJ-1278, provide SSTV capabilities, including the ability to save images to disk. Once on disk, the digital images can be processed with virtually any home computer, using algorithms like those discussed here. ■

Signal Processing, Lim and Oppenheim, editors, Prentice Hall, Englewood Cliffs, New Jersey, 1988.

7. R.K. Palm, *The FCC Rule Book*, American Radio Relay League, Newington, Connecticut, 1988.

8. R.W. Nettleton, J.F. Lindsey, S.V. Varanasi, and D.F. Difonzo, "Communication Systems," *Handbook of Modern Electronics and Electrical Engineering*, Below, editor, John Wiley & Sons, New York, 1986.

9. M.J. Wilson, "Image Communications," *The ARRL Handbook for the Radio Amateur*, Wilson, editor, American Radio Relay League, Newington, Connecticut, 1987.

10. W.T. Orr, W6SAI, "Specialized Amateur Communications Systems and Techniques," *Radio Handbook*, Howard W. Sams & Company, Indianapolis, Indiana, 1987.

11. B.M. Dawson, "Introduction to Image Processing Algorithms," *Byte*, March 1987, page 169.

12. J.L. Star, "Introduction to Image Processing," *Byte*, February 1985, page 163.

13. T. Chard, "Computers as Part of Medical Equipment," *Computing For Clinicians*, Elmore-Chard, London, England, 1988.

14. R. Cloutier, "Plug-in Modules Allow Image Processing on Non-dedicated PCs," *Computer Technology Review*, Fall 1986, page 115.

15. D. Brown and S. Silverman, "Flexible High Speed Image Processing with Non-von Neumann Design," *Computer Technology Review* 8(16): 1986, page 91.

16. K. Preston, "The Abingdon Cross Benchmark Survey," *Computer*, 22(7): 1989, page 9.

17. S. Garcia, "Using the Image Wise Video Digitizer," *Byte*, July 1987, page 113.

SOLID STATE 75S-3 RECEIVER

*Remove the tubes and update your
old receiver*

A few years ago, I published an article in *Ham Radio* that described a solid-state conversion of the Collins 75A-4 receiver! That article generated a number of inquiries from Amateurs expressing an interest, not in the 75A-4, but in Collins 75S series receivers. These inquiries prompted me to attempt a conversion of the 75S-3.

I first tried to convert the 75S-3 by replacing the tubes with homebrewed solid-state equivalents, much like those described by Sartori? These equivalents seemed to do a reasonably good job. However, I felt I could obtain a higher quality conversion with improved frequency stability if I made minor changes to the existing circuits and used more complex oscillators for the VFO and tunable BFO.

I also thought the inside of the receiver would look a lot better if the solid-state circuits were hidden below deck. Consequently, I removed most of the tube sockets, replacing them and the tubes with small perfboard-mounted circuits located under the chassis. I covered the tube socket holes with small rectangular aluminum plates mounted from the underside. On the outside, the receiver still looks like a 75S-3 (Photo A); but when you look inside, you won't see any tubes (Photo B).

Performance characteristics

Table 1 lists comparative performance specifications for those parameters of the solid-state receiver which are different from the vacuum-tube original. Parameters not listed are essentially the same for both versions. The comparative data is the result of



Photo A. Front view of the 75S-3 receiver.

measurements made on the vacuum-tube 75S-3 before its conversion and repeated later on the solid-state version.

I purposely reduced the solid-state version's sensitivity to obtain an improvement in the intermodulation distortion (IMD) and overload capability. The solid-state version's input noise is still reasonably low relative to the typical background and galactic noise from the antenna.

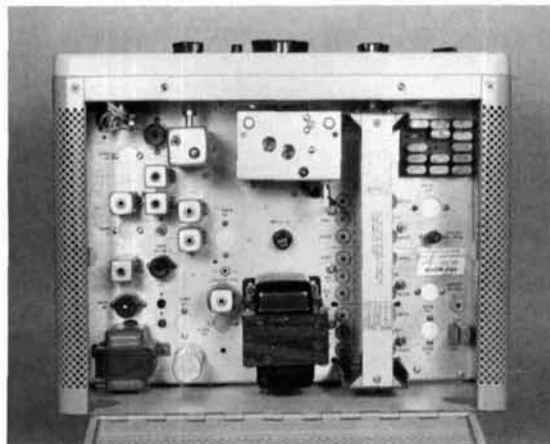


Photo B. Top inside view of the modified 75S-3 receiver.

Circuit description

The overall schematic diagram for the receiver is shown in **Figures 1A** through **1E**. **Figure 1** is basically the same as the schematic shown in the instruction book for the 75S-3, except for the following differences:

- An AGC-controlled input attenuator has been added at the receiver input.
- The AGC bus uses a buffer amplifier.
- The more complex solid-state circuits that replace the tubes are shown only as blocks within the overall diagram.

- Other minor circuit changes have been made.

Crystal calibrator

Figure 2 shows the solid-state, 100-kHz crystal-calibrator schematic and compares it with the original 6DC6 tube circuit. The solid-state circuit's active element is a CD4011B CMOS quad NAND gate. Gate U1a, crystal Y17, resistors R2 and R3, and capacitors C1 and C61 comprise a Pierce oscillator. Gates U1b and U1c square up and buffer the oscillator output. Gate U1d ena-

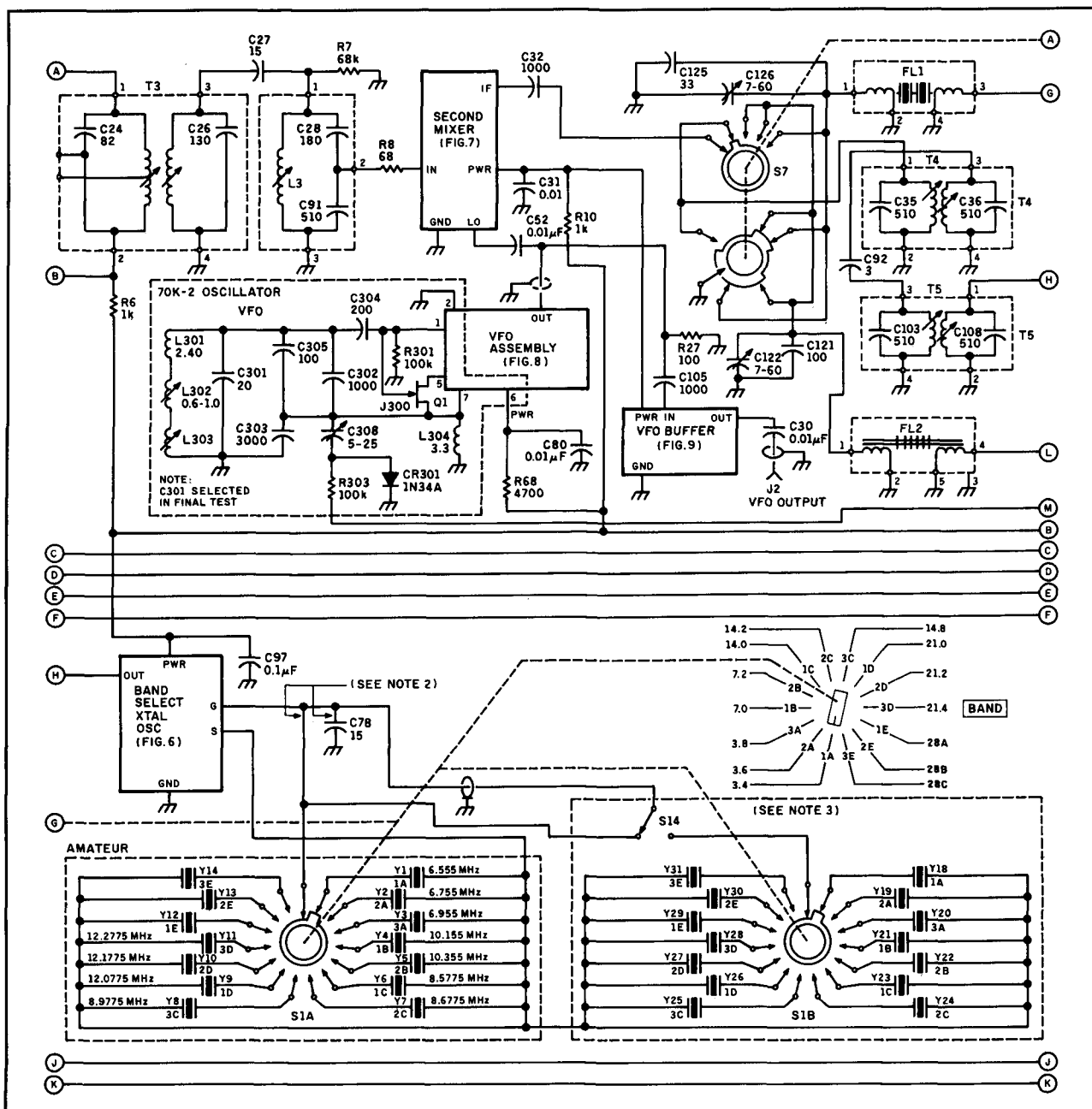


Figure 1B. Part of overall schematic showing the VFO.

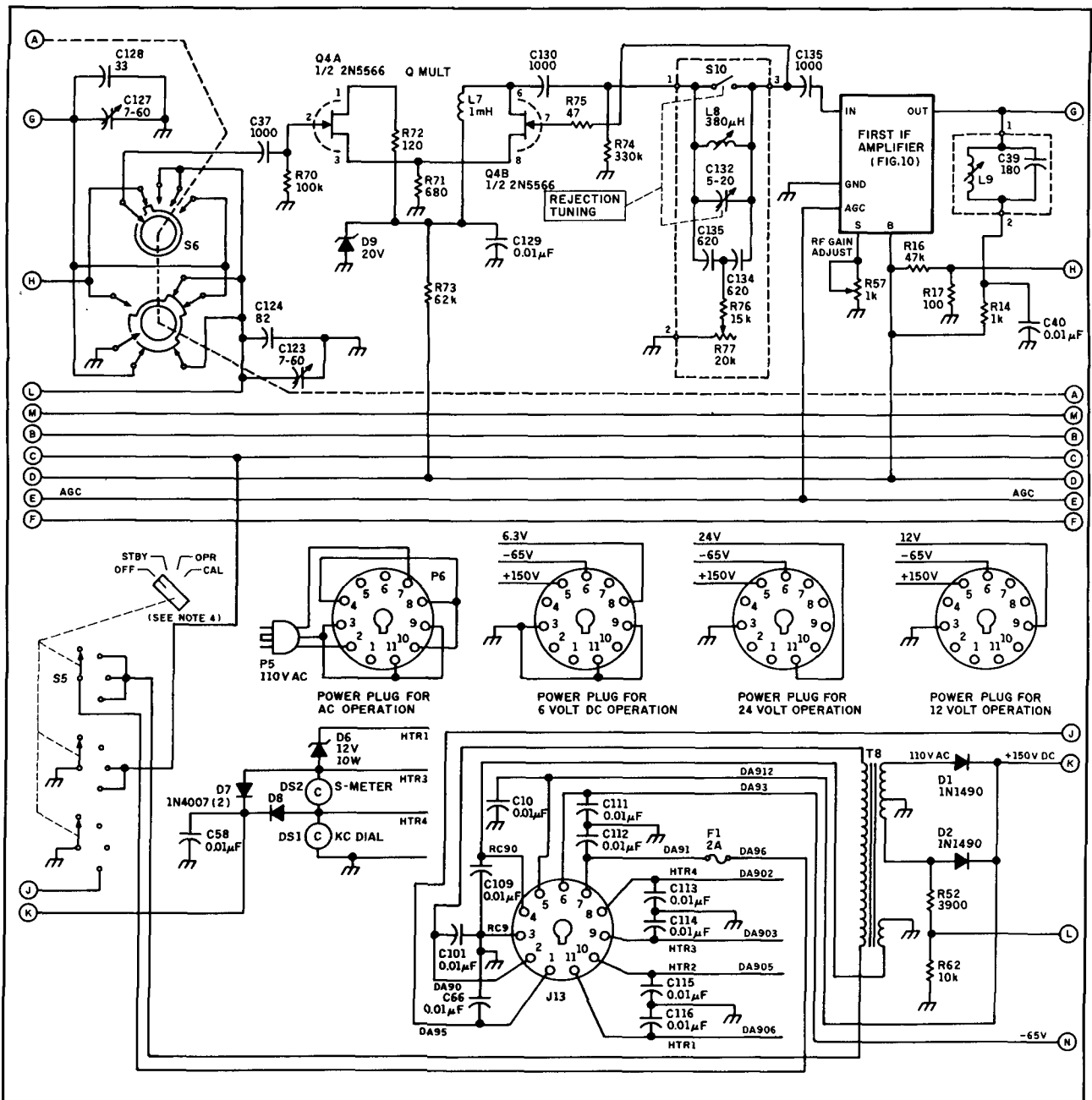


Figure 1C. Part of overall schematic showing the Q multiplier circuit.

bles the oscillator when switch S5 is in the CAL position. The output signal from the calibrator circuit is coupled to the receiver's input through capacitor C12, as shown in Figure 1A.

Input attenuator

I added the AGC-controlled input attenuator block, shown in Figure 1A and schematically in Figure 3, to increase the AGC range. The attenuation provided by this circuit is a function of the voltage on its AGC input. The attenuator provides approximately 20 dB of attenuation when a 0.1-volt signal is applied to the receiver input. The

attenuation is approximately 6 dB for 100 μ V input and can go as high as 40 dB with full AGC.

The input attenuator is a Mini Circuits SAY-1 high-level, double-balanced diode mixer. The signal output at the mixer LO port is proportional to the magnitude of the DC current flowing into the IF port. The mixer IF port is driven by the "current mirror," Q1 and Q2. High AGC levels drive Q1 toward cutoff, reducing its drain current. A corresponding decrease in IF-port current occurs, because Q2b's collector current mirrors Q1's drain current.

Harmonic generation by the SAY-1, and any corresponding increase in receiver IMD,

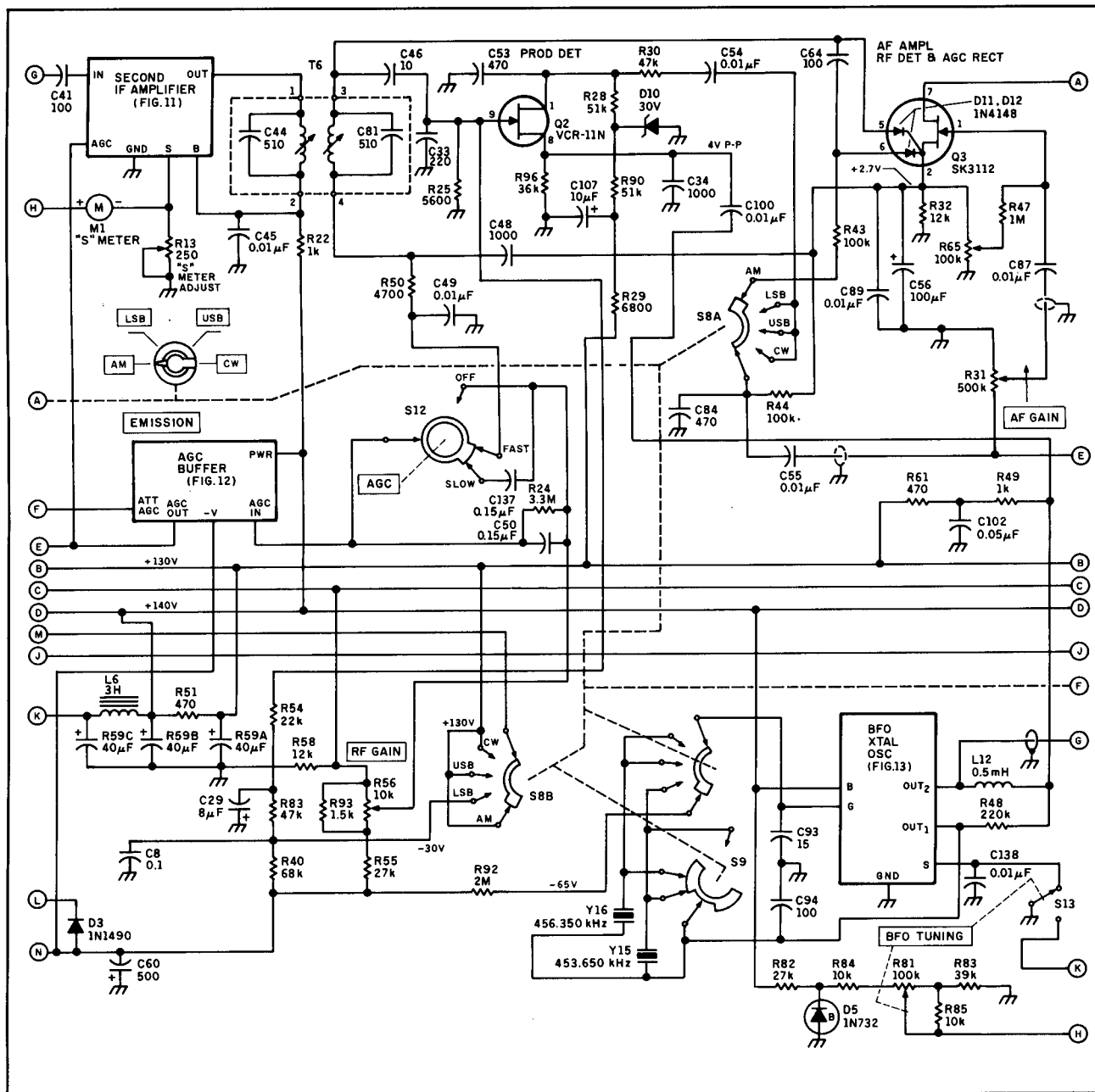


Figure 1D. Part of overall schematic showing the AGC buffer amplifier.

appears to be negligible when the receiver is tuned to signals below the 100 μ V level, where the attenuation of the SAY-1 is at a minimum. When the receiver is tuned to signals greater than 100 μ V, the IMD products generated by the SAY-1 are competing with a much larger received signal and don't seem noticeable.*

The supply voltage for the current mirror circuit is developed from the 6.3-volts AC filament supply through rectifier D1 and filter capacitor C1. The current mirror oper-

ates using AC or DC voltages at the power input. The magnitude of these voltages ranges from 6 to 12 volts, making the circuit compatible with the various power supply modes for which the receiver was originally designed.

The zero-bias drain current I_{dss} of JFET Q1 should be approximately 20 mA.

RF amplifier

Figure 4 shows the schematic of the solid-state RF amplifier compared with the original 6DC6 tube circuit. The new RF amplifier is a dual-gate MOSFET (Q1). Q1 is con-

*A good substitute for the SAY-1 might be a Mini Circuits PAS-3 electronic attenuator which achieves about 50 dB of attenuation and has considerably less harmonic generation. I used the SAY-1 because of its high level capability and because I had them on hand.

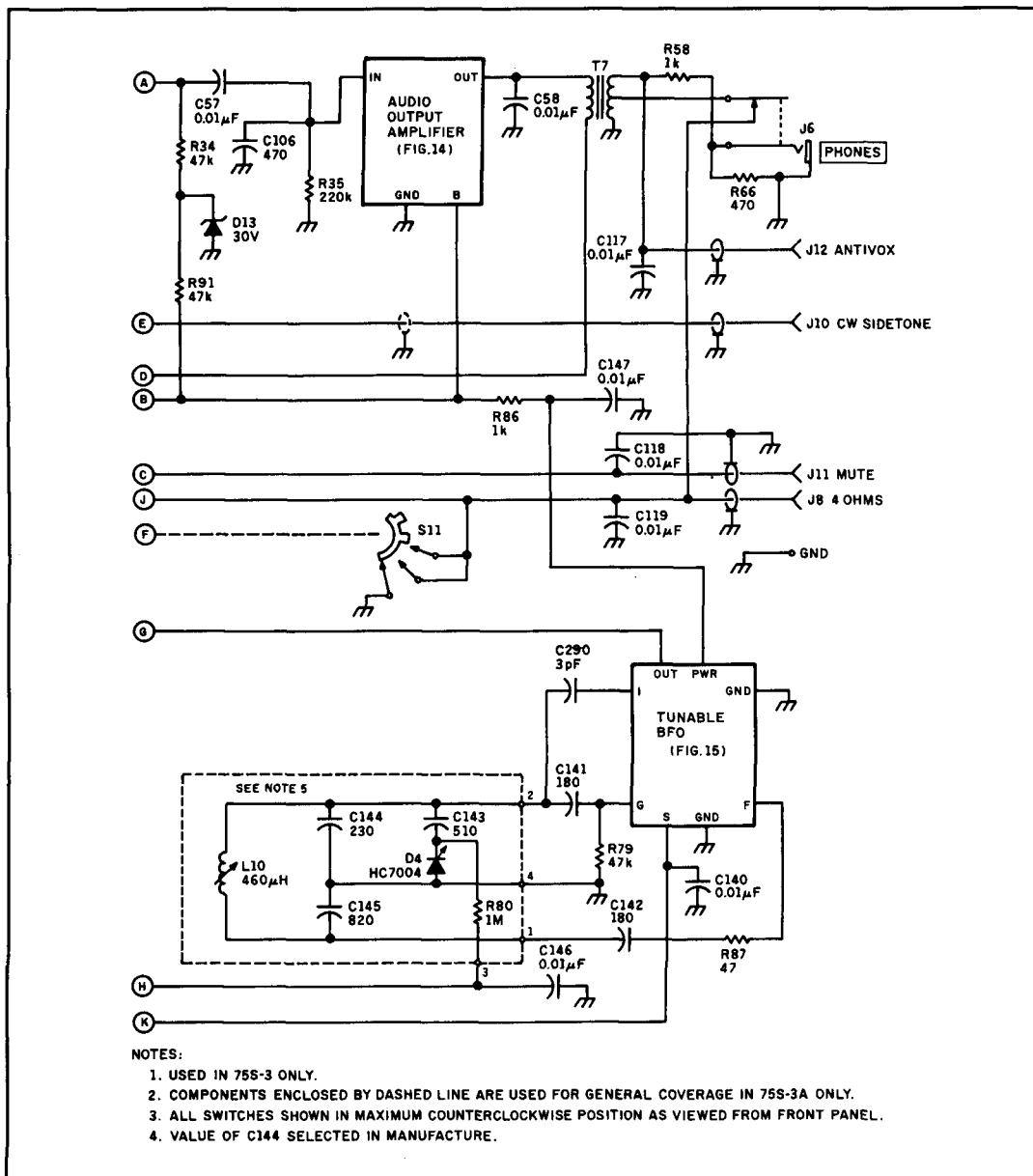


Figure 1E. Part of overall schematic showing the tunable BFO.

nected in cascode with Q2. Transistor Q2 (D40N5) has a 375-volt collector breakdown voltage, making it compatible with the receiver's 140-volt plate supply. Q2 also has a high cut-off frequency and low output capacitance (3 pF), making it a good substitute for the 6CD6 tube.

The screen supply voltage that originally went to the vacuum tube through R2 is reduced to 15 volts by R5 and D1. The 15-volt level is used for Q2 base bias. The AGC bus is connected to Q1 gate 2. R4 keeps the current through Q2 above 1 mA when Q1 approaches cutoff with high AGC levels.

I built this circuit on a piece of copper-clad circuit board mounted to the underside of the chassis near the original RF amplifier

tube location. I soldered a copper-clad shield between Q1 and Q2 to ensure adequate isolation between input and output. The crystal-calibrator circuit is mounted on a spacer directly above the RF amplifier. These circuits are visible in the lower left-hand corner of **Photo C**.

First mixer

Figure 5 shows the solid-state first-mixer schematic and compares it with the original 6U8/6EA8 tube circuit. The triode mixer equivalent consists of JFET Q1 in cascode with Q2. The pinch-off voltage of VCR-11N (Q1) is specified by the manufacturer as between 8 and 12 volts. This large pinch-off

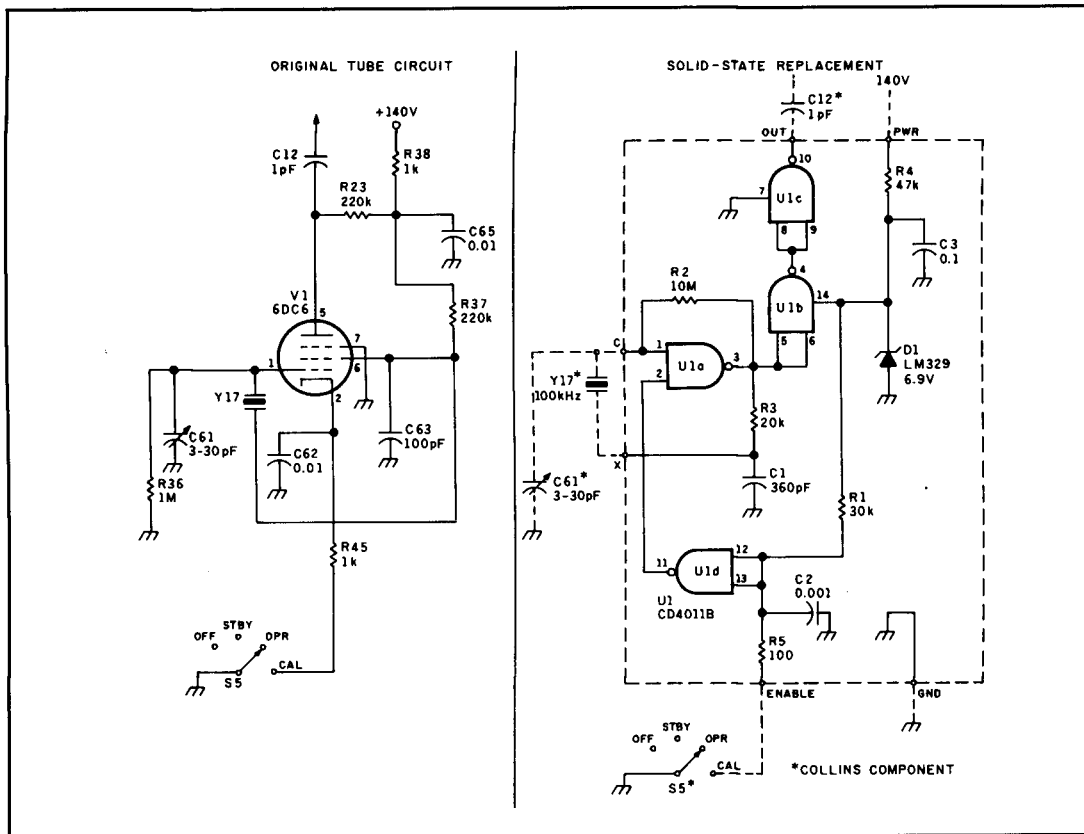


Figure 2. 100-kHz crystal calibrator schematic.

voltage and its relatively tight tolerance make VCR-11N a good substitute for the vacuum-tube triode in this application.

R8 ensures a minimum quiescent current of about 1 mA through Q2. Trimpot R5 is adjusted during receiver alignment to optimize Q1's bias for maximum conversion gain. VCR-11N is a dual device; only half is used in this circuit.

Band-select crystal oscillator

Figure 6 shows the schematic of the solid-state band-select crystal oscillator compared with the original 6U8/6EA8 tube circuit. Chassis-mounted components C79, L14, and L15 are remounted on the circuit board. The cascode connection of Q1 with Q2 and Q3 comprise the pentode equivalent of the original electron-coupled oscillator. The transconductance from grid to screen is simulated by the AC-coupled cascode of Q1 and Q3. Approximately one fifth of the signal current from Q1 is coupled through Q3 and back through the selected crystal of the oscillator to sustain oscillation. The remainder of the signal current from Q1 appears at Q2's collector and drives the oscillator output circuit. Q1 is selected to have a zero-bias drain current of about 20 mA.

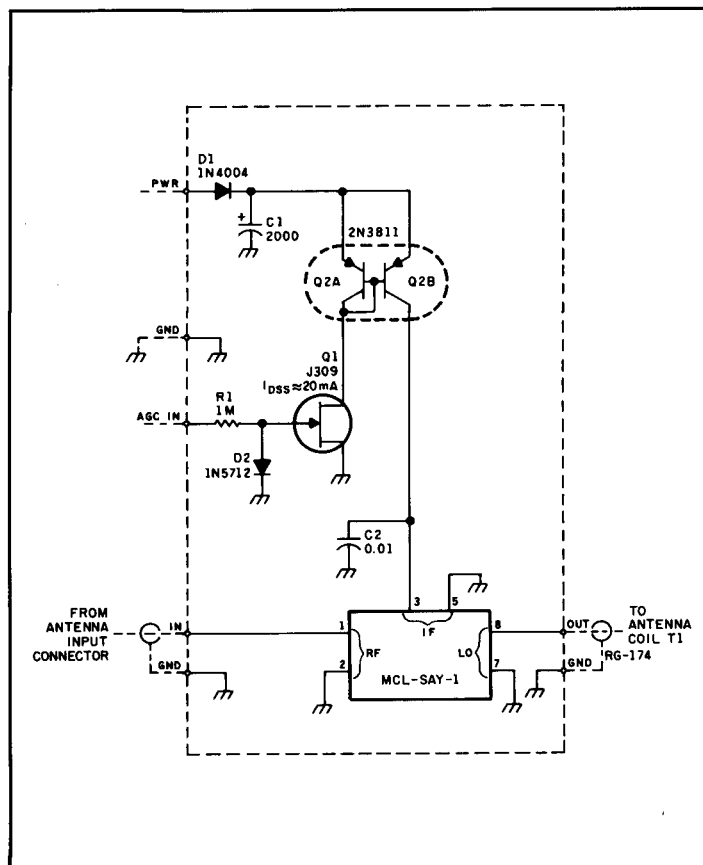


Figure 3. Input attenuator schematic.

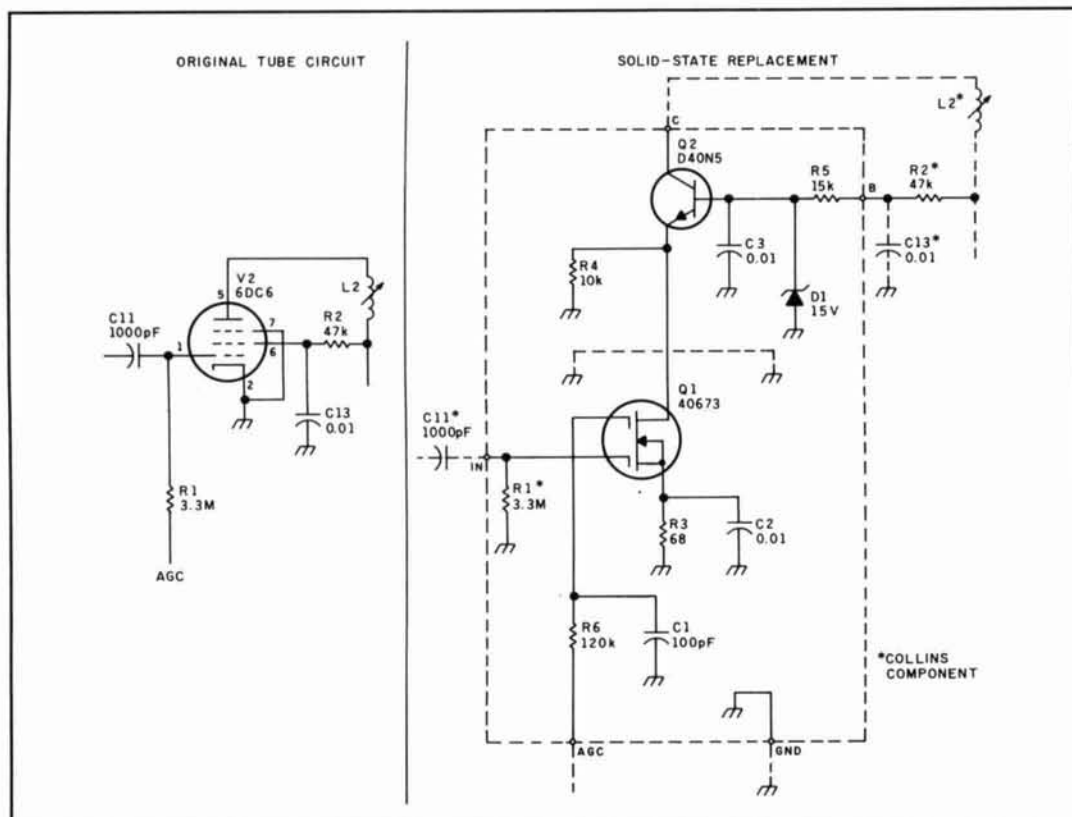


Figure 4. RF amplifier schematic.

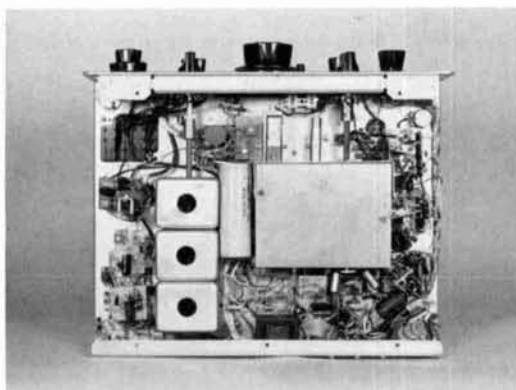


Photo C. Bottom view of the modified 75S-3 receiver.

The crystal band-select oscillator output should be about 6 volts peak-to-peak, as measured at J1 with the 100-ohm crystal oscillator load (R41) in place. The oscillator output is highest on the 40 and 80-meter bands. I reduced the output on 40 and 80 meters to 6 volts peak-to-peak by shunting the output tuned circuits on those bands with resistors R94 and R95, shown schematically in **Figure 1A**.

Second mixer

Figure 7 shows the schematic of the solid-state second mixer and compares it with the original 6U8/6EA8 tube circuit. The circuit

of the second mixer is essentially the same as that of the first. It differs from the first mixer in that the LO signal is AC coupled into the source.

I reduced the gain ahead of the second mixer by taking the mixer input from the tap at terminal 2 of the IF transformer assembly rather than at terminal 1, as was done in the original circuit. This gain reduction improves the receiver's IMD and overload capability.

Permeability tuned VFO

Figure 1B and **Figure 8** show the VFO schematic. **Figure 8** compares the original 6AU6-tube circuit with the solid-state replacement. JFET Q1 is the oscillator's active element. JFET Q2, in cascode with Q3, buffers the oscillator output. Q1 is selected for low zero-bias drain current (I_{DSS}) to minimize heating. I used a J300 with an I_{DSS} of about 3 mA. An SK9161 would probably work as well.

I disassembled the 70K-2 and soldered Q1 directly to the tube-socket solder lugs. T301, C307, the filament leads, and the output coax were removed. R302 was shorted so the 130-volt supply goes directly to tube socket pin 6.

The assembly shown in **Photo D** was constructed as a platform for mounting the

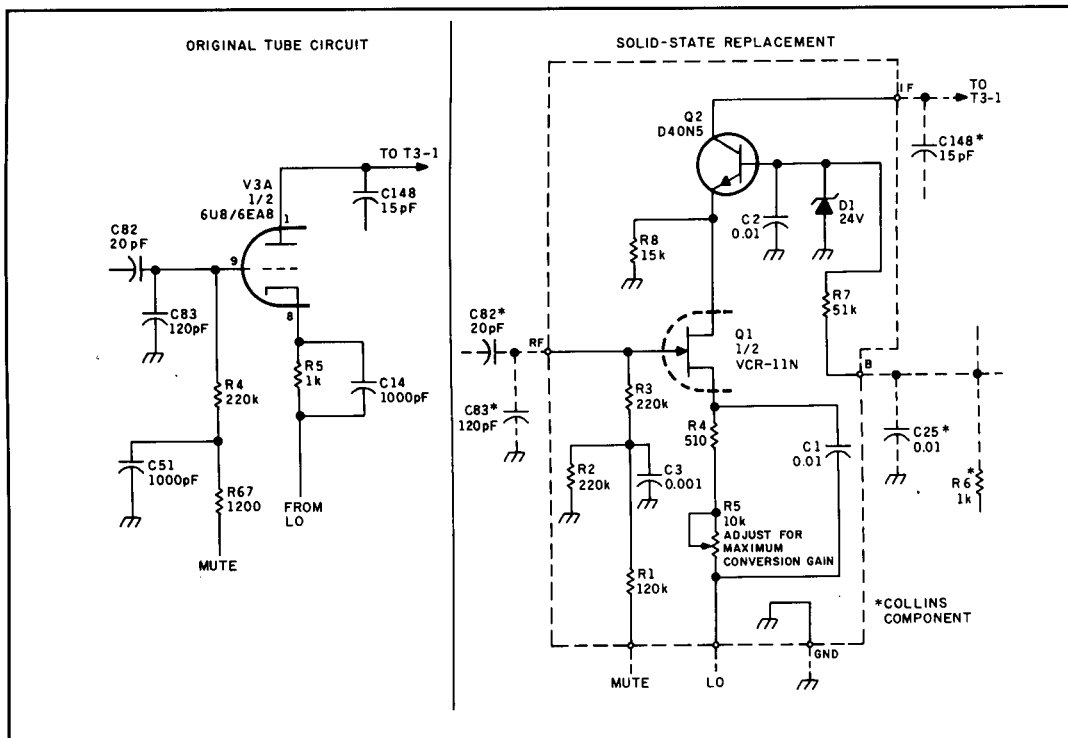


Figure 5. First mixer schematic.

external oscillator components shown in **Figure 8**. This assembly consists of a 7-pin miniature plug attached to an aluminum heat sink. Most of the small components

are mounted around the perimeter of the 7-pin plug on a small perboard. Pin 1 of the 7-pin plug was removed. C4, L1, Q3 and a miniature RF connector are attached to the

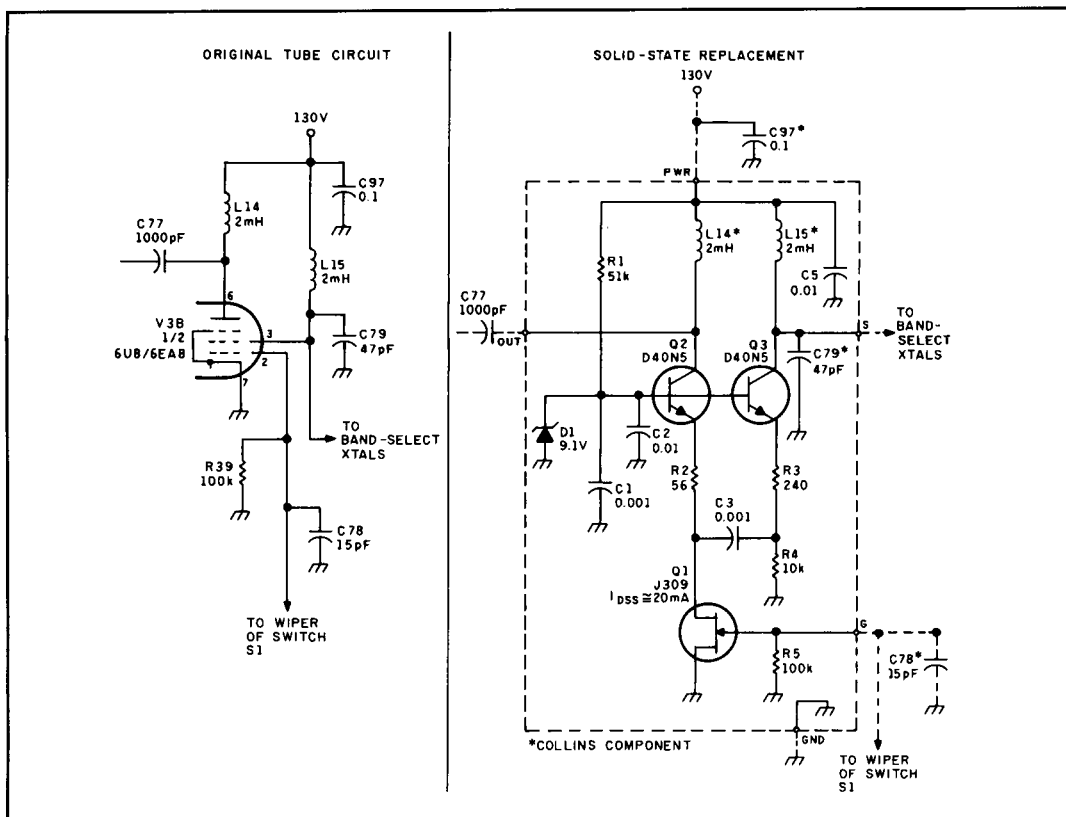


Figure 6. Band-select crystal oscillator schematic.

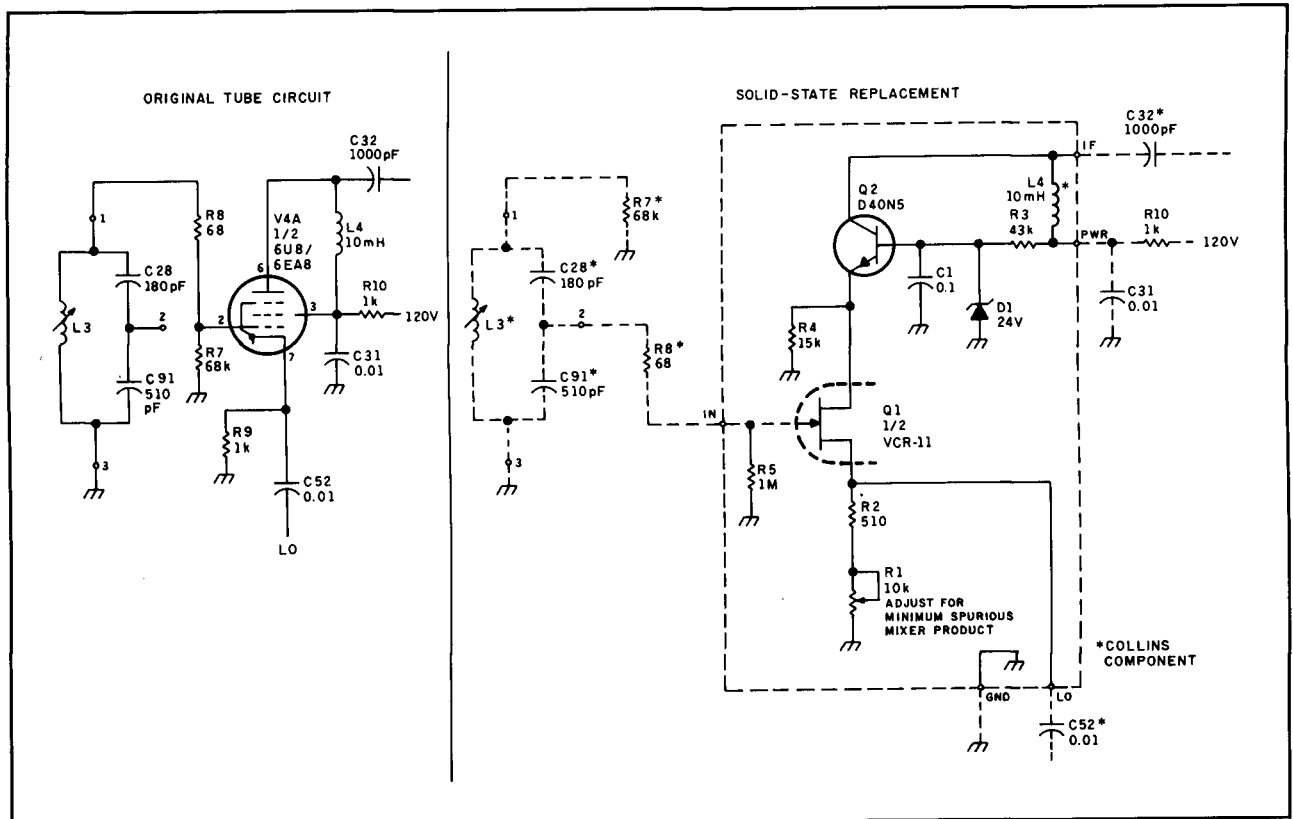


Figure 7. Second mixer schematic.

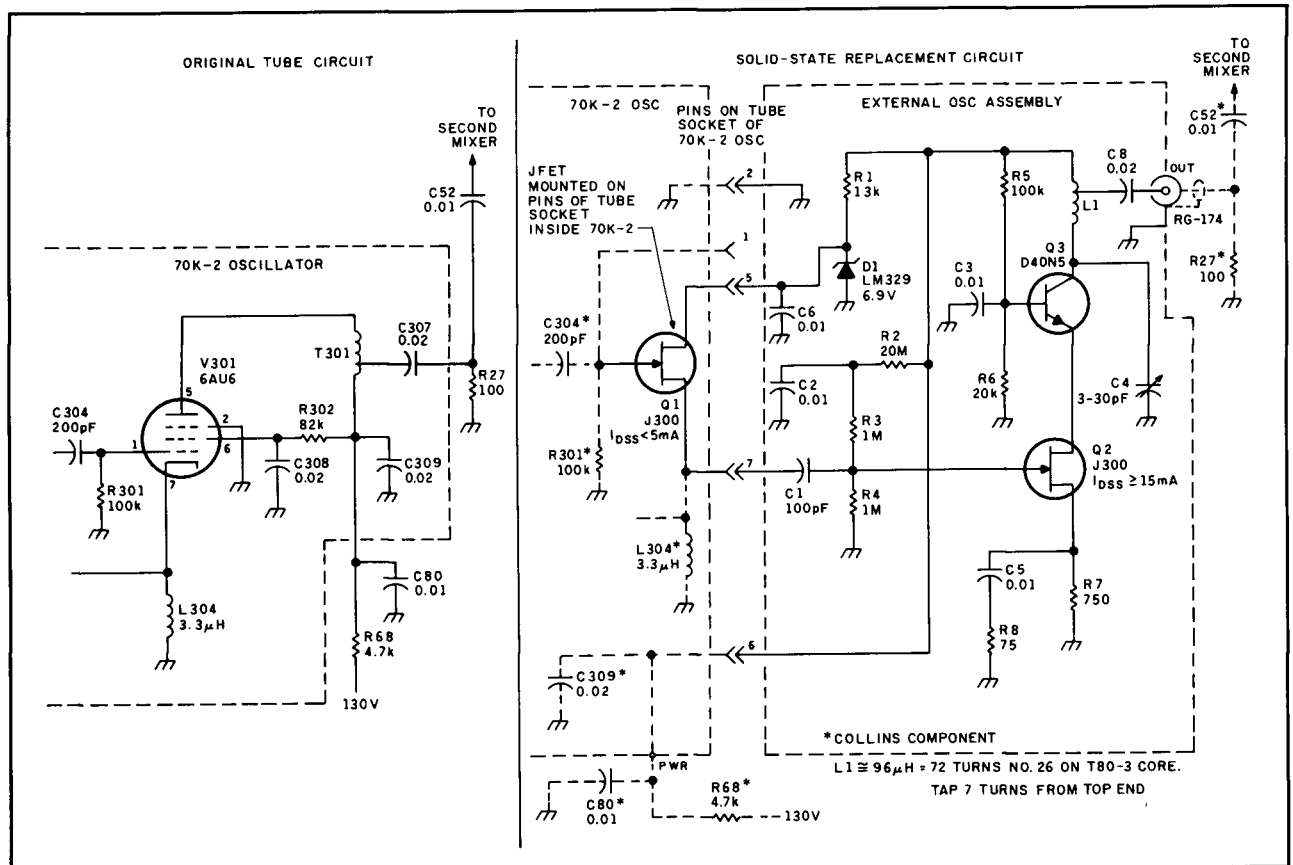


Figure 8. VFO schematic.

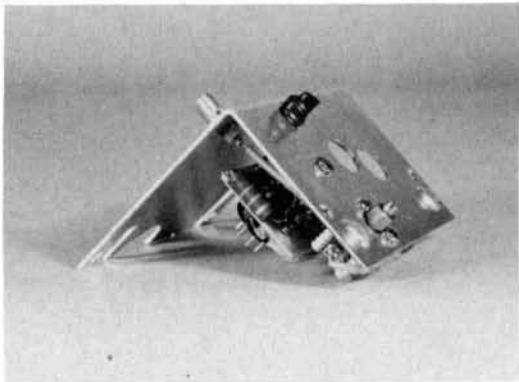


Photo D. VFO assembly.

aluminum heat sink, which is plugged into the tube socket and secured with two threaded lugs extending from the back of the 70K-2 assembly. The VFO RF output is by way of the RF connector mounted on the heat-sink assembly. I punched two holes in the heat-sink assembly top deck to allow access to L302 and C308 on the 70K-2. The main reasons behind this modification of the 70K-2 oscillator are:

- Q1 is soldered firmly to the inside of the oscillator, away from heat and mechanical disturbance.
- The oscillator output is buffered heavily by Q2 and Q3.
- The heat generated by Q3 is diffused and dissipated by the heat sink.
- The external oscillator assembly can be

removed easily.

When the oscillator is completed, trimmer C4 should be adjusted to resonate with L1 at about 2.6 MHz. The value of R8 should be selected so that 8 volts peak-to-peak is developed across R27 (Figure 1B). As a precaution, I used several mica insulators between Q3 and the heat sink to minimize stray capacitance from the Q3 collector to ground. Too much stray capacitance at this point detunes L1 beyond the range of C4.

I measured VFO drift by placing the receiver in the SSB mode and tuning in an external crystal calibrator. The audio-frequency output tone was measured for four hours, beginning from a cold start. A plus and minus 5-Hz drift occurred in the first five minutes after the receiver was turned on. A positive 150-Hz drift then built up gradually over the next two hours as the receiver warmed up. After warm up, the drift stabilized at about 5 Hz per hour. These drift rates are a significant improvement over those measured for the original receiver.

VFO buffer

Figure 9 shows the solid-state VFO buffer schematic and compares it with the original 6U8/6EA8 tube circuit. Q1 and Q2 are a complementary emitter follower. Diodes D1 and D2, in series with R2, provide quiescent

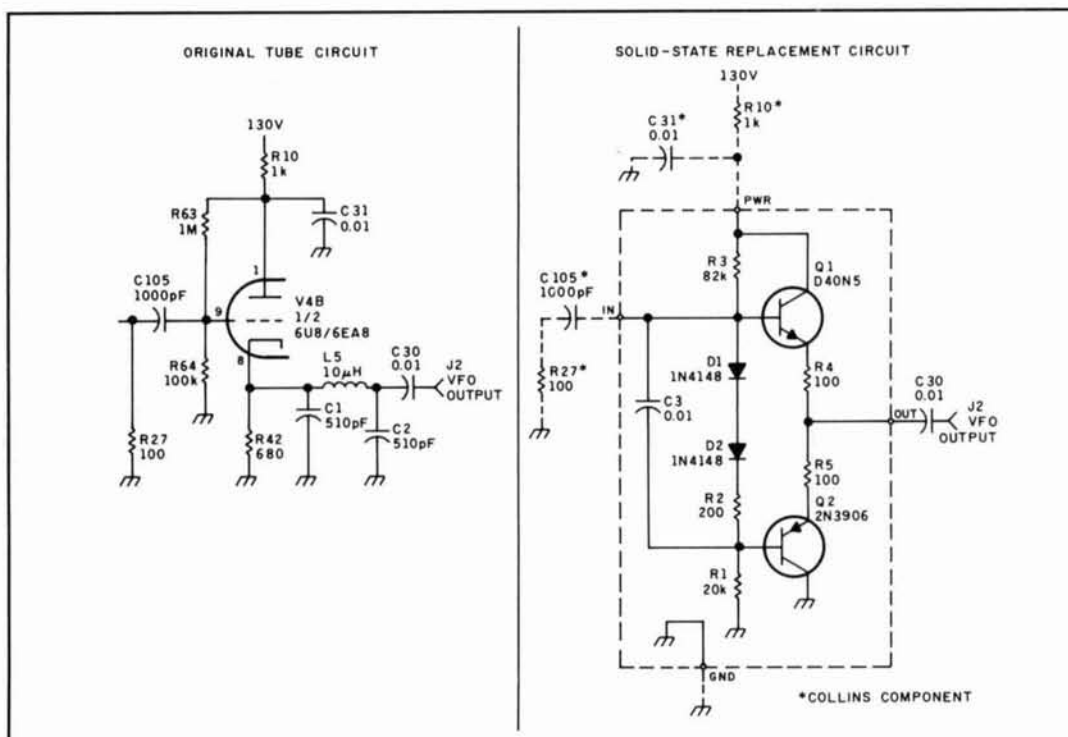


Figure 9. VFO buffer schematic.

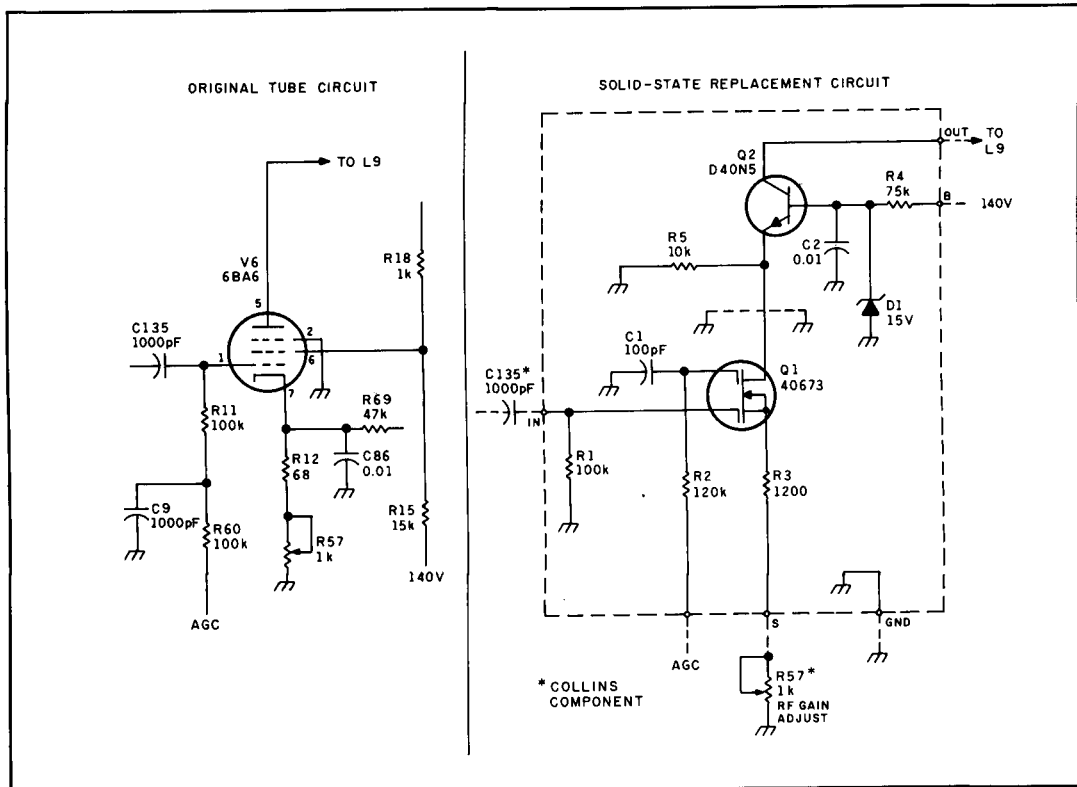


Figure 10. First IF amplifier schematic.

bias for the transistors to eliminate cross-over distortion. The filter network—C1, C2, and L5—used in the original circuit, isn't needed.

Q multiplier

The Q multiplier circuit is shown schematically in **Figure 1C**. This circuit is the first stage in the 455-kHz IF amplifier. The original circuit used a 12AX7 tube. I modified this circuit by changing R73 to 62 k and substituting a 2N5566 dual JFET (Q4) for the 12AX7. (An SK9148 should work as well for Q4.) Zener diode D9, placed at the junction of R73 and C129, sets the JFET drain voltage to 20 volts. I mounted the JFET on a 7-pin miniature plug that substitutes for the tube. The JFET could just as easily have been soldered to the solder lugs of the existing socket.

The value of R76 (15 k), located inside the shielded enclosure with the notch-filter components, may have to be adjusted to obtain adequate narrowness and depth of notch.

First and second IF amplifiers

Figure 10 shows the schematic of the solid-state first IF amplifier and compares it with the original 6BA6 tube circuit. Dual-gate MOSFET Q1 is connected in cascode with Q2. AGC is applied to the second gate

of the MOSFET. The RF gain adjust pot, R57, is retained. Cathode bias resistors R69 and R12 and cathode bypass capacitor C86 are removed.

The second IF amplifier is shown schematically in **Figure 11**. Essentially, this circuit is identical to that of the first IF. The S meter and bias resistors R13, R16, and R17 are retained.

I built the IF amplifiers on copper-clad circuit board, mounted on the underside of the chassis. I mounted a copper-clad shield between the MOSFET and the D40N5 on each circuit. Additional copper-clad shields keep amplified IF signals from feeding back into the second-mixer output and 455-kHz IF-input stages. One of these shields overlies the circuit in the vicinity of the second mixer. This shield and the IF circuit are shown in the center and upper right-hand corner, respectively, of **Photo C**.

AGC buffer

The AGC buffer amplifier (which appears as a block in **Figure 1D**) is shown schematically in **Figure 12**. This buffer adds a DC-offset voltage to the AGC-rectifier output so the AGC voltages are compatible with the dual-gate MOSFET IF and RF amplifiers and the AGC-controlled attenuator. Minimum AGC is applied when the second gates of the RF and IF MOSFET amplifiers

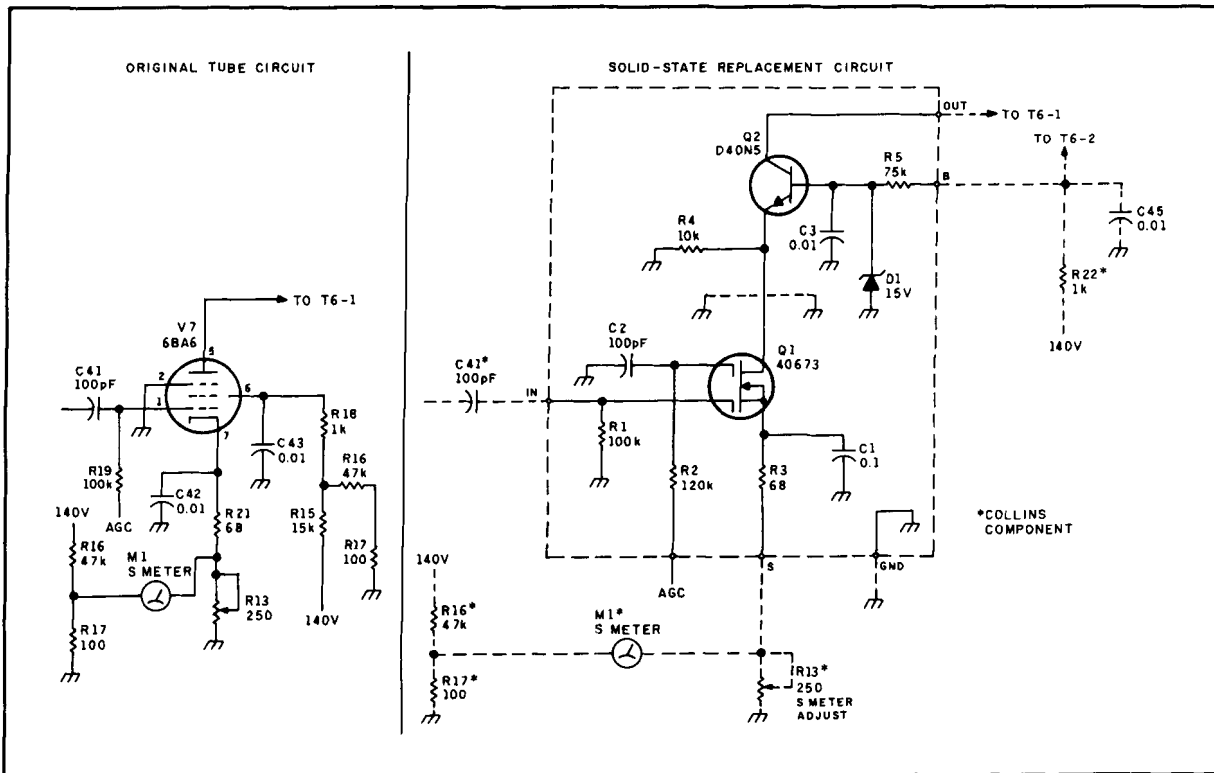


Figure 11. Second IF amplifier schematic.

are at 1.5 volts. The 1.5-volt offset is obtained from the source voltage developed by Q1 on the AGC buffer board. The source voltage of Q1 can be adjusted by trimpot R2, also located on the buffer board. Diode D1 lowers the attenuator AGC voltage to about 0.6 volt below that of the AGC output. Trimpot R2 on the AGC buffer board is adjusted by shorting the buffer-board AGC IN terminal to ground, then adjusting R2 for 1.5 volts at the AGC out terminal.

Product detector

The product detector was originally the triode section of the 6U8/6EA8 tube (V8). The solid-state replacement for this section of V8 is shown in **Figure 1D**. The triode section was replaced by JFET Q2, a VCR-11N.

I substituted a 36-k resistor (R96) for inductor L16. R28 was changed to 51 k. R90 (51 k) and zener diode D10 were added so Q2's drain voltage never exceeds about 30 volts. Q2's quiescent drain voltage should be approximately 18 volts. R96's resistance should be adjusted up or down as necessary to obtain the right drain voltage.

I mounted the JFET on a 9-pin miniature plug that replaces the tube's triode section.

BFO crystal oscillator

Figure 13 shows the solid-state BFO crys-

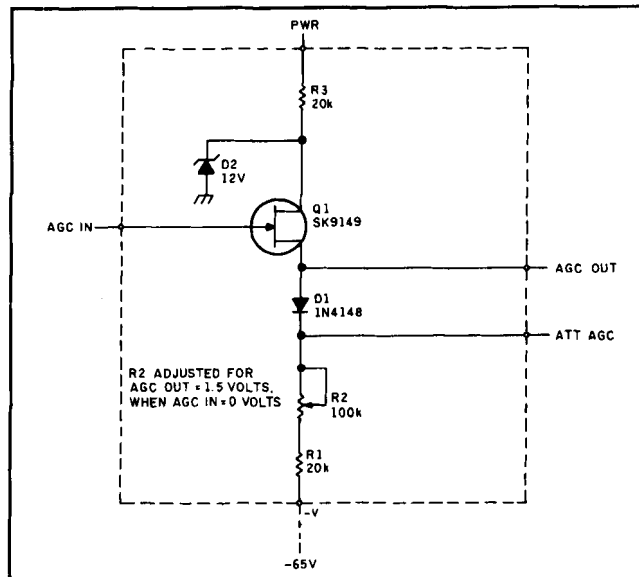


Figure 12. AGC buffer amplifier schematic.

tal oscillator schematic and compares it with the original 6U8/6EA8 tube circuit. This circuitry is built on a small piece of perfboard mounted below tube socket V8. The cascode connection of Q1 with Q2 and Q3 comprise the pentode equivalent of the original electron-coupled oscillator. The transconductance from grid to screen is simulated by the AC-coupled cascode circuit of Q1 and Q3. A fraction of the signal current from Q1 is coupled through Q3 and

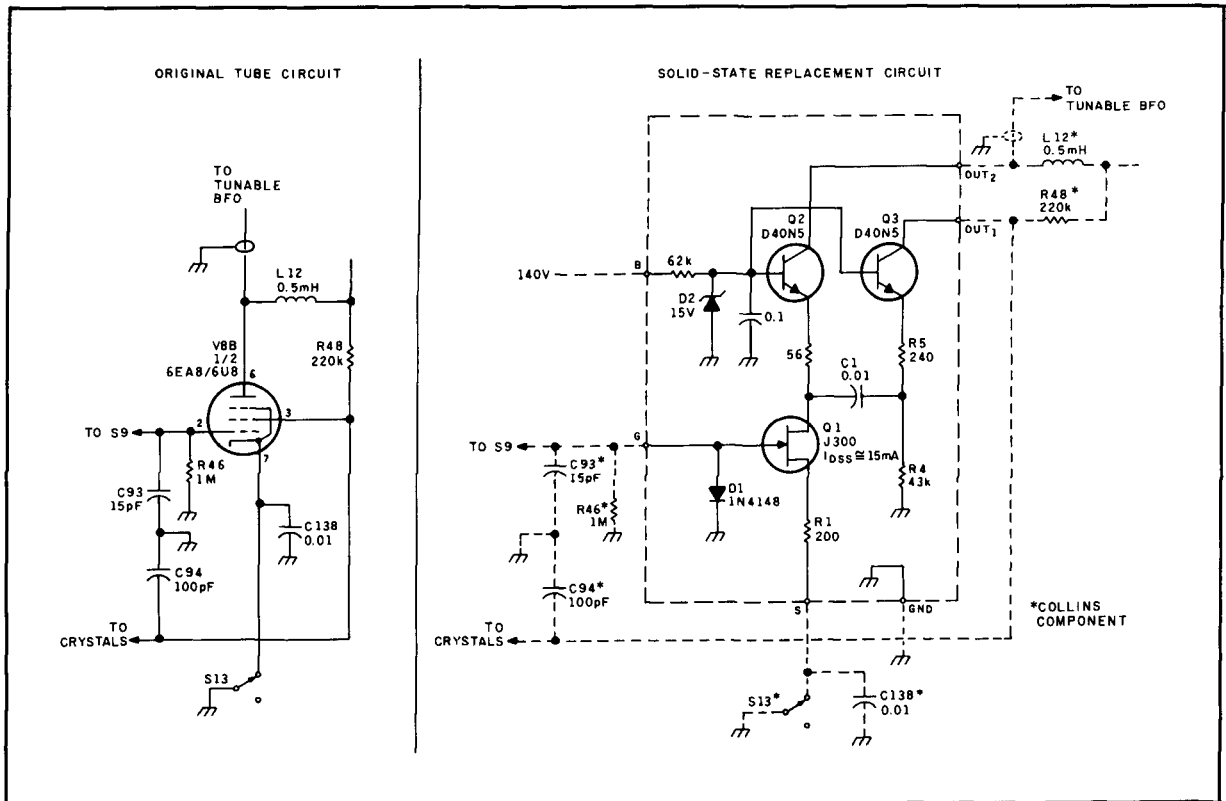


Figure 13. BFO crystal oscillator schematic.

back through the selected oscillator crystal to sustain oscillation. The remainder of the signal current from Q1 appears at Q2's collector and drives the oscillator output circuit.

The BFO output should have an amplitude of approximately 4 volts peak-to-peak measured at the junction of C34 and C100 (refer to **Figure 1D**). These capacitors are located to the right of the product detector in **Figure 1D**.

AF amplifier, AF detector and AGC rectifier

I replaced the 6AT6 tube used for audio and AGC detection, and audio amplification with JFET Q3 and diodes D11 and D12 (see **Figure 1D**). I mounted the JFET and the diodes on a miniature 7-pin plug that substitutes for the tube. These components can be soldered to the tube-socket solder terminals just as easily.

I changed resistor R65 to a 100-k trimpot and reduced R47 to 1 meg. I reconnected R65 and R47 as shown in **Figure 1D**. R65 is adjusted so that a 2.7-volt bias is developed across R32. I reduced R34 to 47 k. I also added R91 (47 k) and D13, as shown in **Figure 1E**, so the drain voltage of Q3 never exceeds 30 volts.

Audio output amplifier

Figure 14 shows the schematic of the audio output amplifier and compares it with the original 6BF5 tube circuit. The new audio amplifier uses paralleled JFETs Q1 and Q2 in cascode with Q3. The total emitter current of Q3 is the sum of the Q1 and Q2 drain currents. R1 and R2 are selected so these drain currents are 15 mA. The Q1 and Q2 zero-bias drain current (I_{dss}) should be 30 mA or greater.

R35 is simply returned to ground in the solid-state replacement circuit.

Q3 dissipates approximately 3.9 watts in this circuit. To provide adequate heat sinking, Q3 is bolted to the receiver chassis. Mica insulators provide electrical isolation between the transistor collector tab and the chassis.

Tunable BFO

Figures 15 and **1E** show the schematic of the solid-state tunable BFO and **Figure 15** compares it with the original 6DC6 tube circuit. The solid-state replacement circuit uses Q1 as the oscillator's active element. The oscillator output signal is taken from resonating network terminal 2. The output signal is routed to buffer amplifier Q2

through 3-pF capacitor C290. C290 is connected directly between resonating network terminal 2 and BFO circuit board terminal 1. Q2 is connected in cascode with Q3. The value of R9 is selected to provide about 4 volts peak-to-peak at the junction of C34 and C100 (see **Figure 1D**).

I measured the BFO drift by placing the receiver in SSB mode with the tunable BFO turned on. Beginning from a cold start, I measured the audio frequency output tone for four hours. A 50-Hz drift occurred in the first thirty seconds after turn on. About 10 Hz of drift occurred in the next ten minutes, followed by a slow drift of 107 Hz over the next two hours as the receiver warmed up. After a 2-1/2 hour warm up, frequency drift was approximately ± 10 Hz per hour.

I performed a second frequency drift test in which the tunable BFO was turned off, but the receiver was allowed to operate and warm up for three hours. At the end of the 3-hour warm up, I turned on the tunable BFO and measured the output-tone drift. After I turned on the tunable BFO, there was a very slow negative drift of about 40 Hz over a 2-hour period. The frequency drift then stabilized at about 10 Hz per hour.

Other circuit modifications

I made other minor circuit modifications to the receiver. These are shown in **Figure 1** and are as follows:

- A 2-meg resistor (R92) was added between R55 and S9, limiting the negative voltage applied to the BFO crystal oscillator JFET gate when S9 is in the AM position.
- A 1.5-k resistor (R93) was paralleled with the RF gain control (R56), and the value of resistor R55 was changed to 27 k. The front-panel manual RF gain control is much too coarse without these changes.
- Resistor R33 (330 ohms), in series with the RF gain control, was short circuited.
- Capacitor C60 was changed to 500 μ F, providing additional filtering of the -65 volt power supply.
- AGC time-constant capacitors C50 and C137 were increased to 0.15 μ F for compatibility with the MOSFET amplifier AGC levels.
- D6, D7, and D8 of **Figure 1C** were added to the filament circuit to provide power to the input-attenuator board of **Figure 3**. D6 provides a fixed 12-volt drop when the receiver is powered using an external 24-volt DC filament supply. D7 and D8 provide a path for 6 or 12-volt DC or AC power to the input-attenuator board.
- The power plug wiring for 6, 12, and 24-volt operation was modified as shown in **Figure 1C**.

Alignment

The receiver is aligned as described in the 75S-3 operator's manual. Before starting the alignment, the trim pots on the first and second mixers should be adjusted for maxi-

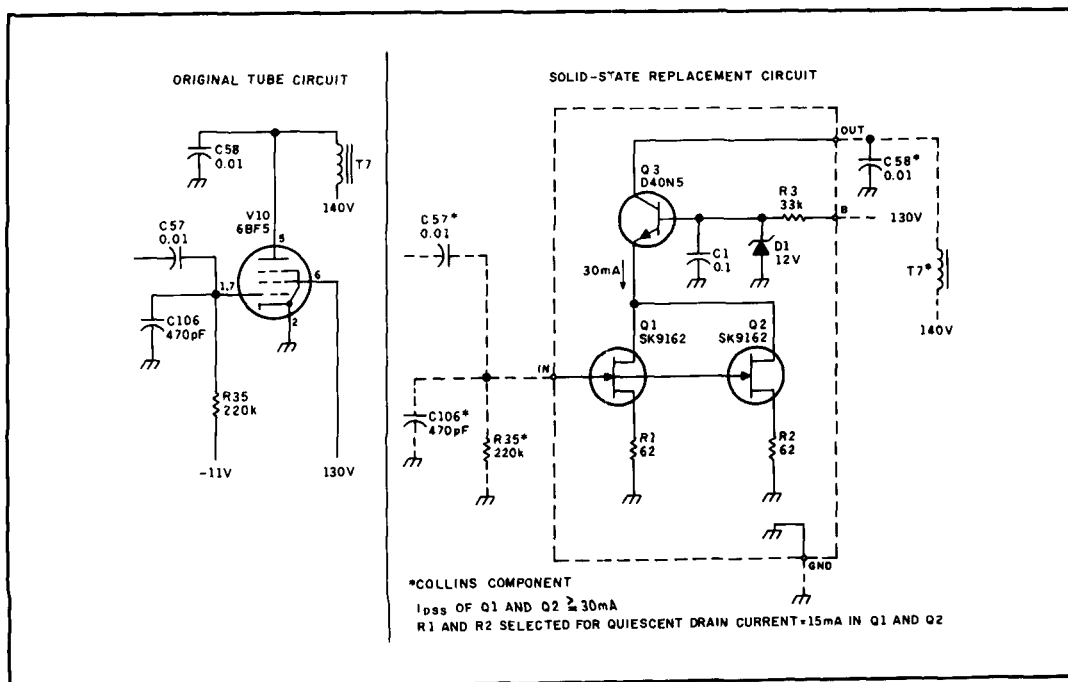


Figure 14. Audio output amplifier schematic.

imum gain, and R65 of **Figure 1D** should be set for 2.7 volts across R32 (AF amplifier, AF detector, and AGC rectifier). Trimpot R2 on the AGC buffer is set properly when the AGC-buffer board AGC out terminal is at 1.5 volts, the AGC switch is in off position, the front-panel RF gain control is fully clockwise, and S5 is in the operate position.

The IF gain is adjusted after the RF and IF stages have been aligned. To make this adjustment, the receiver is set to SSB mode and the AGC is turned to off. An RF generator is set to 14.1 MHz and the generator's attenuator is adjusted for an open-circuit output of 1 μ V rms. The generator is connected to the receiver and tuned for maximum signal. A low-capacitance scope probe is connected across R25 of **Figure 1D** (product-detector input) and RF gain pot R57 (**Figure 1C**) is adjusted for approximately 0.2 volt peak-to-peak, as displayed on the oscilloscope.

Next, the receiver is tuned to the "birdie" at 7.047 MHz. The trimpot on the second mixer board is adjusted for minimum amplitude of the tweet. This adjustment minimizes 5th harmonic generation in the second mixer and should put the amplitude of all tweets within or below the amplitude

specified for the original vacuum-tube receiver.

For S meter calibration, the generator's open-circuit output is set to 100 μ V rms. Pot R13 is adjusted for an S meter reading of S9. This procedure calibrates the S meter to read S9 for a 100- μ V signal.

Some readjustment of RF-gain adjust pot R57 (**Figure 10**) and a corresponding iteration of the S meter adjust pot may be required to get the meter to read accurately over its full range.

Performance measurements

I made sensitivity, two-tone intermodulation distortion (IMD), and blocking measurements using the methods described in *The ARRL Handbook*.

I used a Hewlett-Packard HP606A RF generator and a Boonton Radio Corporation 240A RF generator as the signal sources for these tests. Both of these generators have excellent precision attenuators. A Wavetek 5080.1 precision step attenuator, a Mini Circuits ZSC-2-1 hybrid combiner, and a Ballantine 323 true rms-reading voltmeter made up the balance of the test setup. I used a Tektronix 2235 100-MHz oscilloscope

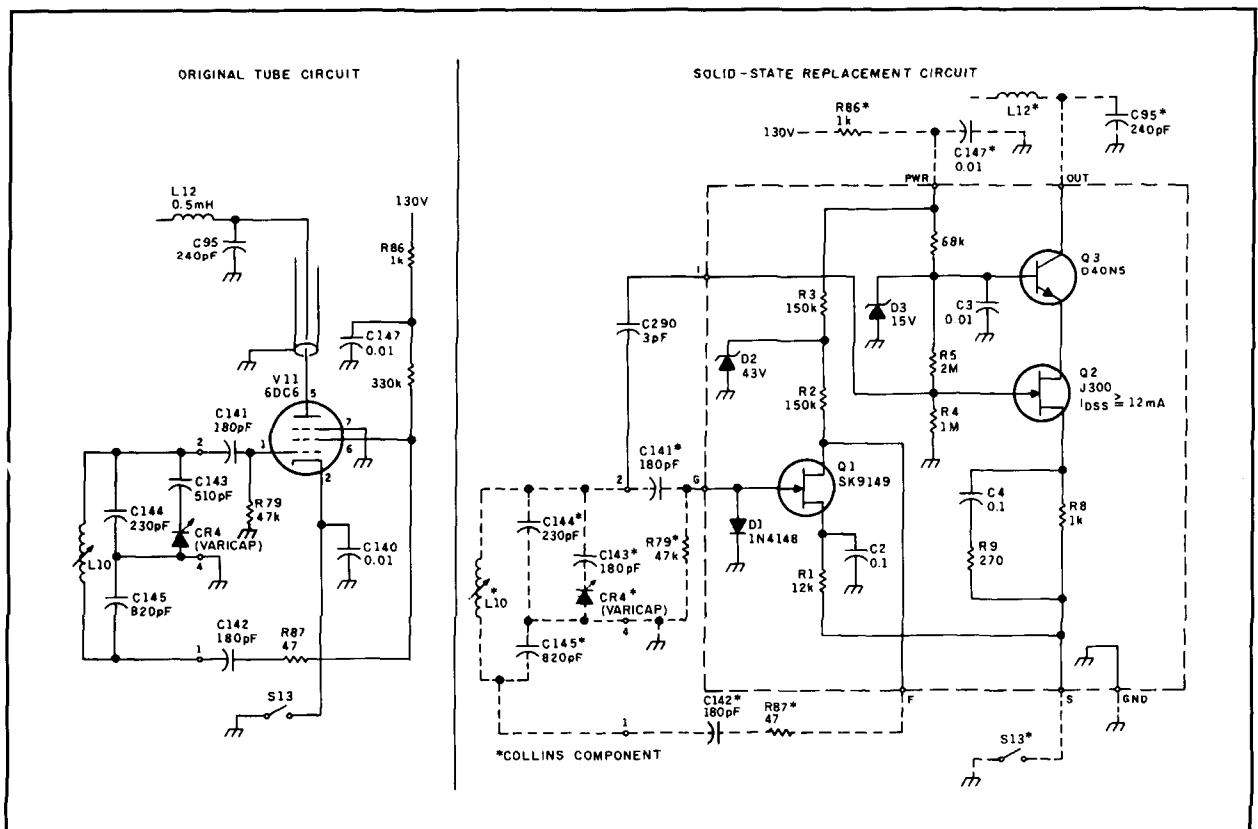


Figure 15. Tunable BFO schematic.

| | | |
|-----------------------------------|--------|---------------------|
| 2N3811 | ECG82 | SK9115 |
| 2N3906 | ECG159 | SK3466 |
| 2N5566 | ECG461 | SK9148 |
| 40673 | ECG221 | SK3050 |
| D40N5 | ECG171 | SK3201 |
| J300 $I_{dss} \leq 5\text{ma.}$ | ECG457 | SK9161 |
| J300 $I_{dss} \geq 12\text{ ma.}$ | ECG453 | Parallel two SK3116 |
| J300 $I_{dss} \geq 15\text{ ma.}$ | ECG453 | Parallel two SK3116 |
| J309 $I_{dss} \geq 20\text{ ma.}$ | ECG467 | SK9162 |
| VCR-11N | ECG466 | SK9163 |

Table 2. Possible semiconductor substitution guide.

to verify all initial signal amplitudes before adding attenuation.

Conversion sequence

If I were to make another 75S-3 conversion, I'd follow these steps in sequence:

- Begin with the crystal calibrator, notch filter, AF amplifier and detector, and the audio-output amplifier stages. Modify each of these stages separately.
- Next, convert the VFO assembly.
- Then convert the first mixer and band-select crystal oscillator.
- Follow this with the second mixer and VFO buffer.
- Then proceed with the product detector and crystal, and tunable BFO oscillators.
- Finally, work on the RF and IF amplifiers, AGC buffer, and input attenuator.

After installing each new modification, I'd make sure that the new addition and the overall receiver were operating *before* moving on to the next stage.

The conversion described in this article

should also work for the 75S-1, as its circuits are nearly identical to those of the 75S-3. The conversion of the 75S-1 should be a little easier, because that receiver doesn't have the rejection filter or tunable BFO.

Parts procurement

The semiconductors are available through the usual distributor channels. I purchased all of mine, with the exception of the SK devices, from Hamilton/Avnet. I found the SK devices at a local parts store.

The D40N5 and the 2N5566 are manufactured by National Semiconductor. The J300, J309, and VCR-11N are manufactured by Siliconix and Intersil. The 40673 is an RCA device. The SAY-1 is manufactured by Mini-Circuits, P.O. Box 166, Brooklyn, New York 11235. See **Table 2** for possible semiconductor substitutions. ■

REFERENCES

1. James M. Larson, KF7M, "A Solid-State 75A-4 Receiver," *Ham Radio*, November 1988, page 67.
2. Howard J. Sartori, "Solid-Tubes—A New Life for Old Designs," *QST*, April 1977, page 45.

VLF-LF AND THE LOOP AERIAL

*Try this antenna with the VLF-LF
receiver*

In the Winter 1991 issue of *Communications Quarterly* we reprinted a design from *Amateur Radio Magazine* for a receiver which tuned the VLF-LF bands. Here's a companion piece which discusses loop aerials as another adjunct to the VLF-LF receiving equipment.

The piece begins with some theory on loop aerials and how they reduce the level of local noise. Some experiments, carried

out by the author, are described together with a circuit for a loop tuner and preamplifier. The discussion extends to the problems of amplifier noise and the advantages of tuning the loop.

Loop aerial theory

As discussed in the previous article, a major problem in receiving VLF and LF

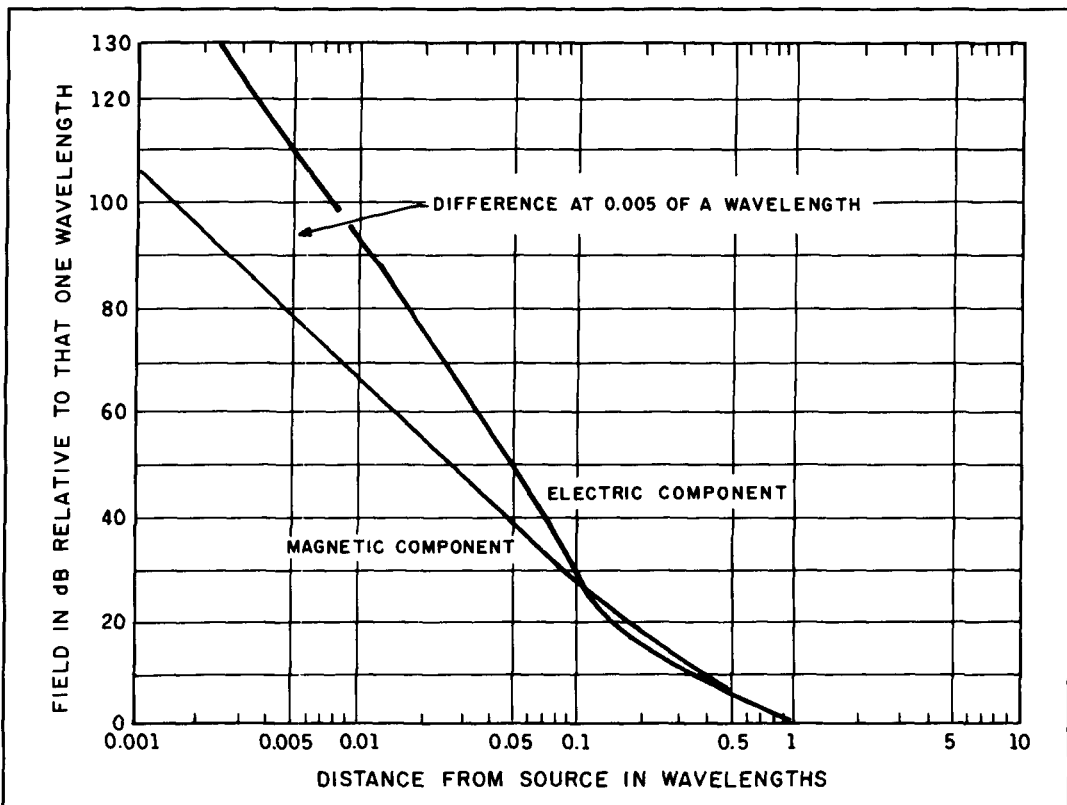


Figure 1. Comparison of electric and magnetic components of received field up to distances of one wavelength from the source.

signals is the high level of local noise generated from noisy power lines and consumer electrical equipment. In the presence of this type of noise, the received signal-to-noise ratio can be improved with the use of a loop aerial.

To explain this, it's necessary to briefly discuss the fields around a radiating element. At distances up to around half a wavelength, the induction or near field is prominent but it falls away at a greater rate with distance than the radiation field. At distances greater than one half wavelength, the radiation field is prominent. The relationship between field strength and distance is as follows:

1. The electric component of the induction field decreases with the cube of the distance and $dB = 60\log(d_2/d_1)$ where d_2 and d_1 are the relative distances.
2. The magnetic component of the induction field decreases with the square of the distance and $dB = 40\log(d_2/d_1)$.
3. Both the electric and magnetic components of the radiation field decrease directly with distance and $dB = 20\log(d_2/d_1)$.

The effect of all this is that, in the near field, the electric component is much stronger than the magnetic component. This is illustrated graphically in **Figure 1**.

At VLF and LF (10 to 300 kHz) you are concerned with half wavelengths between 500 and 15,000 meters, and reception of localized noise is clearly in the induction or near field region. The shielded loop aerial is sensitive only to the magnetic component, and because this is lower in level than the electric component in the near field, the level of noise interference is reduced. Furthermore, if the source of interference is from a different direction than that of the signal to be received, the noise is further reduced by the directional properties of the loop. The loop has a very sharp null at right angles to the plane of the loop and can be rotated to position the noise source at the null.

The equivalent circuit of the loop aerial coupled to a load resistance (R_L) is shown in **Figure 2**. E_s is the voltage induced into the loop, R_T is the resistance of the circuit (the sum of radiation resistance and loss resistance), L is the inductance of the loop, C is the shunt capacitance of the loop with its cable coupled to the load, and E_o is the output voltage across the load.

When the loop plane is in line with the direction of the signal for maximum signal level, induced voltage E_s is given by the fol-

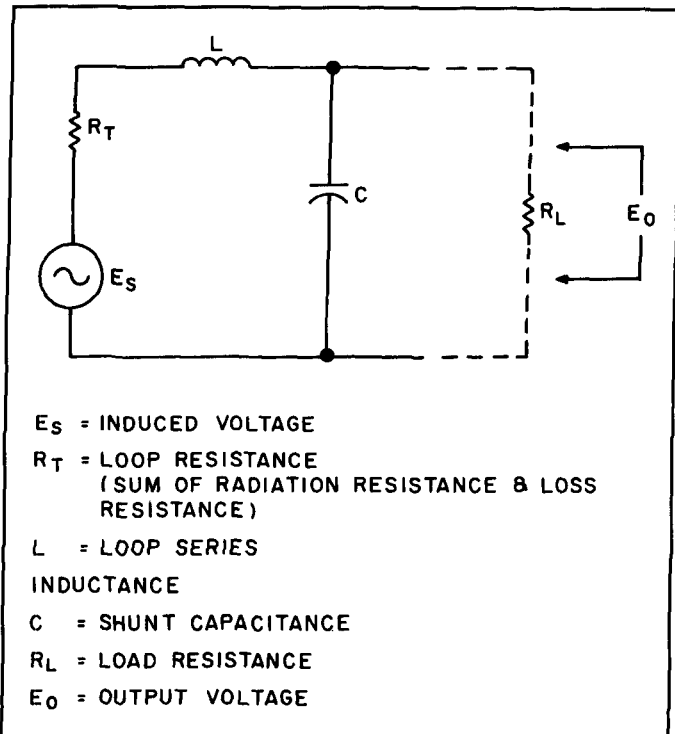


Figure 2. Equivalent circuit of the loop aerial.

lowing formula (valid providing the loop dimensions are small compared to a wavelength):

$$E_s = \frac{(2\pi eNA)}{\lambda} \quad (1)$$

where E_s is expressed in μV
 e = field strength in $\mu V/\text{meter}$
 N = number of turns
 A = area of loop in square meters
 λ = wavelength of the signal in meters

You can also express the formula in terms of frequency (f) as follows:

$$E_s = (2\pi eNAf)/V \quad (2)$$

where $V \approx$ wave velocity (3×10^8 meters/second)

From the formula, it is clear that the induced voltage is directly proportional to both the loop area and the number of turns. The larger you make either of these, the higher the induced voltage. However, increasing these also increases the series inductance and shunt capacitance and, depending on frequency, their reactances have a profound effect on the actual voltage E_o delivered to the load.

Resistance R_T is also in series with the load, but its value is normally low enough to make little difference to the voltage delivered to the load.

Resonance

The loop aerial has a natural resonant frequency at which the reactance of L equals the reactance of C and at which the response peaks such that the output voltage, E_o , equals the induced voltage, E_s , multiplied by the Q factor of the circuit. Clearly, there is much to gain by operating the loop in a parallel-tuned mode. This can be achieved at any frequency lower than the natural resonant frequency by simply adding shunt capacitance across C. At frequencies above the natural resonant frequency, resonance is not possible. Good performance is better achieved by decreasing the number of turns on the loop to make natural resonance equal to or above that of the frequency used.

To obtain good performance in a resonance mode at a wide range of frequencies, a number of loop aerials with different numbers of turns, or one with a selected number of turns, is needed. At low frequencies, a large number of turns is desirable to achieve good signal sensitivity. At higher frequencies a lesser number of turns might have to be used to raise the natural resonant frequency. Referring back to **Formula 2**, you will see that induced voltage E_s is proportional to both the frequency and number of

turns, so while you lose signal level with less turns, this tends to be compensated for by the increase in frequency.

As output voltage E_o is proportional to the Q factor at resonance, it is important to make load resistance R_L a high value to prevent the lowering of Q. This calls for coupling directly into an amplifier with a high impedance input.

Shielded loop

A multi-turn shielded loop can be constructed in many ways. The multi-turns can be spaced laterally, in line, or bunched. They all seem to work, but the essential requirement is that the shield, while fully enclosing the wires, must be discontinuous at one point (usually the loop apex) so it does not form a shorted turn and upset the magnetic properties of the loop.

I found a simple way to make a shielded loop using 12-core computer bus cable. This cable is wrapped in conductive foil and has a heavy drain wire in contact with the foil. The loop of cable (800-mm square) is cleated to two crossed sections of light timber. The ends of the cable terminate at the base of the loop where individual wires are series joined, and the drain wire and foil ends are paralleled to what becomes the cold end of the loop winding. At the apex of the cable loop, the drain wire and foil are cut so that the shield is discontinuous.

Measurements on the loop showed that 12 turns gave a natural resonant frequency of 210 kHz, 6 turns a frequency of 450 kHz, and 3 turns a frequency of 730 kHz. Inductance measured around 500, 120, and 35 μH , respectively, for the different numbers of turns. As it was required to operate the loop aerial up to 500 kHz, a switch was fitted at the base of the loop to select either 12, 6, or 3 turns. The circuit arrangement is shown in **Figure 3**. It should be observed that both ends of the unused turns are disconnected when 6 or 3 turns are in use. This is very important because if one end of the unused turns is left connected, the unused turns add extra capacitance and lower the resonant frequency.

The loop aerial using computer cable is shown in **Photo A**. It is assembled as an experimental unit and not intended, in its present form, to be weatherproof.

To resonate the loop, a 12-position switch connects a range of parallel capacitance values up to 0.47 μF which enables tuning down to 10 kHz with the 12-turn loop. The switched capacitor circuit is included in **Figure 4**. With this arrangement, Q factors

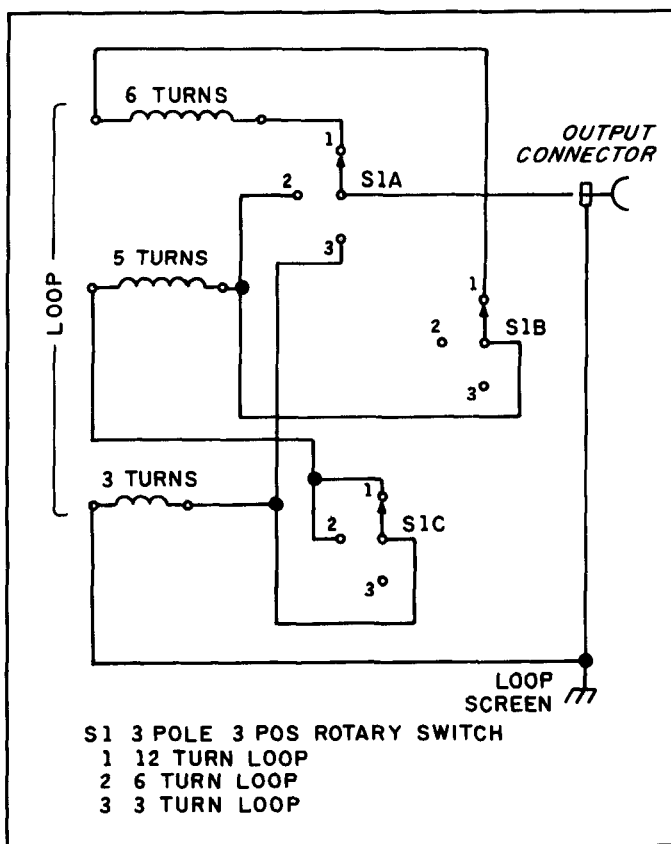


Figure 3. Loop switching circuit.

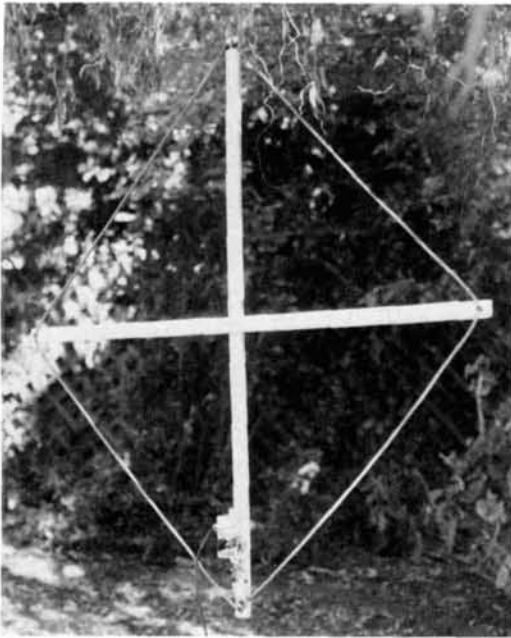


Photo A. Loop aerial assembly using 12-core computer cable.

above 50 kHz were within the range of 13 to 20. At lower frequencies, the Q is lower and was measured as 6 at 18 kHz.

The dynamic impedance of the tuned circuit can be as high as 10,000 ohms at certain frequencies, hence the circuit is interfaced with the high impedance input of an operational amplifier. The amplifier is set for a maximum gain of 10 to increase further the signal level from the loop which, even with tuning, produces a much lower signal than that received from a random wire of reasonable length. The amplifier is provided with a switch to reduce its gain to unity in the event of very high signal levels causing cross modulation. This precaution has so far proved unnecessary.

The tuning capacitors and preamplifier have been fitted into a separate box so they, and the box, can be located at the receiver end of the coax cable which feeds the loop aerial. With this arrangement, the cable capacitance also forms part of the parallel

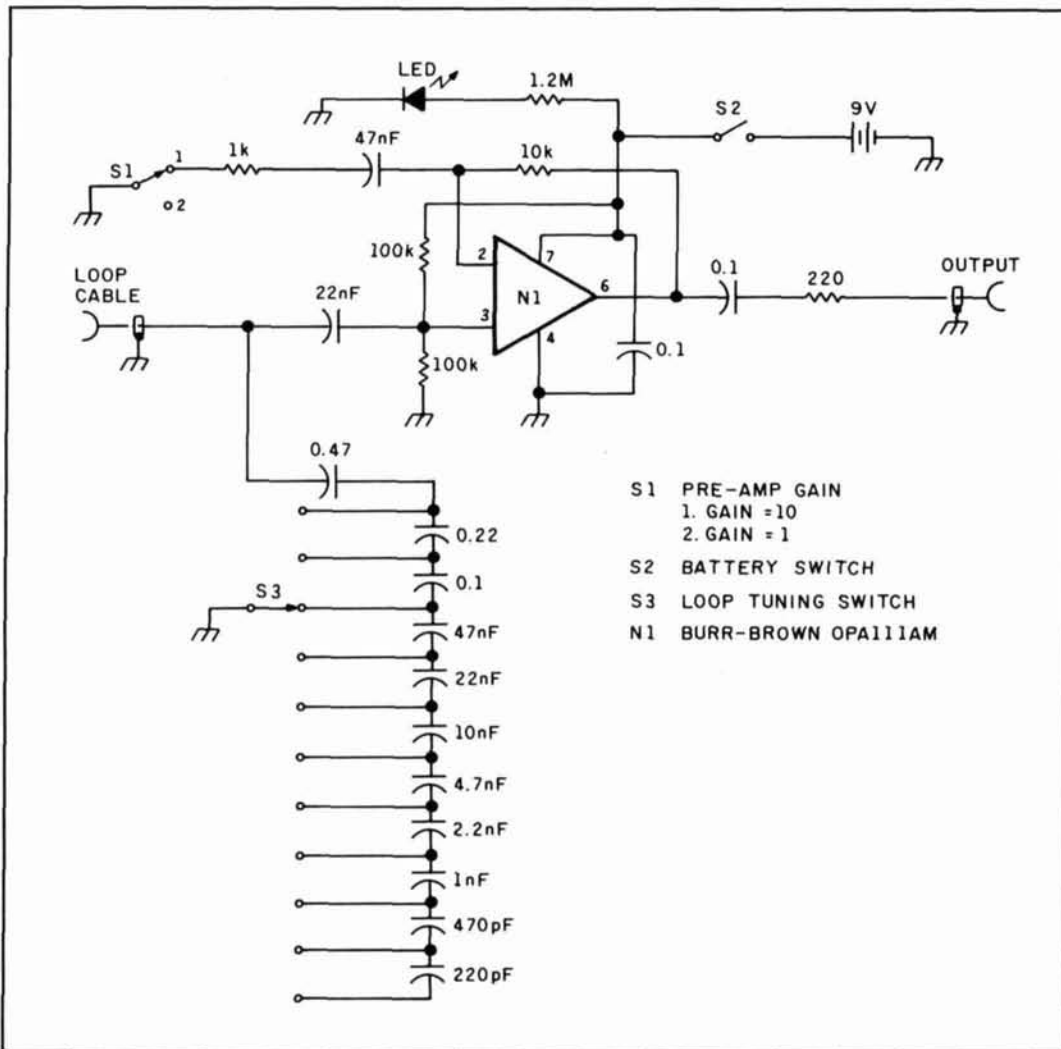


Figure 4. Loop aerial tuning and pre-amp circuit.

tuning capacitance. At these low frequencies, the only effect of this capacitance is to limit the maximum resonant frequency of the loop for a given number of loop turns. Coax cable (such as RG58) has a typical capacitance of around 100 pF per meter. The loop capacitance is around 1 nF so that a few meters of cable do not make a significant difference. The system can still be tuned satisfactorily with 6 meters of coax cable.

The loop tuning system was used in conjunction with the VLF-LF front-end tuning system and the VLF-LF receiver described in **Reference 1**. The complete equipment setup is shown in **Photo B**. The loop tuner is on top of the front-end unit at the left. The receiver is at the right.

In the loop aerial discussed, switching of the number of loop turns is provided by a 3×3 rotary switch. This must be fitted at the base of the loop and could be inconvenient if the loop aerial was located outside and inaccessible. A relay circuit could be devised which would replace the switch and be controlled remotely at the receiver.

Amplifier noise

When operating VLF-LF using a wire aerial, the atmospheric noise level received is normally well above the noise floor of the first amplifier, and amplifier noise is insignificant. With the loop aerial, the signal pickup is much lower, and when the atmospheric noise level is low, the minimum discernible signal level can be set by the amplifier noise floor rather than the atmospheric noise level. It is therefore important to select a preamplifier with a low inherent noise, much as one would do

for a VHF or UHF front end.

For the amplifier used in the circuit of **Figure 4**, a Burr-Brown low-noise FET operational amplifier type OPA111AM was selected. This is specified as having the low voltage noise figure of 6 nV per root hertz of band width, with the negligible current noise characteristic of the FET input circuit. It has a gain-band width product of 2 MHz and hence it can maintain the gain of 10 up to a frequency of 200 kHz with a falling response at higher frequencies down to a gain of 4 at 500 kHz.

Another choice for a low-noise amplifier could have been the bipolar input Precision Monolithics type OP27 amplifier. This has a voltage noise of only 3 nV per root hertz of band width but, having a bipolar input, there is a current noise component which would add noise when connected across the high impedance tuned loop circuit? The amplifier has a gain-band width product of 8 MHz and hence could maintain the gain of 10 well up to 800 kHz. A further approach might have been to use one of the low-noise MOSFET VHF transistors such as the BF981.

Of course, good signal-to-noise ratio also gets back to the design of the loop for highest possible signal voltage. Recapitulating previous parts of this discussion, signal voltage is increased with more turns or larger area (consistent with natural resonance being not less than the operating frequency), or by designing the form of the loop for the highest possible Q factor.

Loop aerial circuits are frequently published with an amplified signal fed back to the loop to form what is called a Q multiplier. This, of course, is a different name for what has been known as regeneration or

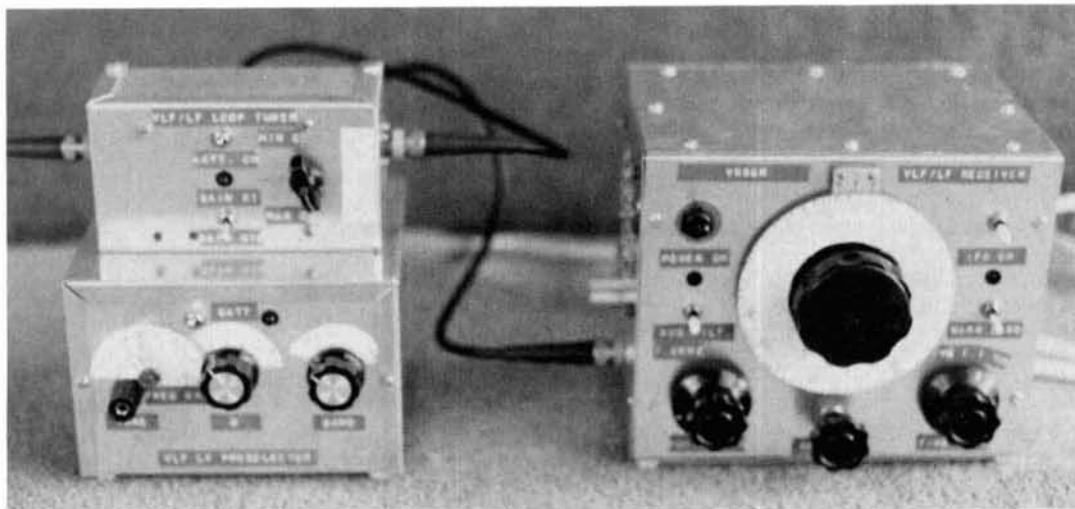


Photo B. The receiving equipment. The loop tuner is on the upper left, the receiver front-end tuner is on the lower left and the receiver is on the right.

reaction. Feedback in phase with the input signal raises the effective Q of the circuit to increase its gain and reduce its band width. For my receiving system, feedback in the loop system was not considered necessary as the loop amplifier was coupled into the VLF-LF front end. This front end, with Q factors up to 200, has itself adequate gain and selectivity.

There is also a disadvantage with using regeneration in that the noise generated by the amplifier is also fed back to be reamplified. While the regeneration narrows the loop band width and reduces the band width of the incoming noise, it actually increases the level of the amplifier noise within the band.

Some other loop forms

The natural resonant frequency of the loop and hence its upper frequency limit for a given number of turns, can be increased by spacing the wires and spacing the shield from the wires so that residual capacitance is reduced. As it turns out, the loop aerial also gives quite good noise rejection without any shield at all. With this arrangement, the residual capacitance can be reduced to provide a considerable increase in the upper frequency of the loop.

Another loop aerial I assembled consisted of 20 turns of unshielded wire spaced in line with a separation of 10 mm between turns, forming a 0.8-meter square. To achieve the spacing, the wire was wound around four pieces of dowelling fitted through two wood cross pieces. This aerial measured an inductance of about 500 μH and had a natural frequency of several hundred kHz. (Unfortunately, the actual frequency was not recorded.)

The wire on the 20-turn loop was eventually replaced with shielded wire. Its second form is shown in **Photo C**. At the apex of the aerial, the shields on each of the 20 wires were cut and all joined together on either side of the cut. The shields were also joined at the base of the aerial and connected to the earth side of the feeder cable. The inductance of this aerial measured much the same as that of the previous aerial with unshielded wire, but natural resonance was lowered to 100 kHz. All in all, the performance in receiving signals at VLF appeared much the same as those for the unshielded loop. This raises a question as to whether the shield is of much value at low frequencies where the loop dimensions are very small compared to a wavelength. At these frequencies, there might be merit in

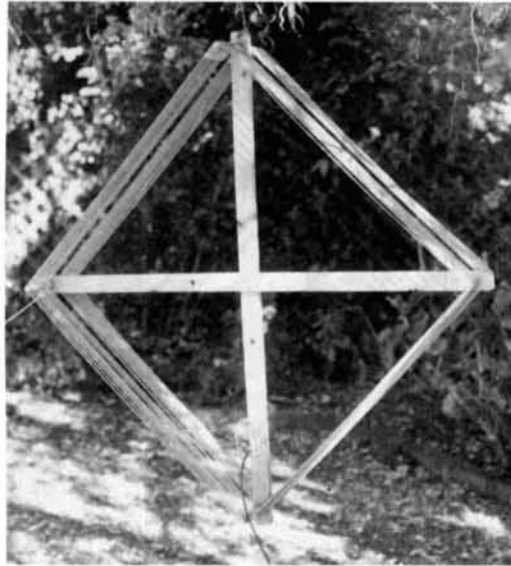


Photo C. The 20-turn loop aerial wound with shielded wire.

using the unshielded loop to take advantage of the higher upper frequency limit achieved.

In a further form of loop aerial, a single turn of large area can be used. Clarrie Castle, VK5KL, described a single turn loop aerial for 1.8 MHz in the March 1982 issue of *Amateur Radio*.³ The aerial was formed by a single loop of around 9 meters of coaxial cable with its outer braid conductor cut at the loop apex. The outer braid thus formed the shield around the inner looped conductor. With lower frequencies in mind, I set up such a loop using 9 meters of RG58 and carried out some tests. The resonance measured 2.5 MHz. At 1.8 MHz, the loop resonated with around 500 pF of parallel capacitance and the circuit had a Q factor of 16. Clearly, the loop was ideal for this frequency. Below 100 kHz, signal pick up was less than adequate and very large values of capacitance were needed to resonate the loop. This particular loop aerial is clearly a very good form for the MF band, but not really suitable for VLF and lower LF. Nevertheless, it was another interesting experiment to find out what would work at the lower frequencies.

Measurement of loop constants

At this point, it might be useful to explain how the loop constants were measured. Having constructed a loop aerial, you need to know its natural resonant frequency and its self inductance so the maximum tunable frequency can be determined and the capacitance values worked out for the

tuning range required. These factors can be measured using a signal generator fed via a fairly high resistance (say 10 k) to the loop as shown in **Figure 5**. More than one signal generator might be needed to tune from VLF to MF. The voltage across the loop is monitored on a CRO (or perhaps a VTVM) via a high impedance probe. The signal generator frequency is adjusted for a peak in voltage at which the natural frequency is indicated. You now add a large capacitance (at least 20 nF) sufficient to make the loop capacitance insignificant by comparison, and retune for a peak at the new lower frequency. Inductance is then calculated from the normal resonance formula (or a resonance chart), using the parallel capacitance as the formula (or a resonance chart), using the parallel capacitance as the value of C and ignoring the self-capacitance of the loop as this makes little difference to the accuracy of calculation.

Having measured the self-resonant frequency and calculated the inductance, the loop self-capacitance can also then be derived from the resonance formula.

As a further operation, Q factor can be measured using the same equipment, except that the resistance in series with the signal generator must be increased to around 100 k to prevent the Q being lowered by the signal source. With extra signal loss across the resistor, a high signal level and a sensitive CRO are needed. The procedure is simply to measure the frequencies either side of resonance which give 0.707 of the voltage at resonance. The Q factor is equal to the resonant frequency divided by the difference between the two frequencies recorded. The Q factor at a range of frequencies can be carried out by varying the value of the shunt capacitor to obtain resonance at each of the frequencies.

To go one step further, you can now calculate the AC resistance of the loop (RT) at

any frequency for which you have derived Q. The inductive reactance at that frequency is calculated from $2\pi fL$ and the reactance is then divided by Q to obtain RT. You now know all the constants RT, L, and D, as shown in **Figure 2**.

Performance

While the level of its signal pickup is low compared to the long wire aerial, it has been clearly demonstrated in my experiments that the loop aerial can separate out signals in the presence of localized noise which overrides the signal on the long wire. As with any directional aerial, it also improves the signal-to-noise ratio for atmospheric noise by restricting noise received—in particular from a direction at right angles to its plane.

Surprisingly, this performance could be achieved with the loop aerial sitting on the cement floor of my shack, which happens to be clad in sheet iron. With a suitably designed loop aerial and highly selective front-end tuning system, good signals at VLF and LF can be received indoors—right down to 10 kHz. This is gratifying if one does not have room for an outdoor aerial. Of course, there are the odd traps. It is very easy to miss a signal if it happens to arrive from a direction close to the null of the loop. It is also very easy to home in on some inside-based signal source such as a frequency counter.

Untuned loop

Discussion has been centered around loop aerials tuned to resonance and giving output voltage as in **Formula 1** or **2** multiplied by Q. However, loop aerials can also be operated in a broadband mode and a design procedure for doing this over a range of frequencies is described in the April 1989 issue of *Lowdown*! The procedure is to load the

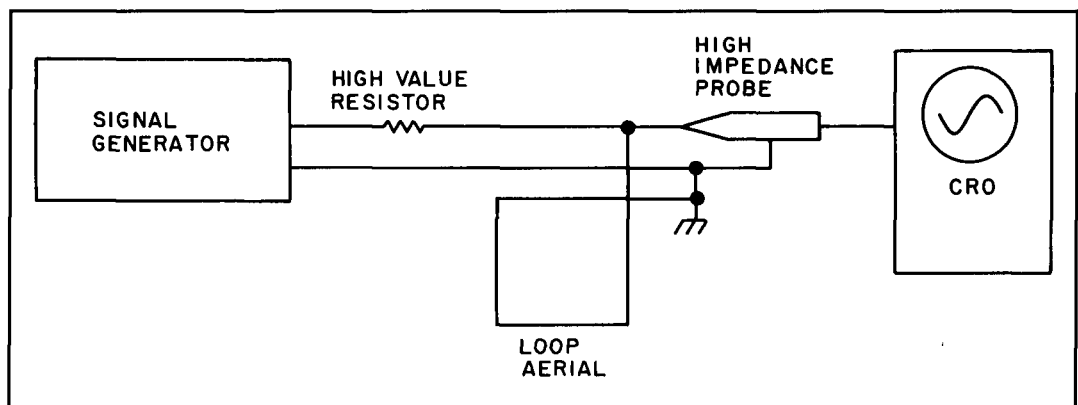


Figure 5. Measurement of loop aerial constants.

loop aerial into a fairly low resistance at the preamplifier input, equal in value to the loop inductive reactance at the lowest frequency of the frequency band required. Parallel resonance is set to a frequency calculated from the geometric mean of the lowest and highest frequency required. According to the article, the design produces a loop response which is flat with frequency.

While the broadband loop eliminates the complication of loop tuning when changing frequency, the loss of Q multiplication can drop atmospheric noise below the noise floor of the amplifier, thus limiting the sensitivity to weak signals. As an example, if you apply **Formula 2** to the 12-turn 0.8-meter square loop described, and use a typical atmospheric noise for 100 kHz (this can be around 0.2 μ V per meter per root hertz), you get a loop output voltage of 3.2 nV per root hertz. This output level is barely comparable with equivalent input noise voltages at low impedance of the best of amplifiers.

Conclusions

A properly designed loop aerial system, with a low-noise preamplifier, is a useful part of the VLF-LF receiving equipment and can enable signals to be picked out from noise which otherwise overrides the signal from the wire aerial. It also provides a means to obtain good signal reception at VLF-LF without the use of a large aerial installation usually considered necessary for low frequency reception.

The signal level received from the loop aerial is low compared to the wire aerial and the signal-to-noise ratio can be limited by the noise generated in the first amplifier. To minimize this problem, a low-noise preamplifier is used, and the loop circuit is tuned so that the signal level into the amplifier is multiplied by the Q factor of the loop circuit.

Some experimental loop aerials and a loop tuning and interface circuit have been described. Operated in conjunction with the high Q front-end tuner, previously described in **Reference 1**, they have provided impressive performance when everything is carefully tuned up. ■

REFERENCES

1. Lloyd Butler, VK5BR, "A VLF-LF Receiver," *Communications Quarterly*, Winter 1991.
2. Lloyd Butler, VK5BR, "Amplifier Noise," *Amateur Radio*, November 1982.
3. C.H. Castle, VK5KL, "A 10-Foot Diameter Receiving Loop on 1.8 MHz," *Amateur Radio*, March 1982.
4. "Analysis & Design of Broadband Low Frequency Loops," *Lowdown*, April and May 1985.

BIBLIOGRAPHY

1. *Direction Finding (Loop Aerials)—Admiralty Handbook of Wireless Telegraphy*, Section T.

HIGH-PERFORMANCE ANTENNA SOFTWARE

MN 3.5 is the fastest, most powerful MININEC antenna analysis program available. MN provides 3-D views of antenna geometry and wire currents, generates presentation-quality polar and rectangular plots of all linear and circular polarization components, handles complex antennas with up to 254 pulses, calculates near-fields for TVI and RF-hazard analysis, has current feed for phased arrays, does automatic frequency sweep, and provides for simple definition of sources and loads. MN 3.5, \$85. 500-pulse option, \$25. MNC 3.5 (1.6-2.4 times faster, copr. req'd), \$110. MNjr 1.5 (same speed and capacity as MN, fewer features), \$35.

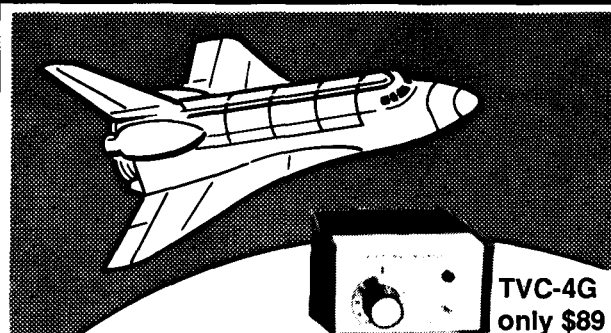
YO 4.0 automatically optimizes Yagi antennas for maximum forward gain, best pattern, and minimum SWR. YO handles designs from HF to microwave, and models Yagis over ground, stacked Yagis, Yagis with dual driven elements, and ohmic conductor losses. YO runs hundreds of times faster than MININEC. YO is calibrated to NEC for high accuracy, and has been extensively validated against real antennas. YO is intuitive, highly graphical, and simple to use. YO 4.0, \$100. YOC 4.0 (1.7-2.7 times faster, copr. req'd), \$130.

NEC For Yagis provides high-accuracy verification of Yagi designs with the professional-standard Numerical Electromagnetics Code. NEC For Yagis 1.0, \$50. Coprocessor, hard disk, and 640K memory required.

MN and YO include both coprocessor and extra-fast no-coprocessor versions, and comprehensive antenna design libraries. All programs include extensive, easy-to-read documentation, and an easy-to-use, full-screen text editor. Add 6% CA, \$5 overseas. U.S. check, cash, or money order. For IBM PC, 3.5" or 5.25" disk.

Brian Beezley, K6STI, 507-1/2 Taylor, Vista, CA 92084
(619) 945-9824, 0700-1800 Pacific Time

AMATEUR TELEVISION



TVC-4G
only \$89

SEE THE SPACE SHUTTLE VIDEO

Many ATV repeaters and individuals are retransmitting Space Shuttle Video & Audio from their TVRO's tuned to Satcom F2-R transponder 13. If it is being done in your area on 70 CM, all you need is one of our TVC-4G ATV 420-450 MHz downconverters, add any TV set to ch 3 and 70 CM antenna. Others may be retransmitting weather radar during significant storms. Once you get bitten by the ATV bug - and you will after seeing your first picture - show your shack with the TX70-1A companion ATV transmitter for only \$279. It enables you to send back video from your camcorder, VCR or TV camera. ATV repeaters are springing up all over - check page 411 in the 90-91 ARRL Repeater Directory. Call for a copy of our complete 70, 33 & 23 CM ATV catalog.

(818) 447-4565 m-f 8am-5:30pm pst.

P.C. ELECTRONICS
2522 S. Paxson Ln Arcadia CA 91007

Visa, MC, COD

Tom (W6ORG)
Maryann (WB6YSS)

By Glenn Leinweber, VE3DNL
Max Pizzolato, VE3DNM
John Vanden Berg, VE3DVV
Jack Botner, VE3LNY

A 4800-BAUD MODEM DAUGHTER BOARD FOR PACKET TNC

*Introducing the HAPN-T, developed by
the Hamilton and Area Packet Network*

Packet radio has become incredibly popular since its introduction in 1979. So popular, in fact, that many local-area networks are rendered nearly useless as a result of peak-period congestion. There are two solutions to this problem — use more channels, and increase the baud rate.

The Hamilton and Area Packet Network (HAPN) has a daughter board 4800-baud modem that plugs into many of today's TNCs, but still uses the same radio equipment and channel bandwidth as 1200 baud.

Background

The HAPN-T 4800-baud modem is the third in a series of high-speed modems developed by HAPN. The modem was originally conceived by Ken Smith, VE3HWB, and Glenn Simpson, VE3DSP! Glen Leinweber, VE3DNL, and John Vanden Berg, VE3DVV, built a practical modem based on their design.

The first version of the 4800-baud modem was designed for external stand-alone use with TNCs like the VADCG TNC+. The modem proved to be a great success and a second version, which could be constructed on the prototype area of the HAPN-1 packet-radio adapter, was developed²

Finally, the HAPN-T modem was introduced. This modem takes advantage of the accessory modem headers on many TNC circuit boards, into which a daughter board modem can be plugged.

Why 4800 baud?

The transmission of packets at 4800 baud (or more correctly, 4800 bits per second) rather than 1200 baud has certain advantages. Most importantly, a given amount of data can be sent in a quarter of the time*. The HAPN-T has a very fast built-in squelch circuit, which substantially reduces the carrier-detect and turnaround times. Although the dynamics of channel use can be quite complex, much more data can be passed over a channel at 4800 baud than at 1200 baud. If the modem is inexpensive and requires no special RF equipment, this can be an attractive way to accommodate many more users on the packet channels.

HAPN-T features

The HAPN-T modem (shown in **Photo A**) consists of a small printed circuit board that plugs into the 20-pin header on many of

*Actually, because of the various overheads associated with packet radio, the difference is a bit less than four times.

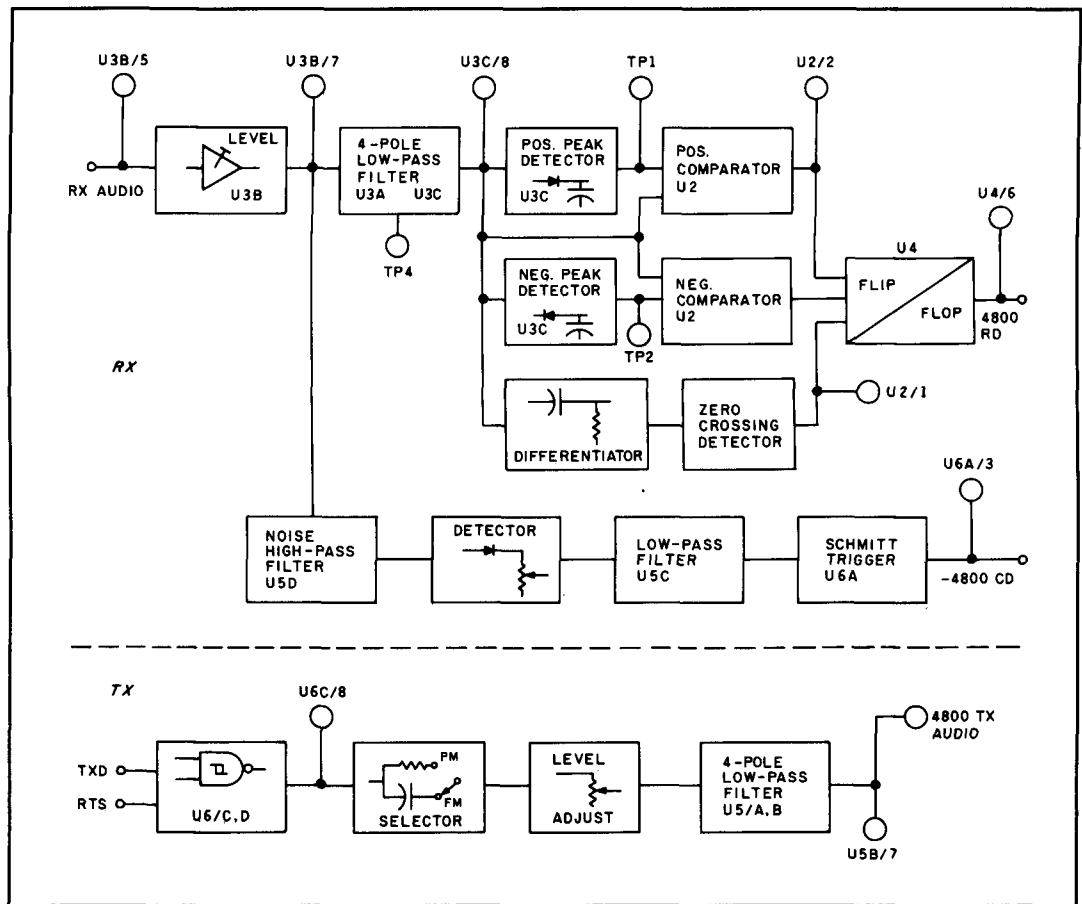


Figure 1. Block diagram of HAPNT 4800-baud modem.

U2/2). When 68 percent of the signal at TP4 exceeds the low-pass filter output, the comparator level will go high again. A similar process occurs for the negative comparator (Figure 3, U2/13).

The zero-crossing detector generates pulses when the low-pass filter output changes direction. The input to the detector is derived by differentiating the low-pass filter output (C10 and R34). This signal is compared with a threshold at the junction of R31/R32 and R33/R35 to generate a pulse on the output. Both sections of the comparators are dot ORed together (Figure 3, U2/1) to produce positive pulses.

The output of the zero-crossing detector gates the output of the data comparators into flip-flop U4. The output at U4/6 (Figure 3) now contains the recovered digital data. Note that a simple cross-wired 74HC00 is used as a flip-flop. Since the modem is decoding continuously, you'd normally see the flip-flop change state due to noise decoding.

The output is ANDed with a carrier detect signal so data is only valid when a radio transmission is received. This reduces

unnecessary decoding attempts by the synchronous controller in the TNC.

Carrier-detect section

The TNC needs a signal to indicate if the channel is busy. This signal prevents the TNC from transmitting when another station is using the channel. Many modern TNCs using modem chips like the AMD7910 or 3505 aren't able to detect a carrier from the data properly, so they usually rely on the radio for audio squelching.

This reliance on the radio presents performance problems. VHF-radio squelches are optimized for voice use and are slow to produce a signal. This is fine for voice, since it prevents marginal signals, like those received by mobiles (mobile flutter), from disturbing you. However, it leads to difficulties in a packet-radio application, because you want short transmissions without unnecessary delay. One popular radio takes about 500 ms to open its squelch. Consequently, short packets, like "acknowledges," may be missed completely. The sender has to com-

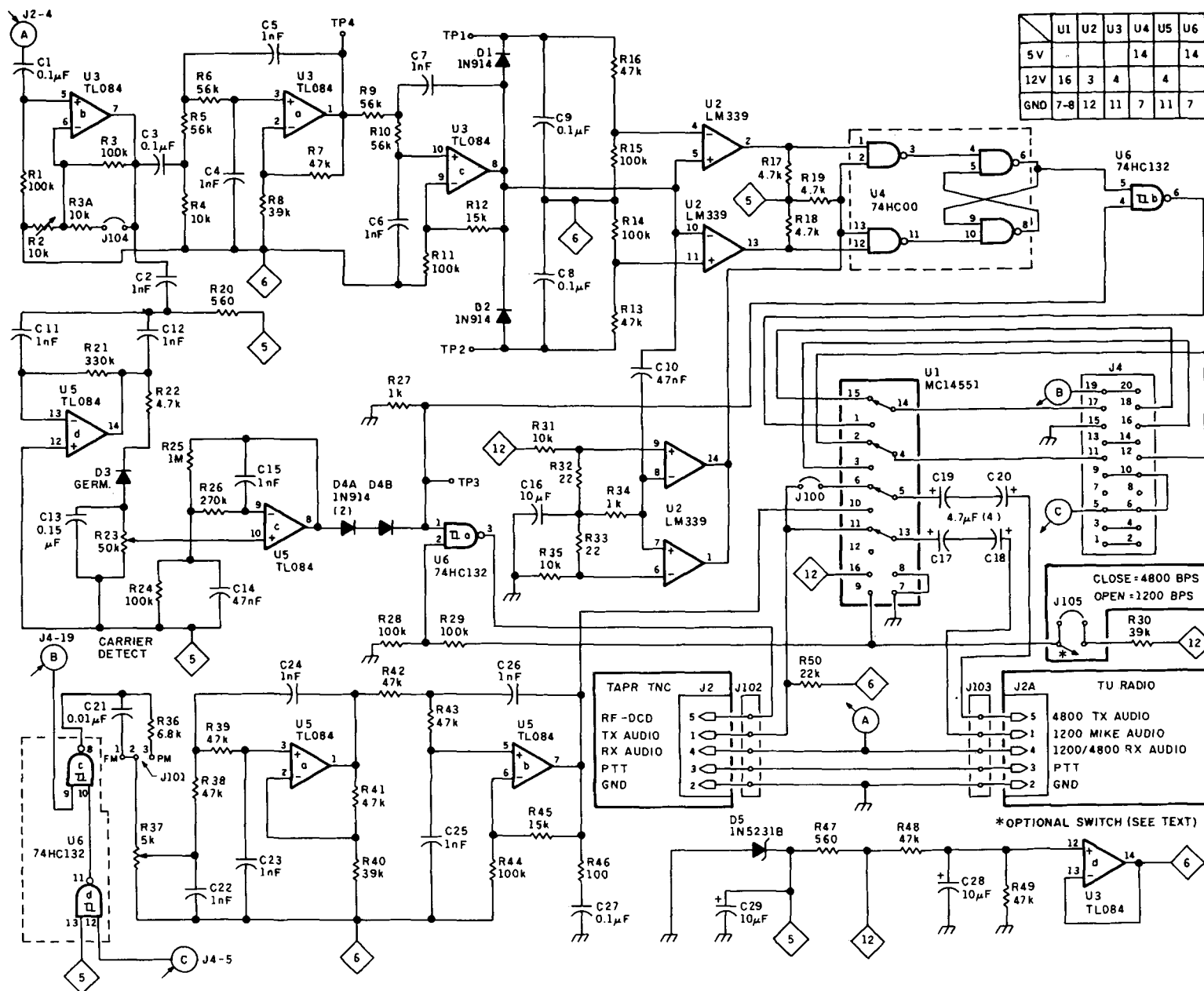


Figure 2. Circuit diagram of HAPN-T 4800-baud modem.

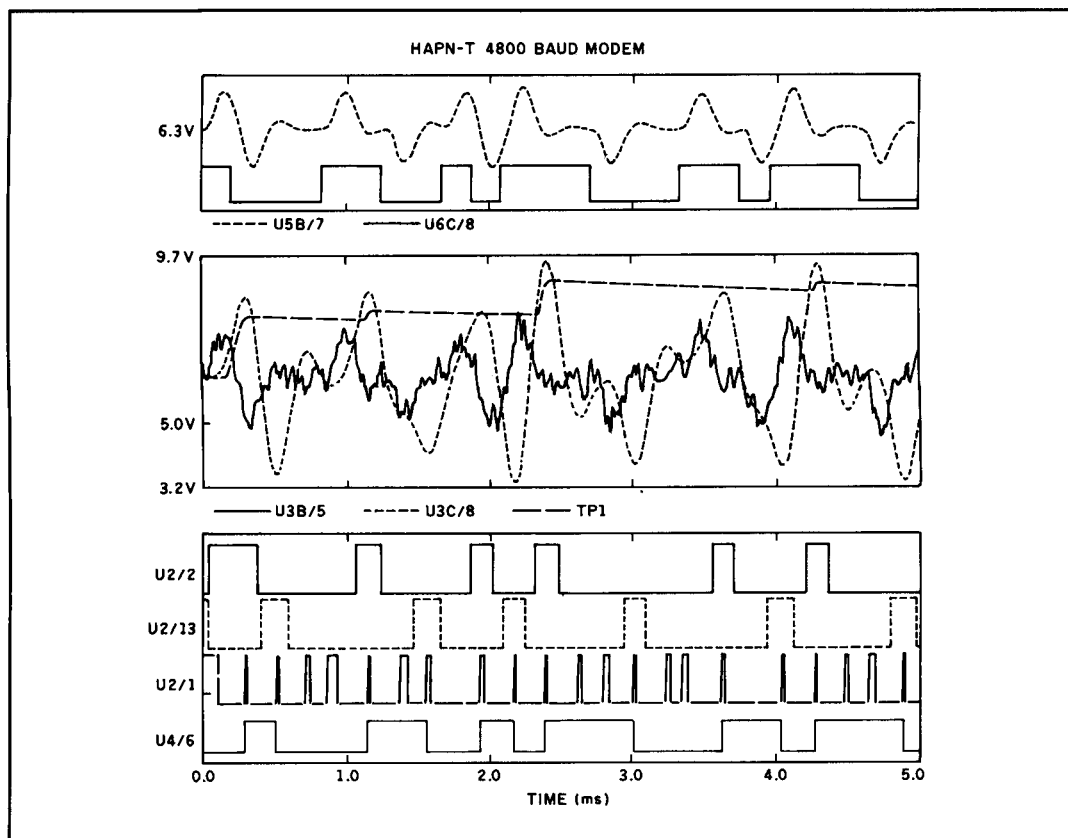


Figure 3. HAPN-T modem waveshapes.

compensate for this by extending the TX delay to 600 ms or more, creating a lot of wasted channel time. The 4800-baud modem described here contains a carrier detect (CD) circuit optimized for packet. It switches in 10 to 15 ms to indicate a busy channel, enabling the TX delay to be kept short as well.

The first part of the carrier-detect circuit is a high-pass filter, U5D, that allows for the separation of the high-frequency noise (around 11 kHz). One stage of a TL084 is used for this circuit.

The noise is rectified by a 1N34 germanium diode. We chose a germanium diode because it has a lower voltage drop than a silicon diode. The level is adjustable by 50-k trim potentiometer R23. The level must be set after the receive data level adjustment has been made. Normally, it is not changed after installation.

Rectified noise is amplified by low-pass filter op amp U5C. The output at U5C/8 will be +5 volts when no noise is received (radio disconnected), because the op amp is biased to +5 volts. When noise is received, the signal will go low toward zero volts. The drop in signal voltage depends on the amount of noise being received.

The analog output of the noise low-pass filter is converted to a digital signal by

carrier-detect squelch gate U6A. The voltage drop across two 1N914 silicon diodes, in conjunction with the 1-k pull-down resistor (R27), shifts the level to the range suitable for the 74HC132 Schmitt trigger input (TP3, Figure 2). The typical 0.9-volt hysteresis of the chip avoids false triggering. The output signal at U6A/3 is logical zero when the radio is disconnected or a carrier is received (in 4800-baud mode).

Transmit section

The digital-transmit data from the TNC is gated with the RTS line to prevent unnecessary audio from getting into the modulator when in receive mode (Figure 3, U6C/8).

Jumper J101 selects either the more common frequency modulation (FM) or less common phase modulation (PM). It's important to match the jumper with the type of modulator in your transmitter. In PM mode, the digital data is sent directly to the low-pass filter; in FM mode the data is first differentiated by C21 and R37. The resulting transmitted signal will then be the same.

Trimpot R37 sets the audio deviation being transmitted. Avoid setting the level too high. This will cause overdeviation and result in an uncopyable signal, because

receiver IF will distort it. A level which is too low results in a poor signal-to-noise ratio. This is similar to what happens when you hear someone with low voice modulation. The optimum deviation is around 3.5 kHz. The adjustments section tells how to determine the proper setting when you don't have access to a deviation meter.

The TX low-pass filter is a four-pole device that removes the higher harmonics from the digital data. It's important to maintain the wave shape shown at U5B/7 in **Figure 3**. Feeding the data through the mike input won't work. The mike audio amplifier and emphasis network normally introduce too many phase and amplitude changes. The output should go directly to the FM or PM modulator.

Multiplexer section

Figure 4 shows the multiplexer block diagram. The multiplexer allows for convenient switching between 1200 and 4800 baud. The radio interface consists of three signals: PTT, RX audio, and TX audio. The TNC requires demodulated data (1200RD or 4800RD), CD (carrier detect), and a clock signal (1200CLK or 4800CLK) for decoding the digital modem data. The TNC outputs the TXD (Transmit Data) and the RTS (Request To Send) lines.

The multiplexer (U1, MC14551) consists of a four-pole two-position CMOS switch

(**Figure 4**) capable of switching analog and digital signals. Section S1 switches the TNC clock between 1200 and 4800. S2 selects the proper receive digital data. S3 sends audio from the 1200-baud modem to the mike input if required. This normally results in an emphasis of the high audio tone (2200 Hz) because of the radio's internal emphasis network.

Some Amateurs prefer a flat response on 1200 baud. You can obtain this by using the 4800-baud modulator input point on 1200 baud, instead of the mike input. In this case, you'd install J100. Switch section S4 feeds TX audio to the modulator.

The CD is derived from the 1200-baud modem as DCD (data carrier detect) and from the 4800-baud modem's internal squelch detect. Both the 1200 and 4800 CD signals are ORed together. Either CD will light the CD LED on the TNC's front panel.

RX audio from the radio is sent to both modems, and each one will try to decode the data. As we mentioned earlier, the proper digital data is selected by S2 of the multiplexer. Since the PTT and watchdog function is the same for both modems, the existing TNC circuit is used for both the 1200 and 4800 mode.

To make selection convenient, you may wish to add a small single-pole two-position switch to the front panel of the MFJ TNC-2 (**Photo B**). The TNC-1 uses the existing

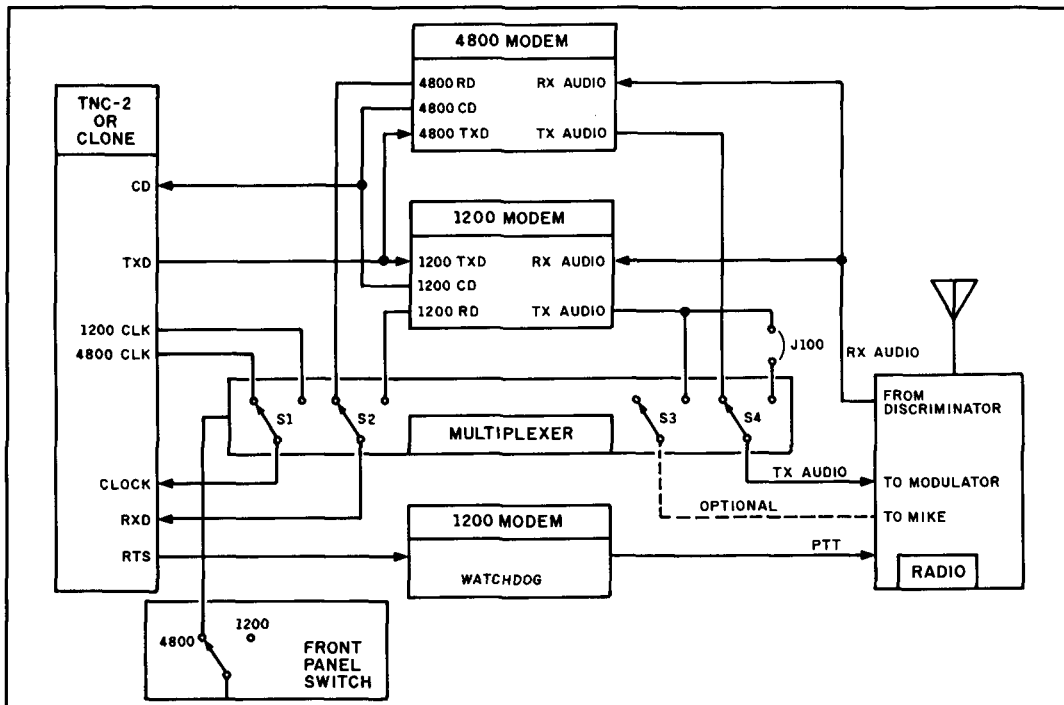


Figure 4. Multiplexer block diagram.

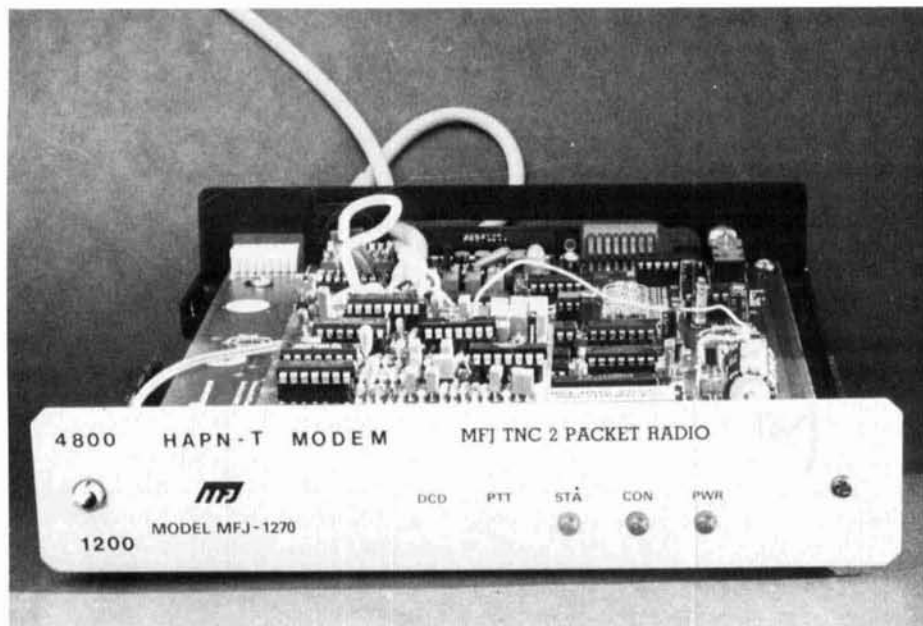


Photo B. A single-pole, 2-position switch on the MFJ TNC-2 is used to switch 1200 and 4800 baud.

bank switch on the front panel to do the switching. The spare LED will light in the 4800 mode.

Circuit modeling

We used a circuit modeling program to plot modem waveforms similar to those seen on an oscilloscope. Modeling programs (like SPICE) are very useful tools and can now be run on personal computers. Most circuits of interest to Amateurs, like audio amplifiers, power supplies, RF-tuned amplifiers, power stages, mixers, and filters (both crystal and LC) can be investigated with good accuracy. We chose SPICE to fine-tune component values and obtain a good transmit waveshape.

Figure 3 shows the digital transmit data of a random sequence of ones and zeros, along with the resulting modem output waveshapes. There are a number of waveshapes from the receiver part of the modem, including the input waveform (with noise added), both before and after the four-pole Butterworth filter. The positive peak-detector (TPI) waveshape is also shown. The four digital waveforms from the receiver are from the positive-peak slicer, negative-peak slicer, zero-crossing detector, and received digital output.

HAPN-T circuit-board assembly

Before assembling the circuit board, make sure all parts are on hand, and inspect the circuit board under a bright light or mag-

nifying glass to make sure there are no flaws. Bend the leads of the resistors and diodes to 0.4 inch (10.4 mm) lead space.

Mount the resistors, following the silk-screen and component mounting diagram. Solder and trim the leads. Mount the diodes, watching the polarity; the band is the cathode. Solder and trim the leads. Mount the IC sockets, watching the direction. The notch side is near pin 1. Mount the tantalum capacitors. Be careful bending leads, and watch the polarity! Mount the remainder of the capacitors. Trim the leads. Mount the trim pots. Mount female connector J4 on the bottom side of the modem board. Cut at length and mount posts J100 (2 pin), J101 (3 pin), J104 (2 pin) and J105 (2 pin). Using an analog ohmmeter, check pin J4/15 (gnd) and the +12 volt lead for about 16-k ohms.

Now install the HAPN-T in your TNC.

Installation

You can use the HAPN-T in both TAPR TNC-1 and TNC-2 TNCs. The following instructions apply to the MFJ TNC-2. Instructions are also available from HAPN for the TNC-1, Tiny-2, and PK232. TNC-1 and TNC-2 instructions are included with HAPN-T orders. Tiny-2 and PK232 instructions are available upon request.

Preparing the TNC-2

Install external modem connector J4 (if not already present), and add one wire to

feed 4800-baud clock pulses to vacant pin 16 of connector J4. Remember, these instructions apply to the MFJ TNC-2; other TNCs may vary to some degree.

Remove the covers from the TNC (on MFJs, you'll also remove the front plate). Remove four screws and the mother board. On the back of the board, cut the trace between the modem interface connector J4 pins 11 and 12 (clock pulses) and the trace between J4 pins 17 and 18 (receive data). Solder in male connector J4. Solder a small-gauge wire from U1 pin 7 to J4 pin 16 (4800-baud clock). You may wish to add a miniature switch for easy switching between 1200 and 4800 baud. A good place for mounting this switch is the left screw hole of the front panel, as shown in **Photo B**. Make sure that J10 on the TNC isn't so high as to interfere with the bottom of the modem board. If it is too high, trim the height of J10 with a pair of side cutters. Reinstall the board in the cabinet.

Test the modifications by temporarily installing jumpers at J4 pins 11-12 and pins 17-18. This restores the original traces and lets you verify that the TNC is still functional before continuing with the modem board installation.

Installing the modem board in the TNC-2

Solder a wire from the 12-volt pad on the modem board (near corner cut) and connect it to a 12-volt source on the TNC (like the cathode of CR7). Plug the modem board into the TNC male header. Make sure the board is plugged in properly by looking at it from the side. Using an ohmmeter, check for zero ohms between square pad J102 pin 2 on the modem board and ground on the TNC (such as RS232 pin 7). This step verifies proper mating of the J4 connector (very important).

For the next step, you'll need four-conductor shielded audio cable and a male DIN plug(s). Use Radio Shack cable part no. 42-2151, cut in half. Refer to the circuit diagram and connect the TNC interface wires to J102 using the cable and DIN plug. The shield goes to J102 pin 2. The 5-pin DIN plug is plugged into TNC radio-connector J2. Refer to **Figure 1**. Connect J103 to the radio using the shielded cable again. The shield goes to J103 pin 2. Test the 1200-baud operation using your old radio interface points, like speaker at J103-4 and audio at J103-1.

Your modem is now installed in the TNC-2. The next section lists modifications you need to make to the radio for the 4800-baud

tie points.

Connecting the HAPN-T to your rig

It's very important to select the proper interface points inside the radio. If you choose the wrong points, the modem will perform poorly, or not at all. The radio modification doesn't interfere with normal voice operation. However, in normal packet use, you should have the mike unplugged when in packet mode to prevent any room noise from being modulated along with the packets. If the mike switch is connected so the audio input to the radio is grounded when the PTT on the microphone isn't activated, you can leave the mike connected. In transmit mode, the modem's output impedance will likely pull the audio level down, so it's advisable to unplug the modem cable when using the radio for voice.

RX audio

The RX audio can't be taken from the speaker output because of: (1) phase distortion of the de-emphasis network in the receiver, and (2) the characteristics of the audio amplifier. The proper take-off point for the receiver is at the discriminator—before the de-emphasis network. This is often the point in the radio where the noise is taken off for the radio's squelch circuit. The HAPN-T modem needs this noise to operate its carrier-detect (squelch) circuit. This CD circuit has been optimized for packet operation and switches in at about 10 to 15 ms.

Some older radios may have a discriminator test point which could be used for take-off. If the discriminator test point has a large bypass capacitor to ground (larger than 1000 pF), the HF-noise component (around 11 kHz) is attenuated along with the IF. In this case, replace the bypass capacitor with 1000 pF to allow the audio noise to pass through.

Many newer radios use ICs in the IF and demodulator sections—almost always the Motorola MC3357 (14-pin dip) or the MC3359 (16 pin). Both chips are similar and lend themselves very well to interfacing. The low output impedance (around 300 ohms) on the audio-out line (pin 9 for MC3357 or pin 10 for MC3359) allows longer shielded cables for the modem, so the radio can be placed further away from the TNC.

You need to be able to place the radio further away from the TNC because the shielded-cable parallel capacitance, which is added to the take-off point capacitance,

might attenuate the audio noise component needed for the modem squelch. It has much less effect on the low 300-ohm output impedance of this chip, than it does on those on older type modulators which have a high output impedance. For example, if you use a 20-foot run of Belden 8723 cable with a cable capacitance of 62 pF/foot, 1240 pF (20×62 pF) is added to the take-off point. The reactance at 11 kHz (audio noise component) would be around 110-k ohms ($1/(6.28 \times 11000 \times 0.0000000124)$). This value has no effect on the 300-ohm output impedance of the demodulator chips, but could load down a high-impedance demodulator. Usually the audio cable to the radio is 10 feet or less, and you'll encounter no side effects in either case. As a precaution, you can use a 10-k series resistor at the take-off point to prevent accidental shorting of the demodulator. This normally won't present a problem, but may give you an added sense of security.

TX audio

Because of the nonlinear characteristics of the audio amplifier (limiter and emphasis network), interfacing through the mike doesn't work. You must go directly to the modulator. The modem output impedance is around 200 ohms and is suitable to drive almost any FM or PM modulator. To find the interface point, look at the radio schematic for the deviation control. You'll usually find it after the limiter/filter. The deviation trimpot output normally goes through a resistor (and often a capacitor, as well) to the modulation varicap diode. The diode capacitance is changed by varying the voltage across the diode (since the diode is reverse biased). The varicap is often mounted in a shielded compartment. Do not connect directly to the diode, but to the resistor that carries the signal to the diode. This is often the same point as the deviation-control wiper.

Determining modulation type

There are two types of modulators, FM and PM. It's important to know which type your rig uses so you can install modulation-selection jumper J101 correctly. If J101 is in the wrong position, the modem won't generate the proper waveshapes for the transmitter, and nobody will be able to copy your signal. The radio manual's specification section should tell you what type of modulation the transmitter uses. However, don't take their word for granted. One HAPN-T user was convinced that his modulator was phase modulated, and set J101 accordingly.

The modem didn't work very well. Interestingly enough, he did receive a short packet on occasion. However, he spent many hours looking for faults until he set J101 for frequency modulation.

An FM modulator changes the oscillator frequency directly, usually by means of a small varicap diode in the tuned section. On the other hand, PM modulators change the phase of the signal in a stage following the oscillator. Most radios use an FM modulator; it's always a good bet to try that first when in doubt.

Examples of receiver interface points

The RX4800 audio must be taken from the discriminator ahead of the audio de-emphasis network. Often, this point is also used for squelch takeoff. It's *important* to use shielded cable.

Yaesu FT480R. Figure 5A shows connections to the Yaesu FT480R. Note that the demodulator is a conventional FM discriminator using one-half of the IF transformer; divider R45 and R46, instead of a center tap; two diodes, D10 and D11, for rectification; and C51 to filter the IF AC voltage. The squelch noise is taken from series filter L05 and C53. The audio is taken from de-emphasis network R47 and C52. The take-off point at D10, D11, and C51 is located in the same place where the receive signal is taken for the modem. Use a 10-k series resistor for isolation.

Kenwood TR-7400A. Figure 5B shows another conventional FM modulator. The RX audio take-off point is similar to that of the FT480R. A 10-k series resistor is added from the modulator output (R44, R46, C48) where it meets the squelch take off (C49) and the audio take off (C65, R62). This is located just before the de-emphasis network R62 and C64.

Kenwood TR-7730. Figure 5C shows another Kenwood. The take-off point is from a 10-k resistor at the junction of the discriminator output (R51, C58), the squelch take-off (C57), and the audio take off (R114).

Santec ST-144 μ p. Figure 5D shows the handheld interface. It uses the MC3357 FM chip. We could have chosen pin 9 for the take-off point, but since this pin is difficult to access in the handheld, we used CT5 (demodulated AF output test point). Note that this take-off point is still before the de-emphasis network (R105 and C146).

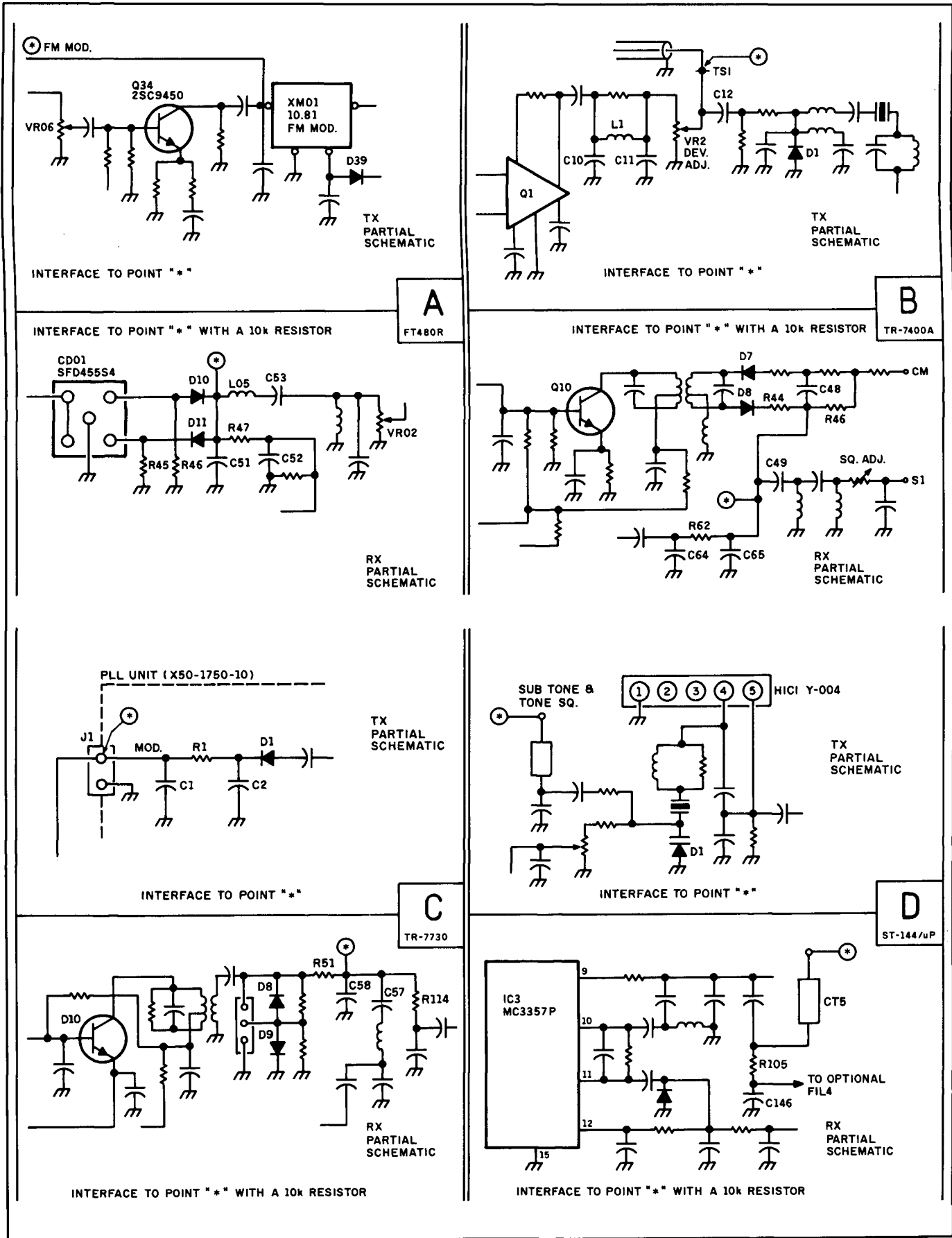


Figure 5. Interface diagrams for four radios.

Examples of transmitter interface points

The 4800TX audio must go directly to the FM or PM modulator to avoid distortion. As we have said, it is *very* important to ascertain the modulator type and set jumper J101 accordingly. Use good shielded cable from the modem to the radio. RF pickup in the TX audio cable will cause distortion in the modulator.

Yaesu FT480R. The TX audio should be tapped into the FM modulator line, as shown in **Figure 5A**.

Kenwood TR-7400A. The connection is shown in **Figure 5B**. The modulating component is D1, a varicap diode, which changes the 10.7-MHz crystal oscillator frequency. Backing up, you see VR2 and the 5-k deviation adjustment pot. Limiter filter C10, C11, and L1 is just ahead of this. You can conveniently interface the 4800TX audio to point TSI going to the wiper of VR2 and coupling capacitor C12.

Kenwood TR-7730. The TX audio can be tapped easily at connector J1, at the point where the modulation enters the PLL board (see **Figure 5C**). The audio goes to a varicap diode, D1, which modulates the PLL-oscillator frequency.

Santec ST-144 μ p hand-held. The TX audio can be connected to the SUB-AUDIO TONE IN entry point (**Figure 5D**). This audio is applied to D1, the frequency modulation varicap diode. We used a 1-k resistor as a limiting resistor, but it's not really required.

Adjusting the HAPN-T

Install the modulation selection jumper on J101 posts (refer to radio manual for modulator type):

- FM modulators (most radios): position the jumper on the side closest to R37 pot (pins 1 and 2).
- PM modulators: position the jumper away from pot R37 (pins 2 and 3).

Adjust the modem potentiometers. Make sure the radio is connected and turned on.

1. **Level adjustment, R2:** Put an analog voltmeter at TP1 and adjust for about 9 volts DC when receiving noise (no antenna). If you have a scope, use U3A/1 (TP4) and adjust until the noise signal is just clipping. If you find that turning R2 doesn't decrease the signal sufficiently, install jumper J104 to decrease the op-amp gain.
2. **Squelch (carrier-detect) adjustment, R23:** Turn until the DCD light on the modem is on when the radio is turned off, and

comes on when the radio is turned on and receiving noise (coarse adjustment). Attach the antenna and connect a voltmeter to TP3. Monitor an active packet channel (1200 or 4800). Turn the pot until you measure about 2.5 volts or higher with carrier and 0.5 volt or lower with no carrier.

3. **Transmit level adjustment, R37:** Make sure jumper J101 is installed, as mentioned earlier. Put the modem in 1200-baud mode by opening the switch on the TNC-2 (J105 removed) or the TNC-1 (select BANK 0 and actuate RESET). Connect an AC voltmeter or scope to J103 pin 5. Key up long 1200-baud packets (or use the CALIBRA command) while observing the meter. Write down this value; it's your 1200-baud operating level.

Temporarily increase the level to maximum by turning the 1200-level pot on the TNC board. If you're like most packeteers, feeding audio through the mike might not cause a further increase because the signal hits the limiters in the radio. Write down this value; it's your limiting value (usually about 5 kHz deviation). Take 70 percent of this value and write it down; it's your preferred transmit level (about 3 to 3.5 kHz deviation). Turn the level pot on the TNC back to the first value you recorded. Now switch to 4800 baud by installing the jumper at J105 (TNC-1 select BANK 1 and actuate reset). Key up the TNC again. This time packets are at 4800 baud. Observe the level. Adjust R37 until you read the third value you recorded.

You've now completed all the adjustments and are ready to try on-the-air tests. If you encounter poor results, make sure your radio is on frequency—both for transmit and receive. Also double-check to make sure that the J101 (FM/PM select) setting is correct for your rig. Finally, cut down on your TXdelay. (You may also have to cut down other delays.) You can make the TXdelay shorter because of the fast-acting modem squelch, which switches in at about 15 milliseconds. This will result in better use of the available radio channel.

If everything is working at this point, and you wish to experiment some more, you can try the 4800-tap points on 1200 baud. This often results in better performance for 1200-baud reception and eliminates the additional interface wires. As an added benefit, you don't have to watch your radio's volume and squelch controls anymore, as they will have been bypassed. For more information on this subject, see the sections on service aids.

There's an additional modification which may improve your 1200-baud reception (it really has nothing to do with the 4800-baud modem). Try bypassing the MF10 filter in the TNC. Some of the newer TNCs, like the MFJ1270B and MFJ1274, have eliminated this filter altogether.

If you still encounter problems at this point, check all previous steps, and then check the sections which follow.

Modem service aids

First, look for poor or missing solder joints. Next, verify that the ICs are plugged in properly and check for bent pins. Finally, check the op amps. With no signal (radio turned off and not transmitting), the outputs of op amps U3B, U3A, U3C, U5A, and U5B should be 6 volts (same level as U3D/14). The outputs of U5D and U5C should be 5 volts (same as zener D5 voltage).

If you're not getting enough high-frequency noise from the receiver for the squelch to operate properly (about 2-volts swing at squelch gate U6A/1 is needed), a bypass capacitor on the line from the RX-audio tap point might be the culprit. Remove or replace the capacitor with a smaller value. If this isn't the case, you can pick up more noise (HF, about 11 kHz) by increasing C2 (try 1500 pF).

Radio service aids

Signals at TP1 and TP2 referenced to U3D/14 should be about equal to the noise amplitude. If not, check to see if you're picking up a weak received signal, like computer noise. If your computer is causing interference, turn it off or change frequency. Disconnect the antenna and check again. If the reading persists, and it's severe, your RX discriminator may not be working properly.

If 4800-baud packet signal levels at TP1 and TP2 vary a lot, but the above noise test is okay, consider the possibility that your receiver (or the sender) is off frequency.

If you're not sure of the correct tie points for the TX audio and/or RX audio for your rig, send us a copy of your circuit diagram and we'll suggest the best connection points.

TNC-2 service aids

To eliminate the "1200-MIC-AUDIO" line and use the "4800-TX-AUDIO" for 1200 baud, try the following: Disconnect the wire at J103 pin 1 (1200-MIC-AUDIO) and install a jumper at J100. Now, readjust the 1200-baud audio level control (R76 on

MFJ1270B) on the main board. If the level is too low, short out series-output resistor R56 and/or increase the coupling capacitor value.

To bypass the MF10 filter in the MFJ1270 (the MFJ1270B and MFJ1274 don't use the MF10), unplug U18 and replace network U17 with a DIP header. Connect pins 1 and 8 on the header. This will result in a flat audio response where the high and low tones (2200 and 1200) should have more equal amplitude. (The XR2206 chip has trouble decoding when the tones are too dissimilar.)

If you'd like to use the 4800-carrier detect for 1200 baud as well, ground the XR2211 DCD line (U20 pin 6 on the TNC-2). Then connect U6 pin 2 to pin 14 (+5 volts) on the modem board. This enables the 4800 CD unconditionally. Next, install jumper J105 and move one of the wires of the baud-rate switch to GND. This should make U1 pin 9 about 10 volts at 4800 baud or 0 volts at 1200 baud.

Available from HAPN

The HAPN-T 4800-baud modem circuit board is available for \$15. You can also purchase the circuit board and a parts kit for \$48. Prices are in United States dollars. To cover shipping costs, please add \$5 for United States and \$8 for overseas orders. Amateurs who are interested in packet radio, and who own an IBM PC or compatible, might also be interested in the HAPN-1 adapter—a complete integrated packet radio system. Write for details. HAPN's address is Hamilton and Area Packet Network, P.O. Box 4466, Hamilton, Ontario, Canada L8V 4S7.

Conclusion

We invite your comments and suggestions on the HAPN-T modem. We can be reached by mail at the address listed above, on CompuServe at 73327,176 (VE3LNY), or by packet radio to John, VE3DVV, at VE3HPL. We're interested in your feedback. We would like to thank VE3LU, VE3NAV, and VE3MCF for their assistance with the HAPN-T project. ■

REFERENCES

1. Ken Smith, VE3HWP, and Glen Simpson, VE3DSP, "Packet Radio with the 1802," *Ipsa Facto newsletter of the Association of Computer Experimenters*, April 1979.
2. Glen Leinweber, VE3DNL, Max Pizzolato, VE3DNM, John Vanden Berg, VE3DVV and Jack Botner, VE3LNY, "A 4800-Baud Modem for VHF/UHF Packet Radio," *Ham Radio*, August 1988.

Dr. Alan Chandler, PHd EE, K6RFK
Vice President Engineering
Advanced Electronic Applications, Inc.
2006 196th SW
Lynnwood, Washington 98036-0918

HF MODEMS FOR DATA TRANSMISSION

A look at the differences between commonly used designs.

In the last ten years, the number of Amateur Radio operators using various data modes has increased dramatically. Two of the primary reasons for this increase were the introduction of inexpensive computers and commercial radio modems that used the computers for data communication (see **Figure 1**). Amateurs were liberated from noisy, heavy, oil-dripping mechanical Teletype™ machines. I finally put my model 28 into storage a few years ago.

There are a number of products designed for Amateur use that provide modems and protocol conversion from many data modes such as Baudot, AMTOR, ASCII, packet, Morse, etc. to ASCII for use with a terminal or a computer. With the exception of Morse, which uses On-Off Keying (OOK), nearly all HF data communications use Frequency Shift Keying (FSK). FSK uses a pair of radio frequencies—one frequency representing the binary 1 and the other the

binary 0 (also referred to as mark and space). The two frequencies are separated by 85 to 1000 Hz depending on the mode. The most common frequencies in use today are 170 and 200 Hz. Amateurs originally used 850-Hz shift, which has some advantages on fading paths. As the stability of Amateur transceivers improved and the bands became crowded, 170 Hz became the most commonly used shift. The originators of packet radio chose a Bell standard 200-Hz shift which is fine for telephone use, but is too narrow for optimum use on HF. (A minimum of 600 Hz provides much better throughput under marginal conditions.) Equipment designed for 200-Hz shift can be used with 170-Hz shift equipment, as there is only 15 Hz offset from each tone. The 15-Hz difference is far too small to be affected by the demodulator filters.

The transmitted data signal can be represented by two on-off keyed signals

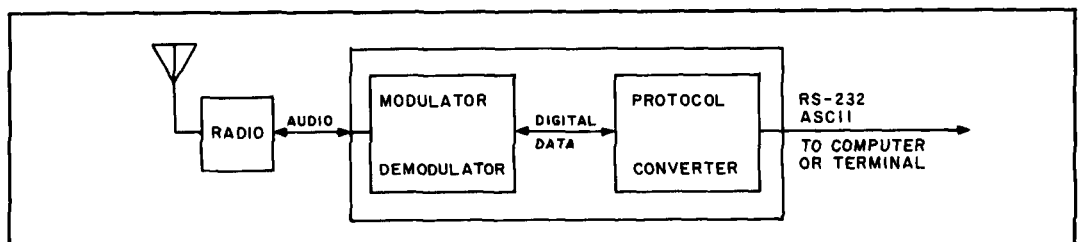


Figure 1. Typical HF data station.

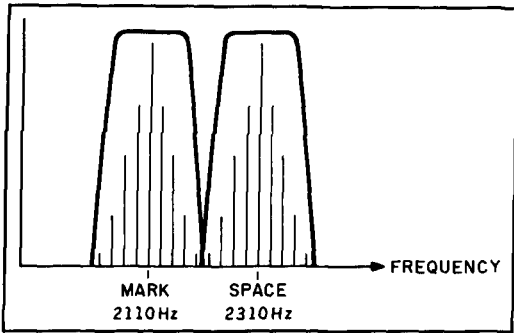


Figure 2. Frequency response of the twin filters and keyed AFSK tones.

separated by the frequency shift. Each of the tones will have a set of sidebands around them due to the on-off keying of the digital data (see Figure 2).

Transmitting FSK

Generation of the transmitted FSK signal is relatively easy. One method is to feed sine wave audio tones into an SSB transmitter. The SSB transmitter translates the audio frequency sine wave to a radio frequency sine wave. The two audio tones are converted to the two radio frequency tones which, by convention, are reversed. What was the lower-frequency audio tone is transmitted as the higher-frequency radio signal and vice versa. LSB is used because it provides the reversal.

Demodulator considerations

The real challenge of designing a data

communication system lies in the design of the demodulator. The variables which must be considered are: data rate, shift, and the real headache, HF radio propagation. The problems with an HF radio link are: selective fading, noise, different path lengths for the two tones, multiple paths, on-channel interference, and near channel signals.

Selective fading occurs during periods of multiple path propagation. One path may interfere destructively with another. This can result in the loss of one particular tone of an FSK pair, but not necessarily the other, because of the slightly different frequencies. The timing of these fades is usually a few seconds. It is very noticeable on AM foreign broadcasts, producing a hollow sound that changes pitch. Different path lengths may produce both tones at the same time for a very short period, or no tones for the same period.

A communications receiver is used to convert the pair of radio frequency signals to a pair of audio tones, called Audio Frequency Shift Keying (AFSK). The demodulator converts these tones back into the binary 1 or 0 that the original tone represented, and minimizes the undesirable effects of HF propagation and interference.

AFSK demodulators

AFSK demodulators can be classified into two basic types: the twin filter-comparator (Figure 3a) and the limiter-discriminator (Figure 3b).

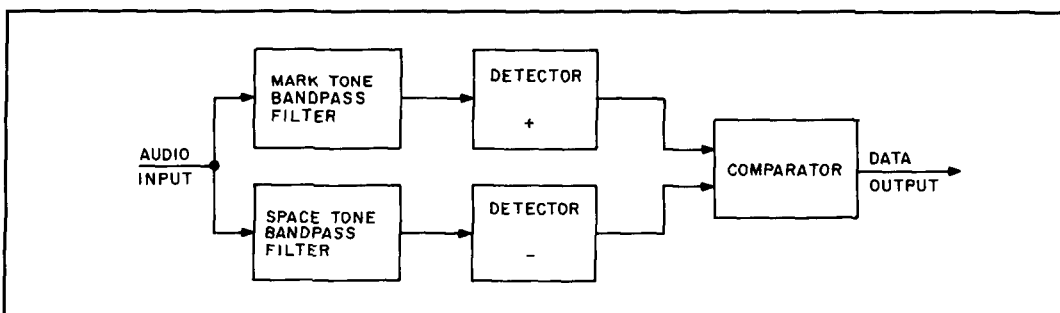


Figure 3A. Basic twin filter-comparator demodulator.

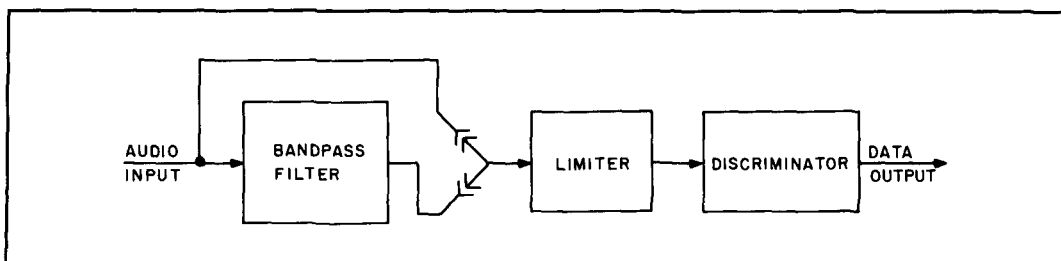


Figure 3B. Basic limiter-discriminator demodulator. Bandpass filter should be used if the receiver doesn't have a narrow bandwidth IF filter.

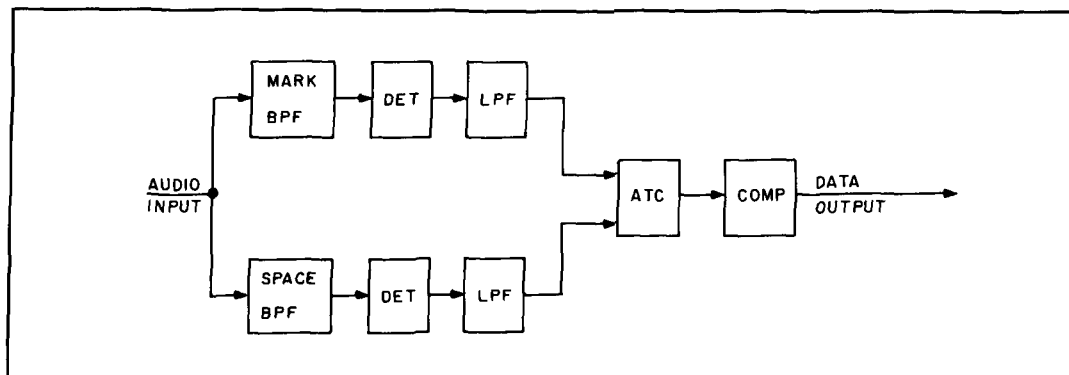


Figure 4. Complete twin filter-comparator demodulator with automatic threshold correction.

Twin filter-comparator demodulator

The twin filter-comparator demodulator uses two bandpass filters. At the output of the filters are detectors and a comparator. One of the filters is centered on one of the tones and the other is centered on the other tone, as shown in **Figure 2**. The comparator decides which of the filters has the largest signal. If both of the bandpass filters have the same bandwidth and are of the same type, the delay through the filters will be the same. It is important that the pulse time delay through the filters be identical so noise bursts cancel at the comparator. If different shifts are to be used, one of the filters must be tunable. The type of filter used is also important. It is desirable to have a filter with narrow skirts to eliminate adjacent channel signals. It is also desirable to have a filter with little or no ringing. Unfortunately, having both requires many sections of a Bessel filter, or some sort of compromise. For the bandwidths used, 100 to 200 Hz, Chebyshev filters can be used with very good skirt selectivity and little During selective fading, one of the two tones may disappear completely and the other may still be present. The comparator should be designed so it will still function with only one tone. For best noise immunity, both detectors should be followed by

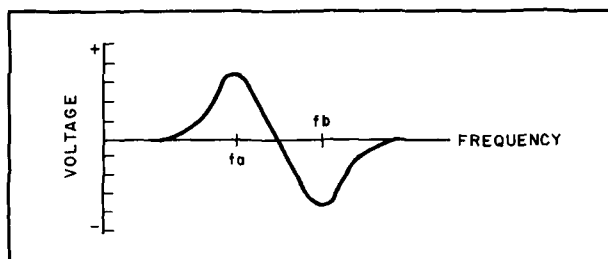


Figure 5. Discriminator response.

low-pass filters. The filter cutoff frequency should be 1.2 to 3 times the baud rate. As a compromise, a single low-pass filter can be used following the comparator. The complete twin filter system is shown in **Figure 4**. Some examples of excellent twin filter systems were the IRL-1000, which used Bessel transitional filters, and the AEA CP-100, which used Chebyshev filters.

The AMD (and other) 7910 integrated telephone modem has also been used with some success on HF circuits. It has Bell 202 (VHF) tone pairs as well as the Bell 103 (200-Hz shift) tones. It is basically a twin filter-comparator system using an analog-to-digital converter followed by digital bandpass filters. Because it was intended for telephone use, it unfortunately has no provision for compensating for selective fading, and its data carrier detection circuit responds to in-channel noise as well as signals.

Limiter-discriminator demodulators

Figure 5 shows the response of a typical frequency discriminator. The discriminator converts frequency to voltage over a selected range of frequencies. In this example, the frequencies would be in the linear range of the response curve, between f_a and f_b . A comparator follows the discriminator. The comparator is set to the voltage corresponding to the frequency midway between the two tones.

There are a number of types of discriminators. Two tuned circuits using coils and capacitors or op-amp resonators may be used as shown in rudimentary form in **Figure 6**. A simple Phase Locked Loop (PLL) integrated circuit, like the 2211, is used in some Amateur products. Integrated circuits intended for use in an FM receiver are also suitable. Most of the PLL and receiver integrated circuits also have the limiter stages.

The limiter is a very high gain amplifier signal to the discriminator. The output of the limiter is the strongest input signal. If the strongest signal is not the signal of interest, or out of range of the PLL, the PLL system will not provide the desired output. For any kind of HF performance, it is necessary to limit the receiver bandwidth or provide an audio bandpass filter ahead of the PLL system.

The 2211 phase-locked loop

The Exar 2211 PLL was designed for tone detection or for FSK demodulation in telephone modems. It works very well on VHF radio circuits, but has several disadvantages for HF use. Since it has a very good limiter, it requires an input bandpass filter to prevent the limiter from being captured by near channel signals that are just a fraction stronger than the desired signal. During periods of selective fading, the PLL has no signal to lock to during the missing tone. The result is poor performance during selective fading. With the 2211 internal comparator reference inaccessible, there really is no good way to compensate for selective fades. I have also found the 2211 to be only fair in terms of weak signal performance, perhaps due to the need to relock. The 2211 should always be used with a narrow bandwidth filter or an audio input bandpass filter.

Because many SSB transceivers do not allow very narrow filters (500-Hz bandwidth) to be used in the SSB mode, an audio bandpass filter is necessary for optimum performance. (The SSB mode is necessary in many radios for the generation of the FSK signal.)

FM receiver integrated circuits

Several FM receiver integrated circuits are suitable for use as AFSK demodulators. An early AMTOR system, the AMT-1, designed in England, used the TBA 120 FM receiver subsystem. The receiver was preceded by an eight-pole Chebyshev bandpass filter. The demodulator performed very well.

Twin resonator discriminators

There are several other ways of designing audio discriminators. Two resonators are tuned to the two audio frequencies as shown in **Figure 6**. The Q s of the resonators (determined by the series resistors) are set so the -3 dB response points are at the geometric mean of the two frequencies. (The geometric mean is the square root of the product of the two tone frequencies. It is generally

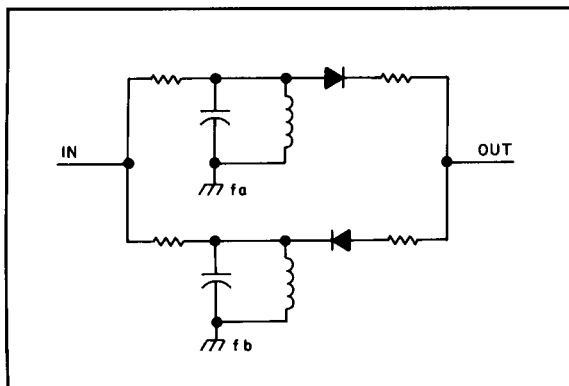


Figure 6. Simple twin-resonator discriminator.

close to the average of the frequencies.) The resonators may be inductor capacitor circuits or one of many types of operational-amplifier resonators. The outputs of the resonators are detected, but with opposite polarity, and the result is summed. The summer output voltage is determined by the input frequency. The discriminator alone could be used as a demodulator, but performance is greatly enhanced when it is preceded by a limiter and a bandpass filter. One advantage of the twin resonator discriminator is that it will provide an output with only one of the two tones during selective fading. A threshold corrector must be used for maximum performance. Examples of the twin resonator system with input bandpass filtering, limiter, and threshold corrector are the AEA CP-1, AEA PK-232, and the Kantronics KAM.

Threshold correction

If the detected output of the discriminator or twin filter systems has equal amplitude input tones, the comparator decision point is halfway between the two voltages

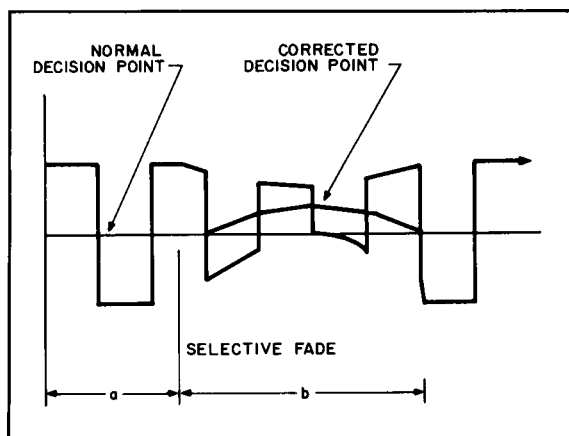


Figure 7. Automatic threshold corrector action.

(see **Figure 7**, region a). During a selective fade, where one of the two tones disappears, a decision point between the two voltages will be incorrect. Since the information desired still exists in the remaining tone, the decision point must automatically move in the direction of the remaining tone (see **Figure 7**, region b). A circuit that stores the amplitude of the two tones averages and divides by two, and will make the necessary correction of the decision point. This system works very well with the twin filter demodulator and the limiter-discriminator demodulator. Because the PLL system loses lock during missing tone periods, the threshold corrector is not appropriate for use with that system.

Conclusions

Both the twin resonator-comparator and bandpass filter-limiter-discriminator

demodulator work very well in HF data communications if care is taken in the system design. The simple PLL system is considered a limiter discriminator system and is the poorest performer on HF. For any performance on HF, it must be used with a narrow receiver IF filter (about 500 Hz). It will still have difficulty with selective fading and impulse noise. Both systems benefit from automatic threshold correctors and post detection low-pass filters. If wide shift, low data rate communications are used, the twin filter system will provide better performance because the noise bandwidth will be smaller than with the limiter discriminator systems.

The Amateur community will soon have digital signal processing modems available which will allow even greater performance for HF data communications. I will save that discussion for a future article. ■



JOIN AMSAT

Support the Amateur Space Program

AMSAT Has Established Amateur Radio As a Permanent Resident in Space!

From operating any of 12 Amateur satellites circling the globe today to participating in Amateur Radio activities from the Space Shuttle, the benefits of space based Amateur Radio are available to you by becoming an AMSAT member. Our volunteers design, build and launch state-of-the-art satellites for use by Radio Amateurs the world over. We provide educational programs that teach our young people about space and Amateur Radio. Most of all, we provide our members with an impressive array of member benefits including:

- Operating aides such as discounted tracking software and land line BBS.
- An extensive network of volunteers to provide you local technical assistance.
- The AMSAT Journal, your bi-monthly periodical devoted to the Amateur Space program.

It's Fun! It's Easy! It's Exciting!

JOIN TODAY. For more information, call or write for your free information packet. Or send your dues now, check or charge: \$30 U.S., \$36 Canada/Mexico, \$45 all else. (\$15 towards the AMSAT journal.)

AMSAT, P. O. Box 27, Washington, D.C. 20044

(301) 589-6062; Fax: (301) 608-3410

SIGNAL-TO-NOISE Voting Comparator



Improve coverage by adding receivers

- Expandable to 32 Channels
- Continuous Voting
- 19" Rack Mountable
- Select/Disable Switches for Manual Override
- Can be used with RF Links or Dedicated Lines
- LED Indicators
- Hundreds in Service
- More

—Competitively Priced—
For more information call or write:

Doug Hall Electronics

815 E. Hudson St.

Columbus, Ohio 43211 • (614) 261-8871

FAX 614-261-8805

YAGI OPTIMIZATION AND OBSERVATIONS ON FREQUENCY OFFSET AND ELEMENT TAPER PROBLEMS

Using computer programs for antenna analysis

In recent years, Yagi modeling programs have taken the hit-or-miss aspect out of antenna design. It used to be that the only practical way to determine Yagi characteristics was to build one, make range measurements of the pattern, and measure the VSWR.

It was only natural that the introduction of the high-speed computer spurred attempts to derive an antenna-analysis program. Of course, the computer can't design an antenna by itself. But, if the physical dimensions of an antenna design are input, the computer program will predict the performance of the array. Once the dimensions have been entered, some programs can even optimize designs according to user-supplied criteria. The accuracy of the antenna analysis program depends upon the algorithms with which the antenna currents, phase, feedpoint type, and radiation patterns are calculated. The computer model can be checked for accuracy against a real antenna with the same physical characteristics.

Numerical Electromagnetic Code (NEC)

The Antenna Modeling Program (AMP) was an early antenna program developed in the 1970s for the Naval Research Laboratories. It was later upgraded and renamed NEC—one of the first of the many computer codes for HF and VHF antennas. The program was developed at the Lawrence Livermore Laboratories in California by G.J. Burke and A.J. Poggio in 1981 under the sponsorship of the Naval Ocean Systems Center (NOSC), the United States Army, and the Air Force Weapons Laboratory! NEC has evolved over time to include features useful in modeling large or small antennas. The most recent versions, written in FORTRAN, are available for use on IBM, UNIVAC, VAX, CDC, and Cray main-frame computers. The NEC programs are very extensive and require an IBM punched-card input format. This is usually a laborious project, particularly for large antennas mounted over real ground. All

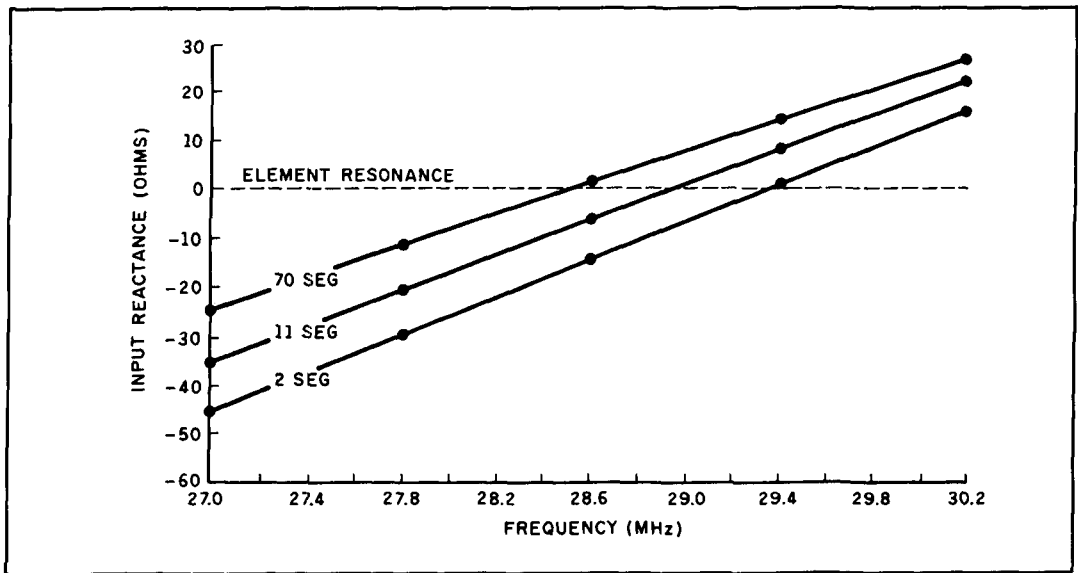


Figure 1. The input reactance of a tapered element analyzed by NEC varies with the number of segments used. This representative element is self-resonant near 28.6 MHz. If only 11 segments are used, element resonance falls about 300 kHz higher in frequency.

dimensions must be scaled to meters (or a special units conversion-card image must be added). Such limitations don't lend themselves to a readily available, user-friendly program for the non-engineer.

NEC operates by dividing the antenna structure into small segments. It then determines the current in each segment by solving the boundary conditions and summing the currents to create radiation patterns. This procedure is called the "method of moments." The user supplies the number of straight wires in the antenna, the number of

segments each wire contains, end coordinates of each wire in X-Y-Z (Cartesian) format, along with the frequency, antenna excitation, and impedance-loading parameters. Finally, the user specifies the physical environment; that is, free space, ideal ground, or real ground. Once the information is processed by NEC, the user must check the model against others for consistency and accuracy, knowing the limitations of the computer code in its ability to accurately model the antenna under examination.

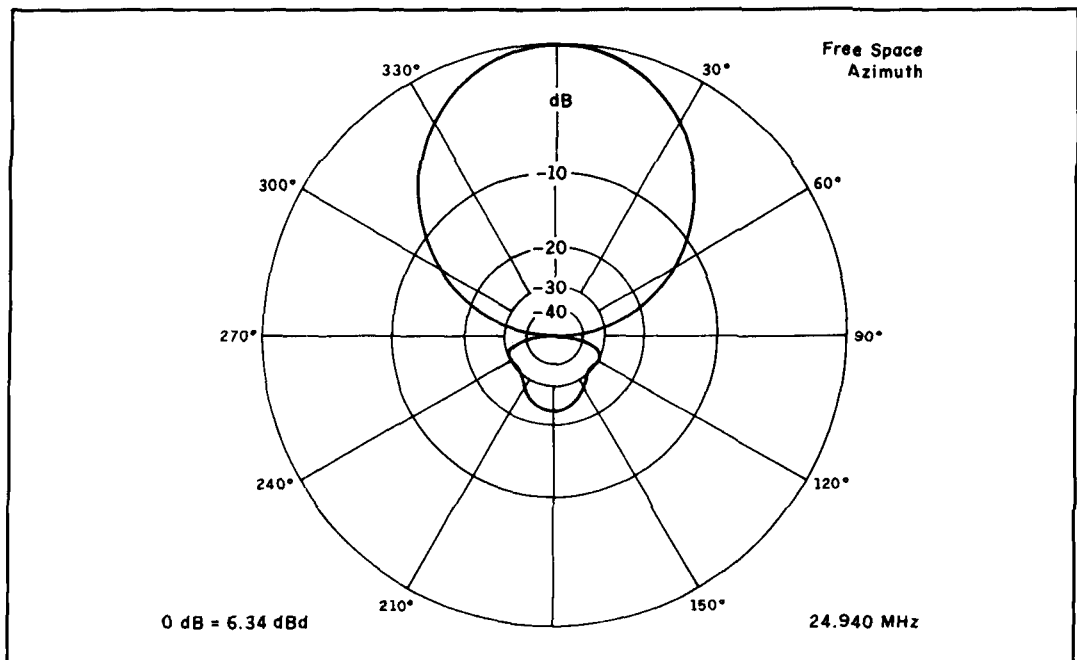


Figure 2. Azimuth plot of a four-element, 12-meter Yagi is provided by K6STI version of MININEC program. Free-space gain is 6.34 dBd, front-to-back ratio is better than 22 dB, and -3dB beam width is about 60 degrees.

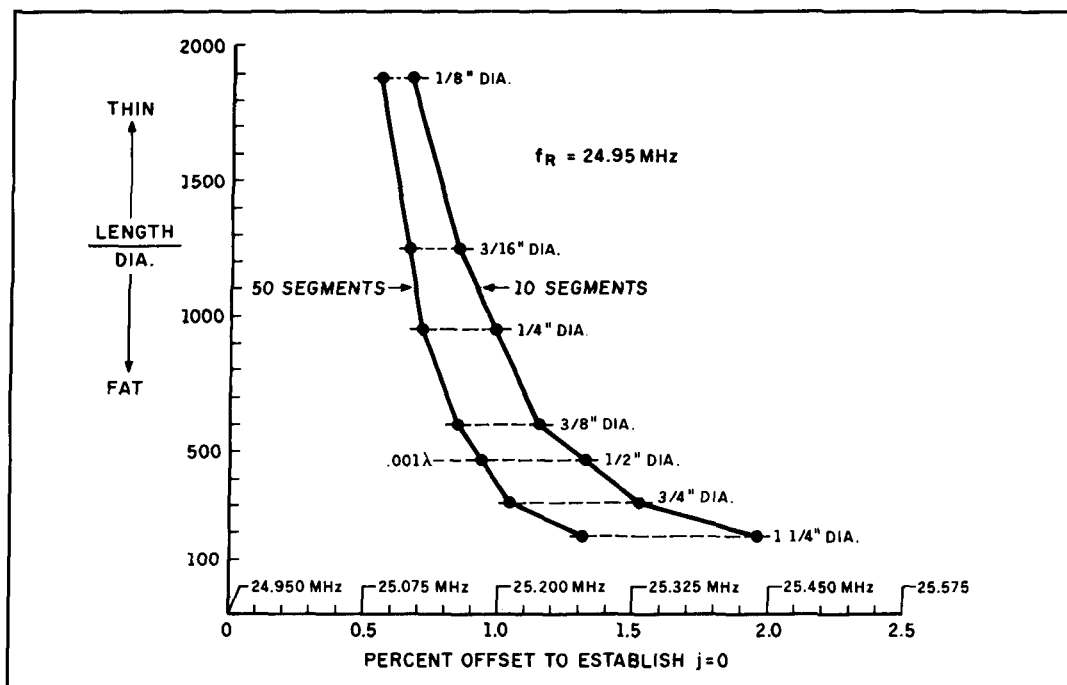


Figure 3. Representative frequency offset of test dipole when examined in MINIMEC-derived program. Percent-age offset is least when many segments are used and element diameter is small compared to length (less than 0.001 wavelength). Once offset is know, it may be factored into final antenna data to provide accurate dimensions.

NEC problems with stepped-radius elements

A comparison of NEC results on a stepped-radius (tapered) element, with antenna-range measurements on the same element, showed that the NEC program introduced a frequency offset and considerable changes in current ratios and phasing. Correct values are essential for an accurate computer model^{2,3} but once this tapered-element frequency offset effect is recognized, it may be accounted for. However, this adds another complication to an already complicated process. As of this writing, the problem is under investigation (see Figure 1).

MININEC

The NEC program is a powerful tool for many engineering applications. In its original form it required the support of and access to a large main-frame computer. Unfortunately, these computers are expensive to run and not readily available to the antenna enthusiast. Recently, however, a simplified version of NEC was made available for personal computer (PC) users. Full NEC capability isn't really required for simple Amateur antennas because the antenna and its environment may not be very complex, or because the information sought requires only a simplified model. NEC,

therefore, is probably overkill for the average Amateur who needs something much simpler and more user-friendly.

The breakthrough came with the development of a stripped-down version of NEC for the personal computer, known as MININEC. The program, designed to analyze thin-wire antennas, was written in BASIC and entered into the computer via the keyboard. MININEC was created by A. Julian, J.C. Logan, N6BRF, and J.W. Rockway⁴ at the Naval Ocean Systems Center in San Diego, California in 1982 and updated in 1986⁵. The program has less capacity than NEC and fewer of the advanced features inherent in NEC. Some ready-to-run versions of MININEC are available on floppy disk with keyboard input, menus, prompts, and data storage/retrieval features. Other versions of MININEC, modified for particular applications, exist. There are also versions aimed specifically at the Amateur market which have files, text editors, plotting programs, graphics, and other features that make them user-friendly⁶.

As with NEC, MININEC requires that the user define the initial antenna geometry and other characteristics. As before, the antenna geometry is specified in X-Y-Z coordinates. Almost any type of antenna can be modeled, provided the coordinates are available. The antenna is divided into wires which the computer then breaks down into smaller segments for analysis.

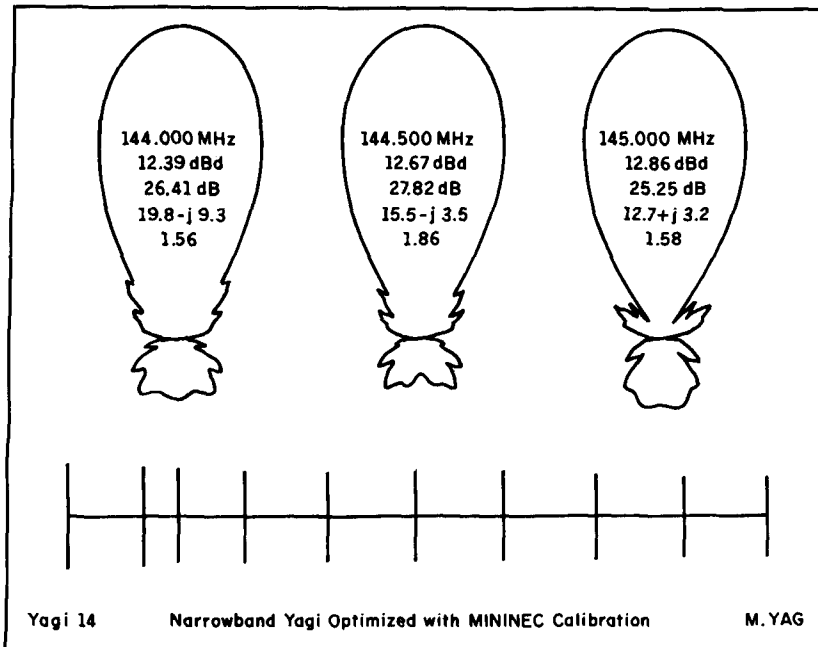


Figure 4. MININEC-optimized VHF beam looks good on paper, but real-life model produced mediocre results.

Once the antenna data is loaded, the MININEC program crunches the numbers and generates all the information needed about the antenna. The user provides antenna parameters and the program determines the gain, front-to-back ratio, bandwidth, and antenna input impedance. Some variations of the program provide patterns on the computer screen in both azimuth (see Figure 2) and elevation. This lets the user

compare these plots with those of another antenna design.

Putting MININEC to work

The original MININEC program wasn't very user-friendly. Some operators swear by it but others, like myself, who have enough trouble finding the on/off switch on the

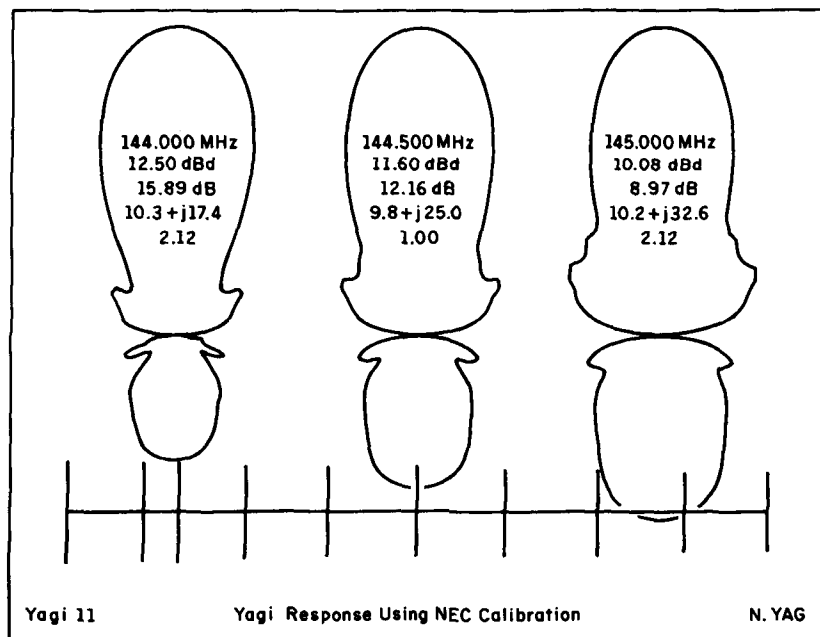


Figure 5. Beam shown in Figure 4 actually performed in the manner predicted by NEC—very poorly. Gain and front-to-back ratio dropped drastically as frequency of measurement was raised. Input impedance was low and VSWR response was poor. Reoptimized by NEC, the beam performed as it should, as predicted in Figure 4.

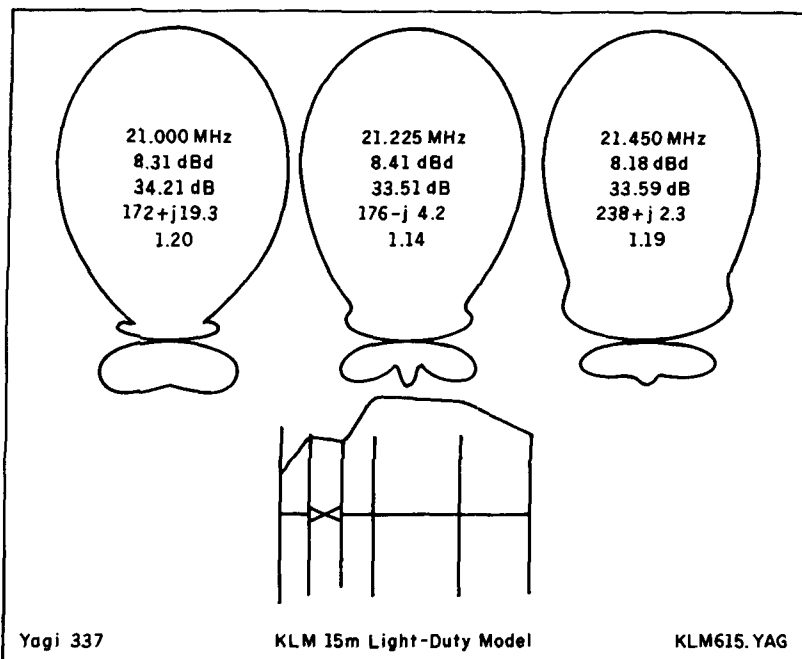


Figure 6. Optimized KLM-615 dual-drive, 15-meter Yagi. Array provides good gain and excellent front-to-back ratio (better than 33 dB) over the whole band. When properly matched, VSWR varies from 1.28 at the low band edge to 1.19 at the high band edge. Current in each element is represented by the varying line running across the top of the elements. Reflector current is very low.

computer, shy away from MININEC's complex keyboard input format.

Various MININEC-derived software programs with user-friendly input requirements are available. These programs have prompts for menu-driven or README files which make data input a relatively simple operation. Such programs quickly became popular in Amateur Radio circles because they provided the means to design and verify the attributes of a particular antenna, before actually building it.

MININEC problems with frequency offset

Recently, Amateurs and others have investigated the accuracy of the different MININEC-based modeling programs. Yagi antennas constructed from program specifications often measured lower in frequency than predicted. The effect was most noticeable on VHF/UHF arrays, particularly with high-Q, narrow-bandwidth designs. (My MININEC-designed multi-element beam required the use of a hacksaw to bring it into alignment with the design frequency.)

In some cases, the design frequencies shifted as much as two percent. The shift seems to be a function of the element length/diameter ratio and the number of segments used in the design program. This gave rise to the thought that some of the "stripping down" of NEC to produce

MININEC may have added built-in problems where large-diameter elements are involved.

Several investigators have confirmed the frequency offset effect.^{7,2} I verified the offset by inserting simple dipole dimensions into my MININEC-derived antenna program, varying element diameter and number of segments, and comparing the answers to known results (Figure 3). If a narrow-band antenna like a Yagi is used, and the frequency offset is known, the experimenter can run the program at the offset frequency and get good results, provided he *does not* use too few segments. As one investigator put it, "Segments should not be as fat as a tuna fish can, nor as long as a clothes pole. Visualize the shape of a cigarette."

The YO 4.0 Yagi Optimizer

MININEC exhibits frequency offsets ranging from 0.25 to more than 2 percent, depending on the diameter of the elements and the number of segments used in the program. NEC, on the other hand, exhibits an offset when elements are tapered. This effect has not been observed with MININEC.

Brian Beezley, K6STI, discovered one solution to these perplexing problems? His new YO 4.0 Yagi Optimizer program is calibrated to NEC using untapered ele-

ments. He used over thirty Yagi designs in the calibration procedure. For example, six four-element Yagis with element diameters of 0.0001 to 0.01 wavelength and almost no rear lobes at a single spot frequency were used to align YO 4.0 to within a couple of kHz of NEC at 14 MHz. By comparison, the alternative MININEC calibration available in YO computes correct patterns at frequencies 30 to 335 kHz higher for these designs.

YO 4.0 offers an advanced element-tapering algorithm. This algorithm, a modification of the classic W2PV tapering method, was developed by matching tapered and equivalent untapered element self-impedances using MININEC. The resulting program takes advantage of the attributes of NEC and MININEC, while avoiding the shortcomings of both.

To date, the accuracy of YO 4.0 appears to be more than adequate for any practical Yagi applications. It has been checked against frequency-swept data for HF Yagis run on a professional antenna range, and has successfully accounted for large frequency shifts observed in several MININEC-designed VHF arrays (see

Figures 4 and 5). The new program predicts front-to-back ratio, sidelobes, and electrical characteristics to a satisfying degree of accuracy.

YO 4.0 also models and optimizes KLM-type Yagis with dual driven elements. It can also automatically optimize their phasing-line impedance and front-to-back ratio (Figure 6).

Frequency graphs

The parameters versus frequency graphs shown in Figure 7 are a helpful addition to YO 4.0. Gain, front-to-back ratio, VSWR, impedance curves versus frequency are displayed and may be printed. A quick overview of a complete Yagi design is given at a glance. Operator-introduced changes in antenna design are reflected in these graphs to provide visual evidence of antenna performance.

Element current profile

YO can draw a profile of element-current magnitudes along the boom of the Yagi (see Figure 8). The profile is normalized so the

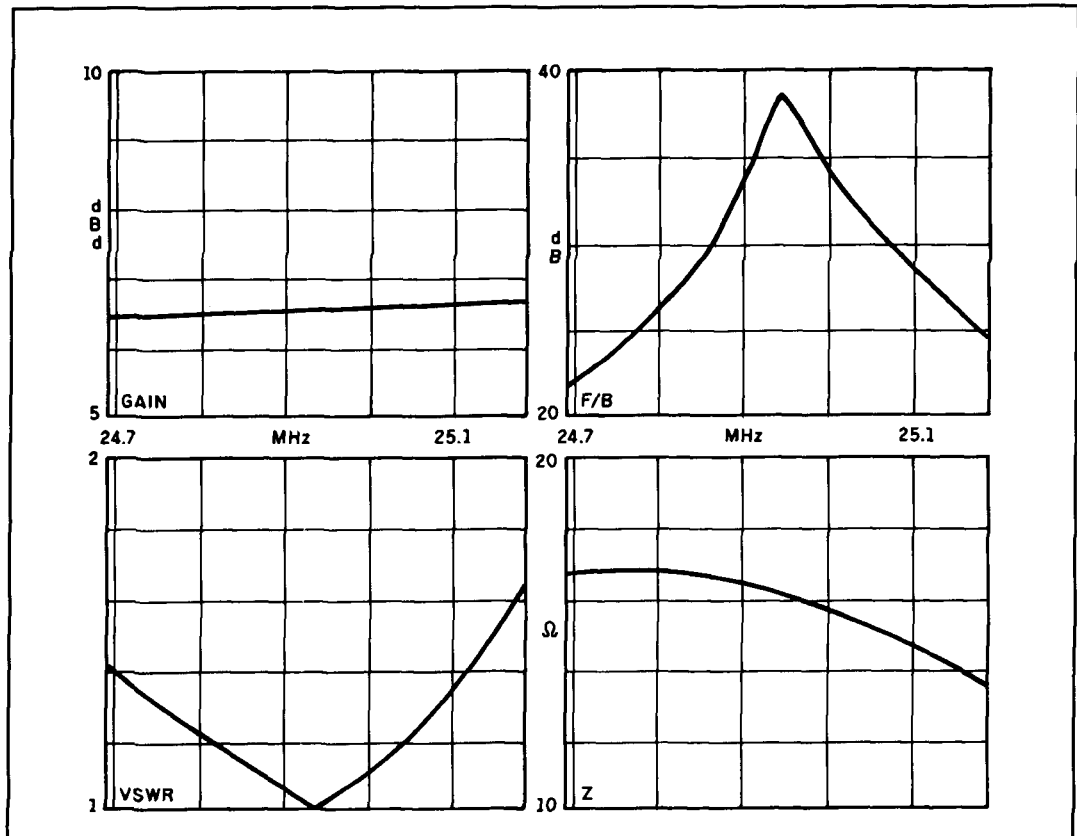


Figure 7. Parameters of a four-element, 12-meter Yagi are provided in four illustrations. The graph on the upper left shows gain in relatively constant at 6.5 dBd across the band. The graph on the upper right shows that front-to-back ratio peaks at about 37 dB at 24.95 MHz. Lower graphs illustrate VSWR match to a 50-ohm line (left) and feedpoint impedance versus frequency (right).

By John A. Wick, *WIHIR*
5749 Camino Del Celador
Tucson, Arizona 85715

WHAT'S THE NEIGHBORHOOD ELECTROMAGNETIC COMPATIBILITY OF YOUR ANTENNA?

Amateur HF antenna design can influence the likelihood of interference with nearby electronic equipment

Amateurs tend to think of antennas in terms of VSWR, forward gain, and radiation angle. For those of us *not fortunate enough to live in the middle of an 80-acre farm*, there's another parameter of vital importance. I call it neighborhood electromagnetic compatibility.

The intensity of electromagnetic fields near your ham station (in your next door neighbor's living room, for example) is a function of the type and placement of your ham antenna, as well as the output power of your transmitter. Experience has taught us that to minimize the likelihood of interference, the higher the antenna we use, the better. Good Amateur etiquette also dictates the use of the lowest transmitted power necessary to maintain communication. Adherence to both of these practices can help maintain neighborhood peace. Those of us who live with antenna restrictions and want to run the legal limit, either to compensate for marginal band conditions or to snare that elusive DX, can minimize interference problems if we consider the field

strength our antenna generates in our neighbor's living room—just as we consider VSWR and radiation angle—when planning an antenna installation.

In the process of producing electromagnetic radiation, antennas create electric and magnetic fields. Some fields are radiated, and some exist only in the vicinity of the antenna. The radiated fields are called *radiation*, or *far fields*. Fields which exist only in the vicinity of the antenna are referred to as *induction*, or, more commonly, *near fields*. They are also called *storage fields*, because energy is stored in the field during portions of the RF cycle and returned to the antenna for radiation during other portions of the cycle. Depending on the antenna configuration, moderate transmitter power levels can generate very high field intensities in the near field. At wavelengths typical of Amateur HF operation, the near field can cover a region that includes your own residence, as well as neighboring ones.

When reading this study, it's helpful to be aware of the difference in how the intensi-

ties of the radiation field and the near field vary in relation to the distance from the antenna. At the distance $d = \lambda/2\pi \approx \lambda/6$ on axis from a dipole antenna in free space, the intensities of the radiation field and the near field are equal. However, the radiation field varies *inversely* with distance from the antenna ($1/d$), while the near field varies inversely as the *square* of the distance from the antenna ($1/d^2$). Consequently, the near field predominates at points close to the antenna, but becomes insignificant at large distances. Of course, the fields may be quite different for an actual antenna located near the ground.

Even the cleanest ham signal can interfere with TV, audio, computer, and other electronic equipment when currents sufficient to cause circuit components to become non-linear are induced into the equipment by high incident RF fields. And the higher the incident field strength, the more likely it is that modern low-power semiconductor equipment will malfunction, and the harder it will be to eliminate the interference.

The availability of computer-based antenna analysis tools like MININEC-3, which compute both the near and far fields for antennas located over realistic ground, greatly simplifies prediction of the impact a proposed antenna type may have on neighborhood tranquility. Even very cooperative neighbors might tire of you making repeated field strength measurements in their living room, as you try various antenna configurations. But the computer lets you repeat simulated tests over and over again, until you find an antenna configuration which minimizes the field strength in neighboring dwellings, while adequately supporting Amateur communication. (Editor's note: If you'd like to correlate the MININEC technique with the older conventional method of calculating field intensity, you can use the following equation for fields in the center of the main antenna beam.)

Field intensity in volts per meter,

$$V/M = \sqrt{30P_t G_t / d_m}$$

where:

P_t = transmitter power in watts

G_t = gain of transmitting antenna (1.64 for a $\lambda/2$ dipole in space, and 3.28 for a $\lambda/4$ ground-mounted vertical over perfect ground)

d_m = distance from antenna in meters

Having spent more than 35 years experimenting with antennas on roof tops and towers, I became intrigued with the possibility of doing some of my antenna work on the ground when I discovered the

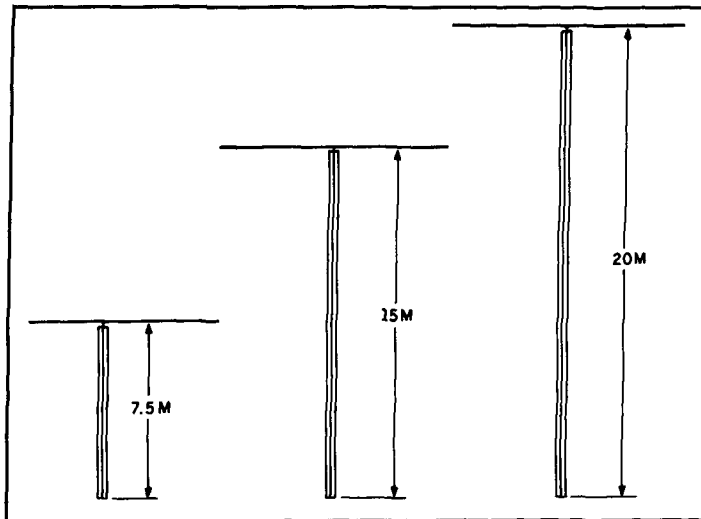


Figure 1. Dipoles.

capabilities of MININEC-3. My first major "armchair antenna" project was this study of the way antenna configuration influences the potential for interference in the neighborhood. To start, I modeled a 20-meter dipole above average ground (dielectric constant 40, conductivity 0.001 mho/m) at a variety of heights from 7.5 to 20 meters. I calculated the combined near and far-field electric field strength for these dipole heights as a function of distance from the base of the antenna tower. The antenna configurations used in this first investigation are shown in Figure 1. The electrical field strengths calculated for these antennas are shown in Figure 2. In each case, I matched the antenna to the transmitter and used a transmitted power of 1-kW CW. Field strengths were calculated for a point one meter above the ground — a distance representative of the height of a piece of electronic equipment on a table or desk, on the first floor of a house.

Without a frame of reference, the predicted field strengths shown don't mean much. To put the numbers in perspective, consider that the old standard for military electronic equipment, given in MIL-STD-461B, dated April 1, 1980, required military electronic equipment to function properly in HF field strengths of less than 5 V/M. The new standard, MIL-STD-461C, dated August 4, 1986, raises the limit to 20 V/M. Note that field strengths in this range are observed within 10 meters of the base low dipole. A recent QST article, discussed a defacto standard of 1 V/M for consumer electronics. Electric field strengths of this magnitude exist up to 100 meters from the base of the tower when the antennas in this example are used at the 1-kW level.

The consumer electronic standard is a

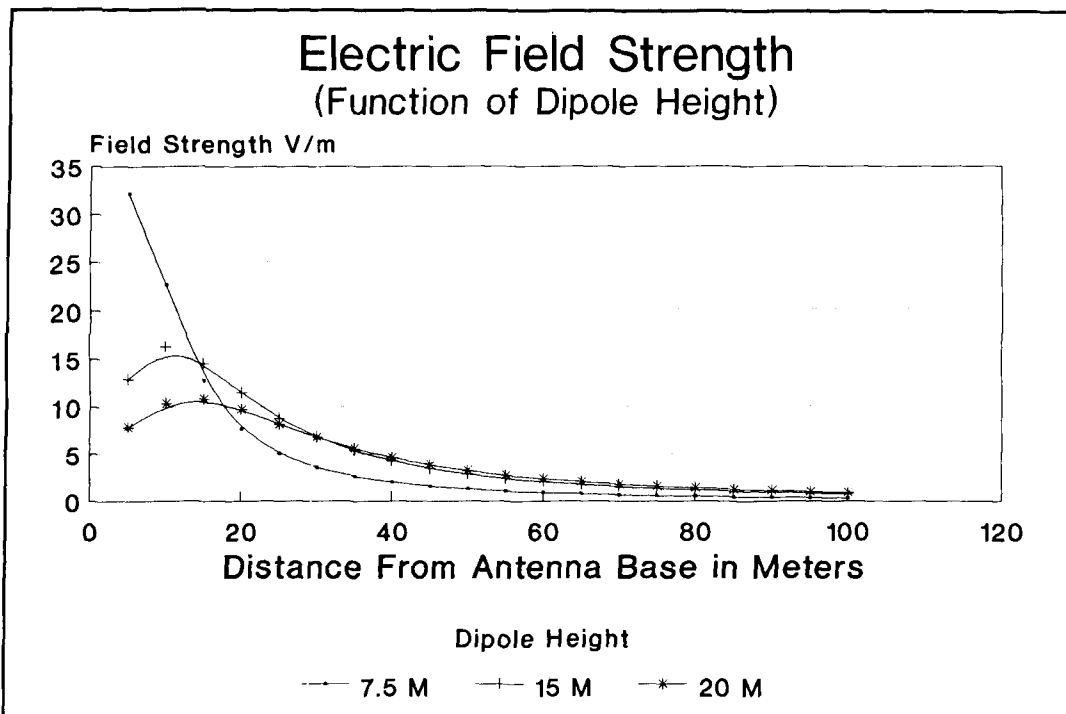


Figure 2. Electric field strength as a function of dipole height.

goal adopted by some companies who make electronic equipment. As yet, there's no law requiring equipment to meet this standard before it can be sold. Consequently, it's possible for a neighbor to have equipment which is more susceptible to interference than the standard would indicate. In fairness to some of the more conscientious consumer equipment manufacturers, there are items on the market that will operate properly in field strengths many times the 1 V/M defacto standard. Though it's possible that field strengths in excess of this level may cause interference in equipment which meets the standard, this is not necessarily so. As the standard is not mandatory, and applies only to new equipment, interference may be experienced at field strengths much less than 1 V/M with older equipment, or with new equipment built without regard to the standard.

The very high field strengths encountered under the low antenna are found beneath the end of the dipole. They are the result of the high voltages present at the dipole's end. At a distance of about 35 feet from the antenna tower, field strength for the low dipole drops below the 1 V/M level. Field strengths from the higher dipoles remain above this level out to about 100 meters from the tower. This is the result of a combination of two factors. First, much of the storage field around the low dipole is confined to the space between the dipole and the ground, producing a very localized high-

intensity field. The storage fields for the higher antenna, on the other hand, are more widely spread. Also, as you move farther from the antenna tower, the importance of the near field decreases and that of the far field increases. Therefore, antennas with a lower angle of far-field radiation will produce higher fields at distances significantly removed from the antenna base than will those with high radiation angles. (If all the power were transmitted straight up, the electric field strength beyond the immediate vicinity of the antenna would rapidly become negligible.) Because the radiation angle is lower for the higher antennas, the intensity of the far field at a point one meter above the ground will be greater for these higher antennas as distance increases and the far field becomes dominant.

To state this in practical terms, a low antenna may cause a high level of interference in your next door neighbor's house, while the neighbor down the block is interference free. When you raise your antenna to decrease the level of interference next door, you may discover that you now have interference problems with some highly susceptible equipment down the block. This might be discouraging, to say the least. It might also send the wrong message to the people who regulate antenna heights in your area. If they were to look at this case, it would appear that the higher the antenna, the more widespread the interference problem.

Fortunately, electric field strengths of 1 or 2 V/M are much less likely to cause interference in well-designed equipment than are higher levels. If interference does occur, it's much easier to cure using commonly accepted techniques than is the severe interference caused by field strengths in excess of 10 V/M. Even though the results of raising the antenna might be disappointing at first, a little additional work might clear up all of your problems and reconfirm the conventional wisdom which states that the best way to decrease high field-strength induced interference is to raise the antenna as high as possible.

Another bit of conventional wisdom says that lowering the transmitter power decreases the potential for interference. This can be verified easily if you consider how the distance from the antenna at which the various standard field strength levels are observed decreases as the power level is lowered. The curves in **Figure 2** can be used for power levels less than 1 kW simply by scaling the field strength by the square root of the ratio of the lower power to 1 kW. For example, for a 100-watt transmitter, multiply the field intensities shown by the square root of 0.1 or 0.316. For a 10-watt transmitter, multiply the field intensities by the square root of 0.01 or 0.1. At the 100-watt level, the high dipoles produce field strengths less than the 1 V/M level at distances greater than about 50 meters and the maximum field strength from the low dipole would be about 10 V/M. At the 10-watt level, all antenna heights would be below the 1 V/M level at distances greater than 25

meters from the antenna tower. Therefore, a reduction power can be very effective in reducing the area over which sufficient electric field strength exists to induce interference in susceptible electronic equipment.

While 20-meter high antenna towers and moderate power levels make neighborhood electromagnetic compatibility likely for all devices that meet the 1 V/M defacto standard, there are many on the market which don't meet this standard. There's no guarantee that such devices will be free of overload interference for *any* usable level of Amateur power, even if your transmitter is clean and your antenna is high. Directional antennas will increase the field strengths "down the block," as they increase the intensity of power being transmitted in one direction. Consequently, they will increase the electric field strength at any given distance in that direction.

Local zoning, aesthetic, physical, and budgetary restrictions may prevent you from erecting a tower 20 meters high. In this is the case, you'll need to make compromises. You may have to use antennas which are not optimal, in any sense. Using MININEC-3, I modeled a variety of vertical, dipole, and loop antennas typically used by Amateurs with limited space and restricted mounting height. The program showed that some configurations create a much higher electric field intensity near the antenna than do others.

Figure 3 illustrates some of the verticals and limited space antennas I investigated. In **Figure 4**, the electric field strengths observed one meter above the ground are

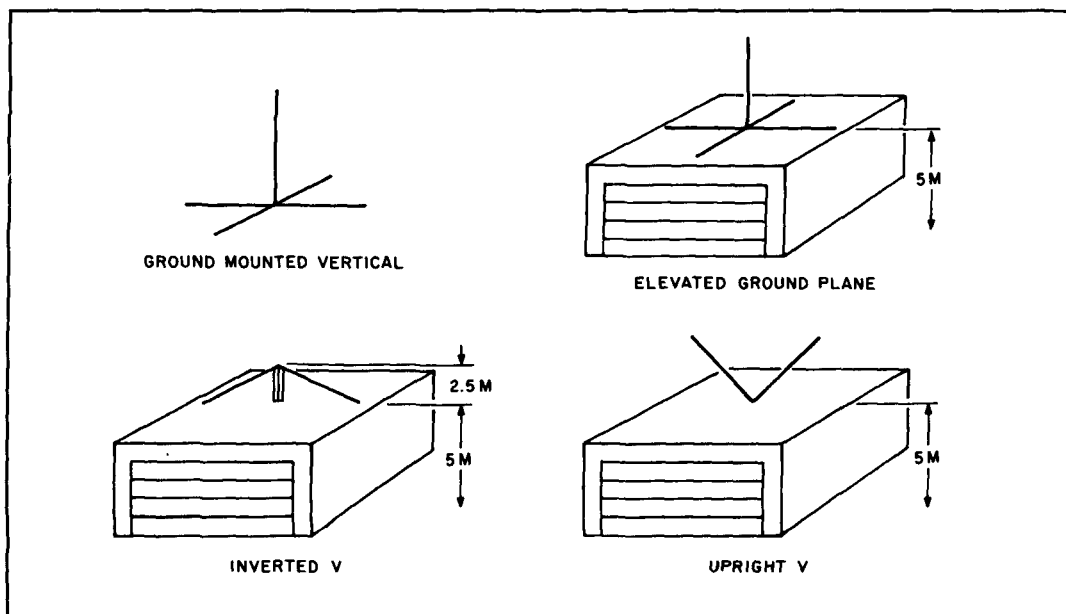


Figure 3. Limited space antennas.

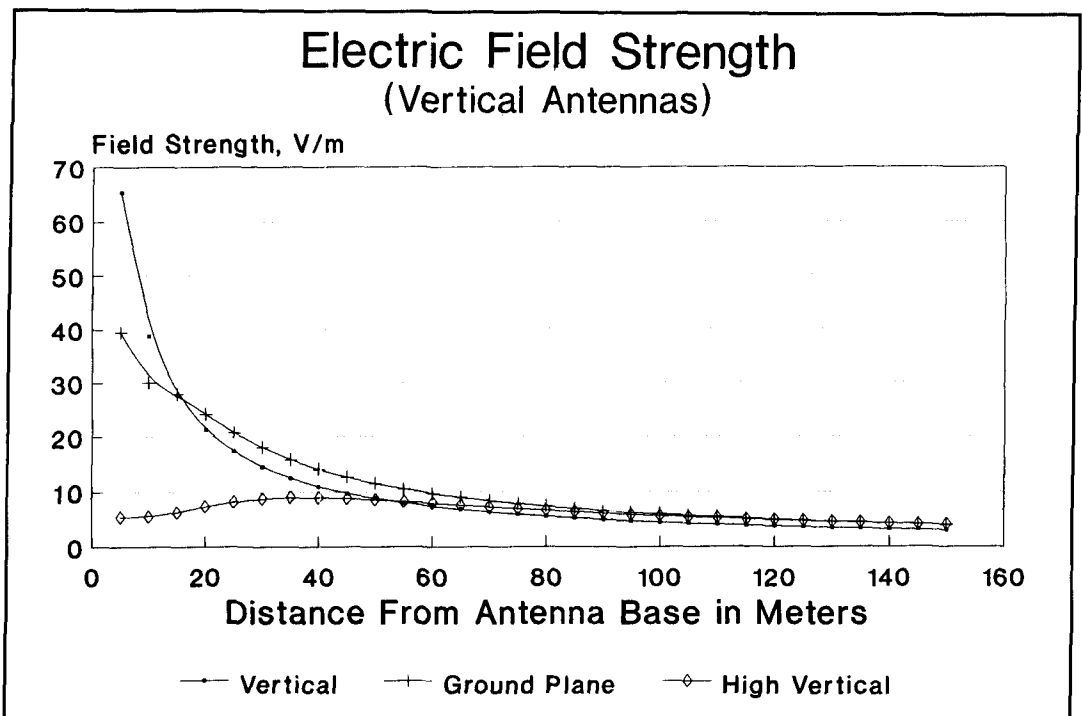


Figure 4. Electric field strength for vertical antennas.

plotted for a ground-mounted vertical, a ground plane 5 meters above the ground, and a vertical dipole 20 meters above the ground, as a function of the distance from the base of the antenna. The electric fields resulting from the ground-mounted vertical and roof-mounted (5-meter high) ground plane are particularly high—both close to the antenna, and at distances of 150 meters. These antennas achieve a much lower angle of radiation than do low dipole antennas; consequently, the far-field electric strengths are higher at the greater distances. This is particularly evident for the high (20-meter height) vertical dipole. Low field strength is observed directly under the antenna as the storage fields are elevated and concentrated in the horizontal plane. Field strength is maximum about 50 meters from the base of the antenna—a point where significant power from the far field pattern of the antenna is observed near the ground. Also note that the field strength curve for the elevated ground-plane antenna merges with that of the high vertical at this point. This further confirms that the reason the vertical antennas generate high field strengths near the ground at distances greater than 50 meters is related to their low angle of radiation.

In the case of the ground-mounted vertical, the peak intensity of electric field strength in the storage fields is located at the same height as your neighbor's stereo, or other equipment, creating a high potential

for interference with electronic devices less than 40 meters from the base of the antenna. The higher radiation angle of the ground-mounted vertical, relative to the roof-mounted ground-plane and elevated vertical dipole, is responsible for the production of somewhat less electric field intensity in this antenna than is found with the other two antennas at distances greater than 50 meters from the antenna base.

Again, some Amateur lore is supported by the antenna analysis. Vertical antennas mounted low to the ground have had a long-standing reputation for creating interference—particularly with inexpensive AM broadcast receivers. The high field strengths predicted by this analysis confirm that, at a given power level, low vertical antennas create higher field strengths in the immediate neighborhood of the antenna than do low horizontal antennas. As a result, devices like inexpensive AM receivers, which are vulnerable to high field strengths, are more likely to be disturbed by high-power Amateur operation using low vertical antennas, than they are by operation using low horizontal antennas.

In Figure 5, the modeled electric field strength is presented as a function of the distance from the center of the antenna for a variety of low horizontal antennas which require only modest support structures. Such antennas might be fastened to low trees, or mounted to a TV roof mount on the top of a garage or single-story house.

Electric Field Strength (Limited Space Antennas)

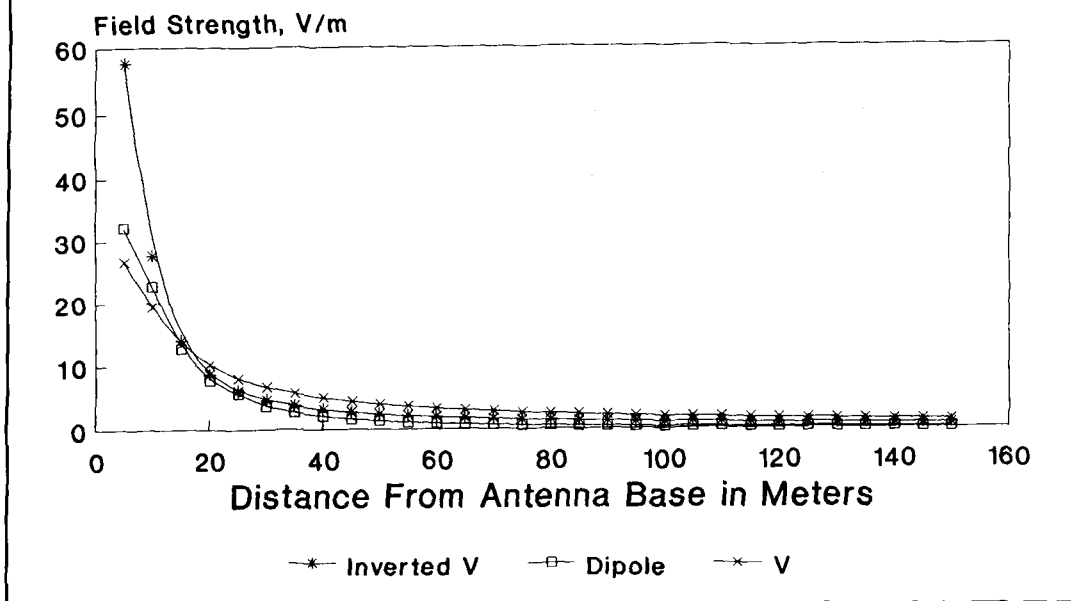


Figure 5. Electric field strength for limited space antennas.

The level of electric field observed one meter above the ground, as a function of the distance from the antenna base, is plotted for three of these antennas in Figure 3.

Of the low horizontal antennas I investigated, the inverted V produces the highest fields in the immediate vicinity of the

antenna, and the lowest fields at 150 meters. The upright V produces the lowest fields near the antenna, and the highest ones at 150 meters. These trends are very similar to those shown in Figure 2 for a horizontal dipole at various heights. They suggest that the height of the ends of the antennas are

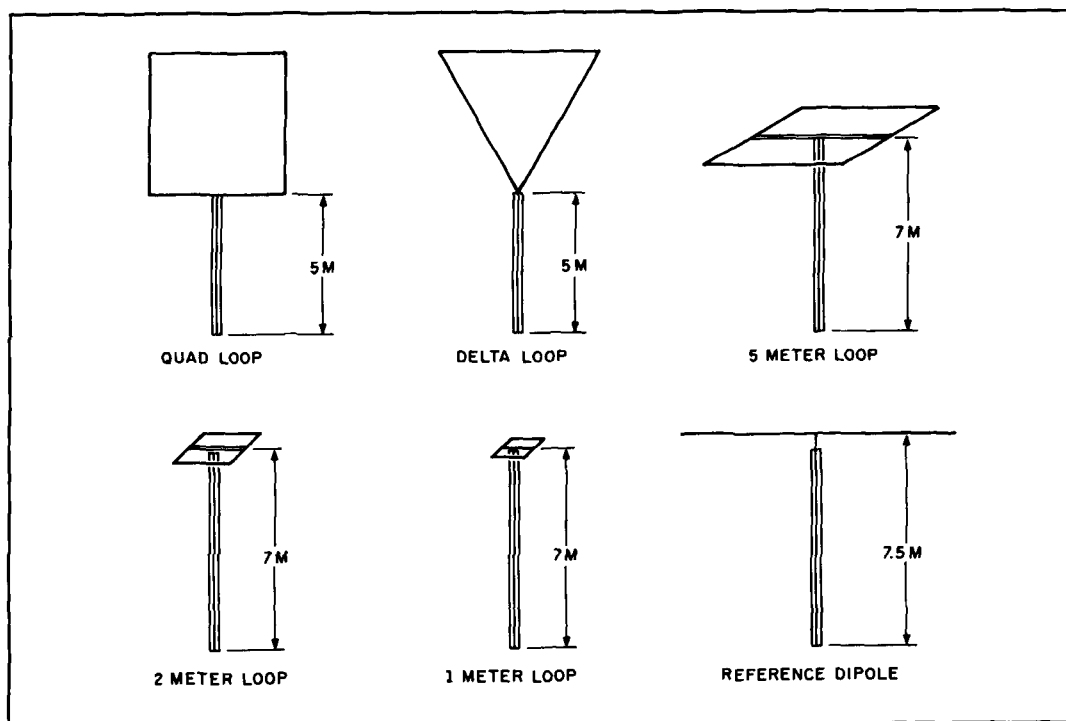


Figure 6. Loop antennas.

important in determining the fields at various distances.

Results obtained for dipoles with heights equal to the end height of the inverted and upright V antennas are identical to those plotted for the corresponding V antennas. This confirms that, as with the dipole, the higher the ends of the antenna, the lower the overall potential for interference. It's interesting to note that the radiation angle for any of these "roof-top" level antennas is quite high, and isn't greatly influenced by small changes in the center height or the particular configuration of the antenna. Therefore, the Amateur with limited antenna tower height might do best with a upright-V antenna located as high as possible—both from the standpoint of potential interference and radiation angle. The inverted-V antenna is definitely the least desirable as far as nearby neighbor interference is concerned, especially if an end of the antenna is tied to a tree just outside your neighbor's house. Remember that the storage fields are excited by the high voltages at the ends of the antennas, and locating the end of the inverted V close to your neighbor's house will tend to maximize the field strength inside the structure.

Reduced-size, loaded antennas are also popular with Amateurs with limited space. I modeled several such antennas, including reduced-size dipoles and short verticals. The field strengths generated at a 1-meter height, as a function of distance from the antenna support structure, were identical to those generated by their full-sized relatives. (Computers can create lossless loading coils and antenna elements, so the reduced-size antennas performed as efficiently as the full-size versions in this study.) Again, height is the most important variable in reducing the level of potential interference. From the standpoint of reducing interference to susceptible electronic devices, a high, reduced-size antenna is preferable to a low, full-sized one.

Loop antennas have often been suggested for Amateur applications but, except for the large loops found in Quad antennas, they have never become popular. Part of the reason is that a loop is essentially a low-impedance current device and, as the loop gets smaller, it becomes more difficult to feed. Its efficiency also decreases because the radiation resistance becomes as small as the ohmic resistance of even the most conductive loops. Using the computer, you can investigate the characteristics of perfect loop antennas without worrying about the mundane problems associated with building them. The computer lets you postulate per-

fectly conducting wires, and transmitters and feed lines which can match very low impedance loads. Consequently, you can perform studies of loop antennas that might have highly desirable characteristics, but which may not be practical to build as efficient antennas. (You can also use the computer to evaluate the efficiency of various practical loops, if you can accurately determine the ohmic resistance of the radiator and the losses of the matching network.)

The loop antennas used in this study are illustrated in **Figure 6**. Because a loop antenna is a current device and generates large nearby magnetic fields, you may expect it to generate relatively small electric storage fields. This will be particularly true for loops which are electrically small with respect to a wavelength.

The electric field strength measured one meter above the ground, as a function of distance from the antenna base, is plotted in **Figure 7** for the large loop antennas. The results for a horizontal low dipole are presented for comparison. Horizontal loop antennas were located seven meters above the ground, and the bottoms of the vertical loop antennas were placed five meters above the ground, to represent antennas with a modest support structure mounted on the roof of a garage or single-story house.

Both the horizontal 5-meter loop and the vertical quad loop behave very much like a dipole. This is to be expected, since they are both full-wavelength loops and have high-voltage points similar to those of the dipole. The delta loop is like the vertical-V antenna with a wire across the top. It's also a full-wavelength loop. The voltage at the delta loop's high-voltage points is greater than that of the other antennas, and its field strength versus distance from the tower curve is more like that presented for the dipole at a 15-meter height.

The electric field strength measured one meter above the ground, as a function of distance from the base of the antenna, is plotted in **Figure 8** for two small horizontal loop antennas—one two meters on a side, and the other one meter on a side. The lowest electric field strength is generated by the horizontal-loop antenna measuring one meter on each side. A plot is also included for a 1-meter loop located 20 meters above the ground (high 1-meter loop) and of a low (7.5 meters high) dipole for comparison. The "best" loop antenna from the standpoint of minimizing electric field generation is the 1-meter loop. The maximum electric field from this antenna at the 1-kW level is 20 V/M immediately under the antenna. The electric field drops to 1 V/M 45 meters

Electric Field Strength (Large Loop Antennas)

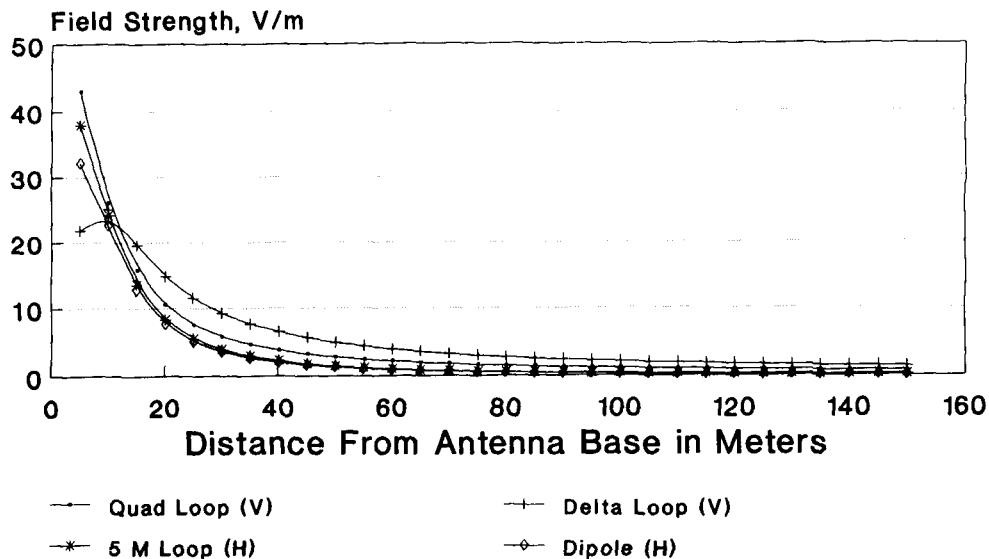


Figure 7. Electric field strength for large loop antennas.

from the base of the antenna support. The interference potential of this antenna is much lower when it is raised to a height of 20 meters. Like the reduced-size dipole antennas discussed previously, greater height is feasible for small loop antennas as their support requirements are modest, and visually they may be mistaken for large tele-

vision antennas. While the small loop antenna is desirable from both the standpoint of low radiation angle and low interference potential, creating an efficient, effective loop is a considerable engineering challenge due to its low radiation resistance and feed impedance.

The results presented here are for the 20-

Electric Field Strength (Small Loop Antennas)

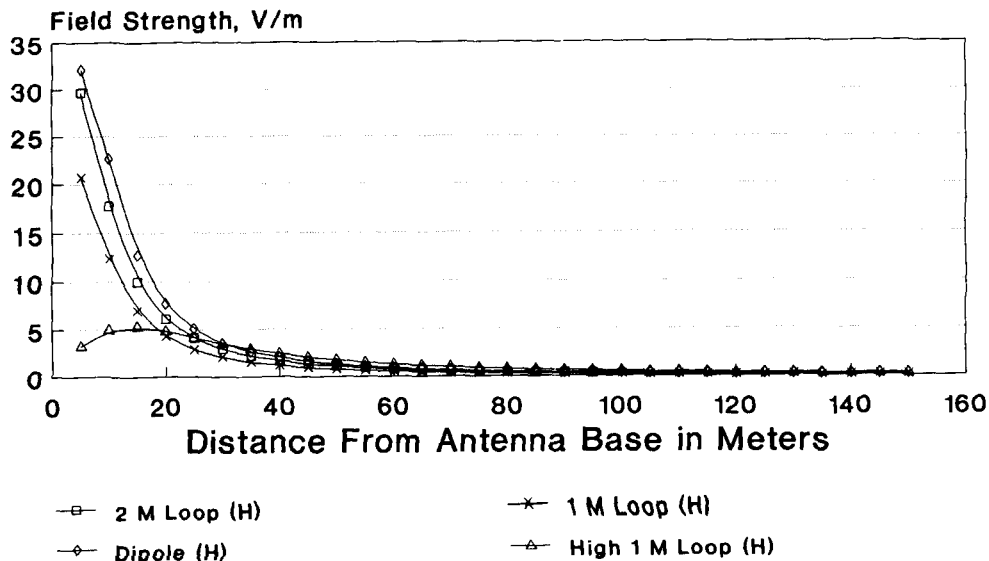
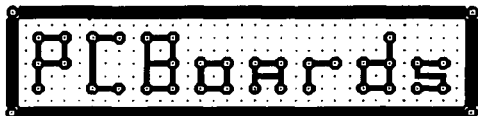


Figure 8. Electric field strength for small loop antennas.



P-C-B ARTWORK MADE EASY I Create and Revise PCB's in a Flash

- * HERC, CGA, EGA, VGA, SUPER-VGA
- * HELP SCREENS
- * ADVANCED FEATURES
- * EXTREMELY USER FRIENDLY
- * AUTO GROUND PLANES
- * DOT- MATRIX, LASER and PLOTTER ART
- * CREATE YOUR OWN FILMS with 1X ART
- * LIBRARIES
- * DOWNLOAD DEMOS from 24 hr. BBS!

REQUIREMENTS: IBM PC or Compatible, 384 K RAM
DOS 3.0 or later. IBM compatible printers.

- PCBoards - layout program 99.00
(PCBoards HP or HI PEN PLOTTER DRIVER 49.00)
- PCRoute - auto-router 99.00
- SuperCAD - schematic pgm. 99.00
- Demo Pkg. - (includes all 3 programs) 10.00

Call or write for more information

PCBoards

2110 14th Ave. South, Birmingham, AL 35205
1-800-473-PCBS / (205)933-1122
BBS / FAX (205)933-2954

meter band, but you can apply the principles involved to antenna structures used anywhere in the Amateur HF spectrum. In this analysis of neighborhood electromagnetic compatibility of antennas, I found the old axiom "the higher the better" was true—especially for the high-voltage end points of dipole or dipole-like antennas. My studies indicate that loop antennas present interesting possibilities for reducing the potential of high electric field-induced interference in the vicinity of the transmitting antenna. Unfortunately, these antennas may be of limited use in Amateur setups because of practical implementation problems. I didn't consider a variety of antennas, like slopers and end-fed random wires, because it's difficult to model all of the relevant conductors that may be part of the ground system or counterpoise of a particular antenna installation. However, you can apply the same basic conclusions to these antenna structures. High-voltage points on such antennas, and their associated ground and/or counterpoise systems which occur near the ground near a neighbor's residence, can greatly increase the potential for RF overload interference.

The configuration of an average Amateur HF antenna is the result of many compromises. The neighborhood electromagnetic compatibility considerations I've presented here, introduce additional constraints which minimize the potential for interference with consumer electronics equipment. While each Amateur antenna installation is unique, I hope you'll find these general principles and ideas useful in defining modifications which will help reduce neighborhood interference. In some cases, a relatively simple change in the direction an antenna wire is run may solve an interference problem. In others, the constraints on the location of your ham antenna may be so severe that you'll have to accept the fact that your antenna system is capable of creating interference at high transmitter power levels. If this is the case, you'll have to choose your operating modes and objectives so you can use moderate power levels if, in fact, interference with neighboring consumer electronics equipment results from the use of higher power levels. ■

REFERENCES

1. DoD MIL-STD-461B (superseding MIL-STD-461A), "Electromagnetic Emissions and Susceptibility Requirements for the Control of Electromagnetic Interference," United States Department of Defense, April 1, 1980.
2. DoD MIL-STD-461C (superseding MIL-STD-461B), "Electromagnetic Emissions and Susceptibility Requirements for the Control of Electromagnetic Interference," United States Department of Defense, August 4, 1986.
3. Howard L. Lester, "Interference Standards Revisited," *QST*, July 1989, pages 27-30.

CQ Bookstore

Greenville, NH 03048

Oscillator Design and Computer Simulation

by Randall Rhea

Includes MS-DOS simulation disk

Simple and easy-to-understand reference on how to design a wide variety of RF and microwave oscillators. Gives you a unified method of design. JFETS, MOSFETS, hybrid/MMIC, bipolar, transmission line, SAW, and piezoelectric resonators are all fully covered so the reader can make use of them.

Simulation program speeds up the design process by automatically handling many of the tedious calculations. © 1990 259 pages, First edition.

PH-ODCS **Hardbound \$59.95**

IONSOUND v 3.19

by Jacob Handwerker, W1FM

Wonder when and on what frequency you'll be able to find the last country you'll need for honor roll? IONSOUND is a state-of-the-art software tool designed to predict propagation to any part of the world. Uses the latest propagation engineering models. Can be customized for a number of different variables. Menu driven and easy-to-use. Manual in an ASCII printable file included. Math co-processor recommended but not required. For IBM PCs and other compatibles.

ION5 (5.25" disk) **\$29.95**

ION3 (3.5" disk) **\$31.95**

Shipping via mail, \$4.00. UPS \$5.00 US Only
Foreign orders FOB Greenville, NH



(800) 457-7373



THE TRAVELING-WAVE AMPLIFIER

A possible solution for your amplifier problems

If you've been watching the recent progress in broadband linear RF amplifiers, you may have noticed one of the "new" innovations—a device called a traveling-wave amplifier, TWA for short. The HMMC-5086 amplifier from Hewlett Packard is one such device! Its bandwidth is 2 to 26.5 GHz. Although the basic principles of the traveling-wave amplifier have been around for a long time, it's not a very common configuration—at least not yet. Nevertheless, it's a very interesting circuit. This short article provides some insight into the design and operation of the TWA.

A brief history of the TWA

The traveling-wave amplifier is a new name given to an earlier amplifier called the distributed amplifier. This amplifier was first proposed by W.S. Percival in British Patent 460,562 in 1936.² The first detailed publication describing the TWA was written by E.L. Ginzton, W.R. Hewlett, et al. in 1948.³ So, although the technology of the traveling-wave amplifier appears new, it's actually years old and dates back to the infancy of the electronic age.

In very basic terms, the distributed amplifier allows a large number of amplifying devices, such as transistors or vacuum tubes, to be operated in *parallel* without the parasitic elements of those devices adding. The parallel operation allows higher power to be delivered than is possible with a single device, and the distributed configuration

preserves the full bandwidth available with a single device. This is perhaps better explained by an example.

Amplifying a broadband signal

Suppose you have a broadband signal from a 50-ohm source that you wish to amplify and use to drive a 50-ohm load. For this example, let the desired bandwidth be 100 kHz to 5 GHz, and the desired output power be 1 watt. Also, suppose that the best device you can find is a broadband FET with: (1) a bandwidth of 10 GHz, (2) a nominal 0.1-watt output capability into a drain load between 25 and 50 ohms, (3) an input capacitance of about 2 pF, and (4) an output capacitance of about 1 pF. If a single such device were used to drive a 50-ohm load, it could deliver 0.1 watt. The upper cutoff frequency, determined by the device output capacitance and the load resistance, would be about 3 GHz. To achieve the desired 1-watt output, at least ten of these devices would need to be combined in some manner.

If you could operate ten devices in parallel, you could conceivably deliver the desired 1 watt. But what would happen to the bandwidth? If the devices are simply paralleled, the output capacitances are effectively connected in parallel. Since capacitors add in parallel, the total output capacitance is the capacitance of a single stage multiplied by the number of stages.

For ten stages, the output capacitance is 10 pF for our example. The upper cutoff frequency determined by the total output capacitance and the load resistance is then about 300 MHz—far below the desired 5-GHz value.

You could tune the output circuit to improve the upper frequency response, but that would result in a narrow-band amplifier. For example, if you were to use a Q of only 5 in a tuned output network with the upper cutoff frequency set at 1 GHz, the lower cutoff would be about 800 MHz. (In a tuned network, Q is approximately the center frequency divided by the bandwidth.)

There are various techniques for near lossless power combining. Unfortunately, those are typically usable only for narrow-band applications. You could look for a higher-power part, but since the physical size of the active device is related to its power capability, it's very likely that a 1-watt part would have an output capacitance close to that of ten 0.1-watt devices in parallel.

Suppose by some trick, you could connect ten of these devices in parallel in such a way that their output powers add, but their output capacitances do not. The total effective output capacitance remains the 1-pF value of the single device. You would achieve the desired 1-watt output. The bandwidth, limited by the effective output capacitance and the load resistance, would be 3 GHz. The distributed amplifier provides this ability. However, you'll lose half the power available from each part, so you must actually use twenty 0.1-watt devices to achieve the desired 1-watt output. That's generally a reasonable price to pay for the very broad bandwidth and high power provided—particularly if there's no other way to obtain the desired power and bandwidth. But, there is an added bonus. The lost power results from the loading of each device by two characteristic impedances. Even though this causes a 50 percent power loss, it doubles the bandwidth limited by the device capacitance and the load impedance. The bandwidth available from this amplifier is then about 6 GHz.

Example using a lumped-element transmission line

To understand how the distributed amplifier works, you must first look at a simple transmission line. A transmission line, such as a length of coaxial cable, is essentially two parallel conductors situated near each other, with a suitable dielectric between them. The transmission line exhibits some

inductance and some capacitance per unit length. There are also some series and shunt resistances per unit length, but assume that those resistances are negligible here. This implies that you have a near-ideal lossless line. The characteristic inductance of the line may be termed L_0 with units of Henries/meter; the capacitance may be termed C_0 , in Farads/meter. The characteristic impedance of the line, Z_0 , and the propagation velocity, V_0 , may be computed in terms of L_0 and C_0 :^{4,5}

$$Z_0 = \sqrt{L_0/C_0} \quad (1)$$

$$V_0 = 1/\sqrt{L_0C_0} \quad (2)$$

You can solve **Equations 1** and **2** for L_0 and C_0 .

$$L_0 = Z_0/V_0 \quad (3)$$

$$C_0 = 1/(Z_0V_0) \quad (4)$$

You may use **Equations 3** and **4** to calculate the inductance and capacitance of a typical cable like RG-58C/U. The propagation velocity of RG-58C/U is approximately two-thirds the speed of light, or about 2×10^8 meters/second, and the characteristic impedance is nominally 50 ohms. Therefore, using **Equation 3**, the inductance per unit length is 250 nH/meter and the capacitance per unit length, using **Equation 4**, is 100 pF/meter. You may check these results by plugging these values into **Equations 1** and **2**, where you'll find that such values of L_0 and C_0 yield a line of 50-ohms characteristic impedance and 2×10^8 meters/second propagation velocity. An equivalent circuit of an ideal lossless transmission line (no resistive components) is shown in **Figure 1**:⁴

Looking at **Figure 1**, you see that a transmission line is, in effect, a number of inductors connected in series, with capacitors connected from each inductor to ground. What would happen if you were to construct a circuit using actual inductors and capacitors connected as shown in **Figure 1**? You'd have a simulated transmission line. Such a line is typically termed a lumped-element line, because the individual inductances and capacitances are lumped into individual elements, rather than distributed

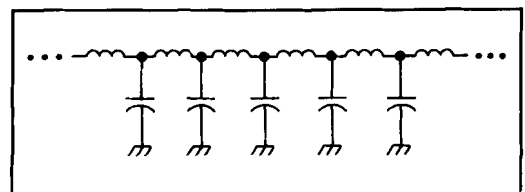


Figure 1. Ideal lossless transmission-line equivalent circuit.

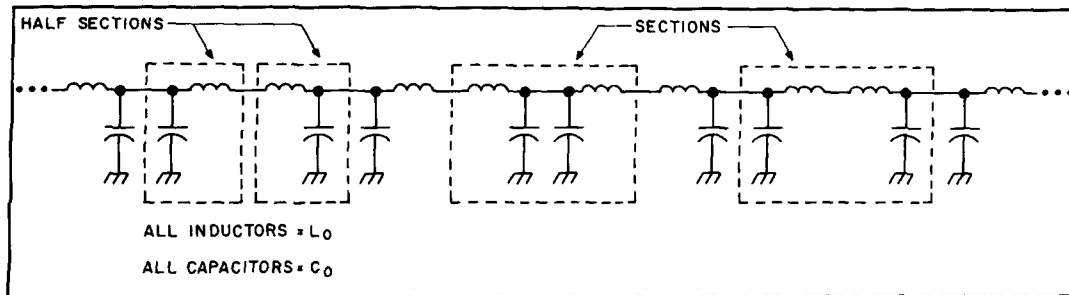


Figure 2. Transmission-line LC filter model.

smoothly along the line as in a coaxial cable. The lumped-element line is a type of LC filter and its detailed design can be very complex. If you wish to explore the actual design of lumped-element lines, start with the references cited at the end of the article.

Another transmission line equivalent circuit is shown in Figure 2. There are various other models which could also be used^{5,6}. The circuit of Figure 2 is essentially the same as that of Figure 1, but each inductor is shown as two series inductors and each capacitor as two parallel capacitors. The network, consisting of one inductor and one capacitor, is termed a half section. Two inductors and two capacitors (either two parallel capacitors to ground with an inductor on either side, or two inductors in series with a capacitor to ground on either side) is considered a section. The inductance and capacitance per half section of a lumped-element line are L_0 and C_0 , respectively, and determine the line characteristics as computed in the equations.

Delay-line example

Suppose that you were to use 125-nH inductors and 50-pF capacitors for each half section. The line impedance would be 50 ohms and the propagation velocity 2×10^8 sections/second,* just as it is for the RG-58C/U coax where the section is defined as a unit length of the lumped line. However, in the coax, a 1-meter length of coax is needed to provide the 250 nH and 100 pF of a section of the lumped line. In the lumped line, you can provide that inductance and capacitance in single components. If the 250-nH inductors (combined inductance of the two series inductors) are about 1 centimeter long, 1 centimeter of the line is equivalent to 1 meter of coax in delay. For example, suppose you want to build a 100-ns

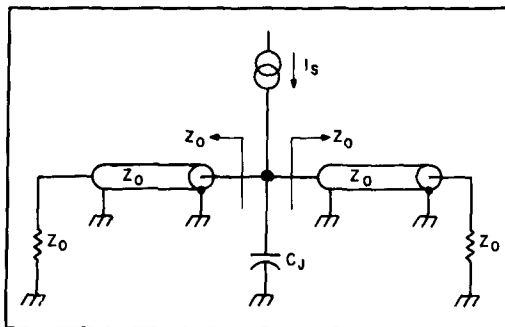


Figure 3. Equivalent device output-node model.

delay line. The delay of RG-58C/U with a propagation velocity of 2×10^8 meters/second is 5 ns/meter, so you'd need 20 meters of coax for a 100-ns delay. The delay of the lumped line is about 5 ns per section, so twenty sections will be required for the 100-ns delay. The total length of lumped line needed is then about 20 centimeters—considerably shorter than 20 meters of coax.

Line cutoff frequency

The lumped line exhibits another property; one that isn't seen in an ideal transmission line. The lumped line exhibits a cutoff frequency. To explain line cutoff simply, suppose that you have a lumped-element line which is very long, or, in other words, composed of a lot of elements. Consider a point near the center of the line, as shown in Figure 3. Capacitor C_j in Figure 3 has two transmission-line segments connected to it in parallel—one on either side. If each section is terminated in the line characteristic impedance, Z_0 , the resistance presented to the capacitor by each section will be the Z_0 . Therefore, the effective resistance connected in parallel with the capacitor is $Z_0/2$. If you were to drive the capacitor node with an RF current source, as illustrated in Figure 3, an upper cutoff frequency would be determined by the time constant of the capacitance and the total resistance across the capacitance. That time constant would be $(Z_0/2)(2C_0)$, or Z_0C_0 . The cutoff fre-

*The velocity of propagation in free space is 3×10^8 meters/second. For RG-58C/U, the velocity of propagation is only 66 percent of the free space velocity because of the dielectric material used. Since a section of the lumped-element line has the same capacitance and inductance as 1 meter of RG58C/U, a section of the lumped-element line has about the same propagation time as 1 meter of RG58C/U. The lumped-element line propagation velocity is then about 2×10^8 sections/second.

quency is then given by **Equations 5 and 6.**

$$F_c = 1/(2\pi Z_0 C_0) \quad (5)$$

But $Z_0 = \sqrt{L_0/C_0}$, thus,

$$F_c = 1/(2\pi\sqrt{L_0 C_0}) \quad (6)$$

This means the 50-ohm lumped line with a 125-nH inductance and 50-pF capacitance per half section would have a line cutoff frequency of about 64 MHz.

Increasing cutoff frequency

You can raise the line cutoff frequency by using more sections of smaller inductance and capacitance with the same inductance-to-capacitance ratio. For instance, you could use 62.5-nH inductors and 25-pF capacitors for each half section. The ratio would be the same as it was previously, so the characteristic impedance would still be 50 ohms. The delay per section would be one half that of the previous example, so forty sections would be needed to provide a 100-ns delay. However, the line cutoff given by **Equation 6** would be 127 MHz—twice that of the previous example.

If you continue reducing the element values, keeping the L/C ratio constant while increasing the number of sections, you'll eventually have a very large number of very small sections. You could then make each inductor from a simple straight length of wire. Each capacitor could be made by surrounding that length of wire with a suitable insulating dielectric and placing that length of insulated wire in a grounded metallic tube, so the proper inductance and capacitance per section are provided. When you then connect many such sections in series, you have a coaxial transmission line.

Lumped-element line in the amplifier

Now that you've examined the lumped-element transmission line, you can apply that technology to an amplifier. Suppose you had ten sections of a line, as shown in

Figure 2, using 62.5-nH inductors and 25-pF capacitors as the half-section values. If the inductors were removed and the capacitors simply tied in parallel, the total capacitance to ground would be 500 pF. The cutoff frequency with a 50-ohm source and load would then be about 12.7 MHz. But you know from the preceding example that the line cutoff is 127 MHz with the 62.5-nH inductors included. Thus, for the same total capacitance to ground, the bandwidth has been improved by a factor of ten by combining the capacitance with some inductance to form a lumped-element transmission line.

Now consider the original amplifier requirement from the example. Instead of simply trying to parallel some number of devices to achieve higher output power, let the devices be connected with inductors between them as shown in **Figure 4**. A lumped-element line is formed with the output capacitance of each device providing the capacitance required for the lumped-element line. Because each device is, in effect, driving two line sections in parallel, one half the power available from each device is delivered to the load. The other half flows along the line in reverse, away from the load, and will eventually be lost. The load impedance presented to each device is one half the characteristic impedance of the output line. With a 50-ohm line, the device load is 25 ohms. With the device specifications given, the circuit is capable of delivering 0.1 watt to 25 ohms, so twenty devices are needed to deliver 1 watt to the load (and 1 watt in reverse).

The device capacitance corresponds to twice the capacitance of a half section. For a 50-ohm line impedance with a device capacitance of 1 pF, or 0.5 pF half-section capacitance, the half-section inductance must then be about 1.25 nH. This means a total inductance of 2.5 nH must be connected between devices. The cutoff frequency of this amplifier is given by **Equation 6** as 6.4 GHz. You can verify this by computing the drain time constant and the corresponding cutoff frequency. The drain

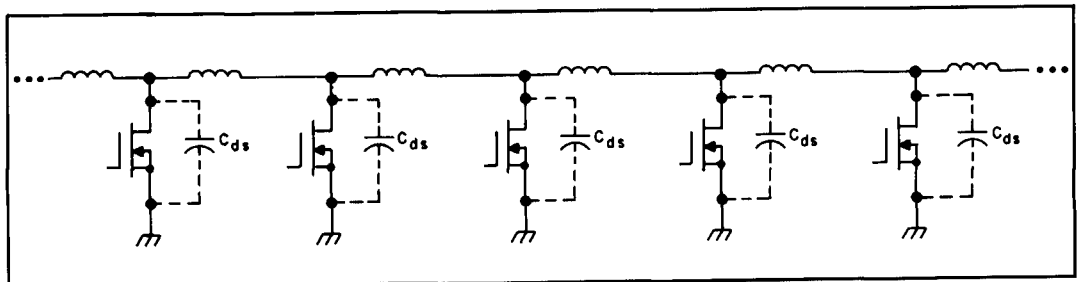


Figure 4. Typical output line.

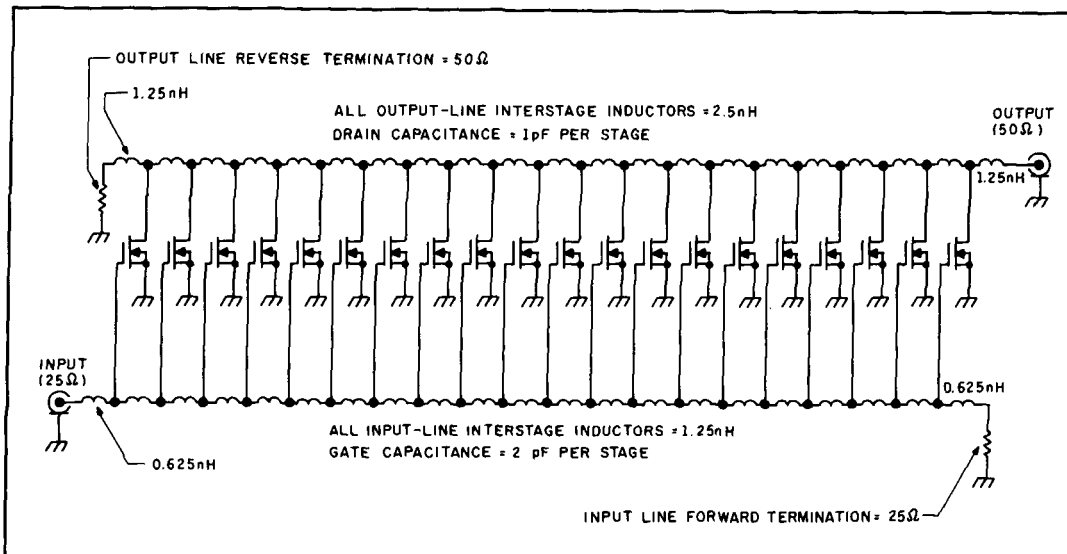


Figure 5. Complete distributed amplifier (DC bias elements omitted).

capacitance is 1 pF and the total load resistance at each drain is 25 ohms. The drain time constant is then 25 ps and the cutoff frequency is 6.4 GHz, as expected.

I've shown that, with the device chosen, you can achieve the desired 1-watt output power by simply paralleling ten devices. However, the bandwidth will be only about 300 MHz. If you connect twenty devices in a lumped-element transmission line, you will achieve the desired 1-watt output power and bandwidth will be more than 6 GHz. This demonstrates the value of this amplifier incorporating the active devices in a lumped-element line.

Timing input signals

One problem remains in the configuration shown in **Figure 4**. The output signal in the output line is in the form of a traveling wave moving in the output line. For the signals from each amplifying stage on the output line to add (provide the desired output over the entire bandwidth), the input signals applied to each stage must be timed precisely so the output signal of each stage is delivered to the output line at precisely the correct time in order to provide proper signal summing. This may seem very difficult to accomplish, but it's actually quite simple.

The device specifications indicate that its input capacitance is 2 pF. Assume that you have an *input* lumped-element line which uses the input capacitance as the line capacitance. For proper signal timing, the propagation velocity (or signal delay) per section of this input line must be exactly the same as that of the output line. The propagation velocity per section is given by **Equation 2**.

For the input line with 2-pF section capacitance to have the same propagation velocity as the output line with 1-pF section capacitance, the half-section inductance must be one half that of the output line, or about 0.625 nH. Because the capacitance of the input line is determined by the device input capacitance, and the inductance by the required input-line propagation velocity, the input line impedance is then determined. According to **Equation 1**, the impedance of the input line must be 25 ohms. The input-line cutoff frequency is then also about 6.4 GHz.

The complete distributed amplifier

The complete 20-stage amplifier is shown in **Figure 5**. (DC biasing is omitted for simplicity.) Note that the transitions at the ends of the lines are made with half sections. If you look at the the complete amplifier in **Figure 5**, you'll find that operation is quite easy to follow once you understand that the device capacitances are incorporated to form *lumped-element* input and output-transmission lines.

A signal at the input terminal travels down the input line, driving each stage in turn, and is finally terminated at the input-line forward termination. At precisely the correct timing, each stage contributes to the output line, adding to the signal component from all previous stages traveling to the load. Because each stage is driving two line segments, one toward the load and one away from the load, some signal components travel in reverse along the output line. The reverse-traveling signals don't add construc-

tively and are of no value as output signals. A reverse termination is included on the reverse end of the output line to terminate the reverse-signal components and prevent reflections in the output line.

Since the gain stages are distributed along the input and output lines, this amplifier was originally termed a distributed amplifier by Ginzton et al. in their 1948 paper.³ Recently, this system has been called a traveling wave amplifier, since a traveling wave passing down the input line results in a traveling wave along the output line to the load.

It's interesting to note that the individual stage gains add in the distributed amplifier. They don't multiply as they would in a more conventional multistage amplifier. Therefore, it's quite acceptable for the available gain from each stage to be less than unity. For example, if the voltage gain of each stage of the twenty-stage amplifier described earlier were only 0.5, the total amplifier would provide an overall voltage gain of 10, or 20 dB.

Commercial systems

Although this amplifier may not be one of the more common ones seen in everyday use, it is common in some applications. One area where the distributed amplifier is quite popular is in very high-power, broad-bandwidth linear RF power amplifiers. Such units are manufactured by Instruments for Industry, Amplifier Research, Kalmus, and others. Typical output powers range from several-hundred watts to several-hundred kilowatts. Typical bandwidths range from a few tens of kilohertz at the low end to several hundred megahertz at the upper end, and perhaps beyond 1 GHz for some units.

Although some of the smaller units are solid state, most of the larger units are vacuum-tube systems. Systems with as many as 48 vacuum tubes (like the 4CX250B) arranged in a distributed-amplifier system, have been constructed. Vacuum-tube operation is identical to that described earlier. However, tetrode devices are typically used to eliminate Miller-capacitance effect, which would produce an excessively high input capacitance. Similarly, in solid-state designs, dual-gate FETs or pairs of FETs connected in a *cascode* (not cascade) configuration are commonly used for the same reason. Bipolar transistors are not commonly used in distributed amplifiers because they exhibit a significant resistive component at their base terminal. That resistance results in a very lossy input line, which limits the stages to a number too small to be of much value.

The Hewlett-Packard HMMC-5026 amplifier

Recently, the basic distributed amplifier has been reintroduced as the traveling-wave amplifier—not so much for high power, but for very high-frequency, wide-bandwidth operation. The distributed amplifier uses many small parallel-connected devices for increased output power, without compromising parasitic-limited bandwidth. It may be used equally as effectively to reduce the size and increase the number of the individual elements needed to provide some specific output power. Reducing the device size generally equates to increasing its high-frequency capability. The HMMC-5026 is one such amplifier. By using the distributed amplifier configuration, the HMMC-5026 can provide more than 15 dBm output power over a bandwidth greater than 2 to 26.5 GHz. Hewlett Packard has used this device in one of their instruments from 100 kHz to 26.5 GHz.⁷ Technically, the HMMC-5026 could be made to provide a bandwidth from DC, or at least a few Hertz, to 26.5 GHz. There is virtually no other means presently available to provide the output power and bandwidth supplied by these traveling-wave devices.

Final remarks

I've briefly reviewed the basic principles of the distributed amplifier. The distributed amplifier lets you operate several devices in parallel, allowing the individual device powers to be summed, while preventing the device parasitic capacitances from adding. This is accomplished by including the device capacitances in lumped-element transmission lines. The individual devices may then be selected to provide the required bandpass performance. A suitable number of devices can provide the desired output power. Although a rather obscure circuit, the distributed amplifier is enjoying renewed popularity as the traveling-wave amplifier for providing very wide bandwidth operation. ■

REFERENCES

1. Hewlett Packard HMMC-5026 data sheet, Hewlett Packard Co., 1989.
2. W.S. Percival, British patent specification 460,562, July 24, 1936.
3. Edward L. Ginzton, William R. Hewlett, J.H. Jasberg, and J.D. Noe, "Distributed Amplification," *Proceedings of the IRE*, August 1948, pages 956-969.
4. G.R. Brown, R.A. Sharp, and W.L. Hughes, *Lines, Waves, and Antennas*, Ronald Press, New York, 1961.
5. *Reference Data for Radio Engineers*, Howard W. Sams Co., New York, fifth edition, 1972.
6. *Reference Data for Engineers: Radio, Electronics, Computer, and Communications*, Howard W. Sams Co., New York, seventh edition, 1986.
7. Dennis Derickson, "A Broadband Instrumentation Photoreceiver," *Hewlett Packard Journal*, February 1990, pages 84-85.

A HIGH- PERFORMANCE 1296-MHz CONVERTER

New techniques and improved components reduce size and complexity while boosting performance

In the last decade, and particularly in the last few years, the 1235 to 1300-MHz Amateur band has become increasingly more populated due to the proliferation of commercially built UHF gear. This type of equipment typically provides 10 watts of transmit output power on continuous wave (CW), single sideband (SSB), and frequency modulation (FM) modes, plus the associated receiving capability. Power amplifiers for 1296 MHz are also becoming available. Many Amateurs use this type of equipment for OSCAR satellite work, terrestrial (point-to-point) communication, and Amateur television (ATV).

Recent advances in compact high-gain antennas like the loop Yagi, together with power amplifiers in the 30 to 200-watt class, now allow over-the-horizon communication on 1296 MHz over ranges of 200 miles or more on a regular basis under "normal" propagation conditions. When propagation becomes more favorable, the range increases considerably.

Background

Many years ago, before commercial versions of 1.2-GHz Amateur equipment were available, I built a 1296-MHz transmitter and a companion down-converter. The con-

verter included a trough-line mixer and a single-point contact diode mixer. The local-oscillator (LO) signal was derived from a tube-type crystal-oscillator-multiplier string. In the 1950s and 1960s, this approach was considered the ultimate in sophistication by many Amateurs. Unfortunately, the Amateur builder in those days was at a distinct disadvantage if he didn't have access to a well-equipped machine shop for bending metal and machining cavity resonators^{1,2,3,4}

In recent years I have completely rebuilt my 1296-MHz converter, taking advantage of new techniques and improved components. In particular, the double-balanced mixer (DBM) has overcome the need for highly selective cavity resonators once needed to isolate the signal, LO, and the intermediate frequency (IF). This makes the unit smaller and less mechanically complex. With the exception of the image filter, the design is a printed circuit, including a low-noise RF preamplifier.

The PLO as the local oscillator

The converter redesign began with the development of a PLO (phase-locked oscillator) to replace the crystal oscillator-multiplier string. This PLO, which operates at 1152 MHz, is described in detail in the

Winter 1991 issue of *Communications Quarterly*.⁵ The PLO is built on a pc board of the same size used for the converter described here. When used together, these two boards constitute a high-performance 1.2-GHz receiving converter.

It's possible, with the addition of appropriate coaxial switches and other RF components, to construct a 1.2-GHz transverter using these two boards. In such a case, the PLO would serve to up-convert a 144-MHz SSB signal to 1.2 GHz on transmit and to perform as the local oscillator on receive. Only the converter is discussed here.

Why a pc-board design?

Over the years, many Amateurs have advocated the use of separate Mini-boxes or similar individual enclosures for each of the circuit blocks of a homebrew system. The input and output connectors are tied together in daisy-chain fashion with short lengths of coaxial cables, thus forming a rather bulky system. This system is advantageous because making changes in one box will have a minimal effect on performance in the other boxes. Using this approach, a converter might consist of an RF preamplifier, a down-converter, a crystal-controlled local-oscillator chain, and a post-IF amplifier. I sometimes use separate enclosures in the early stages of a design when optimizing a particular circuit. But once each of the individual circuits has been worked out, I put the whole system onto a single pc board. This process may take more than one iteration. When I've decided on the final configuration, I prepare the pc board artwork and build a sample board. I then perform tests to verify the artwork.

The pc board approach has advantages not attainable with a chain of individual boxes. The board is much smaller and considerably less expensive to build. Fewer parts are required because the need to repeatedly convert from circuit impedance to 50 ohms and back is eliminated. Furthermore, as the

operating frequency is increased, the pc-board design makes it unnecessary to deal with large and bulky microwave structures.

On the flip side, if you design the board yourself, you can expect to make numerous changes involving many iterations. Recognizing that pc boards are very "final," the easiest approach is to copy the artwork from a magazine article, like this one, and make your own board, or to purchase a ready-made board. In either case, you avoid most of the design work and have a working unit in a very short time. This article not only describes such a board, but includes a 1:1-scale layout and a source for purchasing finished boards.

General description

Commercial UHF transceivers almost always need an external RF amplifier to achieve the lowest possible overall noise figure for the receiver. Sometimes, however, the extra gain produced can push the converter to its dynamic range limit, resulting in spurious mixer products that seem to be everywhere. This overload problem can be reduced by using a DBM for the first converter and limiting RF gain to a level that won't compromise overall noise figure.

I use a Mini-Circuits SRA-11 for the first mixer. The slightly less expensive SRA-5 also works very well. Compared with simpler types of mixers, these suppress harmonics which in turn reduce spurious mixer products (spurs). The relatively high LO power derived from the PLO described in **Reference 5** provides considerable intermodulation distortion (IMD) reduction. In fact, RF signals as high as zero dBm can be tolerated.

A block diagram of the 1.2-GHz converter is shown in **Figure 1**. The PLO is build on a separate board.

Recommended DBM literature

Many technical articles pertaining to optimization of the mixer using a DBM

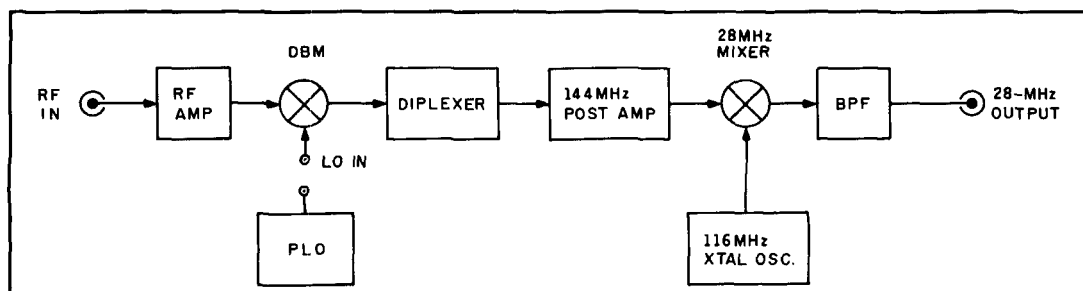


Figure 1. Block diagram, 1.2-GHz converter.

appeared in *QST* and *HAM RADIO* in 1975 and 1976. The principal authors of these articles were Edward L. Meade, Jr., K1AGB^{6,7} and Wes Hayward, W7ZOI⁸. Additional articles by Max Arnold, W4WHN⁹, Doug DeMaw, W1FB¹⁰ and Paul Shuch, WA6UAM¹¹ appeared in 1977 and 1978. These and other articles^{12,13} discuss the application of DBMs over the frequency range from 1.6 MHz through 1296 MHz. Rereading them will give you fresh insights into the DBM—particularly with respect to IF output matching, which is so critical in terms of reducing IMD and maintaining high RF-to-IF conversion efficiency. Some of these pieces address homebrewing the DBM, but this isn't necessary today. For a nominal cost, you can obtain DBMs for operation to 2,000 MHz and above from Mini-Circuits and other manufacturers.

Spurious signals and the diplexer

The spectrum at the DBM output includes the local oscillator (F_{LO}), the signal (F_S), and their harmonics. Also present are the $m \times n$ spurs generated by mixing action between harmonics of the LO and signal:

$$m(1152) \pm n(1296) = IF \quad (1)$$

Using 144 MHz as the first IF, the lowest spur of this type occurs for $m=8$ and $n=7$. Another spur occurs for $m=10$ and $n=9$.

The output signal of interest is F_{LO-F_S} where $m=1$ and $n=1$. If the IF or higher-order mixer products are allowed to reflect back into the DBM, isolation between the signal, local oscillator, and IF will be impaired, and dynamic range and sensitivity may be upset. To retain the desirable features of the DBM, you need a *diplexer* to provide the necessary termination.

The diplexer includes a high-pass filter with a cutoff frequency at approximately 150 MHz. It's terminated with a 50-ohm resistor which absorbs signals above 150 MHz. Below 150 MHz, the low-frequency section of the diplexer couples the desired signal through the low-Q series-resonant circuit consisting of L3 and C7 to the first IF transformer (Figure 2). The combination of the high and low-pass filters provides a good match for all DBM-output signals above about 140 MHz.

Design details

The UHF converter described here includes a low-noise 1.2-GHz bipolar preamplifier which drives the DBM. The

diplexer and low-noise FET post-IF amplifier follow the DBM. The diplexer provides a good match to the post amplifier and adds IF selectivity. Not only must the diplexer terminate unwanted signals, it must also transform the desired signal from the low-output impedance of the DBM to some higher value for the post-amplifier input circuit. The low-frequency terminals of the diplexer should provide a noise-match condition for the post-IF amplifier to minimize overall noise figure. Figures 3A and 3B illustrate the diplexer frequency response.

A second mixer develops the final output signal at 28 MHz. Except for the PLO, these circuits are integrated on a single pc board. The converter board is exactly the same size as the companion PLO board.

The PLO drives the DBM through a 3-dB RF pad. When the PLO output is 10 dBm, the mixer noise figure is about 7 dB. However, when measured at the converter's input terminal, noise figure is about 1.5 dB. Finally, when an external GaAsFET preamplifier like the ICM AG-1200 is added, the receiver noise figure drops to 0.7 dB—a respectable value for 1.2 GHz.

Most experts agree that RF gain ahead of the mixer should not exceed 30 dB, but 20 dB seems to be adequate for weak-signal (over the horizon) communication with this converter. When the GaAsFET is mast mounted, overall system noise figure reduces noticeably, even though overall gain remains the same.

The mast-mounted preamplifier has a gain of about 16 dB and a noise figure of 0.6 dB. My coaxial transmission line has a loss of about 2-1/2 dB, including the loss of an interdigital filter located in the station. To ensure sufficient RF gain, I added a low-noise GaAsFET amplifier in the station. This amplifier is described in Reference 14.

I performed tests to detect and measure the levels of the $m \times n$ and other unwanted responses that might be caused by random 2-meter signals, half-IF signals, and images. With the exception of the image, extremely strong input signals were needed for detection. According to Mini-Circuits test data¹⁵ the 8×7 and 10×9 spurs are 79 and 84 dB, respectively, below a -4 dBm signal at the RF port. Adding the diplexer, reduced these spurs to around the level of the noise threshold. Some, more readily detected, miscellaneous spurs were related to the image and other responses developed in the 10-meter receiver.

Because the bipolar RF amplifier is broadband, it offers very little image rejection at 1008 MHz (see Figure 4). To obtain

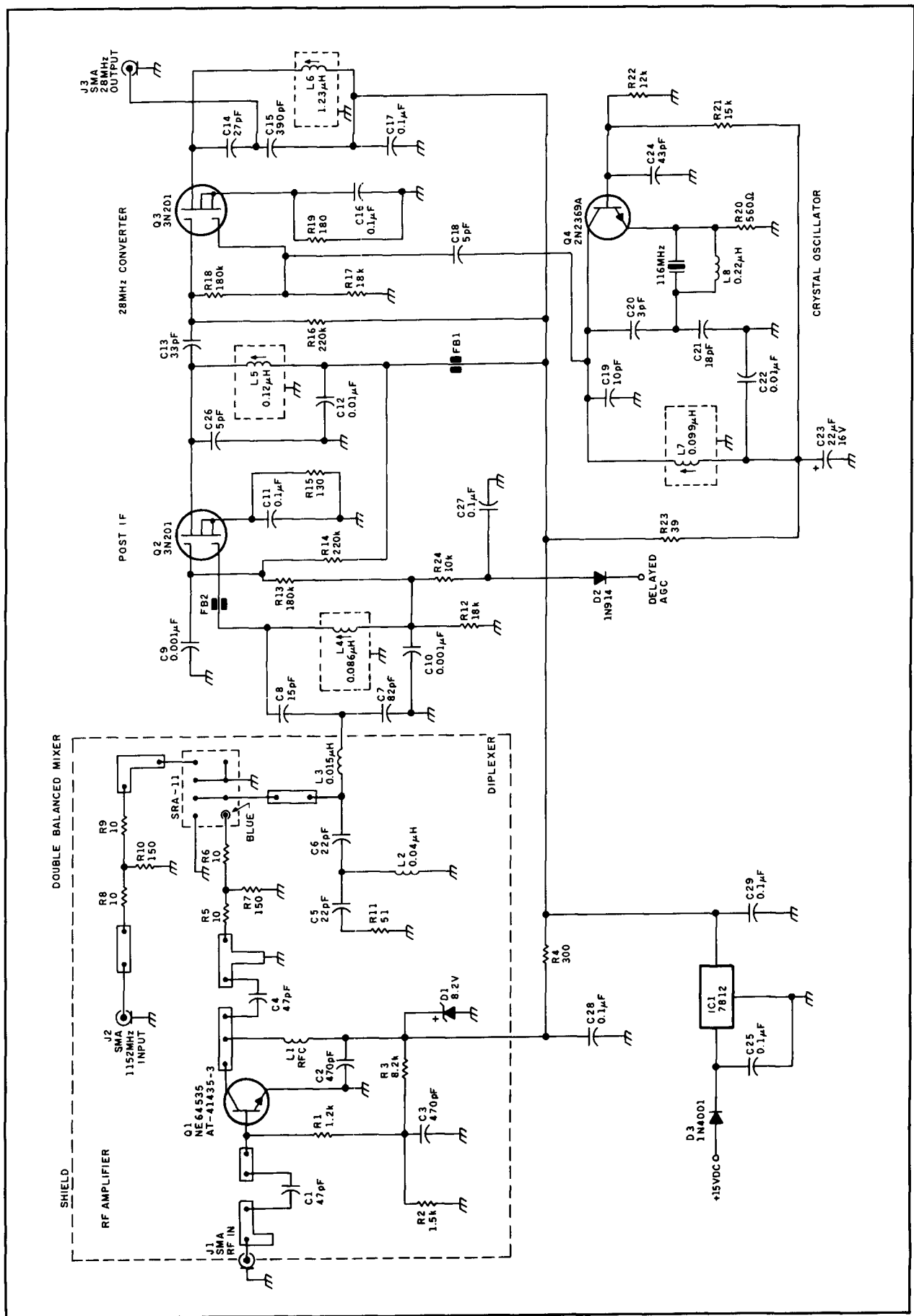


Figure 2. 1296-MHz converter schematic diagram.

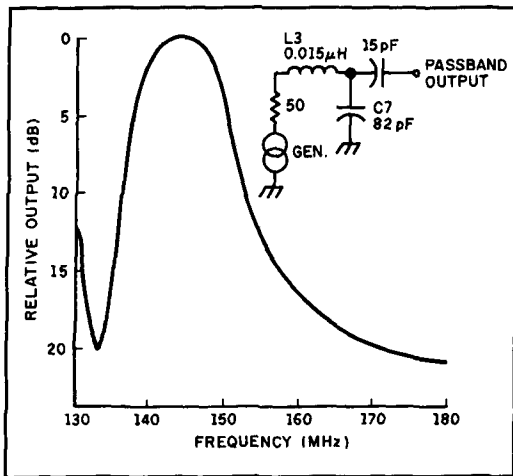


Figure 3A. Diplexer passband.

sufficient RF selectivity, I added an interdigital bandpass filter¹⁶ ahead of the converter. This provides 45 dB image rejection. Even though you may not be bothered by the presence of an actual coherent image signal, the RF filter reduces the amount of noise otherwise fed through the lower sideband to the mixer. This improves the receiver's overall noise figure.

The pc board

As on the companion PLO board, holes are provided for feedthrough grounds. This avoids the need for an expensive plated-through board. A 1:1 scale reproduction of the trace and ground plane sides of the board are shown in Figures 5A and B.

Short lengths of no. 26 tinned busbar are inserted, bent over, slipped short, and soldered on each side. The grounds are effective at 1.2 GHz because they are only a small fraction of a wavelength long. The component side of the board constitutes a ground plane; the circuit side includes soldering pads and interconnecting traces. The

large 1/8-inch pads used for through-grounds are easy to identify.

Circuit analysis

Look at the schematic in Figure 2. Q1 is the microwave bipolar RF amplifier with a gain of 15 dB, measured between the converter's RF input and the SRA-11 input. Q1 can be either an Avantek AT-41435-3 or an NEC 64535. Although these are relatively inexpensive micro-X packages, they yield 1.3 dB noise figures at 1296 MHz. They are rugged and not subject to burnout from static discharges. The circuit I used makes the amplifier unconditionally stable. The stage will not oscillate even when the antenna terminal is an open circuit. Together with a 7-dB mixer NF (noise figure), overall converter NF is 1.5 dB.

The best IMD performance for Q2, the 144-MHz post amplifier, is obtained with a small forward bias on gate 1. The network consisting of R12, R13, and R14 produces 0.5 volts DC on gate 1 and 6.0 volts DC on gate 2. Gain can be reduced by lowering the voltage on gate 2, either manually with a pot, or with automatic gain control (AGC). To maintain good IF stability, ferrite-bead FB2 is surface mounted between the first IF coil and G1 of the 3N201 on the traces provided. The 3N201 bias has been adjusted so drain current is about 12 mA. This is the region where the IF stage is most linear, thus reducing cross modulation should two strong signals be present simultaneously at gate 1.^{17,18} The portion of the DBM matching network coupling the desired signal to gate 1, provides a step-up ratio of 5.5. This represents a voltage gain of 14.8 dB and ensures a low post-amplifier noise figure.

Q3 is a mixer which down converts 144 MHz to 28 MHz, using Q4 as its local oscillator. The 116-MHz crystal is a 5th overtone unit. With this crystal, the converter output frequency would be 28 MHz—corresponding to a 1152-MHz PLO frequency and a

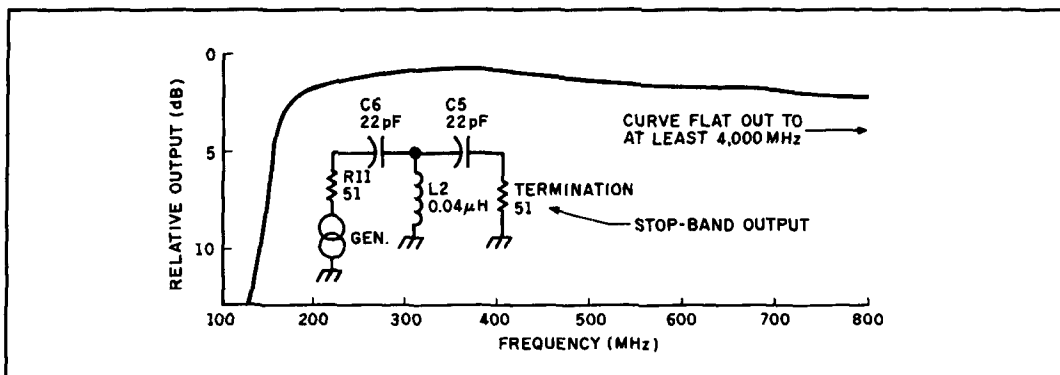


Figure 3B. Diplexer stop band.

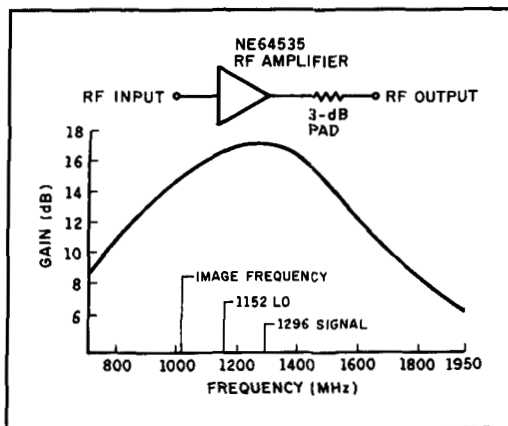


Figure 4. Bipolar RF-amplifier selectivity.

1296-MHz input signal frequency. When using the 1296.1 MHz calling frequency, a 10-meter receiver driven by this converter would be tuned to 28.1 MHz.

ICM part number 473360 defines the crystal case size which fits the pc board. It also specifies overtone number, mode of operation, capacitance, and frequency tolerance. You must specify the operating frequency.

Assembly and test

There's nothing particularly critical about

assembling and testing this converter. There are only four adjustments: the powdered-iron slugs in the oscillator coil, two 144-MHz IF coils, and the 28-MHz output coil. The 116-MHz crystal oscillates only over a narrow tuning range, as indicated by an increase in background noise at the 10-meter receiver output.

The other coils are tuned for maximum output while a weak 1296-MHz signal is applied to the converter input terminal. You can purchase a ready-to-assemble pc board from FAR Circuits. Ordering information is given at the end of the article. The board is designed with an edge-connector which mates with a double 15-pin set of contacts spaced 0.156 inch, like TI H411121-15 or Sullins EMZ150REH, available from Mouser or Digi-Key.

I used Coilcraft T7-144 shielded "uni-coils" for the tunable coils. You can purchase similar coils from Digi-Key (TOKO America Inc., TK1401, TK1402, TK1403, and TK 1411). The board includes holes for either kind of coil. The board doesn't include slots for mounting the coil cans. I bent the mounting tabs at right angles and soldered them to the ground plane instead.

There are two coils hand wound with no. 21 enamel copper wire and one RF choke

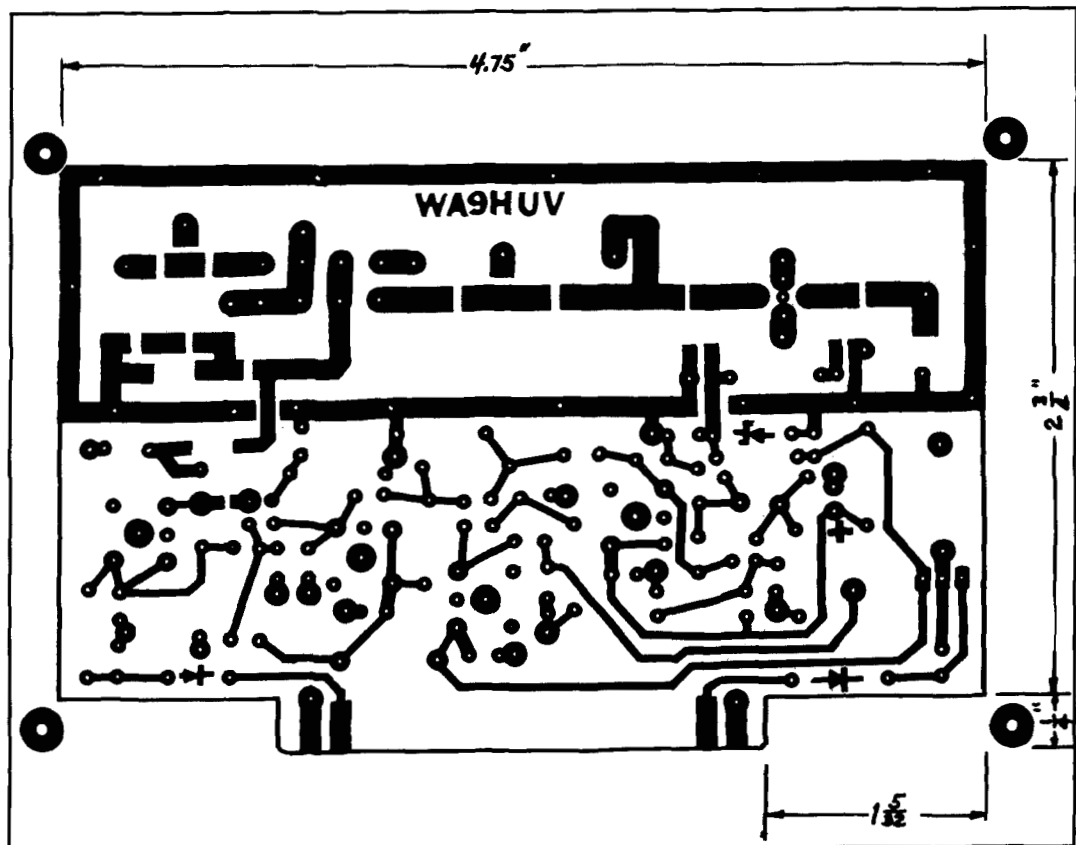


Figure 5A. PC-board artwork, trace side.

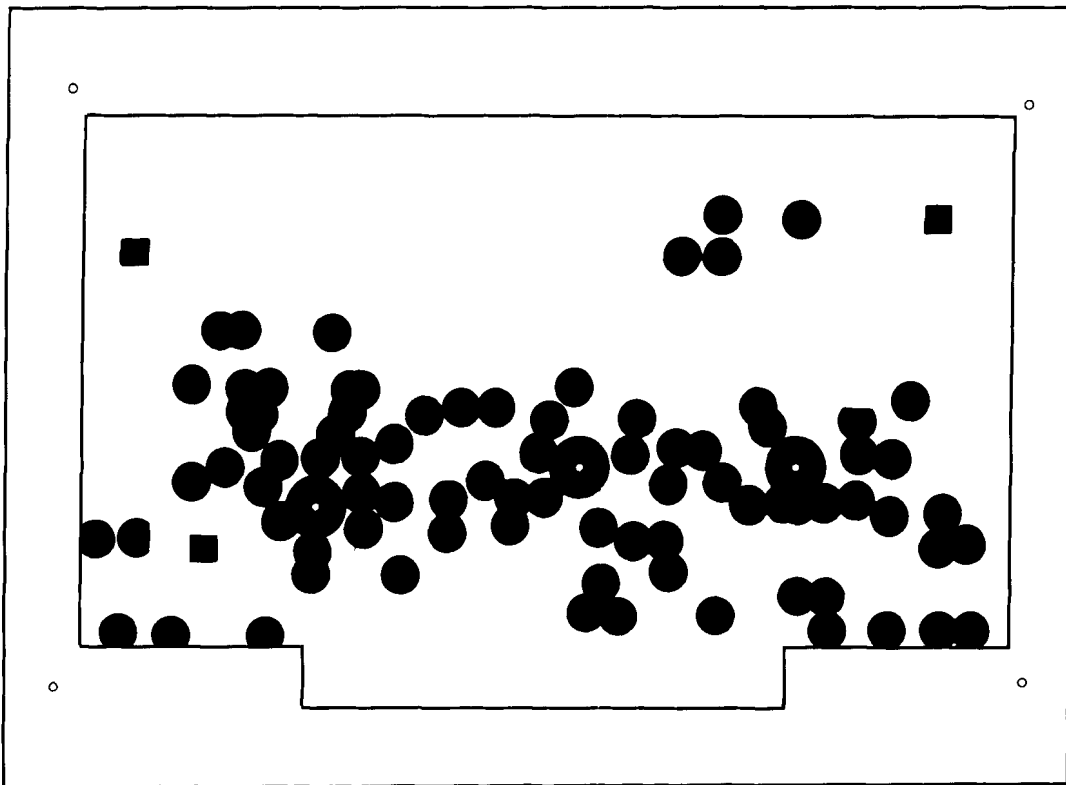


Figure 5B. PC-board artwork, ground-plane side.

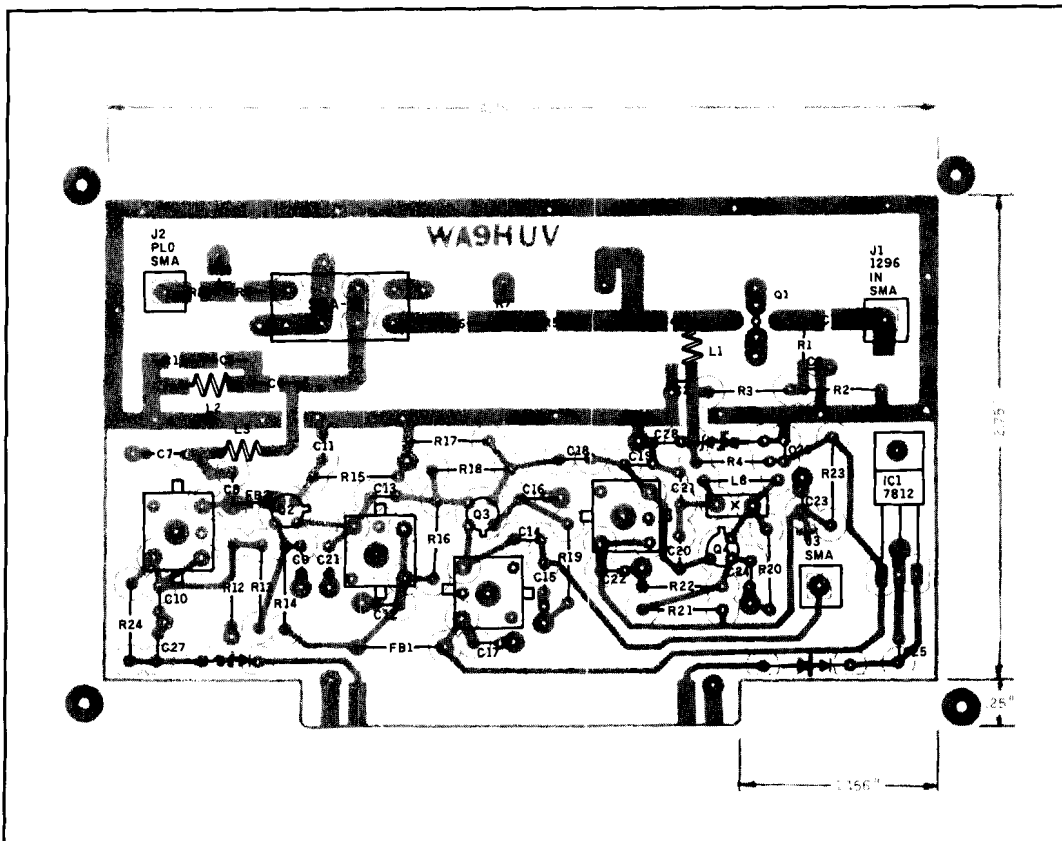


Figure 6. Location of components as seen through trace side of board. The dotted portions are clearance holes in the ground plane.

PARTS LIST

| Symbol | Value | Description | Source |
|--------|-----------------------------|--|--------|
| C1* | 47 pF | ceramic-chip capacitance | 1,2,3 |
| C2* | 470 pF | ceramic-chip capacitance | 1,2,3 |
| C3* | 470 pF | ceramic-chip capacitance | 1,2,3 |
| C4* | 47 pF | ceramic-chip capacitance | 1,2,3 |
| C5* | 22 pF | ceramic-chip capacitance | 1,2,3 |
| C6* | 22 pF | ceramic-chip capacitance | 1,2,3 |
| C7 | 82 pF | dipped mica | 3 |
| C8 | 15 pF | dipped mica | 3 |
| C9 | 0.001 μ F | 50-volt monolithic or polyester | 1 |
| C10 | 0.001 μ F | 50-volt monolithic or polyester | 1 |
| C11 | 0.1 μ F | 50-volt monolithic or polyester | 1 |
| C12 | 0.01 μ F | 50-volt monolithic or polyester | 1 |
| C13 | 33 pF | dipped mica | 3 |
| C14 | 27 pF | dipped mica | 3 |
| C15 | 390 pF | dipped mica | 3 |
| C16 | 0.1 μ F | 50-volt monolithic or polyester | 1 |
| C17 | 0.01 μ F | 50-volt monolithic or polyester | 1 |
| C18 | 5 pF | dipped mica | 3 |
| C19 | 10 pF | dipped mica | 3 |
| C20 | 3 pF | dipped mica | 3 |
| C21 | 18 pF | dipped mica | 3 |
| C22 | 0.01 μ F | 50-volt monolithic or polyester | 1 |
| C23 | 22 μ F/16-volt | electrolytic, radial leads | 3 |
| C24 | 43 pF | dipped mica | 3 |
| C25 | 0.1 μ F | 50-volt monolithic or polyester | 1 |
| C26 | 5 pF | dipped mica (located near L5) | 3 |
| C27 | 0.1 μ F | 50-volt monolithic or polyester (by L4) | |
| C28 | 0.1 μ F | 50-volt monolithic or polyester (by D-1) | |
| C29 | 0.1 μ F | 50-volt monolithic or polyester (by D-1) | |
| D1 | 1N756 | 8.2-volt zener | |
| D2 | 1N914 | silicon diode | |
| D3 | 1N4001 | silicon diode | |
| IC1 | 7812 | voltage regulator | 3 |
| J1 | SMA pc mount p/n 142-0298-1 | | 2 |
| J2 | SMA pc mount p/n 142-0298-1 | | 2 |
| J3 | SMA pc mount p/n 142-0298-1 | | 2 |
| L1* | RFC | 5 turns no. 28 enameled copper wire, 0.064" ID | 5 |
| L2* | 0.04 μ H | 3 turns no. 21 enameled copper wire, 0.154" ID spaced one wire diameter | 5 |
| L3* | 0.015 μ H | 3 turns, no. 21 enameled copper wire, 0.128" ID spaced one wire diameter | 5 |
| L4 | 0.086 μ H | Coilcraft 142-02J08S, 2-1/2 turns, red (alternate) TK1401 | 6 7 |

wound with no. 28 wire. Details are given in the parts list.

Solder the three E.F. Johnson SMA female connectors directly to the pc board after clipping off the four "legs." Allow solder to flow around all four sides, then solder the center pin to the RF pad on the trace side. For the location of these and other parts, refer to **Figure 6**.

The pc board is configured to accept two 22-pF chip capacitors and one 51-ohm chip resistor. These elements form part of the terminated high-pass filter, which operates

into the UHF region. You can use a 51-ohm, 1/8-watt resistor for the termination if you make the lead lengths extremely short.

Make a brass "fence" 4-3/4 inches long and 1-5/16 inches wide from a 1/4-inch wide, 0.032-inch thick brass strip (available from most hobby shops). Tin the strip first, then form it to fit the etched pc board rectangle. Before soldering it to the board, cut two clearance slots with a nibbler to avoid shorting the two pc traces leading out of the box. After soldering the "fence" to the board, make a tight-fitting cover from 0.015-

| | | | |
|---------|--|---|--------|
| L5 | 0.12 μ H | Coilcraft 142-03J08S, 3-1/2 turns, orange (alternate) TK1403 | 6 7 |
| L6 | 1.23 μ H | Coilcraft slot-10-3-02, scramble wound, red (alternate) TK1411 | 6 7 |
| L7 | 0.099 μ H | Coilcraft 144-03J12S, 3-1/2 turns, orange (alternate) TK1402 | 6 7 |
| L8 | 0.22 μ H RFC | 9230-04 J.W. Miller 0.095"D x 0.250"L | 3 |
| Q1 | AT-41435-3 (alternate NE64535) | | 9 |
| Q2 | 3N201 | post IF amplifier (alternate) 40673 | 3 |
| Q3 | 3N201 | 28-MHz converter (alternate) 40673 | 3 |
| Q4 | 2N2369A | 116-MHz crystal oscillator | 3 |
| R1* | 1.2 k, 1/8 watt, 5 percent, carbon film | | 3 |
| R2 | 1.2 k, 1/4 watt, 5 percent, carbon film | | 3 |
| R3 | 8.2 k, 1/4 watt, 5 percent, carbon film | | 3 |
| R4 | 300 ohm, 1/4 watt, 5 percent, carbon film | | 3 |
| R5* | 10-ohm chip resistor | | 1 |
| R6* | 10-ohm chip resistor | | 1 |
| R7* | 150-ohm chip resistor | | 1 |
| R8* | 10-ohm chip resistor | | 1 |
| R9* | 10-ohm chip resistor | | 1 |
| R10* | 150-ohm chip resistor | | 1 |
| R11* | 51-ohm chip resistor | | 1 |
| R12 | 18 k, 1/4 watt, 5 percent, carbon film | | 3 |
| R13 | 180 k, 1/4 watt, 5 percent, carbon film | | 3 |
| R14 | 220 k, 1/4 watt, 5 percent, carbon film | | 3 |
| R15 | 130 ohm, 1/4 watt, 5 percent, carbon film | | 3 |
| R16 | 220 k, 1/4 watt, 5 percent, carbon film | | 3 |
| R17 | 18 k, 1/4 watt, 5 percent, carbon film | | 3 |
| R18 | 180 k, 1/4 watt, 5 percent, carbon film | | 3 |
| R19 | 180 ohm, 1/4 watt, 5 percent, carbon film | | 3 |
| R20 | 560 ohm, 1/4 watt, 5 percent, carbon film | | 3 |
| R21 | 15 k, 1/4 watt, 5 percent, carbon film | | 3 |
| R22 | 12 k, 1/4 watt, 5 percent, carbon film | | 3 |
| R23 | 39 ohm, 1/4 watt, 5 percent, carbon film | | 3 |
| R24 | 10 k, 1/4 watt, 5 percent, carbon film (by L4) | | 3 |
| Crystal | 116 MHz | 473360 | 8 |
| SRA-II | DBM | (blue bead is RF input) | 11 |
| FBI | molded bead | ferrite molded bead, 0.138"D, 0.35"L, with pigtailed | 10 |
| FB2* | bead | Fair-Rite p/n FB-43-101, 1/8"D x 1/8"L | 10 |
| PC | board | see text | 12 |

*surface mount

inch thick brass or aluminum. Slot the side flaps to match the slots in the fence.

Final remarks

As you can see by looking at the references, considerable effort was involved in developing this converter. After sorting through the Amateur literature, I selected a group of circuits that, when used together, promised to provide the best possible converter performance consistent with reason-

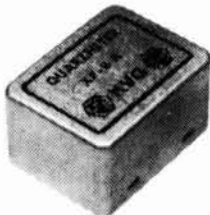
able cost, parts availability, and ease of assembly and test.

Based on the performance I achieved, the effort was well worthwhile. If you decide to duplicate this converter, you may be as pleased with the end result as I have been. ■

REFERENCES

1. Byron Goodman, W1DX, "A Crystal Controlled Converter for 1296 MHz," *ARRL Handbook*, page 420.
2. William O. Troeschel, K6UQH, "1296 Revisited," *QST*, July, 1973, page 40.
3. R.E. Fisher, W2CQH, "Interdigital Converters for 1296 and 2304 MHz," *QST*, January 1974, page 11.

K.V.G. CRYSTAL PRODUCTS



9 MHz CRYSTAL FILTERS

| MODEL | Application | Bandwidth | Poles | Price |
|----------|-------------|-----------|-------|----------|
| XF-9A | SSB | 2.4 kHz | 5 | \$ 75.00 |
| XF-9B | SSB | 2.4 kHz | 8 | 99.00 |
| XF-9B-01 | LSB | 2.4 kHz | 8 | 145.00 |
| XF-9B-02 | USB | 2.4 kHz | 8 | 145.00 |
| XF-9B-10 | SSB | 2.4 kHz | 10 | 170.00 |
| XF-9C | AM | 3.75 kHz | 8 | 110.00 |
| XF-9D | AM | 5.0 kHz | 8 | 110.00 |
| XF-9E | FM | 12.0 kHz | 8 | 120.00 |
| XF-9M | CW | 500 Hz | 4 | 80.00 |
| XF-9NB | CW | 500 Hz | 8 | 165.00 |
| XF-9P | CW | 250 Hz | 8 | 199.00 |
| XF-910 | IF noise | 15 kHz | 2 | 20.00 |

10.7 MHz CRYSTAL FILTERS

| | | |
|------------|---------|---------|
| XF-107A | 12 kHz | \$99.00 |
| XF-107B | 15 kHz | 99.00 |
| XF-107C | 30 kHz | 99.00 |
| XF-107D | 36 kHz | 99.00 |
| XF-107E | 40 kHz | 99.00 |
| XF-107S139 | 100 kHz | 150.00 |

41 MHz CRYSTAL FILTER

| | |
|-----------|----------|
| XF-410S02 | \$199.00 |
|-----------|----------|

Write for full details of crystals and filters.
Shipping: \$6.00 Shipping: FOB Concord, MA
Prices subject to change without notice.

Spectrum International, Inc.
P.O. Box 1084 Dept. Q
Concord, MA 01742 U.S.A.
Phone: 508-263-2145
FAX: 508-263-7008

- Larkin Krutcher, WA5WOW, "An Active Mixer Converter for 1296 MHz," *QST*, August, 1974, page 11.
- Norm Foot, WA9HUV, "Upgrade Your 1296-MHz Converter," *Communications Quarterly*, Winter 1991.
- Edward L. Meade, Jr., K1AGB, "Using the Double-Balanced Mixer in VHF Converters," *QST*, March 1975, page 12.
- Edward L. Meade, Jr., K1AGB, "Double-Balanced Mixer," *QST*, August 1975, page 38.
- Wes Hayward, W7ZOI, "Receiver Dynamic Range," *QST*, July 1975, page 15.
- Max Arnold, W4WHN and Doug DeMaw, W1FB, "Build This High-Performance Top-Band Receiver," *QST*, October 1978, page 72.
- Doug DeMaw, W1CER, "His Eminence-the Receiver," *QST*, June 1976, page 26.
- Paul Shuch, WA6UAM, "Double-Balanced Mixers on 1296," *Ham Radio*, July 1975, page 8.
- Wes Hayward, W7ZOI, "Cer-Ver-ters," *QST*, June 1976, page 22.
- Robert S. Stein, W6NBI, "VHF Techniques," *Ham Radio*, July 1980, page 62.
- Norm Foot, WA9HUV, "The Weekender: A 1296-MHz Low-Noise Amplifier," *Ham Radio*, November 1988, page 60.
- Mini-Circuits, *RF Processing Handbook*, Volume 1, page 58.
- Reed E. Fisher, W2CQH, "Interdigital Bandpass Filters for Amateur VHF/UHF Applications," *QST*, March 1968, page 33.
- RCA Application Note AN-4431.
- Motorola Data Sheet, DS5647.

SOURCES:

- Digi-Key, 701 Brooks Avenue South, P.O. Box 677, Thief River Falls, Minnesota 56701-0677.
- Mouser Electronics, 11433 Woodside Avenue, Santee, California 92071 (West Coast), or 12 Emery Avenue, Randolph, New Jersey 07869 (East Coast).
- Circuit Specialists, Inc., P.O. Box 3047, Scottsdale, Arizona 85271-3047.
- E. F. Johnson, 299 Johnson Avenue, Waseca, Minnesota, 56093. Parts available only through authorized distributors. Mouser is one of many.
- Handmade
- Coilcraft, Inc., 1102 Silver Lake Road, Cary, Indiana 60013.
- TOKO America Inc. 1250 Feehanville Drive, Mt. Prospect, Illinois 60056.
- ICM, P.O. Box 26330, 701 W. Sheridan, Oklahoma City, Oklahoma 73126-0330.
- Avantek, Inc. 3175 Bowers Avenue, Santa Clara, California 95054.
- Fair-Rite Products Corp., Department M, PO Box J, Walkkill, New York 12589.
- Mini-Circuits, P.O. Box 350166, Brooklyn, New York 11235.
- FAR CIRCUITS, Fred Reimers, N9ATW, 18N640 Field Court, Dundee, Illinois 60118*

*To purchase a board, send \$9.50 plus \$1.50 per order for shipping and handling.

NEW BOOKS

WEATHER SATELLITE HANDBOOK New
ARRL 4th Edition
by Ralph Taggart, WB8DQT

Taggart has long been recognized as one of the foremost experts on weather satellite picture reception. This new edition of his famous book has been updated and expanded to include all the latest information on satellite picture reception. Subjects covered include a complete section on what satellites are in orbit, everything you'd want to know on what kind of antenna, receiver, video formats and displays to use, plus much more! You get all the information you need to get your satellite system up and running. © 1990 4th Edition

AR-WSH

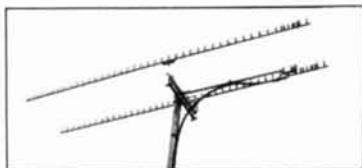
Softbound \$19.95

Call TOLL FREE

(800) 457-7373

Please enclose \$4.00 US mail, \$5.00 UPS brown
CQ's HR Bookstore Greenville, NH 03048
(603) 878-1441 FAX (603) 878-1951

DOWN EAST MICROWAVE



MICROWAVE ANTENNAS AND EQUIPMENT

- Loop Yagis • Power Dividers • Dish Feeds
- Complete Antenna Arrays • Linear Amps
- Microwave Transverters & Kits • GaAs FET Preamps and Kits • Microwave Components
- Tropo • EME • Weak Signal • OSCAR • FM
- Packet • ATV
- 902 • 1269 • 1296 • 1691 • 2304 • 2400 • 3456 • 5760 • 10,386 MHz

ANTENNAS

| | | | | |
|----------|----------|-----------------------------|----------|-------|
| 2345 LYK | 45 el | Loop Yagi Kit | 1296 MHz | \$95 |
| 1345 LYK | 45 el | Loop Yagi Kit | 2304 MHz | \$79 |
| 3333 LYK | 33 el | Loop Yagi Kit | 902 MHz | \$95 |
| 1844 LY | 44 el | Loop Yagi Assembled | 1691 MHz | \$105 |
| 3B Feed | Tri Band | Dish Feed 2.3, 3.4, 5.7 GHz | | \$15 |

Many others and assembled versions available. Shipping extra.

LINEAR AMPS AND PREAMPS

| | | | | |
|-------------|-----------------|---------------------|----------|-------|
| 2303 PA | 1.2 to 1.3 GHz | 3w out | 13.8 VDC | \$130 |
| 2318 PAM | 1.24 to 1.3 GHz | 20w out | 13.8 VDC | \$205 |
| 2335 PA | 1.24 to 1.3 GHz | 35w out | 13.8 VDC | \$325 |
| 2340 PA | 1.24 to 1.3 GHz | high gain 35w out | 13.8 VDC | \$355 |
| 2370 PA | 1.24 to 1.3 GHz | 70w out | 13.8 VDC | \$695 |
| 1302 PA | 2.2 to 2.5 GHz | 3w out | 13.8 VDC | \$430 |
| 13 LNA | 2.3 to 2.4 GHz | preamp | 6 dB NF | \$140 |
| 23 LNA | 1.2 to 1.3 GHz | preamp | 6 dB NF | \$95 |
| 33 LNA | 900 to 930 MHz | preamp | 6 dB NF | \$95 |
| 1691 LNA WP | 1691 MHz | mast mounted preamp | 8 dB NF | \$140 |

Kits, Weatherproof Versions and other Frequencies Available

NO-TUNE TRANSVERTERS AND TRANSVERTER KITS

| | | | | |
|-----------|---|----------------------|-------------|-----------|
| SHF 902K | 900, 1269, 1296, 2304, 2400, 3456, 5760 MHz | 902 MHz Transverter | 40mW, 2m IF | Kit \$139 |
| SHF 1296K | | 1296 MHz Transverter | 10mW, 2m IF | Kit \$149 |
| SHF 2304K | | 2304 MHz Transverter | 10mW, 2m IF | Kit \$205 |
| SHF 3456K | | 3456 MHz Transverter | 10mW, 2m IF | Kit \$205 |

OSCAR and other frequencies available, also Amps and package versions wired and tested.

Write for more information. Free catalog available.

DOWN EAST MICROWAVE
 Bill Olsen, W3HQT
 RR1 Box 2310, Troy, ME 04987
 (207) 948-3741 Fax: 207-948-5157



VHF COMMUNICATIONS

9:00 am - 5:30 pm
weekdays

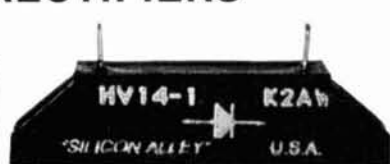
Weekends and evenings
by appointment.

280 Tiffany Avenue
Jamestown, New York 14701

Western New York's finest amateur radio dealer!
 PH. (716) 664-6345
 (800) 752-8813 for orders only

HI-VOLTAGE RECTIFIERS

SUPER FOR
HIGH
POWER
LINEARS



| | | |
|---------------|-------|---------|
| 6 KV @ 1 Amp | | \$5.00 |
| 8 KV @ 1 Amp | | \$11.00 |
| 10 KV @ 1 Amp | | \$13.00 |
| 14 KV @ 1 Amp | | \$15.00 |

Plus \$2.00 Shipping—NY Residents Add 8% Tax

K2AW's "SILICON ALLEY"

175 FRIENDS LANE, WESTBURY, NY 11590
(516) 334-7024

CQ Bookstore

Greenville, NH 03048

Two New Books
for Summer 1991

ARRL 1991-1992

REPEATER DIRECTORY

Over 19,000 listings of repeaters from all corners of the Earth. Great book to have when you travel. You should have one for each car and home! Covers all repeater bands 10M and up. Includes sponsoring clubs. Also has beacon calls and frequencies. ©1991

☐ AR-RD92 Softbound \$5.95

1991 CALLBOOK SUPPLEMENT

Update your 1991 Callbooks with all the latest US and foreign call assignments. Chockfull of information. © 1991

☐ CB-SUP91 Softbound \$9.95

(800)457-7373

Shipping \$4 via Mail. \$5 via UPS.

US only

Foreign orders FOB Greenville, NH 03048



ATV CONVERTERS • HF LINEAR AMPLIFIERS

DISCOVER THE WORLD OF FAST SCAN TELEVISION



HF AMPLIFIERS per MOTOROLA BULLETINS

Complete Part List for HF Amplifiers Described in the MOTOROLA Bulletin.

| | |
|---------------------|---------------------|
| AN758 300W \$160.70 | EB63 140W \$ 88.05 |
| AN762 140W \$ 93.25 | EB27A 300W \$139.20 |
| AN778 20W \$ 83.70 | EB104 600W \$351.05 |
| AN779H 20W \$ 93.19 | AR305 300W \$383.52 |
| AR313 300W \$403.00 | |

NEW!! 1K WATT 2-50 MHz Amplifier

| | | |
|----------------------|-------|----------|
| 600 Watt PEP 2-Port | | \$ 60.05 |
| 1000 Watt PEP 2-Port | | \$ 79.05 |
| 1200 Watt PEP 4-Port | | \$ 89.05 |

100 WATT 420-450 MHz PUSH-PULL LINEAR AMPLIFIER - 990-FM-ATV

| | |
|------------------------|--------------|
| 2 METER VHF AMPLIFIERS | |
| 35 Watt Model 335A | \$ 79.95 Kit |
| 75 Watt Model 875A | \$119.95 Kit |



CCI Communication Concepts Inc.

508 Millstone Drive • Xenia, Ohio 45385 • (513) 426-8600
 FAX (513) 429-3811



UNIVERSAL DIGITAL FREQUENCY READOUT

TK-1 (Wired/tested) \$149.95

HEAT SINK MATERIAL

Model 99 Heat Sink (8.5 x 12 x 1.8) \$24.00

CHS-8 Copper Spreader (8 x 8 x 1/8) \$22.00

We also stock Hard-to-Find parts

CHIP CAPS - Kemet/ATC

METAL CLAD MICA CAPS - Unesco/Semco

RF POWER TRANSISTORS

MINI-CIRCUIT MIXERS

SBL-1 (1-500MHz) \$ 6.50

SBL-1X (10-1000MHz) \$ 7.95

ARCO TRIMMER CAPACITORS

VK200-20/4B RF Chokes \$ 1.20

54-500-65-3B Ferrite Bead \$ 1.20

Broadband HF Transformers

Add \$ 3.50 for shipping and handling.

For detailed information and prices, call or write for our free catalog.

MasterCard

AMERICAN EXPRESS

VISA

MasterCard

AMERICAN EXPRESS

VISA

MasterCard

AMERICAN EXPRESS

VISA

MasterCard

AMERICAN EXPRESS

VISA

MasterCard

AMERICAN EXPRESS

VISA

MasterCard

AMERICAN EXPRESS

VISA

MasterCard

AMERICAN EXPRESS

VISA

MasterCard

AMERICAN EXPRESS

VISA

MasterCard

AMERICAN EXPRESS

VISA

MasterCard

AMERICAN EXPRESS

VISA

MasterCard

AMERICAN EXPRESS

VISA

MasterCard

AMERICAN EXPRESS

VISA

MasterCard

AMERICAN EXPRESS

VISA

MasterCard

AMERICAN EXPRESS

VISA

MasterCard

AMERICAN EXPRESS

VISA

MasterCard

AMERICAN EXPRESS

VISA

MasterCard

AMERICAN EXPRESS

VISA

MasterCard

AMERICAN EXPRESS

VISA

MasterCard

AMERICAN EXPRESS

VISA

MasterCard

AMERICAN EXPRESS

VISA

MasterCard

AMERICAN EXPRESS

VISA

MasterCard

AMERICAN EXPRESS

VISA

MasterCard

AMERICAN EXPRESS

VISA

MasterCard

AMERICAN EXPRESS

VISA

MasterCard

AMERICAN EXPRESS

VISA

MasterCard

AMERICAN EXPRESS

VISA

MasterCard

AMERICAN EXPRESS

VISA

MasterCard

AMERICAN EXPRESS

VISA

MasterCard

AMERICAN EXPRESS

VISA

MasterCard

AMERICAN EXPRESS

VISA

MasterCard

AMERICAN EXPRESS

VISA

MasterCard

AMERICAN EXPRESS

VISA

MasterCard

AMERICAN EXPRESS

VISA

MasterCard

AMERICAN EXPRESS

VISA

MasterCard

AMERICAN EXPRESS

VISA

MasterCard

AMERICAN EXPRESS

VISA

MasterCard

AMERICAN EXPRESS

VISA

MasterCard

AMERICAN EXPRESS

VISA

MasterCard

AMERICAN EXPRESS

VISA

MasterCard

AMERICAN EXPRESS

VISA

MasterCard

AMERICAN EXPRESS

VISA

MasterCard

AMERICAN EXPRESS

VISA

MasterCard

AMERICAN EXPRESS

VISA

MasterCard

AMERICAN EXPRESS

VISA

MasterCard

AMERICAN EXPRESS

VISA

MasterCard

AMERICAN EXPRESS

VISA

MasterCard

AMERICAN EXPRESS

VISA

MasterCard

AMERICAN EXPRESS

VISA

MasterCard

AMERICAN EXPRESS

VISA

MasterCard

AMERICAN EXPRESS

VISA

MasterCard

AMERICAN EXPRESS

VISA

MasterCard

AMERICAN EXPRESS

VISA

Measure Up With Coaxial Dynamics Model 83550 Digital Wattmeter

The "Generation Gap" is filled with the "new" EXPEDITOR, the microprocessor based R.F. AnaDigit System.

The EXPEDITOR power computer...you make the demands, it fills the requirements.

- Programmable forward AND reflected power ranges.
- Can be used with the elements you now have.
- Compatible with all Coaxial Dynamics line sizes and power ranges.
- 18 scales from 100 mW to 50 kW.

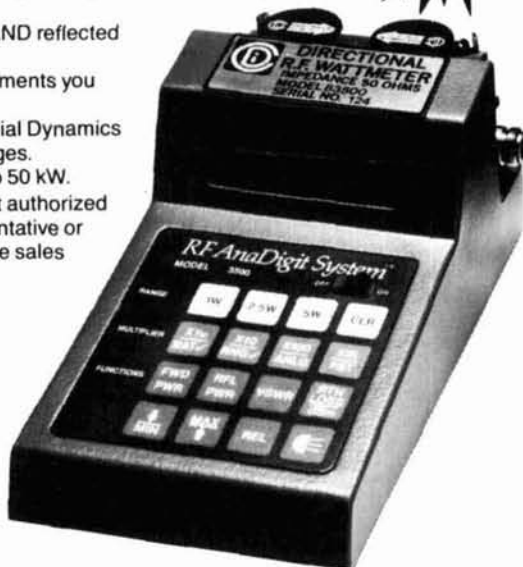
Contact us for your nearest authorized Coaxial Dynamics representative or distributor in our world-wide sales network.



**COAXIAL
DYNAMICS, INC.**

15210 Industrial Parkway
Cleveland, Ohio 44135
216-267-2233 1-800-COAXIAL
Telex: 98-0630

Service and Dependability...A Part of Every Product



TOROID CORES



- Iron Powder
- Ferrite
- Shielding Beads
- Ferrite Rods
- Split Beads

Small orders welcome. All items in stock for immediate delivery. Low cost experimenter's kits: **Iron Powder, Ferrite.** The dependable source for toroidal cores for 25 years.

Call or write for free catalog and tech data sheet.

PALOMAR ENGINEERS

Box 455, Escondido, CA 92033, USA
Tel. (619) 747-3343

Iron Powder and Ferrite Products

Fast, Reliable Service Since 1963

Millions of Parts in Stock for Immediate Delivery.
Low Cost Experimental Kits.

Small Orders Welcome

**Ask For Our FREE 78 Pages
Handbook/Catalog**



Toroidal Cores,
Shielding Beads,
Shielded Coil Forms,
Ferrite Rods,
Pot Cores, Baluns, Etc.

AMIDON
Associates



2216 East Gladwick Street, Dominguez Hills, California 90220

Telephone: (213) 763-5770 FAX: (213) 763-2250

ADVERTISER'S INDEX

| | |
|------------------------------------|--------------|
| Amidon Associates | 112 |
| AMSAT | 78 |
| Astron Corporation | 8 |
| Beezley, Brian, K6STI | 61 |
| Coaxial Dynamics | 112 |
| Communications Concepts, Inc. | 111 |
| CQ Bookstore | 94, 110, 111 |
| Down East Microwave | 111 |
| HAL Communications | 9 |
| Hall Electronics | 78 |
| ICOM America, Inc. | COV. II, 1 |
| K2AW's Silicon Alley | 111 |
| Kantronics | 5 |
| Kenwood USA | COV. IV, 2 |
| L.L. Grace Communications Products | 10 |
| Lewallen, Roy, W7EL | 22 |
| N.E. Litsche | 36 |
| OPTOelectronics | 7 |
| PC Boards | 94 |
| PC Electronics | 61 |
| Palomar Engineers | 112 |
| Quorum Communications | 22 |
| Spectrum International, Inc. | 110 |
| VHF Communications | 111 |
| Yaesu | COV. III |

We'd like to see your company listed here too. Contact Arnie Sposato, N2IQO, at (516) 681-2922 or FAX at (516) 681-2926 to work out an advertising program to suit your needs.

The Tradition Continues...

FT-990 HF All-Mode Transceiver

The benchmark from which all other HF all-mode transceivers are judged was set with the introduction of the FT-1000. Now, the tradition continues.

Features and Options:

- **High Dynamic Range:** Unsurpassed RF circuit design with quad FET first mixer similar to the FT-1000.
- **Dual Digital Switched Capacitance Filter:** The FT-990 is the **only** HF transceiver to feature a SCF with independent hi/lo-cut controls for skirt selectivity providing unmatched audio reception as never before attained.
- **Built-in Convenience:** Unlike the competition's extras the FT-990 was designed as a true self-contained base station. A switching AC power supply is built-in.
- **CPU Controlled RF FSP (RF Frequency-Shifted Speech Processor):** The RF FSP shifts the SSB carrier point by programming a CPU to change audio frequency response and provide optimum speech processing effect.
- **Dual-VFO's with Direct Digital Synthesis (DDS)**
- **Full and Semi Break-in CW Operation**
- **6 Function Multimeter**
- **Adjustable RF Power**
- **Adjustable Level Noise Blanker**
- **90 Memories**
- **Multimode Selection on Packet/RTTY**
- **Front Panel RX Antenna Selection**
- **Digital Voice Storage DVS-2 Option**
- **Band Stacking VFO System**
- **Accessories/Options:** TCXO-2 (Temperature Compensated Crystal Oscillator), XF-10.9M-202-01 (2nd IF SSB Narrow 2.0kHz), XF-445C-251-01 (3rd IF CW Narrow 250Hz), SP-6 (External Speaker), MD1C8 (Desk Microphone), YH-77ST (Headphones), LL-5 (Phone Patch Module).

YAESU

Performance without compromise.SM

© 1991 Yaesu USA, 17210 Edwards Road, Cerritos, CA 90701.
Specifications subject to change without notice.
Specifications guaranteed only within amateur bands.



KENWOOD



TS-950SD

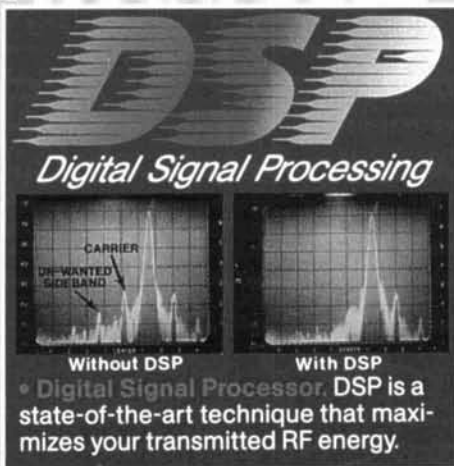
"DX-clusive" HF Transceiver

The new TS-950SD is the first Amateur Radio transceiver to utilize Digital Signal Processing (DSP), a high voltage final amplifier, dual fluorescent tube digital display and digital meter with a peak-hold function.

- **Dual Frequency Receive Function.** The TS-950SD can receive two frequencies simultaneously.
- **New! Digital AF filter.** Synchronized with SSB IF slope tuning, the digital AF filter provides sharp characteristics for optimum filter response.
- **New high voltage final amplifier.** 50 V power transistors in the 150-watt final section, resulting in minimum distortion and higher efficiency. Full-power key-down time exceeds one hour.
- **New! Built-in microprocessor controlled automatic antenna tuner.**
- **Outstanding general coverage receiver performance and sensitivity.** Kenwood's Dyna-Mix™ high sensitivity direct mixing system provides incredible performance from 100 kHz to 30 MHz. The Intermodulation dynamic range is 105 dB.
- **Famous Kenwood interference reduction circuits.** SSB Slope Tuning, CW VBT (Variable Bandwidth Tuning), CW AF tune, IF notch filter, dual-mode noise blanker with level control, 4-step RF attenuator (10, 20, or 30 dB), switchable AGC circuit, and all-mode squelch.

Complete service manuals are available for all Kenwood transceivers and most accessories. Specifications, features and prices subject to change without notice or obligation.

The Ultimate Signal.



- **High performance IF filters built-in†** Select various filter combinations from the front panel. For CW, 250 and 500 Hz, 2.4 kHz for SSB, and 6 kHz for AM. Filter selections can be stored in memory!
- **Multi-Drive Band Pass Filter (BPF) circuitry.** Fifteen band pass filters are available in the front end to enhance performance.

- Built-in TCXO for the highest stability.†
- Built-in electronic keyer circuit.
- 100 memory channels. Store independent transmit and receive frequencies, mode, filter data, auto-tuner data and CTCSS frequency.
- Digital bar meter.

Additional Features: • Built-in interface for computer control • Programmable tone encoder • Built-in heavy duty AC power supply and speaker • Adjustable VFO tuning torque • Multiple scanning functions • MC-43S hand microphone supplied

Optional Accessories

- DSP-10 Digital Signal Processor*
- SO-2 TCXO* • VS-2 Voice synthesizer
- YK-88C-1 500 Hz CW filter for 8.83 MHz IF*
- YG-455C-1 500 Hz CW filter for 455 kHz IF*
- YK-88CN-1 270 Hz CW filter for 8.83 MHz IF*
- YG-455CN-1 250 Hz CW filter for 455 kHz IF*
- YK-88SN-1 1.8 kHz SSB filter for 8.83 MHz IF*
- YG-455S-1 2.4 kHz SSB filter for 455 kHz IF*
- SP-950 External speaker w/AF filter
- SM-230 Station monitor w/pan display
- SW-2100 SWR/power meter
- TL-922A Linear amplifier (not for QSK)

* Built-in for the TS-950SD

† Optional for the TS-950S

KENWOOD U.S.A. CORPORATION
COMMUNICATIONS & TEST EQUIPMENT GROUP
P.O. BOX 22745, 2201 E. Dominguez Street
Long Beach, CA 90801-5745
KENWOOD ELECTRONICS CANADA INC.
P.O. BOX 1075, 959 Gana Court
Mississauga, Ontario, Canada L4T 4C2

KENWOOD

...pacesetter in Amateur Radio

